FIRST LASING OF FERMI FEL-2

E. Allaria[1], D. Castronovo[1], P. Cinquegrana[1], M.B. Danailov[1], G. D'Auria[1], A. Demidovich[1], S. Di Mitri[1], B. Diviacco[1], W.M. Fawley[1], M. Ferianis[1], L. Froehlich[1], G. Gaio[1], R. Ivanov[1], N. Mahne[1], I. Nikolov[1], G. Penco[1], L. Raimondi[1], C. Serpico[1], P. Sigalotti[1], C. Spezzani[1], M. Svandrlik[1], C. Svetina[1], M. Trovo[1], M. Veronese[1], D. Zangrando[1], Benoît Mahieu[1,2], M. Dal Forno[3,1], L. Giannessi[4,1*], M. Zangrando[5,1], G. De Ninno [7,1], E. Ferrari[8,1], F. Parmigiani[8,1], D. Gauthier [7]

[1]Elettra-Sincrotrone Trieste S.C.p.A., Basovizza, Italy
[2]CEA/DSM/DRECAM/SPAM, Gif-sur-Yvette, France
[3]DEEI, Trieste, Italy
[4]ENEA C.R. Frascati, Frascati (Roma), Italy
[5]IOM-CNR, Trieste, Italy
[6]PSI, Villigen, Switzerland
[7]University of Nova Gorica, Nova Gorica, Slovenia
[8]Università degli Studi di Trieste, Trieste, Italy

Abstract

The FERMI@Elettra seeded Free Electron Laser (FEL) is based on two separate FEL lines, FEL-1 and FEL-2. FEL-1 is a single stage cascaded FEL delivering light in the 65-20nm wavelength range, while FEL-2 is a double stage cascaded FEL where the additional stage extends the frequency up-conversion process to the spectral range of 20-4nm.

The FEL-1 beam line has been in operation since the end of 2010, with user experiments carried on in 2011-2013 and user beam time allocated until the first half of 2014. Fermi FEL-2 is a seeded FEL operating with a double stage cascade in the "fresh bunch injection" mode [1]. The two stages are two high gain harmonic generation FELs where the first stage is seeded by the 3rd harmonic of a Ti:Sa laser system, which is up converted to the 4th-12th harmonic. The output of the first stage is then used to seed the second stage. A final wavelength of 10.8 nm was obtained (the 24th harmonic of the seed wavelength) during the first commissioning in October 2012. The experiment demonstrated that the FEL is capable of producing single mode narrow bandwidth pulses with energy of several tens of microjoules. The commissioning of FEL-2 continued in March and June 2013, where the wavelength of operation was extended down to 4nm and below, demonstrating that an externally seeded FEL is capable of reaching the soft X-ray range of the spectrum.

*Corresponding author: luca.giannessi@elettra.eu. This work has been supported in part by the Italian Ministry of University and Research under grants FIRB-RBAP045JF2 and FIRB-RBAP06AWK3

FERMI FEL-2 FREE ELECTRON LASER

We have addressed the FERMI FEL-2 First lasing experience elsewhere in these proceedings. We address therefore the reader to Ref. [2-4] for a general overview of FERMI, and to Ref. [5, 6] for a detailed description of FEL-2 first lasing details.

REFERENCES

[1] I. Ben-Zvi, K.M. Yang, L.H. Yu, "The `fresh-bunch´ technique in FELs", NIM A 318 (1992), p 726-729.
[2] L. Giannessi, et al., "FERMI@Elettra Status Report", WEPSO22, FEL2013.
[3] E. Allaria et al., Nat. Phot. 6, 233 (2012).
[4] E. Allaria et al., New J. Phys. 14, 113009 (2012).
[5] E. Allaria et al., "Double Stage Seeded FEL with Fresh Bunch Injection Technique", THIANO01, FEL2013.
[6] E. Allaria et al., submitted to Nat Photonics.

ISBN 978-3-95450-126-7

GENERATION OF A TRAIN OF SHORT PULSES BY MEANS OF FEL EMISSION OF A COMBED ELECTRON BEAM

V. Petrillo, Università degli Studi di Milano-INFN, Milan, Italy
M. Artioli, ENEA, Bologna, Italy
F. Ciocci, G. Dattoli, A. Petralia, C. Ronsivalle, M. Quattromini, E. Sabia, ENEA, Frascati, Italy
L. Giannessi FERMI, Elettra, Basovizza, Italy
M.P. Anania, M. Bellaveglia, E. Chiadroni, D. Di Giovenale, G. Di Pirro, M. Ferrario, G. Gatti, R. Pompili, C. Vaccarezza, F. Villa, INFN-LNF, Frascati, Italy
A. Bacci, A.R. Rossi, INFN-Milano, Milan, Italy
J. V. Rau, ISM-CNR, Roma, Italy
P. Musumeci, UCLA, Los Angeles, California, USA
A. Cianchi, Università di Roma II Tor Vergata, Roma, Italy
A. Mostacci, Università La Sapienza, Roma, Italy

Abstract

We present the experimental demonstration of a novel scheme for the generation of ultrashort pulse trains based on the FEL lasing from a multi-peaked eletron energy distribution. At SPARC we generated two electron beamlets with relative energy difference larger than the FEL parameter ρ by illuminating the cathode with a combed laser, followed by a manipulation of the longitudinal phase space by velocity bunching in the linac. The SASE FEL radiation obtained by sending such beam in the undulator is analyzed by a FROG diagnostic revealing the double-peaked spectrum and temporally modulated pulse structure.

INTRODUCTION

Radiation pulse trains with atto-femtosecond time spacing represent a real possibility for a breakthrough in science and technology, permitting unprecedented insights into the atomic, multielectron and nuclear dynamics [1,2,3]. Since attosecond electronic motion is relevant to chemical processes leading to the formation of new materials and to chemical/biological transformations, the studies of time-resolved electron and nuclear rearrangements could lead to significant advances in understanding of intermolecular processes, chemical bond breaking and formation, and interaction of photoactivated molecules with their environment.

The ultrafast electron dynamics can be studied in atomic and molecular systems by using trains of ultrashort pulses, that allow not only the ultrafast electron imaging in atomic and molecular systems [4] or the investigation of the electronic response accompanying collective electron motion in nanomaterials, but find further applications in other technical fields as the enhancement of transmission or reflectivity in materials, the resonant inelastic X ray scattering, or the ab-initio phasing of nanocrystals. Sequences of spikes have been so far synthesized by means of the High Harmonic Generation driven by lasers in gases [HGHG] and regularly used in experiments, but with the intrinsic frequency limitations of this kind of sources.

The Free Electron Laser, in the self-amplified spontaneous emission (SASE) mode of operation, generates radiation with limited temporal coherence, time duration of the order of the electron bunch length and structured in a chaotic succession of random peaks. Several techniques have been explored to increase longitudinal coherence and stability and shorten the time scale towards the attosecond domain, and the progresses along this route have allowed the systematic generation of femtosecond EUV/x-ray pulses at the Fourier limit. The amplification of one single SASE spike has been demonstrated by compressing the electron beam below the radiation coherence length [5-6], by using a chirped bunch energy combined with a negative undulator taper [7-9], or by spoiling the whole electron beam except a limited fraction [10,11], a technique that has also been implemented to produce double pulse two color radiation for pump and probe experiments [12]. UV or soft X-ray short single or multiple pulses have been also produced in seeded or cascaded FELs [13], guaranteeing phase stability and coherence from shot to shot.

Another technique [14,15], relying on concepts adapted to FELs from mode-locked cavity lasers, has been proposed for reducing the duration of X-ray pulses generated by SASE FELs to less than the atomic unit of time and foresees the generation of trains of high peak coherent power flashes with large contrast ratio. Such scheme provides a comb of longitudinal modes by applying a series of spatiotemporal shifts between the co-propagating radiation and electron bunch, and is foreseen operating in the X-ray range of wavelength.

In this paper we present the experimental demonstration of a novel scheme for the generation of a regular short FEL pulse sequence [16] based on lasing from a multipeaked electron energy distribution.

DESCRIPTION OF THE METHOD

The experiment was carried out at the SPARC FEL facility in the IR-optical frequency range. The electron

ISBN 978-3-95450-126-7

EMITTANCE CONTROL IN THE PRESENCE OF COLLECTIVE EFFECTS IN THE FERMI@ELETTRA FREE ELECTRON LASER LINAC DRIVER*

S. Di Mitri#, E. Allaria, D. Castronovo, M. Cornacchia, W.M. Fawley, L. Fröhlich, E. Karantzoulis, G. Penco, C. Serpico, C. Spezzani, M. Trovo', M. Veronese, Elettra Trieste, Basovizza, Italy
L. Giannessi, ENEA, Frascati (Roma) & Elettra Trieste, Basovizza, Italy
P. Craievich, Elettra Trieste, Basovizza, Italy & PSI, Villigen, Switzerland
A.A. Lutman, Elettra Trieste, Basovizza, Italy & SLAC, Menlo Park, CA, USA
G. De Ninno, S. Spampinati, Elettra Trieste, Basovizza & University of Nova Gorica, Slovenia
M. Dal Forno, Elettra Trieste, Basovizza & University of Trieste, Trieste, Italy
E. Ferrari, Elettra Trieste, Basovizza & Università degli Studi di Trieste, Trieste, Italy

Abstract

Recent beam transport experiments conducted on the linac driving the FERMI@Elettra free electron laser (FEL) have provided new insights concerning the transverse emittance degradation due to both coherent synchrotron radiation (CSR) and geometric transverse wakefield (GTW), together with methods to counteract such degradation. For beam charges of several 100's of pC, optics control in a magnetic compressor helps to minimize the CSR effect by manipulating the H-function. We successfully extended this approach to the case of a modified double bend achromatic system, opening the door to relatively large bending angles and compact transfer lines. At the same time, the GTWs excited in few mm diameter iris collimators and accelerating structures have been characterized in terms of the induced emittance growth. A model integrating both CSR and GTW effects suggests that there is a limit on the maximum obtainable electron beam brightness in the presence of such collective effects.

INTRODUCTION TO FERMI FEL

FERMI@Elettra is a single-pass fourth generation light source user facility in operation at Elettra – Sincrotrone Trieste in Trieste, Italy [1, 2]. Table 1 shows the main electron and photon beam parameters.

Table 1: FERMI FEL Main Operational Parameters

Parameter	FEL-1	FEL-2	Unit
Charge	500	500	pC
Energy	0.9–1.2	1.0–1.5	GeV
Peak Current	600	400	A
Bunch Length, fw	0.7	1.0	ps
Norm. Emittance rms, slice	< 1.2	1.0	μm
Energy Spread rms, slice	< 250	< 250	keV
Fund. Wavelength	100 – 20	20 – 4	nm
Energy per pulse	< 400	< 100	μJ

*Work supported in part by the Italian Ministry of University and Research under grants FIRB-RBAP045JF2 and FIRB-RBAP06AWK3
#simone.dimitri@elettra.eu

An electron beam in the energy range 0.9–1.5 GeV drives two seeded FELs in the fundamental wavelength range 4–100 nm. The accelerator and FEL complex comprise the following parts: a photo-injector, and a main linac in which the beam is time-compressed in one or two-stages by a total factor of ~10; the transport system to the undulators; the undulator complex where the FEL radiation is generated; the photon beamlines, which transport the radiation from the undulator to the experimental area; and the experimental area itself.

IMPORTANCE OF PROJECTED TRANSVERSE EMITTANCE

Unlike linear colliders, where particle collisions effectively integrate over the entire bunch length, the FEL process takes place over short fractions of the electron bunch length. In fact, slice transverse emittance and slice energy spread may vary significantly along the bunch and thus give local regions where lasing may or may not occur. One could therefore argue that only *slice* electron beam quality is of interest, each slice typically being as long as the FEL slippage length. In this section we make the case that other considerations related to the electron beam control and optimization of the FEL performance justify an optimization of the four-dimensional electron beam normalized brightness, $B_{4D,n}$ that is defined as the final bunch peak current divided by the product of the transverse normalized *projected* emittances, *i.e.* integrated over the entire bunch length.

Electron –Photons Interaction in the Undulator

The need to control beam size and angular divergence along the undulator calls for measurements and manipulation of the electron beam optical parameters. The incoming electron beam optics must be matched to the design Twiss functions [3–5]. As a practical matter, optics matching is routinely performed by measuring the projected electron bunch transverse size [6, 7]. From an operational point of view, it is therefore important to ensure a projected emittance as close as possible to the slice one because this guarantees that most of the bunch slices are matched to the design optics; as a consequence, $B_{4D,n}$ is maximized.

ISBN 978-3-95450-126-7

MULTI-OBJECTIVE GENETIC OPTIMIZATION FOR LCLSII X-RAY FEL†

L. Wang# and T. O. Raubenheimer, SLAC, Menlo Park, CA, USA

Abstract

The Linac Coherent Light Source II (LCLS-II) will build on the success of the world's most powerful X-ray laser, the Linac Coherent Light Source (LCLS). It will add two new X-ray laser beams and room for additional new instruments, greatly increasing the number of experiments carried out each year. Multiple operation modes are proposed to accommodate a variety of user requirements. There are a large number of variables and objectives in the design. For each operation mode, Multi-Objective Genetic Algorithm (MOGA) is applied to optimize the machine parameters in order to minimize the jitters, energy spread, collective effects and emittance.

INTRODUCTION

LCLS-II will provide beam with difference charge. For each beam, the bunch compressors, R56 at BC1 and BC2, accelerating structure phase and voltage are optimized using MOGA program to satisfy the required peak current, and to minimize the energy spread, energy chirp, current jitter, energy jitter and time jitter. We briefly summarize the MOGA optimization for LCLS, LCLSII and the two beam configuration.

The transverse emittance growth due to CSR is minimized by choosing appropriate phase advance between BC2 and the downstream bending magnets. The final emittance at the beginning of the undulator is just about 1um and even lower for low charge.

BENCHMARK WITH LCLS BEAM

It is important to have a comparision of the simulation with the measurements. A series of data, for instance, the voltage and phase of Linac 1and 2, energy at BC1, BC2 and DL2, beam current at BC1 and BC2, were taken at the LCLS to set-up the variations and then compare the jitters in beam current and energy. One example of the variation of L2 voltage and DL2 energy are shown in Fig. 1. We uses these varations to study the enegy and beam current jitter. The main machine parameters used in the simulation are listed in Table 1 as oeprational model. The values of these parameters are not exactly the same as the readings from MCC. Some parameters, especially the phase of RF, are tweaked to get flat top current profile and zero energy chirp at the beginning tof the undulator similar to the measured values. The bunch charge is 150 pC. FIG.2 shows the bunch profile before the undulator by LiTrack simulation, which gives a simliar bunch current ~ 3kA. The measured energy jitter in the machine is about 0.049%, which is slighly larger than the the simulation result of 0.033%. The L0 jitter is not included in the simulation since the simulation starts after L0 and this will cause the simulated jitter to be low [1].

†Work supported by DOE contract No. DE-AC02-76SF00515
Email address: wanglf@slac.stanford.edu

The main contributions of the energy jitters in the operational mode are L1 phase and voltage, LX phase and L2 phase. One of the optmized configurations is also listed in Table 1. This optmized configuration reduces the energy jitter by a factor 2. Fig.3 shows the comparision of the energy jitter for the optmized mode and the operational one. There are large reductions for the four major contributions. The energy jitter of the optimized mode is widely distributed compared with the operational mode. It clearly shows the benefit from optmization. We are doing detail benchmark with the measurement: taking the OTR4 phase space data as the input of the simulation and comparing the phase space in the middle of BC1, BC2 and DL2. New features are being added to Litrack code for such comparision.

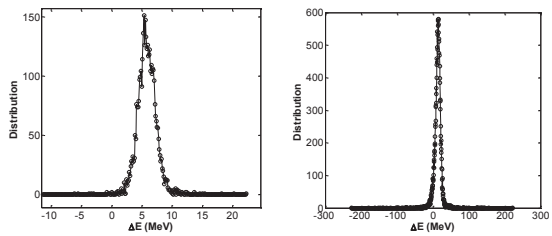

Figure 1: Variation of the L2 voltage and DL2 energy at LCLS.

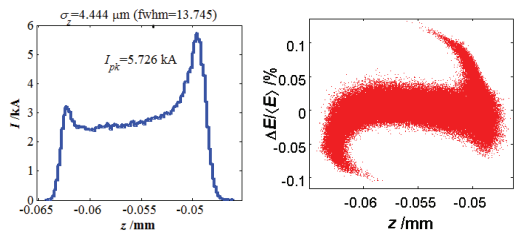

Figure 2: The bunch profile and phase space at the beginning of the undulator for 150pC beam at LCLS. Bunch head is on the left.

Table 1: Example of LCLS operational and optimized model.

Variables	optimized	~operational
I_{pk} (kA)	3	3
ϕ_{L1} (degree)	-19.3	-26.1
V_{L1}(MV)	111	118
ϕ_{Lx} (degree)	-154	-160
V_{Lx}(MV)	22	22
ϕ_{L2} (degree)	-19	-38.7
V_{L2}(GV)	5.06	6.15
ϕ_{L3} (degree)	-10.3	0
V_{L3}(GV)	8.79	7.667
R_{56}@BC1(mm)	-45.5	-45.5
R_{56}@BC2(mm)	-51.3	-20.6
(ΔI/I) (%)	10	7
(ΔE/E) (%)	0.014	0.033

ISBN 978-3-95450-126-7

USING A LIENARD-WIECHERT SOLVER TO STUDY COHERENT SYNCHROTRON RADIATION EFFECTS

R.D. Ryne*, C.E. Mitchell, J. Qiang, Lawrence Berkeley National Laboratory, Berkeley, CA, USA
B. Carlsten, N. Yampolsky, Los Alamos National Laboratory, Los Alamos, NM, USA

Abstract

We report on coherent synchrotron radiation (CSR) modeling using a massively parallel, first-principles 3D Lienard-Wiechert solver. The solver is able to perform simulations with hundreds of millions to billions of simulation particles, the same as the real-world number of electrons per bunch typically present in modern accelerators. We have recently extended this tool to model a variety of beam transport systems including undulators. In this paper we provide an overview of the tool and present several examples. We also describe the concept of a Lienard-Wiechert particle-mesh (LWPM) code, and how such a code might make it possible to perform parallel, self-consistent modeling using a Lienard-Wiechert approach.

INTRODUCTION

Particle accelerators are among the versatile and important tools of scientific discovery and technology advancement. They are responsible for a wealth of advances in materials science, chemistry, bioscience, high-energy physics, and nuclear physics. They also have important applications to the environment, energy, national security, and medicine. Given the enormous benefit of particle accelerators and their extreme complexity, high performance computing using parallel computers has become an essential tool for their design and optimization to reduce cost and risk, maximize performance, and explore advanced concepts.

Early examples of parallel simulation in the U.S. accelerator community date from the late 1980's and early 1990's [1]. By the mid-1990's parallel beam dynamics codes had been developed to run on the Thinking Machines CM-5 computer at LANL's Advanced Computing Laboratory [2, 3]. In 1997 the U.S. Department of Energy (DOE) approved a "Grand Challenge" project in Computational Accelerator Physics [4]. This later evolved into a DOE Scientific Discovery through Advanced Computing (SciDAC) project [5, 6]. This, as well as other R&D efforts in parallel accelerator simulation worldwide, led to the parallelization of existing beam dynamics codes and the development of new codes. Examples include ASTRA [7], BeamBeam3D [8], CSRtrack [9], elegant/SDDS [10], GENESIS [11], G4Beamline [12], ICOOL [13], IMPACT [14, 15], MaryLie/IMPACT [16], OPAL [17], SPUR [18], Synergia [19], TRACK [20],TREDI [21], and WARP [22], to name a few.

From the mid-1990's to the present, significant attention was devoted to parallel 3D space-charge modeling, multi-physics modeling, and increasingly large-scale simulation. In regard to 3D space-charge modeling, many parallel Poisson solvers were developed to treat a variety of boundary conditions, e.g., [23, 24, 25]. Integrated Green functions (IGFs) were introduced to increase solver performance and address grid aspect ratio issues [26, 27, 28], and are now used in several codes worldwide [7, 8, 14, 16, 17]. IGFs have also been applied to model 1D CSR [29, 30]. In regard to multi-physics modeling, split-operator methods were introduced as a means to combine high-order optics effects with parallel 3D space-charge and other effects [31], and are used in several codes [14, 16, 17, 19]. In general, parallel beam dynamics codes now contain, and are routinely used to model, a variety of phenomena including high-order optics, space-charge effects, wakefield effects, 1-D CSR effects, electron-cloud effects, and beam-material interactions. Regarding the trend toward increasingly large-scale simulation, a start-to-end 2-billion-particle simulation of a future light source, based on the single parallel executable containing IMPACT-T, IMPACT-Z, and GENESIS, requires 10 hours on 2048 cores [32].

Despite these major advances in parallel multi-physics modeling, the simulation of 3D CSR effects has remained a major challenge. A first-principles classical treatment usually involves the Lienard-Wiechert (L-W) formalism. Since this involves quantities when the radiation was emitted (i.e. at retarded times and locations), it requires storing a history of each particle's trajectory. Also, CSR phenomena can exhibit large fluctuations which are physical, not numerical, hence it is often necessary to use a large number of simulation particles if those fluctuations are to be modeled correctly. Storing a large number of particles over a lengthy time history imposes a huge memory requirement. Furthermore the calculation of retarded quantities is iterative and extremely time consuming. Consider that the calculation of an electric field component on a grid in an electrostatic code, e.g., $x/|r|^3$, requires only a small number of floating point operations at each grid point; by contrast the calculation of the L-W field at just a single grid point requires a small simulation code itself to implement the iteration to find the retarded quantities, and furthermore the iteration involves numerical integration of trajectories. In summary a L-W solver involves large memory and many floating point operations, and obviously requires parallel computing. In addition, to embed such a capability in a self-consistent beam dynamics code would greatly compound the computational requirements.

Despite these computational challenges, in the following we will present results that point to the possibility of a mas-

* RDRyne@lbl.gov

ISBN 978-3-95450-126-7

MEASUREMENT OF ELECTRON-BEAM AND SEED LASER PROPERTIES USING AN ENERGY CHIRPED ELECTRON BEAM*

E. Allaria[1], S. Di Mitri[1], W. M. Fawley[1], L. Froehlich[1], G. Penco[1], P. Sigalotti[1], C. Spezzani[1], M. Trovo[1], G. De Ninno[1,2], S. Spampinati[1,2,3], E. Ferrari[1,4]

[1]Elettra-Sincrotrone Trieste S.C.p.A., Basovizza, IT
[2]University of Nova Gorica, Nova Gorica, SLO
[3]The Cockcroft Institute, Liverpool, UK
[4]Università degli Studi di Trieste, Trieste, IT

Abstract

We present a new method that uses CCD images of the FERMI electron beam at the dump spectrometer after the undulator to determine various electron beam and external seed laser properties. By taking advantage of the correlation between time and electron beam energy for a quasi-linearly chirped electron beam and the fact that the FERMI seed laser pulse (~180 fs) is much shorter than the electron beam duration (~1 ps), measurements of the e-beam pulse length and temporally local energy chirp and current are possible. Moreover, the scheme allows accurate determination of the timing jitter between the electron beam and the seed laser, as well as a measure of the latter's effective pulse length in the FEL undulators. The scheme can be also provide an independent measure of the energy transferred from the electron beam to the FEL output radiation. We describe the proposed method as well as some experimental results obtained at the seeded FERMI FEL.

SEEDED FEL AT FERMI

FERMI is a seeded Free Electron Laser user facility based on normal conducting linac [1]. Electron beams generated in the photocathode [2] are compressed and accelerated up to the final energy of 1.2 GeV. A schematic layout of the FERMI complex is shown in Fig. 1. Electron beam compression is obtained by introducing a linear chirp in the beam before entering into the compressor chicane (BC1). If not properly removed by operating the second part of the linac off crest the linear chirp needed for the compression remains on the beam. As a result the electron beam entering in the radiator has a linear correlation between energy and time as shown in Fig. 2.

FERMI FEL is based on a HGHG scheme. An UV external laser is used to induce into the electron beam an energy modulation after the interaction that occurs in the modulator. Energy modulation is converted into spatial modulation and bunching at the seed laser wavelength and his harmonics. The final radiator is tuned to one of the harmonics and the electron beam produces coherent emission, finally FEL emission is amplified along the radiator.

As a result of the seeding the electrons that interact with the laser become energy modulated and a local energy bump is created.

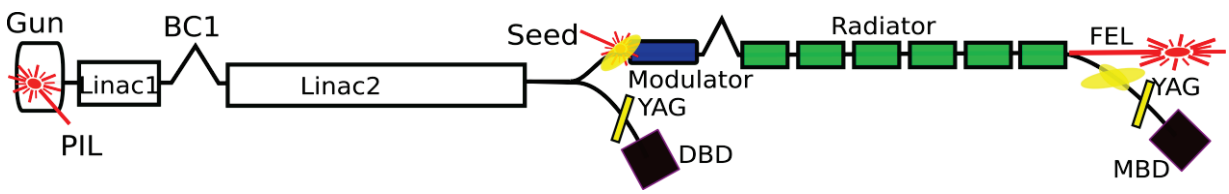

Figure 1: Layout of the FERMI linear accelerator and FEL.

*Work partially supported by the Italian Ministry of University and Research under grants FIRB-RBAP045JF2 and FIRB-RBAP06AWK3
#enrico.allaria@elettra.eu

ISBN 978-3-95450-126-7

THEORETICAL ANALYSIS OF A LASER UNDULATOR-BASED HIGH GAIN FEL

Panagiotis Baxevanis and Ronald Ruth
SLAC National Accelerator Laboratory, Menlo Park, CA 94025, USA

Abstract

The use of laser (or RF) undulators is nowadays considered attractive for FEL applications, particularly those that aim to utilize relatively low-energy electron beams. In the context of the standard theoretical analysis, the counter-propagating laser pulse is usually treated in the plane-wave approximation, neglecting amplitude and phase variation. In this paper, we develop a three-dimensional, analytical theory of a high-gain FEL based on a laser or RF undulator, taking into account the longitudinal variation of the undulator field amplitude, the laser Gouy phase and the effects of emittance and energy spread in the electron beam. Working in the framework of the Vlasov-Maxwell formalism, we derive a self-consistent equation for the radiation amplitude in the linear regime, which is then solved to good approximation by means of an orthogonal expansion technique. Numerical results obtained from our analysis are used in the study of an example of a compact, laser undulator-based, X-ray FEL.

INTRODUCTION

In recent years, the free-electron laser (FEL) has emerged as one of the leading methods for producing bright, coherent radiation up to the X-ray region. The push for higher photon energy is facilitated by the use of higher electron energy and/or shorter undulator period. For magnetic undulators, implementing the latter option is generally limited by technical considerations to periods of a few mm at best. On the other hand, the wide availability of lasers with very high peak power (in the TW level) often raises the possibility of generating X-rays through the head-on collision of an electron beam with a counter-propagating laser pulse, where the field of the pulse acts as an undulator with period equal to half the laser wavelength. Though this process is usually studied in the framework of incoherent, inverse Compton scattering sources, one can also consider the production of coherent radiation from an FEL that uses such a laser undulator, provided a high-brightness electron beam is available [1]. Here, we present a theoretical description of such a device, paying particular attention to the effects introduced by variations in the amplitude and phase of the effective undulator field. A specific numerical example for a soft X-ray, laser undulator-based FEL is included in order to illustrate the main points of our analysis and also to highlight some the main challenges involved in the realization of this concept.

THEORY

FEL Configuration and Single Particle Motion

To begin with, let us assume that the laser radiation is monochromatic, linearly polarized along the x direction and has a Gaussian transverse profile. The electric field of the laser pulse - which is propagating along the negative z direction - can then be written as $\mathbf{E}_L = E_L(r,z)\hat{x}$, where

$$E_L = -E_0 \frac{w_0}{w} \exp\left(-\frac{r^2}{w^2}\right) \sin[k_L(z+ct) + \frac{k_L r^2}{2R} - u]\,. \tag{1}$$

Here, $r^2 = x^2 + y^2$, $k_L = 2\pi/\lambda_L$ (λ_L is the laser wavelength), $w = w(z) = w_0(1 + \bar{z}^2/z_R^2)^{1/2}$ is the laser spot size, $R = R(z) = \bar{z} + z_R^2/\bar{z}$ is the radius of curvature and $u = u(z) = \tan^{-1}(\bar{z}/z_R)$ is the Gouy phase. In these relations, $\bar{z} = z - z_w$, where $z = z_w$ is the position of the laser waist, z_R is the Rayleigh length, E_0 is the field amplitude at the waist and $w_0 = (2z_R/k_L)^{1/2}$ is the minimum spot size. Moreover, the counter-propagating electron beam is also assumed to be round and Gaussian, with transverse size $\sigma_e(z) = (\sigma^2 + \sigma'^2\bar{z}^2)^{1/2}$, where σ and σ' are the rms beam size and divergence at the location of the electron beam waist, which we take to be the same as that of the laser. Both the laser pulse and the electron beam are characterized by a uniform longitudinal profile, with temporal durations t_L and t_e respectively ($t_L \gg t_e$). For simplicity, we can also assume that their front ends collide at $z = 0$, when $t = 0$. Each electron in the beam interacts with the laser field for a time $t \approx L_I/c = t_L/2$, where $L_I = ct_L/2$ is the corresponding interaction length. For the configuration under consideration, we assume that the interaction region is centered around the common waist, so that $L_I = 2z_w < z_R$. The laser power P_L is given by the relation $P_L = \pi c\varepsilon_0 E_0^2 w_0^2/4$ - where ε_0 is the vacuum permittivity - while the total energy in the laser pulse is $U_L = P_L t_L$.

Next, we consider the motion of electrons in the combined field of the laser and the emitted FEL radiation. As is the case with standard FEL schemes, the transverse motion is predominantly determined by the undulator field. The vertical magnetic field of the laser is $B_L \approx -E_L/c$ so the total force in the x direction is $F_x \approx -e(E_L - v_z B_L) \approx -2eE_L$ (the electric and magnetic force contributions are equal and add up). This force gives rise to an oscillatory motion similar to that in a conventional magnetic wiggler. To establish this connection in a way that takes into account the dominant effects of the undulator field inhomogeneities, we consider the equation of motion in the hori-

ISBN 978-3-95450-126-7

PARAXIAL APPROXIMATION IN CSR MODELING USING THE DISCONTINUOUS GALERKIN METHOD*

D. A. Bizzozero†, J. A. Ellison, K. A. Heinemann, S. R. Lau
Department of Mathematics and Statistics, University of New Mexico,
Albuquerque, New Mexico 87131, USA

Abstract

We continue our study [1, 2] of CSR from a bunch moving on an arbitrary curved trajectory. In that study we developed an accurate 2D CSR Vlasov-Maxwell code (VM3@A) and applied it to a four dipole chicane bunch compressor. Our starting point now is the well-established paraxial approximation [3–7] with boundary conditions for a perfectly conducting vacuum chamber with uniform cross-section. This is considerably different from our previous approach [1, 2] where we calculated the fields from an integral over history, using parallel plate boundary conditions. In this study, we present a Discontinuous Galerkin (DG) method for the paraxial approximation equations. Our basic tool is a MATLAB DG code on a GPU using MATLAB's `gpuArray`; the code was developed by one of us (DB). We discuss our results in the context of previous work and outline future applications for DG, including a Vlasov-Maxwell study.

STATEMENT OF THE PROBLEM

Statement of the Mathematical Problem

We study the initial boundary value problems for two nonhomogeneous Schrödinger type equations which arise in a paraxial approximation to Maxwell's equations. The PDEs are

$$\partial_s E_x^r = \frac{i}{2k}\nabla_\perp^2 E_x^r + \frac{ikx}{\rho}E_x^r + \frac{ikx}{\rho}E_x^b(x,y) \qquad (1a)$$

$$\partial_s E_y^r = \frac{i}{2k}\nabla_\perp^2 E_y^r + \frac{ikx}{\rho}E_y^r + \frac{ikx}{\rho}E_y^b(x,y), \qquad (1b)$$

on the domain $0 \le s \le L, -a \le x \le a, -b \le y \le b$. Here the 2D Laplacian is $\nabla_\perp^2 := \partial_x^2 + \partial_y^2$, the real parameters $k \in \mathbb{R}$ and $\rho > 0$, and the nonhomogeneous terms are determined by

$$E_x^b = C\frac{x}{x^2+y^2}, \quad E_y^b = C\frac{y}{x^2+y^2}, \qquad (2)$$

where C is defined in the next subsection. The boundary conditions for $E_x^r = E_x^r(x,y,s;k)$ are

$$\begin{aligned} \partial_x E_x^r &= \partial_y E_y^b, \quad \text{on} \quad x = \pm a \\ E_x^r &= -E_x^b, \quad \text{on} \quad y = \pm b, \end{aligned} \qquad (3)$$

and the boundary conditions on $E_y^r = E_y^r(x,y,s;k)$ are

$$\begin{aligned} E_y^r &= -E_y^b, \quad \text{on} \quad x = \pm a \\ \partial_y E_y^r &= \partial_x E_x^b, \quad \text{on} \quad y = \pm b. \end{aligned} \qquad (4)$$

The initial conditions are given uniquely by

$$\nabla_\perp^2 E_x^r = 0, \quad \nabla_\perp^2 E_y^r = 0, \quad \text{at} \quad s = 0, \qquad (5)$$

with the same boundary conditions, i.e. (3), (4). We note that the above two initial boundary value problems are uncoupled and that the boundary and initial conditions are independent of k.

In addition, the field quantity $E_s^r = E_s^r(x,y,s;k)$, defined by

$$E_s^r = \frac{i}{k}(\partial_x E_x^r + \partial_y E_y^r), \qquad (6)$$

is needed for $0 \le s \le L$ in order to compare with the impedance calculation in [5]. The impedance in our notation is given by

$$Z = -\frac{Z_0}{2\pi C}\int_0^\infty ds E_s(0,0,s;k), \qquad (7)$$

where Z_0 is the free space impedance, C is the parameter in (2), and the calculation of $E_s(0,0,s;k)$ for $s \ge L$ is discussed in the numerical implementation section. Note that C simply scales the fields.

Statement of the Physical Problem

Derivations of the paraxial approximation can be found in [3], [6] and [7]. The starting point is Maxwell's equations with a source given by a line charge moving at near the speed of light, on a circular arc of radius ρ and length L, and in a perfectly conducting rectangular vacuum chamber. As in [3], [6] and [7], we take the special case where the line charge is reduced to a single point. Maxwell equations are written in beam frame coordinates (x, y, s) where the arc is in the (x, s) plane, s is the distance along the arc, and (x, y) are perpendicular to the arc. Thus the electric field can be written

$$\boldsymbol{\mathcal{E}}(x,y,s,t) = (\mathcal{E}_x, \mathcal{E}_y, \mathcal{E}_s). \qquad (8)$$

where $(\mathcal{E}_x, \mathcal{E}_y, \mathcal{E}_s)$ are the components of the field along the unit vectors $(\mathbf{e}_x(s), \mathbf{e}_y, \mathbf{e}_s(s))$ along the reference curve

* Work supported by DOE under DE-FG-99ER41104
† dbizzoze@math.unm.edu

ISBN 978-3-95450-126-7

CHANNELING RADIATION WITH LOW-ENERGY ELECTRON BEAMS: EXPERIMENTAL PLANS & STATUS AT FERMILAB*

B. Blomberg[1], C. A. Brau[2], B. K. Choi[2,3], W. E. Gabella[2], B. Ivanov[2], M. Mendenhall[2], D. Mihalcea[2], H. Panuganti[1], P. Piot[1,4], W. Wagner[5]
[1] Dept. of Physics and Northern Illinois Center for Accelerator & Detector Development, Northern Illinois University DeKalb, IL 60115, USA
[2] Dept. of Physics and Astronomy, Vanderbilt University, Nashville, TN 37235, USA
[3] Dept. of Electrical Engineering and Computer Science, & Vanderbilt Institute of Nanoscale Science and Engineering Vanderbilt University, Nashville, TN 37235, USA
[4] Accelerator Physics Center, Fermi National Accelerator Laboratory, Batavia, IL 60510, USA
[5] Institute of Radiation Physics, Helmholtz-Zentrum Dresden-Rossendorf, Dresden, Germany

Abstract

Channeling radiation is an appealing radiation process to produce x-ray radiation with low-energy electron beams. In this contribution we describe the anticipated performance and preliminary results from a channeling-radiation experiment to produce $\sim$ 1.2-keV radiation from a $\sim$ 4-MeV electron beam at Fermilab's high-brightness electron source lab (HBESL). We also discuss plans to produce x-ray radiation ($[10, 80]$-keV photon energy) at Fermilab's advanced superconducting test accelerator (ASTA).

INTRODUCTION

The quest for short wavelength compact light sources has applications in many fields including fundamental science, medical imaging and homeland security. For some applications, e.g., medical imaging, important requirements on the x-ray source include high brilliance, efficiency and compactness. Channeling radiation (CR) generated as ultra-low-emittance electron beams channel in thin crystals provide a viable path toward such requirements [1].

CR was first theoretically predicted by Kumakhov [2, 3] in 1974, and since then has been experimentally verified by several groups. It has generally been found that experiments and theory are in decent agreement [4, 5, 6, 7, 8]. Normally when relativistic electrons are accelerated into a crystal target they will be incoherently scattered emitting a broad spectrum of bremsstrahlung radiation. However, when relativistic electrons are focused onto a crystal target, at a small angle near to parallel with a crystallographic axis or plane the scattering becomes an oscillatory motion about the axis or plane not unlike that of electrons propagating through undulators and wigglers [9]. This motion emits electromagnetic radiation dubbed CR in a forward directed cone of $1/\gamma$. In the rest frame of the electron this radiation is in the optical region however the Doppler effect shifts it into the x-ray regime in the lab frame when the electron beam has a sufficient energy. This allows creation of x-rays from moderate energy electron beams (20-50 MeV). The frequency of CR scales as $\omega = 2\gamma^2\omega_0/(1+\gamma^2\theta^2)$, where ω_0 is the oscillation frequency about the lattice plane, θ is the observation angle with respect to the electron direction and γ is the Lorentz factor. The transverse force experienced by an electron traveling along a crystal plane are comparable to those in a 10^4-T magnetic undulator or a 1-TW laser undulator focused to a 10-μm spot [10].

For high-energy beams a description of channeling radiation is more concurrent with a classical treatment however below 100-MeV, the region we are concerned with, it is more accurately described by a quantum mechanical treatment. When the electrons enter the crystal lattice the ions making up the lattice planes are Lorentz contracted increasing the charge density of the plane causing it to appear as a sheet of charge in the rest frame of the electrons. While the longitudinal motion of the electrons is relativistic the oscillatory or transverse motion about the charged plane remains non-relativistic. The average potential associated to the crystal axis or plane can then be used in the Schrödinger equation to describe the non-relativistic transverse motion of the electrons [8, 11].

For the calculations presented in this paper, we use the MATHEMATICA©-based package described in [12]. The package was benchmarked with experiments [13] but some limitations were recently found and summarized in [14].

The brilliance $\mathscr{B}$ associated with CR scales with beam size $\sigma_\perp$, the two scale as $\mathscr{B} \propto \sigma_\perp^{-2}$ where $\sigma_\perp$ is the transverse root-mean-square (rms) beam size. In addition, the beam size has to satisfy $\sigma_\perp = \varepsilon_x/(\gamma\psi_c)$ where ε_x is the rms normalized beam emittance, and ψ_c is the critical angle. In order to channel, electrons must be incident on the crystal surface at an angle smaller than ψ_c [15]. Therefore in order to increase brilliance of CR the beam emittance must be decreased. One of the main goals of our CR studies is to produce x-ray radiation with photon energies $\mathcal{E} \in [10, 80]$ keV and brilliance $\mathscr{B} \sim 10^{12}$ photon.(mm-mrd)$^{-2}$.(0.1%BW)$^{-1}$.s^{-1}. Achieving such a goal requires electron beams with nano meter normalized transverse emittances and $\sim$ 200-nA average current.

Our experimental plans are two fold: we first plan to investigate the generation of CR using the low-energy beam produced at the Fermilab high-brightness electron source

* Work supported by the DARPA Axis program under contract AXIS N66001-11-1-4196 with Vanderbilt University and Northern Illinois University and by in-kind contribution from the Institute of Radiation Physics at the Helmholtz-Zentrum Dresden-Rossendorf in Germany.

ISBN 978-3-95450-126-7

UNAVERAGED MODELLING OF A LWFA DRIVEN FEL

L.T. Campbell[1,2], A.R. Maier[3,4,5], F.J. Grüner[3,4,5] and B.W.J. M[c]Neil[1]
[1]SUPA, Department of Physics, University of Strathclyde, Glasgow, UK,
[2]ASTeC, STFC Daresbury Laboratory and Cockcroft Institute, Warrington, United Kingdom
[3]Center for Free-Electron Laser Science, Notkestrasse 85, Hamburg, Germany
[4]Institut für Experimentalphysik, Universität Hamburg, Hamburg, Germany
[5]Department für Physik, Ludwig-Maximilians Universität, Garching, Germany

Abstract

Preliminary simulations of a Laser Wake Field Accelerator driven FEL are presented using the 3D unaveraged, broad bandwidth FEL simulation code Puffin. The radius of the matched low-emittance electron beam suggests that the FEL interaction will be strongly affected by radiation diffraction. Parameter scaling and comparison between 3D and equivalent 1D simulations confirm this. The Puffin 1D simulations indicate that the energy spread conditions for FEL lasing are met, even without any beam phase space manipulation prior to injection into the undulator. The large diffraction in the Puffin 3D simulations creates boundary problems that will need to be overcome before further progress is made.

INTRODUCTION

With several linac driven X-ray FEL's currently in operation or construction around the world, there is much interest in the next generation of FEL facilities. The plasma based Laser Wakefield Accelerators (LWFA's) are a promising driver for future FEL facilities. Due to their large acceleration gradients compared to conventional RF-linacs, their compact size could dramatically reduce facility costs.

No plasma accelerator driven FEL has yet reported successful lasing primarily as the beam energy spreads from these accelerators are too large by approximately an order of magnitude. Some other plasma accelerator schemes exist that may promise an improvement in beam quality, but these are yet to be realised. A pragmatic approach was taken in a study [1], which considered a design that uses beams currently available from LWFA's to enable modest FEL gains to generate power levels measurably above the spontaneous power to be observed. A cryogenic undulator design with a small undulator period and large on-axis magnetic field was used. This design is chosen to maximise the FEL ρ parameter for a given beam and thus relax the energy spread requirement in the FEL $\sigma_\gamma/\gamma \lesssim \rho$. A chicane to stretch the beam before insertion into the undulator was utilized to both increase the beam length with respect to the cooperation length, and so increase the interaction length between radiation and electrons, and to reduce the localised energy spread. Genesis [2] simulations predicted a modest gain of ~ 6 over the spontaneous emission without bunch stretching, and a gain of $\sim 10^3$ when the stretching was optimized.

In averaged FEL simulation codes where the Slowly Varying Envelope Approximation (SVEA) is applied, the electron beam and radiation fields are modelled by a series of phase space 'slices' within which periodic boundary conditions are applied. Modelling the FEL interaction and electron phase space evolution with beams that are short, have correlated energy spreads (chirps) etc, such as those generated by plasma accelerators, can therefore be problematic. The 3D FEL simulation code Puffin [3] does not perform the Slowly Varying Envelope Approximation or averaging of the electron or radiation parameters and so may be better suited to such circumstances. Furthermore, the effects of dispersion in short beams, either from the chirp or from energy spread induced from the FEL interaction, may be more dramatic than equivalent effects in a longer pulse.

In the following the 3D parameters and likely consequences on the FEL interaction for a plasma accelerator driven FEL interaction are discussed. Puffin simulations of the FEL interaction using the parameter set of [1] are then presented, first in 1D, showing the requirement on the beam energy spread is satisfied. A 3D simulation is also presented. However, the small matched electron beam radius results in a large radiation diffraction which, for the field sampling size used, cannot be modeled properly.

PARAMETERS

Much information can be gained regarding a potential FEL interaction by calculating the scaled parameters that describe the interaction and comparing against a known set of limits which the scaled parameters must meet before good FEL lasing action can occur. Several works have derived these criteria over a period as summarised in [4, 5].

The physical parameters of the study of [1], in the scaled parameters of Puffin [3], are shown in Table 1. In [1], the electron beam was matched in one transverse direction to the natural focusing of the planar undulator. However, the Puffin model assumes a uniform focusing in *both* transverse directions. This results, in the case of the planar wiggler, in the beam being over-focused when using the same betatron wavelength. In the following, the beam is focused to give a matched beam of radius equal to the rms radius used in [1], giving the same diffraction length. This gives an incorrect betatron wavelength, but it is assumed this will

ISBN 978-3-95450-126-7

INVESTIGATION OF A 2-COLOUR UNDULATOR FEL USING PUFFIN

L.T. Campbell[1,2], B.W.J. M[c]Neil[1] and S. Reiche[3]
[1]SUPA, Department of Physics, University of Strathclyde, Glasgow, UK,
[2]ASTeC, STFC Daresbury Laboratory and Cockcroft Institute, Warrington, United Kingdom
[3]Paul Scherrer Institute, Villigen PSI, Switzerland

Abstract

Initial studies of a 2-colour FEL amplifier using one monoenergetic electron beam are presented. The interaction is modelled using the unaveraged, broadband FEL code Puffin. A series of undulator modules are tuned to generate two resonant frequencies along the FEL interaction and a self-consistent 2-colour FEL interaction at widely spaced non-harmonic wavelengths at 1nm and 2.4nm is demonstrated.

INTRODUCTION

With X-ray SASE FELs now in operation around the world, there is now user interest in the simultaneous delivery of two distinct wavelengths. This may be possible by preparing the beam before injection into the undulator, or by using two electron beams of different energy, known as a two-beam or two-stream FEL. Another method, the so-called 2-colour FEL, generates two radiation wavelengths simultaneously from a single mono-energetic electron beam by injecting it through alternative undulator modules that are tuned to the two different wavelengths. There may also be a need for more broadband broadband sources, which may be achievable using an energy chirped electron beam in a 2-colour FEL configuration, and matching together the spectra generated by each of the undulator modules.

Averaged FEL simulation codes such as [1, 2, 3, 4] that make the Slowly Varying Envelope Approximation (SVEA) [5], can readily model 2-colour FEL interactions when the radiation wavelengths are about a fundamental wavelength λ_1 and e.g. its third harmonic $\lambda_3 = \lambda_1/3$. This requires the radiation to be described by two distinct computational fields as the field sampling at any resonant radiation wavelength λ_r means the frequency range able to be sampled is limited by the Nyquist condition to $\omega_r/2 < \omega < 3\omega_r/2$. Furthermore, the accuracy of the model decreases the further away from the central resonant frequency ω_r. For a fundamental and say its 3rd harmonic field, the sampling can be over a common set of 'slices' each an integer number of fundamental wavelengths in length. However, for cases where the two wavelengths in a 2-colour FEL are strongly non-harmonic and well separated in frequency, e.g. where $\lambda_2 = 2.4 \times \lambda_1$, modeling of two computational fields using the averaged SVEA approximation becomes problematic - integer wavelength long slices of the two fields cannot be coincident and so when radiation propagation effects are modeled, electrons within these different length slices are driven asymmetrically in phase space leading to unphysical instabilities.

The unaveraged free electron laser simulation code Puffin [6] does not make the SVEA approximation and is therefore not restricted to the limited bandwidth of conventional averaged FEL codes. Furthermore, because Puffin also models the electron beam dynamics without averaging, the electrons are not confined to localised 'slices' of width the fundamental radiation wavelength, and a realistic electron beam interaction can occur over a broad bandwidth of radiation wavelengths. Puffin (along with other unaveraged codes e.g. [7, 8, 9, 10]) is then ideally suited to simulating and investigating the physics of a multi-color FELs.

In what follows, the Puffin code was modified to allow for undulator modules of different undulator parameters $\bar{a}_w$. This code was then used to simulate a high-gain 2-colour FEL amplifier at distinct, well separated, non-harmonic wavelengths. It is not immediately clear how such an interaction would be expected progress and in particular how the electron phase space in interacting resonantly with two distinct radiation wavelengths would develop. The interaction is therefore first seeded, rather than starting from noise, to allow a cleaner picture of the electron beam and radiation evolution in the 2-colour interaction. An example is then given of an unseeded, 2-colour SASE FEL interaction.

MATHEMATICAL MODEL

Puffin uses a system of equations which utilizes scaled variables developed in [11]. These dimensionless variables are scaled with respect to the FEL parameter, defined as

$$\rho = \frac{1}{\gamma_r}\left(\frac{\bar{a}_w \omega_p}{4ck_w}\right)^{2/3}, \qquad (1)$$

where $\bar{a}_w \propto B_w\lambda_w$ is the usual rms undulator parameter, B_w is the rms undulator magnetic field strength, λ_w is the undulator period and $k_w = 2\pi/\lambda_w$. In the cases simulated in this paper, the undulator tuning of $\bar{a}_w$ is obtained by varying the rms undulator magnetic field alone. This tuning therefore also changes the FEL parameter and it is convenient to re-scale the equations in a general way for the different undulator module tunings by introducing the undulator module dependent parameter $\alpha \equiv \bar{a}_w/\bar{a}_{w1}$, where the sub-script '1' refers to the value of $\bar{a}_w$ of the first module. By similarly re-defining

$$\rho = \alpha^{2/3}\rho_1, \qquad (2)$$

again where sub-script '1' refers to the values of the first module, the parameter α becomes an explicit parameter in

ISBN 978-3-95450-126-7

THE PRESENT STATUS OF THE THEORY OF THE FEL-BASED HADRON BEAM COOLING*

Andrey Elizarov†, Vladimir Litvinenko‡, BNL, Upton, NY 11973, USA,
and Stony Brook University, Stony Brook, NY 11794, USA

Abstract

The coherent electron cooling (CeC) [1] device is one of the new facilities under construction at Brookhaven National Laboratory (BNL). The CeC is a realization of the stochastic cooling with an electron beam serving as a pick-up and a kicker. Hadrons generate electron density perturbations in the modulator section, then these perturbations are amplified in an FEL, and then, they accelerate (or decelerate) hadrons in the kicker by their electric field with respect to the hadrons' velocities. Here we present the theoretical description of the modulator sector [2, 3], where the electron density perturbations are formed, and our new results on the time evolution of these perturbations in the FEL section, where they are amplified.

INTRODUCTION

The scheme of the CeC device is depicted in Fig. 1. It

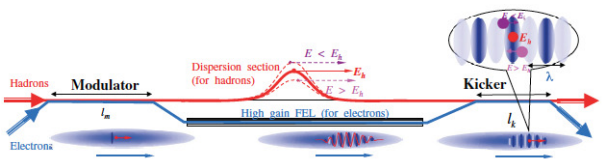

Figure 1: The scheme of the coherent electron cooler.

consists of three sections: the modulator section, where the electron density perturbations are created by hadrons, the FEL section, where these perturbations are amplified, and the kicker section, where the amplified perturbations accelerate (decelerate) hadrons moving slower (faster) than the one with the desired energy, before the kicker, hadrons pass through the dispersion section, where they are delayed in accordance with their energy deviations. In the present article, we describe theoretical models for all these sections.

THE MODULATOR SECTION

In the modulator section, each hadron in a hadron beam creates density perturbations in a co-propagating electron beam. The dynamical shielding of a charged particle in an infinite beam was considered in [4] and for the certain distribution the density perturbation was expressed as a one-dimensional integral, the more general method for a finite beam taking into account focusing fields was proposed in [2]. In the present article, we just quote some results from [3], where this problem was solved via the numerical evaluation of the inverse integral transforms for a variety of equilibrium distributions for a finite electron beam.

General Solution

Here we describe the dynamical shielding of a charged particle in an infinite isotropic electron beam via the Fourier and Laplace transforms. We introduce the following dimensionless variables:

$$\vec{\mathsf{x}} = \frac{\vec{x}}{r_\mathrm{D}}, \quad \vec{\mathsf{v}} = \frac{\vec{v}}{v_\mathrm{rms}}, \quad \mathsf{t} = \frac{t}{t_\mathrm{p}} \equiv t\omega_\mathrm{p}, \quad r_\mathrm{D} = \frac{v_\mathrm{rms}}{\omega_\mathrm{p}},$$

where

$$v_\mathrm{rms} = \sqrt{\frac{1}{\rho}\int v^2 f_0(\vec{v})d\vec{v}}, \quad \omega_\mathrm{p} = \sqrt{\frac{e^2\rho}{m_0\gamma\epsilon_0}}, \qquad (1)$$

and the dimensionless equilibrium density $\mathsf{f}_0(\vec{\mathsf{v}})$:

$$f_0(\vec{v}) = \rho f_\mathrm{d}\mathsf{f}_0(\vec{\mathsf{v}}), \quad \int f_0(\vec{v})d\vec{v} = \rho. \qquad (2)$$

For a unitary point charge moving along a straight line $\vec{\mathsf{y}}(\mathsf{t}) = \vec{\mathsf{x}}_0 + \vec{\mathsf{v}}_0\mathsf{t}$, we have for the induced electron density perturbation for any number of spacial dimensions d:

$$\mathsf{n}_1(\vec{\mathsf{x}},\mathsf{t}) = \mathsf{L}^{-1}\mathsf{F}^{-1}\left[\frac{\mathrm{e}^{-i\vec{\mathsf{k}}\cdot\vec{\mathsf{x}}_0}}{\left(\frac{f_\mathrm{d}^{-1}v_\mathrm{rms}^{-d}}{\mathsf{LF}_{\vec{\mathsf{k}}\mathsf{t}}(\mathsf{tf}_0(\vec{\mathsf{v}}))}+1\right)\left(\mathsf{s}+i\vec{\mathsf{k}}\cdot\vec{\mathsf{v}}_0\right)}\right], \qquad (3)$$

where $\mathsf{LF}_{\vec{\mathsf{k}}\mathsf{t}}(\mathsf{tf}_0(\vec{\mathsf{v}}))$ depends on the equilibrium distribution:

$$\mathsf{LF}_{\vec{\mathsf{k}}\mathsf{t}}(\mathsf{tf}_0(\vec{\mathsf{v}})) = \int_0^\infty \mathrm{e}^{-\mathsf{ts}}\mathsf{t}\int \mathsf{f}_0(\vec{\mathsf{v}})\,\mathrm{e}^{-i\vec{\mathsf{k}}\cdot\vec{\mathsf{v}}\mathsf{t}}d\vec{\mathsf{v}}d\mathsf{t}, \qquad (4)$$

$f_\mathrm{d}^{-1}v_\mathrm{rms}^{-d}$ is a dimensionless factor, and L^{-1}, F^{-1} are the inverse Laplace and Fourier transforms, respectively.

Solutions for Some Distributions

We consider several distributions for the 1D, 2D and 3D cases. v_rms, f_d, and $f_\mathrm{d}^{-1}v_\mathrm{rms}^{-d}$ can be computed via (1) and (2) for all distributions excepting the Cauchy. The solution (3) is valid for all these cases, we only need to

* Work is supported by the U.S. Department of Energy.
† aelizarov@bnl.gov
‡ vl@bnl.gov

ISBN 978-3-95450-126-7

STUDY OF CSR EFFECTS IN THE JEFFERSON LABORATORY FEL DRIVER*

Christopher Hall, Sandra Biedron, Theodore Burleson, Stephen Milton, Auralee Morin
CSU, Fort Collins, CO, USA
Stephen Benson, David Douglas, Pavel Evtushenko, Fay Elizabeth Hannon, Rui Li,
Chris Tennant, Shukui Zhang, JLAB, Newport News, VA, USA
Bruce Carlsten, John Lewellen, LANL, Los Alamos, NM, USA

Abstract

In a recent experiment conducted on the Jefferson Laboratory IR FEL driver the effects of coherent synchrotron radiation (CSR) on beam quality were studied. The primary goal of this work was to explore CSR output and effect on the beam with variation of the bunch compression in the IR recirulator. This experiment also provides a valuable opportunity to benchmark existing CSR models in a system that may not be fully represented by a 1-D CSR model. Here we present results from this experiment and compare to initial simulations of CSR in the magnetic compression chicane of the machine. Finally, we touch upon the possibility for CSR induced microbunching gain in the magnetic compression chicane, and show that parameters in the machine are such that it should be thoroughly damped.

INTRODUCTION

The Jefferson Laboratory energy recovery linac (ERL) IR FEL Driver [1] consists of a superconducting radio frequency (SRF) linac, allowing for CW operation, and a recirculating transport system. This recirculation of the beam back to the linac, after it has passed through the wiggler, allows for recapture of the RF energy before the beam is dumped. The IR FEL can operate at a repetition rate of 75 MHz with a charge per bunch of up to 135 pC and a beam energy of 160 MeV. This gives a very high average power of as much as 14 kW in the 0.9 to 10.5 μm range, from the FEL. ERL operation allows for a much more efficient machine, in terms of RF power required, however, this mode of operation necessitates a layout that allows for the electron bunches to recirculate back to the linac (see Figure 1 for machine layout) raising many challenges with respect to maintaining necessary beam quality and suppressing instabilities. The primary concern of this paper is coherent synchrotron radiation (CSR) which can occur from the passage of very short electron bunches through bending magnets. This effect can cause losses in beam energy and an increase in energy spread from the coherent radiation emission as well as growth in the beam emittance in the bending plane. Understanding and controlling CSR's effect on the electron beam is an important facet to optimizing the performance of an FEL.

* Work supported by the Office of Naval Research and the High Energy Laser Joint Technology. Jefferson Laboratory work also received supported under U.S. DOE Contract No. DE-AC05-06OR23177

OVERVIEW OF RELEVANT BEAM EFFECTS

While there are a number of important effects that must be taken into account for operation of the ERL FEL driver, here, we restrict ourselves to the examination of two that are often interrelated and may cause problems. CSR and microbunching are an important set of collective effects that have been the focus of much attention recently, particularly, in X-ray FELs. CSR is especially a concern in the operation of high average current machines. For the Jefferson Laboratory FEL the power output of CSR has been measured to be around 0.2% which gives about 200 W/mA of CSR; this can produce undesirable heating and cause a measurable rise in vacuum pressure [1]. The microbunching instability has been an important consideration in the design and operation of many recent FELs. However, for the Jefferson Laboratory FEL no signs of the microbunching instability have been observed in measurements. This lack of microbunching gain is supported by calculations shown later in this paper.

CSR

Like incoherent synchrotron radiation (ISR), CSR is produced when the beam experiences acceleration, such as in a bending magnet. When the radiation wavelength is on the order of the bunch length, though, the emission will be coherent. Coherent emission produces a power output that scales as N^2 where N is the number of electrons in the bunch, as opposed to linear scaling with N of ISR. Because of the desire for high peak currents for FEL operation magnetic compression chicanes are commonly employed to reduce bunch length. Because the bunch becomes very short within the chicane, while it is traversing several bending magnets, CSR is always a serious concern in chicanes. The other place where CSR may be a concern, and which is unique to the ERL, is in the two 180 arcs. The effect of CSR when it occurs is the production of a CSR wake that travels from tail to head along the bunch. This wake will cause different changes in energy within different slices along the bunch, increasing the slice energy spread. Because this occurs in a dispersive region this change in energy is coupled to position in the bending plane and may cause a rise in emittance. In addition, there is obviously a net loss in energy from the CSR radiation. In a high average current machine this power loss may be considerable

ISBN 978-3-95450-126-7

SIMPLE SETUPS FOR CARRIER-ENVELOPE-PHASE STABLE SINGLE-CYCLE ATTOSECOND PULSE GENERATION

J. Hebling, G. Almási, J. Fülöp, M. Mechler
MTA-PTE High Field Terahertz Research Group, 7624 Pécs, Hungary
Z. Tibai, Gy. Tóth, Institute of Physics, University of Pécs, 7624 Pécs, Hungary

Abstract

A robust method for producing half-cycle—few-cycle pulses in mid-infrared to extreme ultraviolet spectral ranges is proposed. It is based on coherent undulator radiation of relativistic ultrathin electron layers (nanobunches), which are produced by nanobunching of ultrashort electron bunches by a TW power laser in a modulator undulator. According to our numerical calculations it is possible to generate shorter than 7 nm long nanobunches in this way, where the key points is to use a single-period modulator undulator, rather than a multi-period one, having an undulator parameter of only $K = 0.25$ and a significantly shorter period than the resonant period length. By using these electron nanolayers the production of carrier-envelope-phase stable pulses with up to a few nJ energy and down to 18 nm wavelength and 35 as duration is predicted.

INTRODUCTION

Waveform-controlled few-cycle laser pulses enabled the generation of isolated attosecond pulses and their application to the study of electron dynamics in atoms, molecules, and solids [1]. Intense waveform-controlled extreme ultraviolet (EUV)/X-ray attosecond pulses could enable precision time-resolved studies of core-electron processes by using e.g. pump-probe techniques [2]. Examples are time-resolved imaging of isomerisation dynamics, nonlinear inner-shell interactions, or multi-photon processes of core electrons. EUV pump–EUV probe experiments can be carried out at free-electron lasers (FELs) [3, 4]; however, the temporal resolution is limited to the fs regime and the stochastic pulse shape is disadvantageous. The shortest electromagnetic pulses reported to date, down to a duration of only 67 as, were generated by high-order harmonic generation (HHG) in gas targets [5, 6]. Isolated single-cycle 130-as pulses were generated by HHG using driving pulses with a modulated polarization state [7]. One drawback of gas HHG is the relatively low EUV pulse energy due to the ionization depletion of the medium. The use of long focal length for the IR driving field, or using strong THz fields for HHG enhancement [8] were proposed to increase the EUV pulse energy. The generation of half-cycle 50-as EUV pulses with up to 0.1 mJ energy is predicted for coherent Thomson backscattering from a laser-driven relativistic ultrathin electron layer by irradiating a double-foil target with intense few-cycle laser pulses at oblique incidence [9, 10]. Various schemes, such as the longitudinal space charge amplifier [11, 12], two-color enhanced self-amplified spontaneous emission (SASE) [13, 14], the interaction of an ultrarelativistic electron beam with a few-cycle, intense laser pulse and an intense pulse of the coherent x-rays [15], or ultraviolet laser induced microbunching in electron beams [16] were proposed for attosecond pulse generation at FELs. However, the realization of these technically challenging schemes has yet to be demonstrated and precise waveform control is difficult. In our previous work we proposed a robust method for producing half-cycle–few-cycle pulses in the MIR-EUV spectral range [17, 18]. It is based on coherent undulator radiation of relativistic ultrathin electron layers, which are produced by nanobunching of ultrashort electron bunches by a TW-power laser in a nanobuncher undulator. In this contribution we further examine this method and discuss in more detail the important findings of optimal electron nanobunching in a non-resonant undulator.

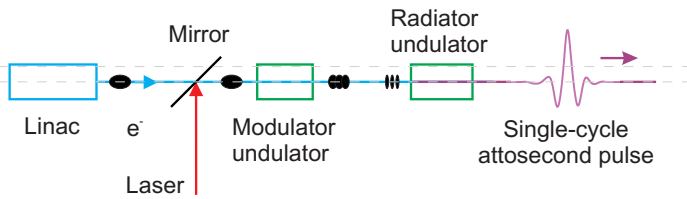

Figure 1: Scheme of the proposed setup.

SIMPLE SETUP

The proposed setup is shown in Fig. 1. The method based on ultrahin electron layer generation and subsequent coherent undulator radiation. A relativistic electron beam, e.g., from a linac is sent through a single-period modulator undulator where a TW-power laser beam is superimposed on it in order to generate nanobunches by inverse free-electron laser (IFEL) action. The nanobunched electron beam then passes through a radiator undulator consisting of a single or a few periods. The radiator undulator is placed at a position behind the modulator undulator where the nanobunch length is shortest.

Efficient ultrashort pulse generation by coherent undulator radiation is possible only if the (micro/nano)bunch length is shorter than the radiation's half period. We note that the previously reported shortest microbunch length was about 800 nm, where the beam of a CO_2 laser was used in the modulator undulator [19].

ISBN 978-3-95450-126-7

QUASIPERIODIC METHOD OF AVERAGING APPLIED TO PLANAR UNDULATOR MOTION EXCITED BY A FIXED TRAVELING WAVE *

K.A. Heinemann†, J.A. Ellison‡,UNM, Albuquerque, NM, USA
M. Vogt§, DESY, Hamburg, Germany

INTRODUCTION

We summarize our mathematical study in [1] on planar motion of energetic electrons moving through a planar dipole undulator, excited by a fixed planar polarized plane wave Maxwell field in the X-Ray FEL regime.

We study the associated 6D Lorentz system as the wavelength of the traveling wave varies. The 6D system is reduced, without approximation, to a 2D system. There are two small parameters in the problem, $1/\gamma_c$, where γ_c is a characteristic energy γ, and ε which is a measure of the energy spread. Using these parameters, the 2D system is then transformed into a system for a scaled energy deviation, χ, and a generalized ponderomotive phase, θ, both of which are slowly varying. When the two small parameters are related the system is in a form for an application of the Method of Averaging (MoA); a rigorous long time perturbation theory which leads to error bounds relating the exact and approximate solutions. As the wavelength varies the system passes through resonant and nonresonant zones and we develop nonresonant and near-to-resonant normal form approximations based on the MoA. For a special initial condition, on resonance, we obtain the well-known FEL pendulum system.

In [1] we prove nonresonant and near-to-resonant first-order averaging theorems, in a novel way, which give optimal error bounds for the approximations. The nonresonant case is an example of quasiperiodic averaging where the small divisor problem enters in the simplest possible way and the near-to-resonant case is an example of periodic averaging. To our knowledge the analysis has not been done with the generality in [1] nor has the standard FEL pendulum system been derived with error bounds. Our main emphasis here is to summarize the derivation of the normal form approximations, discuss their behavior and state in a rough way the results of the error analysis. The FEL pendulum appears on resonance in the near-to-resonant normal form and we discuss the near-to-resonant behavior with phase plane plots.

* Work supported by DOE under DE-FG-99ER41104 and DESY
† heineman@math.unm.edu
‡ ellison@math.unm.edu
§ vogtm@mail.desy.de

GENERAL PLANAR UNDULATOR MODEL

In this section we state the basic problem and put the equations of motion in a standard form for the MoA.

Lorentz Force Equations

The 6D Lorentz equations of motion in SI units with z as the independent variable are

$$\frac{dx}{dz} = \frac{p_x}{p_z}\,, \quad \frac{dy}{dz} = \frac{p_y}{p_z}\,, \quad \frac{dt}{dz} = \frac{m\gamma}{p_z}\,, \tag{1}$$

$$\frac{dp_x}{dz} = -\frac{e}{c}[cB_u\cosh(k_u y)\sin(k_u z) - \frac{p_y}{p_z}cB_u\sinh(k_u y)\cos(k_u z) + E_r(\frac{m\gamma c}{p_z} - 1)h(\check{\alpha}(z,t))]\,, \tag{2}$$

$$\frac{dp_y}{dz} = -\frac{e}{c}\frac{p_x}{p_z}cB_u\sinh(k_u y)\cos(k_u z)\,, \tag{3}$$

$$\frac{dp_z}{dz} = -\frac{e}{c}[-\frac{p_x}{p_z}cB_u\cosh(k_u y)\sin(k_u z) + E_r\frac{p_x}{p_z}h(\check{\alpha}(z,t))]. \tag{4}$$

Here (x, y, z) are Cartesian coordinates, z is the distance along the undulator, $t(z)$ is the arrival time at z, (p_x, p_y, p_z) are Cartesian momenta, $\gamma^2 = 1+\mathbf{p}\cdot\mathbf{p}/m^2c^2$, m is the electron mass, $-e$ is the electron charge and c is the vacuum speed of light.

The planar undulator model magnetic field which we use satisfies the Maxwell equations and is given by

$$\mathbf{B}_u = -B_u \cdot[\cosh(k_u y)\sin(k_u z)\mathbf{e}_y + \sinh(k_u y)\cos(k_u z)\mathbf{e}_z]\,, \tag{5}$$

where $B_u > 0$ is the undulator strength, $k_u > 0$ is the undulator wave number and $\mathbf{e}_x, \mathbf{e}_y, \mathbf{e}_z$ are the standard unit vectors.

The traveling wave radiation field we choose is also a Maxwell field and is given by

$$\mathbf{E}_r = E_r h(\check{\alpha})\mathbf{e}_x\,,$$
$$\mathbf{B}_r = \frac{1}{c}(\mathbf{e}_z\times\mathbf{E}_r) = \frac{E_r}{c}h(\check{\alpha})\mathbf{e}_y\,, \tag{6}$$

ISBN 978-3-95450-126-7

HIGHLY EFFICIENT, HIGH-ENERGY THz PULSES FROM CRYO-COOLED LITHIUM NIOBATE FOR ACCELERATOR AND FEL APPLICATIONS*

Kyung-Han Hong#,[1] Wenqian Ronny Huang,[1] Ravi Koustuban,[1] Shu-Wei Huang,[1] Eduardo Granados,[1] Luis E. Zapata,[1] and Franz X. Kärtner[1,2,3]

[1]Department of Electrical Engineering and Computer Science and Research Laboratory of Electronics, Massachusetts Institute of Technology,
77 Massachusetts Avenue, Cambridge, MA, 02139, USA
[2]Center for Free-Electron Laser Science, DESY, Notkestraße 85, D-22607 Hamburg, Germany
[3]Department of Physics, University of Hamburg, Notkestraße 85, D-22607 Hamburg, Germany

Abstract

Intense, ultrafast terahertz (THz) fields are of great interest for electron acceleration, beam manipulation and measurement, and pump-probe experiments with coherent soft/hard x-ray sources based on free electron lasers (FELs) or inverse Compton scattering sources. Acceleration at THz frequencies has an advantage over RF in terms of accessing high electric-field gradients (>100 MV/cm), while the beam delivery can be treated quasi-optically. In this paper, we present highly efficient, single-cycle, 0.45-THz pulse generation by optical rectification of 1.03-um pulses in cryogenically cooled lithium niobate (LN). Using a near-optimal duration of 680 fs and a pump energy of 1.2 mJ, we report conversion efficiencies above 3%, >10 times higher than previous report (0.24%). Cryogenic cooling of LN significantly reduces the THz absorption, which will enable the scaling of THz pulse energies to the mJ. As a preliminary experiment, we demonstrate low-energy electron acceleration or streaking by THz pulses.

INTRODUCTION

The intense and ultrafast THz fields have many interesting applications, such as THz time-domain spectroscopy, the study of carrier dynamics in semiconductors, electric field gating of interlayer charge transport in superconductors, or THz-assisted attosecond pulse generation [1-3]. More recently, high peak power THz sources have been proposed for acceleration, undulation, deflection and spatiotemporal arbitrary manipulation of charged particles, enabling compact linear accelerators for FEL facilities and inverse Compton scattering X-ray sources. These applications benefit from the scaling the energy and peak power of the THz pulses.

Optical rectification (OR) is one of the common methods for optically pumped THz generation together with difference frequency generation (DFG). In contrast to DFG, OR has been widely used to generate pulses at low THz frequencies [4]. Since the nonlinear process can be cascaded, over 100% of photon conversion efficiency has been demonstrated [5]. Compared to ZnTe, one of the common nonlinear materials used for OR, LN has multiple advantages such as large d_{eff}, high damage threshold, low THz absorption, and large bandgap, but it requires tilted pulse front pumping techniques to achieve phase matching between the IR pump and the THz wave [6]. The highest THz pulse energy that has been reported is still only 0.24%, achieved by pumping a room-temperature LN crystal with 100 mJ, 1.2 ps pulses [7].

Recent theoretical studies have shown that OR in LN can be further improved in terms of efficiency by optimizing the pump pulse duration [8], lowering the distortion produced by the imaging techniques, and reducing the photo-refractive losses in the LN crystal by cooling it down to cryogenic temperatures [9]. The optimum pump pulse duration is found to be ~500 fs because it maximizes the effective length of the nonlinear interaction for THz generation [7]. In addition, maintaining a moderate pumping fluence ensures no saturation of the THz generation process due to three-photon absorption. The maximum efficiency predicted at room temperature is ~2%. Stoichiometric lithium niobate (sLN) is more beneficial for a high efficiency than congruent lithium niobate (cLN), but growing sLN to a large size is limited. In this paper, we demonstrate an efficient THz generation in a cryogenically cooled cLN using a near optimal pump pulse duration of 680 fs.

EXPERIMENTAL SETUP AND RESULTS

The pump laser for OR is a diode-pumped sub-ps Yb:KYW chirped pulse amplification system (s-Pulse, Amplitude Systemes) at 1-kHz repetition rate. The pulses have a center wavelength at 1029 nm with 2.6 nm of spectral bandwidth. The regenerative amplifier was seeded by a mode-locked Yb-doped fiber oscillator [10] followed by a fiber stretcher and pre-amplifier. After the further stretching in a grating stretcher and the regenerative amplification to 2 mJ, the pulses were compressed to 680 fs using a grating compressor. The maximum available energy was 1.2 mJ for the experiments.

*Work supported by DARPA AXiS program under contract number N66001-1-11-4192.
#kyunghan@mit.edu

ISBN 978-3-95450-126-7

CLARA ACCELERATOR DESIGN AND SIMULATIONS

P. H. Williams*, D. Angal-Kalinin, J. A. Clarke, F. Jackson,
J. K. Jones, B. P. M. Liggins, J. W. McKenzie & B. L. Militsyn
STFC Daresbury Laboratory, Sci-Tech Daresbury, UK

Abstract

We present the accelerator design for CLARA (Compact Linear Accelerator for Research and Applications) at Daresbury Laboratory. CLARA will be a testbed for novel FEL configurations. The accelerator will consist of an RF photoinjector, S-band acceleration and transport to 250 MeV including X-band linearisation and magnetic bunch compression. We describe the design of the accelerator. Beam dynamics simulations are then used to define an operating working point suitable for the seeded FEL scheme.

INTRODUCTION

The aims of the CLARA project are presented in an accompanying paper [1] and the recently published conceptual design report [2]. CLARA will build on VELA, a 6 MeV injector currently being commissioned at Daresbury Laboratory. Previously presented work has detailed the RF photocathode gun design, longitudinal phase space linearisation scheme and variable magnetic bunch compressor [3], the diagnostics sections and dogleg for transferring the beam to the seed laser axis [4] and initial studies of tolerance and jitter [5]. In this paper we detail the full machine layout and electron transport including modulator and radiator sections together with full tracking simulations.

LAYOUT

A major aim of CLARA is to be able to test seeded FEL schemes. This places a stringent requirement on the longitudinal properties of the electron bunches, namely that the slice parameters should be nearly constant for a large proportion of the full-width bunch length. In addition, CLARA should have the ability to deliver high peak current bunches for SASE operation and ultra-short pulse generation schemes, such as velocity compressed bunches. This flexibility of delivering tailored pulse profiles will allow a direct comparison of FEL schemes in one facility. An overview of the proposed layout is shown in Fig. 1. The S-band (2998 MHz) RF photocathode gun [6] is followed by linac 1. This is a short ($\sim$ 2 m long) structure, chosen such that it may be used in acceleration or bunching configurations. A spectrometer line which also serves as injection to VELA branches at this location. Linac 2 follows which is $\sim$ 4 m long and capable of accelerating up to 150 MeV. Space for a laser heater is reserved at this point, initially this will not be installed however we expect that in the ultra-short bunch mode the beam properties will be degraded by microbunching instability (predominantly driven by longitudinal space-charge impedance). This effect will be quantified and the case for installing the laser heater determined in the future. A fourth harmonic linearising X-band cavity (11992 MHz) is situated before the magnetic compressor to correct for longitudinal phase space curvature. A variable magnetic bunch compressor is then followed by the first dedicated beam diagnostics section, incorporating transverse deflecting cavity and spectrometer, enabling measurement of emittance, bunch length and slice properties. Linacs 3 & 4 (each $\sim$ 4 m long) accelerate to 250 MeV, these are followed by a second diagnostics section. It has also been proposed to divert this high energy beam for other applications. The beamline then passes a dogleg, offsetting the FELs from the linacs transversely to enable co-propagation of long wavelength laser seeds. Immediately following the dogleg is the energy modulator and phase-space shearing chicane. A dedicated matching section ensures that periodic optics is achievable in the radiators for the entire wavelength range. Seven FEL radiators and a space for a FEL afterburner complete the accelerator and the beam is then dumped.

ELECTRON TRANSPORT

The full machine optics are shown in Fig. 2. Particular care was taken in the FEL section. We require an offset of the FEL transversely from the linacs as we must insert the seed laser co-linearly with the undulator axis. A dogleg was chosen instead of a chicane in order to min-

Table 1: Machine Parameters for Seeded Bunch

Section	Value	Unit
Gun Gradient	100	MV/m
Gun ϕ	-25	°
Linac 1 V	21.0	MeV/m
Linac 1 ϕ	-20	°
Linac 2 V	11.5	MeV/m
Linac 2 ϕ	-31	°
Linac X V	7.3	MeV/m
Linac X ϕ	-168	°
BC θ	95.0	mrad
Linac 3 V	22.5	MeV/m
Linac 3 ϕ	$+0$	°
Linac 4 V	22.5	MeV/m
Linac 4 ϕ	$+0$	°

* peter.williams@stfc.ac.uk

ISBN 978-3-95450-126-7

HIGH POWER LASER TRANSPORT SYSTEM FOR LASER COOLING TO COUNTERACT BACK-BOMBARDMENT HEATING IN MICROWAVE THERMIONIC ELECTRON GUNS*

J.M.D. Kowalczyk†, M.R. Hadmack, J.M.J. Madey, E.B. Szarmes, and M.H.-H.E.H. Vinci,
Department of Physics and Astronomy, University of Hawai'i at Manoa, Honolulu, HI, USA

Abstract

Heat from a high power, short pulse laser deposited on the surface of a thermionic electron gun cathode will diffuse into the bulk producing a surface cooling effect that counteracts the electron back-bombardment (BB) heating intrinsic to the gun. The resulting constant temperature stabilizes the current allowing extension of the gun's peak current and duty cycle. To enable this laser cooling, high power laser pulses must be transported to the high radiation zone of the electron gun, and their transverse profile must be converted from Gaussian to top-hat to uniformly cool the cathode. A fiber optic transport system is simple, inexpensive, and will convert a Gaussian to a top-hat profile. Coupling into the fiber efficiently and without damage is difficult as tight focusing is required at the input and, if coupled in air, the high fluence will cause breakdown of the air resulting in lost energy. We have devised a vacuum fiber coupler (VFC) that allows the focus to occur in vacuum, avoiding the breakdown of air, and have successfully transported 10 ns long, 85 mJ pulses from a 1064 nm Nd:YAG laser through 20 m of 1 mm diameter fiber enabling testing of the laser cooling concept.

INTRODUCTION

A method to counteract back-bombardment (BB) heating in microwave thermionic electron guns [1, 2] is being tested at the University of Hawaii. A fiber optic transport system has been developed to deliver the high energy laser pulses required for laser cooling from the optics lab where the laser and its radiation sensitive electronics reside to the high radiation zone of the electron gun. The fiber is a very simple, flexible, and cost effective means of laser transport and has the additional advantage of converting the quasi-Gaussian input from the Nd:YAG laser used into a near top-hat beam. Most of the system consists of off-the-shelf parts (mirrors, lenses, fiber optic cable), but a special vacuum fiber coupler (VFC) [3] was necessary to couple the high power laser into the fiber without damage. Previous authors have shown that a 50 mm lens system in air with a 'mode scrambler' or a fiber-to-fiber injection method has the ability to transport over 100 mJ, 13.5 ns pulses [4]. These two methods have the effect of more evenly distributing power over the supported optical modes in the fiber to prevent damage; necessary since the input beam's divergence angle is much less than the numerical aperture (NA) of the fiber. Our method employs an short focal length lens focusing the beam in a small vacuum chamber that couples light to the fiber. This has the advantage of utilizing nearly the entire NA of the fiber so the input beam is much less likely to damage the fiber.

* Financial support provided by the U.S. Department of Homeland Security under Federal Grant Identifying # 2011-DN-077-AR1055-03.

† jeremymk@hawaii.edu

DESIGN AND EXPERIMENT

A schematic of the VFC appears in Figure 1 and illustrates the concept. The laser is focused in vacuum to avoid breakdown of the air witnessed at any pulse energies over a couple millijoule. The vacuum level is 65 mTorr and is provided by a rotary vane pump. The vacuum seals for the lens and fiber are made with buna o-rings coated with a thin layer of vacuum grease. The focal plane is initially placed slightly back from input face of the fiber to decrease the laser fluence at the entrance. The input beam to the VFC is a fundamental Nd:YAG at 1064 nm with a quasi-Gaussian TEM_{00} transverse profile with width w =2.15 mm and z_R =13.7 m at the VFC. The shortest focal length lens tested, 8 mm, at the input to the VFC provides a divergence (half) angle $\theta \approx 15^o$ which fills the majority of acceptance (half) angle of 23° of the NA=0.39, 1 mm diameter fiber (Thorlabs part number FT1000EMT). The fabricated VFC is shown in Figure 2.

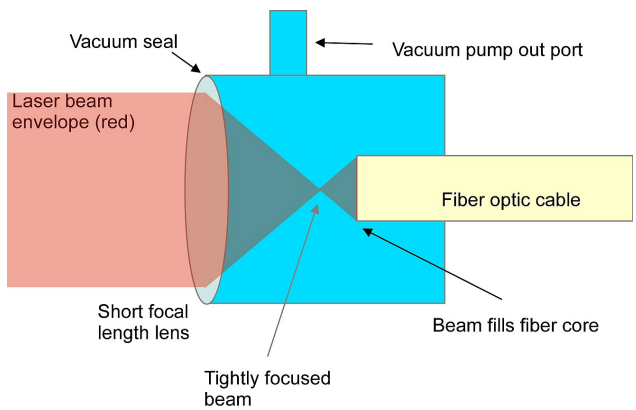

Figure 1: Schematic of the VFC. The laser beam (red) is focused with a short focal length lens sealed to the front of an aluminum (blue) vacuum chamber with ports for vacuum pumping and a vacuum seal to the input fiber optic cable. The input face of the cable is placed such that the beam expands to fill the fiber diameter.

ISBN 978-3-95450-126-7

LASER COOLING TO COUNTERACT BACK-BOMBARDMENT HEATING IN MICROWAVE THERMIONIC ELECTRON GUNS*

J.M.D. Kowalczyk†, M.R. Hadmack, and J.M.J. Madey,
Department of Physics and Astronomy, University of Hawai'i at Manoa, Honolulu, HI, USA

Abstract

A theoretical study of the use of laser cooling to counteract electron back-bombardment heating (BB) in thermionic electron guns is presented. Electron beams with short bunches, minimum energy spread, and maximum length pulse trains are required for many applications, including the inverse-Compton X-ray source being developed at UH. Currently, these three electron beam parameters are limited by BB which causes the cathode temperature and emission current to increase leading to beam loading. Beam loading elongates the bunches by shifting the electrons' relative phases, introduces energy spread by reducing the energy of electrons emitted later in the macropulse, and forces the use of shorter macropulses to minimize energy spread. Irradiation of the electron gun cathode with a short laser pulse prior to beam acceleration allows the laser heat to diffuse into the cathode bulk effectively cooling the surface and counteracting the BB. Calculation of the the cooling produced by laser pulses of various duration and energy is presented.

INTRODUCTION

The principle limitation to the average current delivered by thermionic electron guns is due to back-bombardment heating (BB). Due to the oscillatory nature of the accelerating field in these guns, some electrons that are emitted from the cathode turn around before exiting the accelerating cavity and hit the cathode, increasing its temperature. The temperature increase can be decreased by use of a deflection magnet [1], but cannot be eliminated (our deflection magnet at UH provides a 28% decrease in BB rate [2]). This rise in temperature limits the macropulse length to 5 μs in our gun at UH, similar to other guns [3]. However, if the cathode is maintained at a lower temperature between macropulses (typically by a slow response time heater and feedback circuit) and the surface is heated with a laser just prior application of the RF accelerating voltage, the diffusion of the laser heat from the higher temperature cathode surface into the lower temperature bulk produces cooling of the surface as proposed by Madey [4]. In this work, the cooling effect of various length and energy laser pulses is simulated using a finite difference method (FDM). Results are shown indicating that macropulse lengths up to 23 μs can be achieved with heat from a 7 μs, 300 mJ laser pulse.

* Financial support provided by the U.S. Department of Homeland Security under Federal Grant Identifying # 2011-DN-077-AR1055-03.

† jeremymk@hawaii.edu

SIMULATION

The temperature of the cathode is simulated with the one dimensional heat diffusion equation [5]:

$$\frac{\partial T}{\partial t} = D\frac{\partial^2 T}{\partial z^2} - P_{\text{rad}}/(C_v V) + P_{\text{BB}}/(C_v V), \quad (1)$$

with D the temperature dependent diffusivity from Tanaka [6]. The radiated power, P_{rad}, is non-zero only at the emitting surface (we neglected radiation at the other surfaces as it is small compared to BB due to the small temperature difference between the other surfaces and surrounding) and is defined by:

$$P_{\text{rad}} = \epsilon\sigma A(T^4 - (300K)^4), \quad (2)$$

with ϵ the emissivity of LaB_6 [7], σ Stefan's constant, A the cathode area, C_v the temperature dependent volumetric heat capacity [6], and V the volume. Note that P_{rad} at the surface is also small compared to the BB in all cases except where the cathode surface temperature is brought to high values by short, high energy laser pulses. The BB power, P_{BB}, depends on many parameters include the energy distribution of BB electrons and the cathode material properties (in this case LaB_6) and has been calculated for our gun by McKee [8] at an emission current of 600 mA. Since the emission current changes with temperature according to the Schottky equation,

$$I_{gun} = AA_G T^2 e^{(\phi_{LaB_6} - d\phi)/(k_B T)}, \quad (3)$$

and the number of BB electrons is roughly 30% of the emission current in the narrow temperature range of interest [8], P_{BB} is scaled linearly with emission current. In equation 3, A is the cathode area, ϕ_{LaB_6} is the work function, T is the temperature, and $d\phi = \sqrt{e^3 E/(4\pi\epsilon_o)}$ with E the applied electric field. The value of the work function, ϕ_{LaB_6}=2.43 eV, is determined empirically by fitting measured surface temperature and output current pairs to the Schottky equation with ϕ_{LaB_6} as a free parameter and is in rough agreement with values in the literature [3, 9, 10]. The Richardson constant for LaB_6 is $A_g = 29$ A/(cm^{2}K) [10].

Equation 1 is solved for 1.52 mm long, 1.5 mm radius cylinder with an FDM via:

$$T(n+1,j) - T(n,j) = \frac{D\triangle t}{\triangle z^2}(T(n,j+1) - 2T(n,j) + T(n,j-1)) \quad (4)$$

ISBN 978-3-95450-126-7

NUMERICAL ACCURACY WHEN SOLVING THE FEL EQUATIONS*

R.R. Lindberg †, ANL Advanced Photon Source, Argonne, IL 60439, USA

Abstract

The usual method of numerically solving the FEL equations involves dividing both the e-beam and radiation field into "slices" that are loaded one at a time into memory. This scheme is only first order accurate in the discretization of the ponderomotive phase because having only one slice in memory effectively results in a first order interpolation of the field-particle coupling. While experience has shown that FEL simulations work quite well, the first order accuracy opens the door to two possible ways of speeding up simulation time. First, one can consider higher order algorithms; unfortunately, these methods appear to require all the particle and field data in memory at the same time, and therefore will typically only be important for either small (probably 1D) problems or for parallel simulations run on many processors. Second, one may consistently solve the equations to some low order using faster, simpler algorithms (replacing, for example, the usual RK4). The latter is particularly attractive, although in practice it may be desirable to retain higher order methods when integrating along z. We investigate some of the possibilities.

INTRODUCTION

Numerical simulation of free-electron lasers (FELs) is an integral part of understanding existing FEL devices and planning for future machines. Presently there are several codes (Ginger [1], genesis 1.3 [2], FAST [3], MEDUSA [4], etc.) that have shown remarkable agreement with experimental measurements. While the current FEL algorithms are based on several physical approximations designed to increase their speed and efficiency, certain problems can still require many hours (or even weeks/months) of CPU time. Here we discuss some of the factors that play a role in FEL simulation time, and show an algorithm that can reduce the computational time for certain FEL problems by a factor of two without sacrificing numerical stability or accuracy.

For simplicity, the present paper predominantly restricts itself to treating the FEL equations in 1D, but our general discussion is relevant to the full 3D system. We begin by reviewing some of the numerical algorithms/tricks used to reduce computational time, and show that for time dependent simulations the resulting FEL codes are limited to being first order accurate in the discretization of the ponderomotive phase. Hence, traditional FEL codes at best converge $\sim(\Delta\theta)$. Before more fully discussing time dependence, however, we introduce some of the issues regarding numerical accuracy using the single frequency/time independent equations. We present an explicit algorithm that integrates the FEL interaction while exactly conserving the total (kinetic + field) energy, and compare its performance to more the traditional second and fourth order Runge-Kutta solvers, abbreviated by RK2 and RK4, respectively.

Then, we turn to the fully time dependent equations. Here, we show how to develop a fully second order (in both Δz and $\Delta\theta$) FEL algorithm. However, this method requires that all the particles and field data be simultaneously accessible in memory, and hence is probably only practical for small problems or those run on multiple processors. Furthermore, the accuracy requirements for a typical FEL simulation do not require a fully second order method, and we show that our conservative algorithm is probably sufficient for almost all problems, and is twice as fast as the typical RK4 scheme. Finally, we indicate how our conservative 1D algorithm can be extended to 3D.

NUMERICALLY SOLVING THE 1D FEL EQUATIONS

The longitudinal FEL particle phase space is comprised of the ponderomotive phase $\theta_j \equiv (k_u + k_1)z - ck_1t_j$ and the scaled energy difference (Lorentz factor) $\eta_j \equiv (\gamma_j - \gamma_r)/\gamma_r$. Here, the coordinate z is the distance along the undulator and t_j is the particle time, while $k_u \equiv 2\pi/\lambda_u$ and $k_1 \equiv 2\pi/\lambda_1$ are the undulator and resonant radiation wavevector, respectively, which are related to the reference energy γ_r through the FEL resonance condition $\lambda_1 = \lambda_u(1 + K^2/2)/2\gamma_r^2$ (the undulator deflection parameter $K \equiv eB_0/mck_u$, with B_0 being the peak magnetic field and e, m, c the electron charge magnitude, mass, and the speed of light).

We use the standard Bonifacio-Pelligrini-Narducci scaling for high gain FELs [5], defining the scaled energy, distance, and electric field via $\hat{\eta} \equiv \eta/\rho$, $\hat{z} \equiv 2\rho k_u z$, and $a(\theta,\hat{z}) \equiv [eK[\mathrm{JJ}]/(\rho^2mc^2\gamma_r^2)]E(\theta;\hat{z})$; the dimensionless FEL parameter ρ is given by

$$\rho \equiv \left[\frac{1}{8\pi}\frac{I}{I_A}\left(\frac{K^2[\mathrm{JJ}]}{1+K^2/2}\right)^2\frac{\gamma_r\lambda_1^2}{2\pi\sigma_x^2}\right]^{1/3}, \qquad (1)$$

where I is the peak current, $I_A \equiv 4\pi\epsilon_0 mc^3/e \approx 17$ kA is the Alfvén current, ϵ_0 is the permittivity of free space, σ_x is the rms beam size, and the Bessel function factor $[\mathrm{JJ}] \equiv J_0[K^2/(4+2K^2)] - J_1[K^2/(4+2K^2)]$. We assume

* Work supported by U.S. Dept. of Energy Office of Basic Energy Sciences under Contract No. DE-AC02-06CH11357

† lindberg@aps.anl.gov

ISBN 978-3-95450-126-7

FEASIBILITY OF AN XUV FEL OCILLATOR AT ASTA*

A.H. Lumpkin#, Fermi National Accelerator Laboratory, Batavia, IL USA
H. Freund, Los Alamos National Laboratory, Los Alamos, NM USA
M. Reinsch, Lawrence Berkeley National Laboratory, Berkeley, CA USA

Abstract

The Advanced Superconducting Test Accelerator (ASTA) facility is currently under construction at Fermilab. With a 1-ms macropulse composed of up to 3000 micropulses and with beam energies projected from 45 to 800 MeV, the possibility for an XUV free-electron laser oscillator (FELO) is evaluated. We have used both GINGER with an oscillator module and MEDUSA: OPC codes to assess FELO saturation prospects at 120 nm, 40 nm, and 13.4 nm.

INTRODUCTION

A significant opportunity exists at the Advanced Superconducting Test Accelerator (ASTA) facility [1] presently under construction at Fermilab to enable the *first* extreme ultraviolet (XUV) free-electron laser oscillator (FELO) experiments. The ultrabright beam from the L-band photoinjector will provide sufficient gain to compensate for reduced mirror reflectances in the VUV-XUV regimes, the 3-MHz micropulse repetition rate for 1 ms will support an oscillator configuration, the SCRF linac will provide stable energy, and the eventual GeV-scale energy with three TESLA-type cryomodules will satisfy the FEL resonance condition in the XUV regime. Concepts based on combining such beams with a 5-cm-period undulator of 4.5-m length and with an optical resonator cavity in an FEL oscillator configuration are described. We used the 68% reflectances for normal incidence on multilayer metal mirrors developed at LBNL [2]. Simulations using GINGER [3]with an oscillator module and MEDUSA:OPC [4] show saturation for a 13.4-nm case after 300 and 350 passes, respectively, of the 3000 pulses. Initially, VUV experiments could begin in the 180- to120-nm regime using MgF_2-coated Al mirrors with only one cryomodule installed after the injector linac and beam energies of 250-300 MeV

ASTA FACILITY ASPECTS

The ASTA linac with photocathode (PC) rf gun, two booster L-band SCRF accelerators (CC1 and CC2), and beamline is schematically shown in Fig. 1. The L-band accelerating sections will provide 40- to 50-MeV beams before the chicane, and an additional acceleration capability up to a total of 800 MeV will eventually be installed in the form of three cryomodules after the chicane with eight 9-cell cavities with highest possible average gradient (up to ~31 MV/m). The phase of the CC2 section can be adjusted to energy chirp the beam entering the chicane to vary bunch-length compression. Maximizing the far infrared (FIR) coherent transition radiation (CTR) in a detector after the chicane will be used as the signature of generating the shortest bunch lengths. Micropulse charges of 20 - 3200 pC will be used typically as indicated in Table 1. The nominal micropulse format is 3 MHz for 1 ms.This aspect is unique for test facilities in the USA and highly relevant to the next generation of FELs. The macropulse repetition rate will be 5 Hz.

First photoelectrons were generated in the rf PC gun on June 20, 2013 using a Mo photocathode as a precursor to the planned Cs_2Te photocathode [5]. In this demonstration the gun rf was at partial power at 1.8 MW resulting in an approximate gradient of 35 MV/m and a beam energy of 3.5 MeV exiting the gun. A small suite of diagnostics including the YAG;Ce beam profiling station, resistive wall current monitor, two rf beam position monitors, and a Faraday Cup are in commissioning. The low Q.E. of 2 $x10^{-4}$ with a few μJ of the UV drive laser results in a few pC per micropulse. The Cs_2Te photocathodes with about 1000 times better Q.E. have been prepared and are waiting in the cathode preparation area for the gun rf conditioning to be completed. A photocathode transfer assembly has also been constructed and will allow changing of PCs in situ at the gun. The plans are for completing the 50-MeV linac in FY14 by installing one more booster cavity and the beamline transport to the low-energy dump. One cryomodule is installed and cool down is expected in FY13 with rf power tests first and then beam tests later in FY14.

Table 1: Summary of Planned Electron Beam Properties at ASTA

Parameter	Units	Values
Bunch charge	pC	20-3200
Emittance, norm	mm mrad	1-3
Bunch length, rms	ps	3-1
Micropulse Number		1-3000

lumpkin@fnal.gov
*Work supported under Contract No. DE-AC02-07CH11359 with the United States Department of Energy.

ISBN 978-3-95450-126-7

MEASUREMENT OF WIGNER DISTRIBUTION FUNCTION FOR BEAM CHARACTERIZATION OF FELs*

T. Mey#, B. Schäfer and K. Mann, Laser-Laboratorium e.V., Göttingen, Germany
B. Keitel, S. Kreis, M. Kuhlmann, E. Plönjes and K. Tiedtke, Deutsches Elektronen Synchrotron DESY, Hamburg, Germany

Abstract

Free-electron lasers deliver VUV and soft x-ray pulses with the highest brilliance available and high spatial coherence. Users of such facilities have high demands on phase and coherence properties of the beam, for instance when working with coherent diffractive imaging (CDI).
To gain highly resolved spatial coherence information, we have performed a caustic scan at BL2 of FLASH using the ellipsoidal beam line focusing mirror and a movable XUV sensitive CCD detector. This measurement allows for retrieving the Wigner distribution function, being the two-dimensional Fourier transform of the mutual intensity of the beam. Computing the reconstruction on a four-dimensional grid, this yields the Wigner distribution which describes the beam propagation completely. Hence, we are able to provide comprehensive information about spatial coherence properties of the FLASH beam including the mutual coherence function and the global degree of coherence. Additionally, we derive the beam propagation parameters such as Rayleigh length, waist diameter and the beam quality factor M².

INTRODUCTION

Operating a free-electron laser, detailed knowledge of its beam properties is required by users performing experiments as well as by beam scientists intending to maintain and improve the beam quality. Phase distribution and beam propagation factor M^2 can be retrieved by single shot wavefront measurements [1, 2]. A standard approach to gain information on the coherence properties of the beam is Young's double pinhole experiment [3]. Nevertheless, measuring the entire mutual coherence function $\Gamma(\vec{x},\vec{s})$ is an elaborate task since each single point $(\vec{x},\vec{s})$ in the four-dimensional phase space represents one experiment. For an adequate rasterization, quickly, this exceeds hundreds of thousands of shots.

We follow an alternate strategy to recover $\Gamma(\vec{x},\vec{s})$: measuring the Wigner distribution function (WDF) $h(\vec{x},\vec{u})$ offers access to the mutual coherence function since it is defined as the two-dimensional Fourier transform of the latter [4]. Similarly to measurements with UV lasers and synchrotron sources [5, 6] we have performed a caustic scan at BL2 of FLASH using the ellipsoidal beam line focusing mirror and a movable XUV sensitive CCD detector. For separable beams this is sufficient to completely map out the phase space of the Wigner distribution function [7]. The global degree of coherence is computed from $h(\vec{x},\vec{u})$ directly. A subsequent two-dimensional Fourier back-transform of the WDF yields the mutual coherence function and the coherence length of the beam is retrieved.

In this paper, we briefly summarize the theoretical background of the applied formalism and describe the experimental settings at FLASH. Subsequently, we present the resulting Wigner distribution and mutual coherence function together with the corresponding coherence parameters. Finally, we propose an extended experimental setup which offers an additional degree of freedom allowing an entire mapping of the phase space also for non-separable beams. First results carried out at this setup with several modes of an IR laser are presented proving the performance of the system.

THEORY

The Wigner distribution $h(\vec{x},\vec{u})$ of a quasi-monochromatic paraxial beam is defined in terms of the mutual intensity $\Gamma(\vec{x},\vec{s})$ as a two-dimensional Fourier transform of the latter [8]

$$h(\vec{x},\vec{u}) = \left(\frac{k}{2\pi}\right)\int \Gamma\left(\vec{x}-\frac{\vec{s}}{2},\vec{x}+\frac{\vec{s}}{2}\right)e^{ik\vec{u}\cdot\vec{s}}ds_x ds_y \qquad (1)$$

where $\vec{x}=(x,y)$ and $\vec{s}=(s_x,s_y)$ denote spatial and $\vec{u}=(u,v)$ angular coordinates in a plane perpendicular to the direction of beam propagation and k is the mean wave number of light. As Γ is Hermitian, h is real, although it may become negative in some regions. However, its marginal distributions with respect to $\vec{x}$ and $\vec{u}$ are always non-negative and yield the irradiance (near field) $I(\vec{x})$ and the radiant intensity (far field) $\hat{I}(\vec{u})$, respectively [9].

Propagation of the Wigner distribution through static and lossless paraxial systems, signified by a 4x4 optical ray propagation $ABCD$ matrix S from an input (index i) to an output (index o) plane writes [9, 10]

$$h_i(D\vec{x}-B\vec{u},-C\vec{x}+A\vec{u}) = h_o(\vec{x},\vec{u}). \qquad (2)$$

Likewise, the four-dimensional Fourier transform $\tilde{h}$ of h obeys a similar transformation law under propagation [10]

$$\tilde{h}_i\left(A^T\vec{w}+C^T\vec{t},B^T\vec{w}+D^T\vec{t}\right) = \tilde{h}_o\left(\vec{w},\vec{t}\right), \qquad (3)$$

where $(\vec{w},\vec{t})$ are the Fourier space coordinates corresponding to $(\vec{x},\vec{u})$. Considering a set $\{p\}$ of

*Work supported by Deutsche Forschungsgemeinschaft within Sonderforschungsbereich SFB755 "Nanoscale Photonic Imaging"
#tobias.mey@llg-ev.de

ISBN 978-3-95450-126-7

THE INFLUENCE OF THE MAGNETIC FIELD INHOMOGENEITY ON THE SPONTANEOUS RADIATION AND THE GAIN IN THE PLANE WIGGLER

Koryun B. Oganesyan*, A.I.Alikhanyan National Science Lab, Yerevan, Armenia

Abstract

We calculate the spectral distribution of spontaneous emission and the gain of electronsmoving in plane wiggler with inhomogeneous magnetic field. We show that electrons do complicated motion consisting of slow(strophotron) and fast(undulator) parts. We average the equations of motion over fast undulator part and obtain equations for connected motion. It is shown, that the account of inhomogenity of the magnetic field leads to appearence of additional peaks in the spectral distribution of spontaneous radiation and the gain.

INTRODUCTION

Free-Electron Lasers are powerful, tunable, coherent sources of radiation, which are used in scientific research, plasma heating, condensed matter physics, atomic, molecular and optical physics, biophysics, biochemistry, biomedicine etc. FELs today produce radiation ranging from millimeter waves through to ultraviolet, including parts of the spectrum in which no other intense, tunable sources are available [1], [2]. This field of modern science is interesting from the point of view of fundamental research and very promising for further applications.

Usually FEL [3], [4] use the kinetic energy of relativistic electrons moving through a spatially modulated magnetic field(wiggler) to produce coherent radiation. The frequency of radiation is determined by the energy of electrons, the spatial period of magnetic field and the magnetic field strength of the wiggler. This permits tuning a FEL in a wide range unlike atomic or molecular lasers. In usual FEL magnetic field of wiggler is supposed to be uniform. But really the magnetic field is inhomogeneous in transverse direction(see for example [5]). It is important to take into account this inhomogeneity. This account leads to complex motion of electrons: fast undulator oscillations along the wiggler axis and slow strophotron motion [6], [7], [8], [9], [10], [11] in transverse direction .

In the Sec II we describe the equation of motion of electrons moving along the axis of the wiggler with transversal inhomogeneous magnetic field. In the Sec. III and IV we calculate the spectral distribution of spontaneous emission and the gain correspondingly.

* bsk@yerphi.am

EQUATIONS OF MOTION

The vector potential of undulator's magnetic field has a form [12]

$$\overrightarrow{A_W} = -\frac{H_0}{q_0}\cosh q_0 x \sin q_0 z \;\; \hat{j} \tag{1}$$

where H_0 is the strength of magnetic field and $q_0 = 2\pi/\lambda_0$, λ_0 - period of wiggler, $\hat{j}$ unit vector in y direction.

Corresponding magnetic field is

$$\begin{aligned}\vec{H} &= rot\vec{A} = \hat{i}\left(\frac{\partial A_z}{\partial y} - \frac{\partial A_y}{\partial z}\right) + \hat{j}\left(\frac{\partial A_x}{\partial z} - \frac{\partial A_z}{\partial x}\right) \\ &+ \hat{k}\left(\frac{\partial A_y}{\partial x} - \frac{\partial A_x}{\partial y}\right) = -\hat{i}\frac{\partial A_y}{\partial z} + \hat{k}\frac{\partial A_y}{\partial x} \\ &= \hat{i}H_0 \cosh q_0 x \cos q_0 z - \hat{k}H_0 \sinh q_0 x \sin q_0 z \end{aligned} \tag{2}$$

So

$$H_x = H_0 \cosh q_0 x \cos q_0 z; H_y = 0; \quad H_z = -H_0 \sinh q_0 x \sin q_0 z. \tag{3}$$

These fields satisfy Maxwell's equations $div\vec{H} = 0$ and $\Delta\vec{H} = 0$.

Equations of motion in the fields (3) have a form

$$\begin{aligned}\frac{dp_x}{dt} &= e[\vec{v}\vec{H}]_x = e(v_y H_z - v_z H_y) = ev_y H_z \\ \frac{dp_y}{dt} &= e[\vec{v}\vec{H}]_y = e(v_z H_x - v_x H_z) = ev_z H_x - ev_x H_z \\ \frac{dp_z}{dt} &= e[\vec{v}\vec{H}]_z = e(v_x H_y - v_y H_x) = -ev_y H_x \end{aligned} \tag{4}$$

and change of energy

$$\frac{d\varepsilon}{dt} = 0, \quad \varepsilon = const \tag{5}$$

Further we consider paraxial approximation when

$$q_0 x < 1 \tag{6}$$

Taking into account (6) the magnetic field (2) becomes

$$H_x = H_0\left(1 + \frac{q_0^2 x^2}{2}\right)\cos q_0 z; H_y = 0; \quad H_z = -H_0 q_0 x \sin q_0 z \tag{7}$$

Then we can write equations of motion

ISBN 978-3-95450-126-7

CHANNELED POSITRONS AS A SOURCE OF GAMMA RADIATION

Koryun B. Oganesyan*,
A.I.Alikhanyan National Science Lab, Yerevan, Armenia

Abstract

A possibility of channeling of low-energy ($5 \div 20\, Mev$) relativistic positrons with coaxial symmetry around separate crystal axes of negative ions in some types of crystals, is shown. The annihilation processes of positrons with medium electrons are investigated in details. The lifetime of a positron in the regime of channeling is estimated $10^{-6}\, sec$ which on a $10^9 \div 10^8$ is bigger than at usual cases.

INTRODUCTION

Studying of ways of generation of short-wave coherent radiation always was an essential problem of a science and was stimulated by its wide applied application. In work [1] one of the first the mechanism of radiation of relativistic electrons at their movement in periodic structures (see also [2]) was offered (later such types of structures have been named undulators). It at first sight imperceptible work later has essentially accelerated a process of creation of of modern devices the synchrophasotrons and the lasers on free electrons (see for example review [3]). In spite of the fact that the technology of generation of undulator radiation steadily is being developed and successes are obvious [4], however the problems also are obvious and they remain unresolved up to now. Let's note that the frequency of undulator radiation is being defined by length of its periodic element which in FELs and the undulators devices are macroscopic. Other defects of undulators their big sizes and used big energies of electrons. After opening of channeling of electrons (positrons) in crystals [5–7] and accompanying by its short-wave radiation [8] was appeared a hope to solve all the aforementioned problems. However these hopes up to now is justified only partially. In particular the problems of generation of short-wave radiation (x-ray) from less energetic electrons (of order a several Mev) on very small distances (of order a several micron) have been solved. Now a new problem arise. The point is that in the regime of channeling the particle (electrons and positrons) usually live very short time $\sim 10^{-14} \div 10^{-15}\, sec$. However this time is very short for conversion of a appreciable part of particle energy to energy of radiation. The short lifetime as well doesn't conduce to use of external factors for control by beam of channeling particles and to improving of spectral characteristics of radiation.

The quantum theory of channeling for electrons and positrons has been elaborated by many authors [8–10]. It is important to note that an electron in a crystal can commit both planar and axial channeling. At the same time only one type of real channeling for the positrons is known, the regime where a particle is localized between two adjacent planes. The possibility of axial channeling of positive particles has not been investigated, seriously up to now, because the crystallographic axes, irrespective of grade of crystal are been charged positively. However investigation of possibilities of axial channeling of positrons and, hence, the formation of metastable relativistic positron systems (PS) is a problem of utmost importance for a radiation physics.

In earlier studies [11] we investigated the possibilities of ionic crystals of type $CsCl$ and have shown that at channeling of positrons around the axises of negatively charged ions Cl^- the main factor of de-channeling the scattering of particles on phonons subsystem is absent. However such channels for positrons, as shows an analysis there are and in other more realistic crystals, for example in crystal SiO_2.

In this work a role of different processes (scattering of positron on media electrons, the annihilation processes etc) in the expansion of energy levels of relativistic PS is analyzed and shown that PSs are metastable.

FORMATION OF RELATIVISTIC POSITRON SYSTEM (PS)

In previous work [12] we have shown, that if a low-energy relativistic positrons ($5 \div 20\, Mev$) are scattering under a small corners $\vartheta \leq \vartheta_L$ (where ϑ_L is a Lindhard angle) on the axis $\langle 100 \rangle$ of chlorine ions Cl^- that they fall into regime of axial channeling. Moreover the motions of positrons concentrate between two cylinders that is very important from the point of view of movement stability. In particular, as was shown the effective $2D$ potential of channeling don't depend from temperature of media in a broad range of temperatures and has an order $-10\, eV$ depths of potential which is sufficient for formation a several quantum states of transverse motion. Recall that this type of effective potential can be in other crystals too. For example the effective potential of negatively charged ions O_2 axes often used in experiments of crystal SiO_2 is such.

In other words, the relativistic positrons in described regime of channeling don't interact with phonons subsystem. That means a main factor of de-channeling of particles in considered case is absent.

Taking into account the symmetry of effective potential for positrons around of the negative ions axis we can write the following analytical formula:

$$U_0(\rho) \quad = \quad D_0(e^{-2\alpha\overline{\rho}} - 2e^{-\alpha\overline{\rho}}), \overline{\rho} = (\rho - \rho_0)/\rho_0,$$

* bsk@yerphi.am

ISBN 978-3-95450-126-7

MODULATED MEDIUM FOR GENERATION OF TRANSITION RADIATION

Koryun B. Oganesyan*, A.I.Alikhanyan National Science Lab, Yerevan, Armenia

Abstract

It is shown on an example of amorphous quartz, under the influence of a standing microwave field, at its certain parameters, superlattice is created in the medium where difference in values of dielectric constants of neighboring layers can be up to third order. This superlattice exists during the nanosecond, however it is sufficient for using it as a radiator for generation of transition radiation by relativistic electrons.

INTRODUCTION

The formation and governing of periodically modulated refractive index in media is a most important problem of solid state physics and material science. First of all it is related to the possibility of developing compact UV or X-ray Free-Electron Lasers (FEL) based on emission of transition radiation (TR) (see for example [1]). Currently the following two problems are discussed intensely:

1. A gas-plasma medium with periodically varied ionization density [2–9],

2. A special periodical solid-state superlattice-like (SSL) structures composed of layers with different refraction indexes [10–20].

TR is generated due to the difference in frequency-dependent dielectric constants (permittivity functions) of adjacent layers (remember that the radiation power is proportional to $[\epsilon_1^R(w) - \epsilon_2^R(w)]^2$, where $\epsilon_{1;2}^R(w) = Re[\epsilon_{1;2}(w)]$) [21]. Therefore, the possibility of controlling this difference by means of an external field is highly important. In other words, the problem here is to construct a superlattice with difference in dielectric constants of neighboring domains having the form $[\epsilon_1^R(w,\mathbf{g}) - \epsilon_2^R(w,\mathbf{g})]^2$, where $\mathbf{g}$ describes the controlling parameters, $\epsilon_1(w,\mathbf{g})$ and $\epsilon_2(w,\mathbf{g})$ are dielectric permittivity functions in neighboring regions. According to theoretical and experimental studies, the periodical structures may be formed in condensed matter by means of external electromagnetic or acoustic fields [22–25].

This idea was recently realized in TR generation experiments [26]. In particular, it was shown that at the passage of a beam of 20 Mev electrons through amorphous silicon dioxide $a - SiO_2$ with a standing electromagnetic wave (of 10 GHz frequency) inside, anomalous high short-wave radiation was produced. Preliminary studies explain this high intensity radiation as a result of multiple passage of the electron beam through interfaces between regions with different permittivity functions. Theoretically the appearance of $1D$ superlattice order in random media is explained by the polarization of media due to the orientational relaxation of elastic dipoles in the direction of external electromagnetic field propagation [27].

So, the main objective of this work is a systematic investigation of relaxation processes and critical effects in $a - SiO_2$ compound type disordered $3D$ systems under the action of external electromagnetic field that forms a standing wave in the medium, and in particular, to prove the possibility of formation of $1D$ periodic superlattice of permittivity function in the scales of space-time periods of standing wave.

FORMULATION OF THE PROBLEM

The starting point in our discussion will be the Clausius-Mossotti relation for dielectric constant. It is known that in isotropic media (as well as in crystals of cubic symmetry) the dielectric constant is well described by the Clausius-Mossotti equation [28–30]:

$$\frac{\epsilon_s - 1}{\epsilon_s + 2} = \frac{4\pi}{3}\sum_m N_m^0 \alpha_m^0, \qquad (1)$$

where N_m^0 is the concentration of particles (electrons, atoms, ions, molecules) with given m types of polarizability and α_m^0 correspondingly are polarizability coefficients. It follows from this formula that the static dielectric constant ϵ_s depends on the polarizability properties of particles as well as on their topological order. In the external field the homogeneity and isotropy of the medium is often lost. Then, it is expected that the formula (1) will be applicable after slight generalization.

The object of our investigation are solid state dielectrics of the amorphous silicon dioxide $a-SiO_2$ type. According to numerical $ab\ initio$ simulations [31], the structure of this type compound may be well described by the model of $3D$ disordered spin system.

In particular the $3D$ spin system we can represent as a $3D$ lattice with the lattice's constant $d_0(T) = \{m_0/\rho_0(T)\}^{1/3}$, where m_0 is the molecule mass, ρ_0 is the density and T is the temperature. We will assume also, that in each cell of this lattice there are only one randomly distributed spin (roughly polarized molecule).

We will suppose that the media under the influence of external standing electromagnetic field the electrical part

* bsk@yerphi.am

ISBN 978-3-95450-126-7

SUPPRESSION OF WAKEFIELD INDUCED ENERGY SPREAD INSIDE AN UNDULATOR THROUGH CURRENT SHAPING *

J. Qiang† and C.E. Mitchell, LBNL, Berkeley, CA 94720, USA

Abstract

Wakefields from resistive wall effects inside an undulator can cause significant growth of the beam energy spread and limit the performance of x-ray FEL radiation. In this paper, we propose a method to mitigate such wakefield-induced energy spread by appropriately conditioning the electron beam current profile. Numerical examples and potential applications will also be discussed.

INTRODUCTION

Wakefields such as the resistive wall wakefield and the surface roughness wakefield inside an undulator can cause significant electron beam energy loss and energy spread growth. Such energy loss inside an undulator can heat the vacuum pipe and also induce energy variation along the bunch length that will limit the performance of the undulator and the quality of the final FEL radiation. For a seeded FEL, such energy variation will increase the bandwidth of the radiation. If the relative energy variation inside the beam is larger than the FEL Pierce parameter, the coherent radiation from part of the beam can even be suppressed. In previous studies, the relative energy change due to the resistive wall wakefield was calculated for a room-temperature normal conducting LCLS undulator using a double-horn beam distribution from the LCLS linac [1]. The resistive wall heating of the undulator from the wakefield was also calculated for a high repetition rate FEL [2]. In this paper, we report on a method to suppress the energy variation along the bunch length induced by the resistive wall wakefield inside an undulator through longitudinal current profile shaping. A similar method was previously proposed to suppress the emittance growth driven by coherent synchrotron radiation inside a bunch compressor chicane [3].

The total wakefield-induced energy loss per meter from a single bunch of the electron beam inside an undulator is given by

$$E_{tot} = \int_{-\infty}^{\infty} E_w(z)\rho(z)dz \quad (1)$$

where

$$E_w(z) = \int_{-\infty}^{z} w(z-z')\rho(z')dz'. \quad (2)$$

Here $w(z)$ is the single-particle wake function for an electron inside the undulator, z and z' denote the electron longitudinal coordinate with respect to the head of the beam (on the left), $\rho(z)$ is the electron longitudinal line charge density, $E_w(z)$ is the energy loss per meter per Coulomb along the beam, and E_{tot} is the total energy loss per meter of the electron bunch. The power loss to the vacuum pipe per meter for a high repetition light source is given by the product of the repetition rate and the single bunch total energy loss (1). The rms energy spread per meter of the beam induced by such energy loss is given by

$$E_{rms} = \sqrt{\int_{-\infty}^{\infty} (E_w(z) - E_{tot})^2 \rho(z) dz} \quad (3)$$

The single-particle wake function used in (2) is related to the impedance [1] by

$$w(z) = \frac{2c}{\pi} \int_{-\infty}^{\infty} Re(Z(k)) \cos(kz) dz \quad (4)$$

where $Re(Z(k))$ denotes the real part of the resistive wall impedance Z inside the undulator and c is the speed of light in vacuum.

CONTROL OF ENERGY MODULATION INDUCED BY WAKEFIELD THROUGH CURRENT PROFILE SHAPING

For a given current profile, the wakefield-induced energy loss along the beam can be calculated using (2). This equation can also be used to control the energy variation along the beam by choosing an appropriate longitudinal current profile. For a given single-particle wake function w and a desired wakefield E_w, (2) defines an integral equation for the current profile ρ. Such an integral equation can be solved analytically or numerically for the desired current profile.

First, we consider the case when the resistive wall wake function can be approximated by an analytical resonator wake function of the form [1]:

$$w(z) = \frac{1}{\pi\epsilon_0 a^2} \exp(-z/\sigma_l) \cos(\omega z) \quad (5)$$

where $\sigma_l = 4c\tau$, $\omega = \sqrt{2k_p/a}$, $k_p = \sqrt{Z_0\sigma/(c\tau)}$, τ is the pipe material relaxation time, σ is the pipe material DC conductance, a is the pipe radius, Z_0 is the vacuum impedance, c is the speed of light in vacuum, and ϵ_0 is the vacuum permittivity. To induce a uniform (step function) energy loss along the beam, with the above resonator wake function, the electron line density distribution can be obtained by solving the integral equation (2) using a Laplace transform method. The resulting density distribution is

$$\rho(z) = \rho_0[\delta(z) + \frac{H(z)}{\sigma_l} + \sigma_l\omega^2(1 - e^{-z/\sigma_l})H(z)] \quad (6)$$

* Work supported by the U.S. Department of Energy under Contract No. DE-AC02-05CH11231 using computing resources at the NERSC.

† jqiang@lbl.gov

ISBN 978-3-95450-126-7

START-TO-END SIMULATION OF A NEXT GENERATION LIGHT SOURCE USING THE REAL NUMBER OF ELECTRONS*

J. Qiang† J. Corlett, P. Emma, C.E. Mitchell, C.F. Papadopoulos, G. Penn, M. Reinsch, R.D. Ryne, M. Venturini, LBNL, USA
S. Reiche, PSI, Switzerland

Abstract

Start-to-end simulation plays an important role in the design and optimization of next generation light sources. In this paper, we will present start-to-end (from the photocathode to the end of the undulator) simulations of a high repetition rate FEL-based Next Generation Light Source driven by a CW superconducting linac with the real number of electrons (∼2 billion electrons/bunch) using the multi-physics parallel beam dynamics code IMPACT. We will discuss the challenges, numerical methods and physical models used in the simulation. We will also present simulation results of a beam transporting through the photoinjector, the beam delivery system, and the final X-ray FEL radiation.

INTRODUCTION

Next generation x-ray light sources provide an important tool for scientific discovery in biology, chemistry, physics, and material science. A high repetition rate, soft x-ray free electron laser (FEL), Next Generation Light Source is being studied at LBNL [1]. High resolution start-to-end macroparticle simulation is an important tool for evaluating and optimizing the design of the light source. For example, a microbunching instability starting from the electron shot noise or initial laser temporal fluctuations can significantly degrade the electron beam quality at the end of the accelerator beam delivery system and lower the resulting performance of the FEL x-ray radiation. Accurate modeling of the microbunching instability with a large number of macroparticles will help to determine the final electron beam properties for generating x-ray radiation. For a given number of macroparticles, N_{mp}, the shot noise in the simulation can be artificially magnified by a factor of $\sqrt{N/N_{mp}}$, where N is the real number of electrons. In previous studies, a low pass filter was proposed to suppress the numerical noise associated with the use of a small number of macroparticles in comparison with the real number of electrons [2]. Applying such a low pass filter does not completely suppress the artificial numerical noise in our simulations. Figure 1 shows the final uncorrelated energy spread at the exit of a beam delivery system using direct sampling of 1 billion macroparticles, 100 million macroparticle sampling with a low pass filter (c1=0.2, c2=0.25) from [2], with a low pass filter (c1=0.03, c2=0.167) and with a low pass filter (c1=0.125, c2 = 0.167). It is seen that even with the use of the low pass filter and with different choices of filter parameters, the 100 million macroparticle simulations still predict larger energy modulation than the one-billion macroparticle simulation. In order to understand these effects, we use an FFT to calculate the difference between the Fourier coefficients of an analytical Gaussian function and a randomly sampled Gaussian function using 10 thousand, 100 thousand, one million, and 10 million macroparticles. The results as a function of the mode number (proportional to the wave number of the input) are shown in Fig. 2. It is seen that the sampled shot noise amplitude goes down with the use of a larger number of macroparticles. Sampling using a small number of macroparticles over-estimates the level of shot noise through the whole frequency domain, not just in the high frequency region. A low pass filter helps to suppress the high frequency numerical noise as-

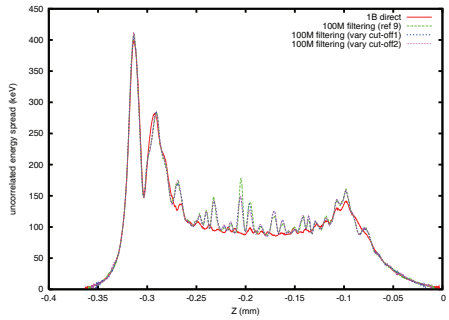

Figure 1: Final uncorrelated energy spread using 1 billion macroparticle direct sampling (red), using 100 million macroparticle sampling with the low pass filter from [2] (c1=0.2, c2=0.25) (green), with a low pass filter and c1=0.03, c2=0.167 (blue), and with a low pass filter and c1=0.125, c2 = 0.167 (pink).

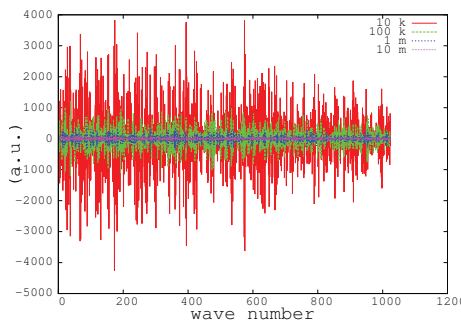

Figure 2: Fourier Coefficient Differences from the FFT of an Analytical Gaussian Function and a Sampled Gaussian Function with 10k, 100k, 1M and 10M Macroparticles.

* Work supported by the U.S. Department of Energy under Contract No. DE-AC02-05CH11231 using computing resources at the NERSC.
† jqiang@lbl.gov

ISBN 978-3-95450-126-7

FREE-ELECTRON LASERS DRIVEN BY LASER-PLASMA ACCELERATORS USING DECOMPRESSION OR DISPERSION*

C.B. Schroeder, E. Esarey, W.P. Leemans, J. van Tilborg, LBNL, Berkeley, CA 94720, USA
F.J. Grüner, A.R. Maier, CFEL, 22607 Hamburg, Germany
Y. Ding, Z. Huang, SLAC, Menlo Park, CA 94025, USA

Abstract

Laser-plasma accelerators (LPAs) are a compact source of fs electron beams with kA peak current and low (submicron) transverse emittance. Presently, the energy spread (percent-level) hinders the free-electron laser (FEL) application. Given experimentally-demonstrated LPA electron beam parameters, we discuss methods of beam phase space manipulation after the LPA to achieve FEL lasing. Decompression is examined as a solution to reduce the slice energy spread. Beam dispersion, coupled to a transverse gradient undulator (TGU), is also discussed as a path to enable LPA-driven FELs. Using a TGU has several advantages, including maintaining the ultrashort LPA bunch length, radiation wavelength stabilization, and higher saturation power.

INTRODUCTION

Laser-plasma accelerators (LPAs) have the ability to generate ultra-high accelerating gradients, several orders of magnitude larger than conventional RF accelerators. Laser-plasma acceleration is realized by using a high-intensity laser to ponderomotively drive a large plasma wave (or wakefield) in an underdense plasma [1]. The plasma wave has relativistic phase velocity, and can support large electric fields in the direction of the laser propagation. When the laser pulse is approximately resonant (pulse duration on the order of the plasma period) and the laser intensity is relativistic, with normalized laser vector potential $a = eA/m_e c^2 \sim 1$, the size of the accelerating field supported by the plasma is on the order of $E_0 = m_e c\omega_p/e$, or $E_0[\mathrm{V/m}] \simeq 96\sqrt{n_0[\mathrm{cm}^{-3}]}$, where $\omega_p = k_p c = (4\pi n_0 e^2/m_e)^{1/2}$ is the electron plasma frequency, n_0 is the ambient electron number density, m_e and e are the electronic mass and charge, respectively, and c is the speed of light in vacuum. For example, an accelerating gradient of $\sim$100 GV/m is achieved operating at a plasma density of $n_0 \sim 10^{18}$ cm^{-3}. Owing to these ultra-high accelerating gradients, LPAs are actively being researched as ultra-compact sources of energetic electron beams for a variety of applications. Electron beams up to $\sim$1 GeV have been experimentally demonstrated using high-intensity lasers interacting in centimeter-scale plasmas [2]. These LPA electron beams contain tens of pC of charge, percent-level relative energy spread, and have ultra-low normalized transverse emittances $\epsilon_n \sim 0.1$ mm rad [3, 4]. In addition to extremely large accelerating gradients, plasma-based accelerators intrinsically produce ultra-short (fs) electron bunches with bunch lengths that are a fraction of the plasma wavelength [5, 6]. Because of the short beam durations, LPAs are sources of high peak current beams ($\sim$1–10 kA), and, hence, it is natural to consider LPA electron beams as drivers for a compact free-electron laser (FEL) producing high-peak brightness radiation [7–14]. LPA electron beams have been coupled into magnetostatic undulators to produce spontaneous radiation in the visible [15] and soft-x-ray [16] wavelengths.

Presently, the FEL application is hindered by the relatively large energy spread (few percent) of the LPA electron beam. LPA research has focused on methods to provide detailed control of the injection of background plasma electrons into the plasma wave, thereby controlling the LPA beam phase space characteristics and to improve the shot-to-shot stability and tunability of the beam parameters [17–19]. Although LPA beam phase space properties continue to improve, application of FEL beams may be accomplished using present experimentally-demonstrated LPA electron beam properties. In this paper we discuss post-LPA beam phase-space manipulation (i.e., beam decompression [11, 13] or dispersion [14]) to enable lasing of the LPA-driven FEL.

BEAM MANIPULATION FOR GAIN LENGTH REDUCTION

The fundamental resonant wavelength emitted in the FEL is $\lambda = \lambda_u(1 + K^2/2)/(2\gamma^2)$, where λ_u is the undulator wavelength and K is the undulator strength parameter. The ideal (with diffraction, energy spread, space charge, and emittance effects neglected) gain length (e-folding length of the fundamental radiation power) is [20]

$$L_{g0} = \lambda_u/(4\pi\sqrt{3}\rho), \tag{1}$$

where ρ is the FEL parameter

$$\rho = \frac{1}{4\gamma}\left[\frac{I}{I_\mathrm{A}}\left(\frac{K[JJ]\lambda_u}{\pi\sigma_x}\right)^2\right]^{1/3}, \tag{2}$$

with σ_x the average rms beam transverse size (assuming a round beam $\sigma_x = \sigma_y$), I the peak beam current, $I_A = m_e c^3/e \approx 17$ kA is the Alfvén current, $[JJ] = [J_0(\chi) - J_1(\chi)]$ (planar undulator), $\chi = K^2(4 + 2K^2)^{-1}$, and J_m are Bessel functions.

* Work supported by the Director, Office of Science, of the U.S. Department of Energy under Contract Nos. DE-AC02-05CH11231 and DE-AC02-76SF00515.

ISBN 978-3-95450-126-7

CRYSTAL CHANNELING ACCELERATION RESEARCH FOR HIGH ENERGY LINEAR COLLIDER AT ASTA FACILITY

[1, 2]Young-Min Shin, [2]Jayakar C. Tobin, [2]Dean A. Still, [2]Kermit Carlson, [2]Michael Church, and [2]Vladimir Shiltsev

[1]Department of Physics, Northern Illinois University, Dekalb, IL, 60115, USA

[2]Fermi National Accelerator Laboratory (FNAL), Batavia, IL 60510, USA

Abstract

Crystal channeling technology has offered various opportunities in accelerator community with a viability of ultrahigh gradient (TV/m) acceleration for future HEP collider in Energy Frontier. The major challenge of the channeling acceleration is that ultimate acceleration gradients might require relativistic intensities at hard x-ray regime (~ 40 keV), exceeding those conceivable for x-rays as of today, though x-ray lasers can efficiently excite solid plasma and accelerate particles inside a crystal channel. Moreover, only disposable crystal accelerators are possible at such high externally excited fields which would exceed the ionization thresholds destroying the atomic structure, so acceleration will take place only in a short time before full dissociation of the lattice. Carbon-based nanostructures have great potential with a wide range of flexibility and superior physical strength, which can be applied to channeling acceleration. This paper present beam-driven channeling acceleration concept with CNTs and discuss feasible experiments with the Advanced Superconducting Test Area (ASTA) in Fermilab and beyond.

INTRODUCTION

The cost models of the modern colliders are quite complicated, but one may safely assume that a future facility should not exceed a few tens of km in length and simultaneously require less than 10 to a few tens of MW of beam. To get to the energies of interest within the given footprint, fast particle acceleration is inevitable. Plasma-wakefield acceleration (PWA) has become of great interest because of the promise to offer extremely large acceleration gradients, on the order of $E_0 \approx n_0^{1/2}$ [GeV/m], where n_0 is the ambient electron number density (n_0 [10^{18}cm^{-3}]), on the order of 30-100 GV/m at plasma densities of $n_0 = 10^{17} - 10^{18}$ cm^{-3}.[1] The density of charge carriers (conduction electrons) in solids $n_0 = \sim 10^{20} - 10^{23}$ cm^{-3} is significantly higher than what was considered above in plasma, and correspondingly, wakefields of up to 100 GeV/cm or 10 TV/m are possible. In the solid plasma, as escaping from a driving field due to fast pitch-angle diffusion resulting from increased scattering rates, particles must be accelerated along major crystallographic directions. This is called "channeling acceleration". Normally, crystal channeling has been applied to high energy beam control such as collimation, bending, and refraction [2]. For high energy beam optics, carbon nanotubes (CNTs) have been considered for bending and collimation [3,4,5]on account of the much wider range of flexibility, including superior physical strength, which also ideally fits with channeling acceleration. CNTs, composed of graphene sheets rolled into seamless hollow cylinders with diameters ranging from 1nm to about sub-micron, exhibit unique physical and chemical properties as a quasi-one dimensional material[6 ,7,8,9]. In principle, both straight and bent CNTs can effectively be used for high-energy particle channeling [10], provided the technological challenge of achieving an almost perfect alignment of CNTs with respect to the beam direction could be tackled effectively in the synthesis of samples.

Recently, Fermilab built the Advanced Superconducting Test Accelerator (ASTA) facility (50 MeV and several hundreds of MeV energy beams) that will enable a broad range of electron beam-based experiments to study fundamental limitations to beam intensity and to developing transformative approaches to particle-beam generation, acceleration and manipulation, which is ideally suited for the channeling acceleration experiment. We plan to detect a measurable energy gain from the electron bunches passing through CNTs. Successful demonstration of the experiment with this beam driven method will verify the viability of CNT channeling interaction for ultra-high gradient acceleration, which will also prove the feasibility of the laser-driven channeling acceleration. The experimental setup will be accommodated to a 50 MeV main stream beamline and high energy (50 – 300 MeV) beamline in our plan. In the research, beam energies and radiation spectra of CNT samples will be mainly characterized by beam tests at relativistic regimes.

CHANNELING ACCELERATION

Plasma acceleration provides the highest acceleration gradient ($E_0 = m_e c \omega_p / e \approx 100 \times n_0^{1/2}$ [GeV/m], where n_0 is the ambient plasma density (n_0 [10^{18}cm^{-3}]), corresponding to 30 – 100 GV/m. The density of charge carriers (conduction electrons, $n_0 \sim 10^{20-23}$ cm^{-3}) in solid media is 3 ~ 5 orders of magnitude higher than those in gaseous plasma, so in principle, a wakefield of 0.3 – 30 TeV/m can be created in crystals, which consists of the longitudinal component, $\varepsilon_z \approx - 8eN/a^2(1 - r^2/a^2)\cos(kz - \omega_p t)$, for acceleration and a transverse component, $\varepsilon_z \approx - 16eN/a^2(r/ka^2)\sin(kz - \omega_p t)$, for beam focusing ($N$: the number of electrons and a : the beam spot size).

ISBN 978-3-95450-126-7

SURFACE ROUGHNESS WAKEFIELD IN FEL UNDULATOR*

G. Stupakov
SLAC National Accelerator Laboratory, Menlo Park, CA, USA
S. Reiche
Paul Scherrer Institute, Villigen-PSI, Switzerland

Abstract

We derive wakefield of a round pipe with a sinusoidal wall modulation and use this model for study of wakefields due to wall roughness of the undulator vacuum chamber of free electron lasers.

INTRODUCTION

In free electron lasers the wakefield due to the wall roughness of the vacuum chamber in the undulator can have important implications on the required smoothness of the beam tube. Detailed theoretical studies of the roughness induced impedance has been carried out in the past [1–4] and provided a useful tool for computation of the wakes and practical recommendations for the undulator vacuum chamber design.

Among several wakefield models a simple sinusoidal wall modulation with a small ratio of height to wavelength is especially attractive because of its simplicity [5]. The model neglects a so called resonant mode wakefield [6, 7] because, as it was shown in [8], the contribution of the resonant mode is small for a shallow wall perturbation. The wake derived in [5] has a singularity at the origin and shows a typical resistive behavior. While the wake singularity is integrable, and applied to a smooth beam profile gives a finite wakefield, it requires a special care in implementation of the numerical algorithm. In addition, for some idealized beam profiles, such as flat-top, the resulting bunch wake exhibits non-physical singularities at the beam edges.

In this paper we generalize the result of [5] to include the effect of the resonant mode. As it turns out this also eliminates the wake singularity at the origin and facilitates numerical calculations of wakes.

SINUSOIDAL WALL MODULATION

We consider a round pipe of radius a and represent the roughness profile of the wall by a sinusoidal perturbation

$$r = a - h\sin\kappa z, \tag{1}$$

where $2\pi/\kappa$ is the period of corrugation, and h is its amplitude. It is assumed that both the wavelength and the amplitude are small compared to the pipe radius, $h \ll a$ and $\kappa a \ll 1$. This allows one to neglect in calculations the curvature of the round wall and to consider the surface locally as a plane one. It is also assumed that the corrugation is shallow,

$$h\kappa \ll 1, \tag{2}$$

that is the amplitude of the corrugation bumps is much smaller then their period.

Using the perturbation theory developed in [1], the following expression for the wakefield (per unit length of pipe) of a point charge was obtained in [5]

$$w(s) = \frac{h^2\kappa^3}{a} f(\kappa s), \tag{3}$$

where the function f is

$$f(\zeta) = \frac{1}{2\sqrt{\pi}}\frac{\partial}{\partial\zeta}\frac{\cos(\zeta/2)+\sin(\zeta/2)}{\sqrt{\zeta}}, \tag{4}$$

for $\zeta > 0$ and $f = 0$ otherwise. The wake function in (3) is defined so that positive w corresponds to the energy loss, and positive s corresponds to the test particle behind the source one. The plot of this function is shown in Fig. 1. One can see that $f(\zeta)$ has a singularity at the origin, $f \propto \zeta^{-3/2}$, similar to the resistive wall wake in a round pipe in the standard approximation [9] of long wavelengths. The negative sign of the wake (3) near the origin seems to suggest that the source charge gains energy in the process of interaction with the wall. This conclusion however is incorrect as we will see below.

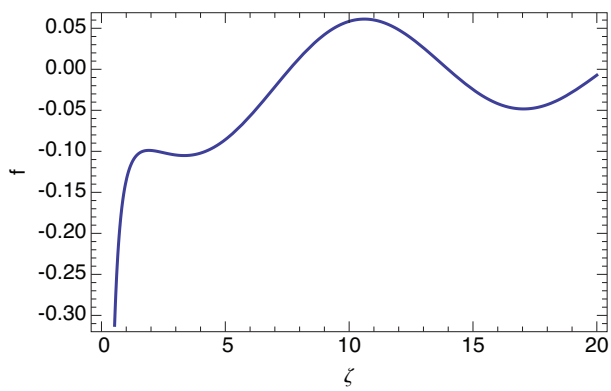

Figure 1: Function $f(\zeta)$.

In a seemingly different approach to the problem, using the concept of surface impedance of the sinusoidal corrugation (1), an expression for the beam longitudinal impedance

* Work supported by the U.S. Department of Energy under contracts No. DE-AC02-76SF00515.

ISBN 978-3-95450-126-7

REEVALUATION OF COHERENT ELECTRON COOLING GAIN FACTOR*

G. Stupakov
SLAC National Accelerator Laboratory, Menlo Park, CA 94025, USA
M. S. Zolotorev
Center for Beam Physics, Lawrence Berkeley National Laboratory, Berkeley, CA 94720, USA

Abstract

An important element in the concept of coherent electron cooling [1] is amplification of the electric field induced by a point charge in an electron beam passing through an FEL amplifier. We calculate this factor in 1D FEL theory and show that it is equal to the conventional FEL gain (for the field) multiplied by the relative bandwidth of the FEL amplifier, which is typically a small parameter of the order of 10^{-3}. The obtained amplification factor is more than two orders smaller than quoted in Ref. [1]. We also discuss the recent reply [2] of the authors of [1] to our comment [3] and show that critical remarks in the reply with regard to the comment are unjustified.

INTRODUCTION

In Ref. [1] the authors put forward a concept of coherent electron cooling of hadrons. At the core of the concept lies the following idea: a density perturbation induced by an hadron in a co-propagating electron beam is amplified by several orders of magnitude in a free electron laser (FEL). After the FEL the electron beam is merged again with the hadron one and the amplified electric field in the electron beam acts back on each hadron resulting, after many repetitions, in a cooling of the hadron beam. The efficiency of the process is critically determined by the amplification factor of the longitudinal electric field induced by the hadron in the electron beam. The authors associate this amplification with the FEL gain factor. In this note we show that it is actually considerably smaller than the (conventionally defined) FEL gain with the smallness parameter to be the relative bandwidth σ_ω/ω_0 of the FEL amplifier.

This paper is an expanded and detailed version of the comment [3] on the original publication [1].

AMPLIFICATION OF THE LONGITUDINAL FIELD INDUCED BY HADRON

In our analysis we use a standard one-dimensional linear FEL theory which gives a reasonably good approximation for typical parameters of modern FELs, (see, e.g., [4, 5]). For simplicity we assume a helical undulator with the undulator parameter K, the undulator period $\lambda_u = 2\pi/k_u$ and length l_u. An electron beam with a localized line density perturbation $\delta n_0(z)$ induced by an hadron (δn_0 has dimension of inverse length, z is the longitudinal coordinate inside the bunch in the direction of propagation) enters the FEL. Following [5] we use the dimensionless undulator length $\tau = k_u l_u$.

We expand $\delta n_0(z)$ into Fourier integral and use linear FEL theory to propagate each harmonic from the beginning to the end of the FEL assuming a high-gain FEL process. The density at the exit $\delta n_0(z,\tau)$ is Fourier transformed over z

$$\delta n_q(\tau) = \int_{-\infty}^{\infty} dz e^{-ik_0(1+q)z} \delta n_0(z,\tau), \qquad (1)$$

where $k_0 = \omega_0/c = 2\gamma^2 k_u/(1+K^2)$ corresponds to the fundamental FEL frequency and q is the dimensionless detuning. In a linear approximation, assuming a cold beam, the FEL instability develops as $\delta n_q \propto e^{s\tau}$ with s satisfying the dispersion equation

$$s^2(s+iq) = i(2\rho)^3, \qquad (2)$$

with ρ the standard FEL parameter defined by

$$(2\rho)^3 = \frac{2\lambda_u}{\gamma k_0 S}\frac{K^2}{1+K^2}\frac{I}{I_A}, \qquad (3)$$

where γ is the beam Lorentz factor, S is the beam area, I is the beam current and $I_A = mc^3/e \approx 17$ kA is the Alfvén current. The three roots of (2), s_1, s_2 and s_3, for small detuning q, can be approximated [5] by

$$s_i \approx 2\rho\left[\mu_i - \frac{i}{3}\frac{q}{2\rho} - \frac{1}{9\mu_i}\left(\frac{q}{2\rho}\right)^2\right], \; i = 1,2,3, \qquad (4)$$

with $\mu_1 = \frac{\sqrt{3}}{2} + \frac{i}{2}$, $\mu_2 = -\frac{\sqrt{3}}{2} + \frac{i}{2}$ and $\mu_3 = -i$. In what follows we assume a large gain, then the terms involving s_2 and s_3 can be neglected and only the fastest growing exponential term involving s_1 is kept. The Fourier transform $\delta n_q(\tau)$ at the exit of the FEL in this limit can be expressed through the initial value $\delta n_q(0)$ [5]

$$\delta n_q(\tau) = (s_1 + iq) H_q(\tau) \delta n_q(0), \qquad (5)$$

where

$$H_q(\tau) = \frac{s_1 e^{s_1\tau}}{(s_1 - s_2)(s_1 - s_3)}. \qquad (6)$$

Let us assume that $\delta n_0(z)$ corresponds to a localized perturbation at $z = 0$ that carries a charge Ze. If the width

* Work supported by the U.S. Department of Energy under contracts No. DE-AC02-76SF00515 and DE-AC02-05CH11231.

ISBN 978-3-95450-126-7

FEL OPERATION WITH THE SUPERCONDUCTING RF PHOTO GUN AT ELBE

J. Teichert[1#], A. Arnold[1], H. Büttig[1], M. Justus[1], T. Kamps[2], P. Lu[1,3], P. Michel[1], U. Lehnert[1], P. Murcek[1], J. Rudolph[2], R. Schurig[1], W. Seidel[1], H. Vennekate[1,3], R. Xiang[1], I. Will[4],
[1]Helmholtz-Zentrum Dresden-Rossendorf, Germany,
[2]Helmholtz-Zentrum Berlin, Germany,
[3]Technische Universität Dresden, Germany,
[4]Max-Born-Institut, Berlin, Germany

Abstract

The superconducting RF photoinjector (SRF gun) operating with a 3½-cell niobium cavity and Cs_2Te photocathodes is installed at the ELBE radiation center. Since 2012 a new UV driver laser system developed by MBI has been installed for the SRF gun. It delivers CW or burst mode pulses with 13 MHz repetition rate or with reduced rates of 500, 200, and 100 kHz at an average UV laser power of about 1 W. The new laser allows the gun to serve as a driver for the infrared FELs at ELBE. In the first successful experiment a 260 μA beam with 3.3 MeV from the SRF gun was injected into the ELBE linac, further accelerated, and then guided to the FEL. First lasing was achieved at 41 μm wavelength. The spectrum, detuning curve and further parameters were measured.

INTRODUCTION

High-brightness electron sources for CW operation with megahertz pulse repetition rates and bunch charges up to 1 nC are still a topic for research and development. One promising approach is a superconducting radio-frequency photoelectron injector (SRF gun), which is able to combine the high brightness of normal conducting RF photo guns with the advantages of superconducting RF, i.e. low RF losses and CW operation. At present, R&D programs are conducted in a growing number of institutes and companies. (See Ref. [1].)

Details of the ELBE SRF gun design have been published in [2]. The SRF gun is able to inject an electron beam into the ELBE linac using a dogleg-like connection beamline since 2010. In 2012 a new ultraviolet driver laser for the SRF gun was installed which had been developed at the MBI, Berlin. This laser delivers pulses with 13 MHz (ELBE FEL mode) as well as lower repetition rates (500, 250, 100 kHz) for high-charge operation. The new laser allows applying the SRF gun for the FEL operation at ELBE, and in this paper we will report on the first successful attempt.

SRF GUN

Photocathodes and Laser

The SRF gun has been designed for the use of high quantum efficiency (QE), semiconductor photocathodes. Up to now Cs_2Te has been used. This material has both high QE and robustness against vacuum deterioration. The photocathode plug with a diameter of 10 mm was made of Mo polished to a roughness of 8 nm. A Cs_2Te photo emission layer of 4 mm diameter was deposited on top by successive evaporation of Te and Cs in an ultra-high-vacuum preparation system [3]. The currently used photocathode was prepared 12 months ago with a fresh QE of 8.5 %, while a recent measurement has shown 0.6%. The QE decrease happened during storage in the first weeks. Inserted in the SRF gun, the experience is that the photocathodes have lifetimes of months and relatively stable QE. For the present photocathode the total charge extracted is 265 C at an average current up to 0.5 mA.

The driver laser consists of a Nd:glass oscillator at 52 MHz, a pulse picker generating the 13 MHz with an electro-optical modulator, a fiber-laser preamplifier, a multipass amplifier, and a frequency conversion stage with lithium triborate (LBO) and beta-barium borate (BBO) crystals. The UV laser pulse had a Gaussian shape in time with a FWHM value of about 3 ps. The transverse profile can be shaped with a variable aperture. Here the aperture was completely opened in order to obtain maximum laser pulse energy. Thus, the transverse profile was also Gaussian with 1.2 mm FWHM. The UV laser power on the laser table was measured as 600 mW. Considering the transportation losses of 50 %, the laser pulse energy at the photocathode was about 23 nJ. The laser spot was centred on the photocathode and the laser parameters were optimized to maximize the electron current. A value of 260 µA which corresponds to a bunch charge of 20 pC was obtained und held stable during the whole beam time.

Cavity Performance

The cavity performance, i.e. the intrinsic quality factor Q_0 versus the peak electric field, has been measured regularly since the commissioning of the gun in 2007. Fig. 1 shows some results of these measurements. The practical limitation for the peak field value of the acceleration field is the strong field emission. The acceptable heat loss is about 30 W. From 2007 until 2011 the values for the peak fields were 16 M/m in CW and 21.5 MV/m for pulsed RF. A temporary improvement was obtained by high power processing (HPP) of the cavity. In autumn 2011 a number of photocathodes where exchanged within a short time for testing new designs and

#j.teichert@hzdr.de

ISBN 978-3-95450-126-7

TIMING JITTER MEASUREMENTS OF THE SWISSFEL TEST INJECTOR

C. Vicario, M. Csatari Divall, M. G. Kaiser, M. Luethi, S. Hunziker, B. Beutner, T. Schietinger, M. Pedrozzi, Paul Scherrer Institute, Villigen PSI, Switzerland
C. P.Hauri, Ecole Polytechnique Federale de Lausanne, Lausanne, Switzerland and Paul Scherrer Institute, Villigen PSI, Switzerland

Abstract

To reach nominal bunch compression and FEL performance of SwissFEL with stable beam conditions for the users, less than 40fs relative rms jitter is required from the injector. Phase noise measurement of the gun laser oscillator shows an exceptional 30 fs integrated rms jitter. We present these measurements and analyze the contribution to the timing jitter and drift from the rest of the laser chain. These studies were performed at the SwissFEL Injector Test Facility, using the rising edge of the Schottky-scan curve and on the laser system using fast digital signal analyzer and photodiode, revealing a residual jitter of 150 fs at the cathode from the pulsed laser amplifier and beam transport, measured at 10Hz. Spectrally resolved cross-correlation technique will also be reviewed here as a future solution of measuring timing jitter at 100 Hz directly against the pulsed optical timing link with an expected resolution in the order of 50 fs. This device will provide the signal for feedback systems compensating for long term timing drift of the laser for the gun as well as for the pulsed lasers at the experimental stations.

INTRODUCTION

For SwissFEL to provide the high brightness ultra short hard X-ray pulses, the 4-10 ps FWHM electron bunches at the injector source have to be compressed by a factor ranging from 140 to 300 depending on the operating mode [1,2]. For stable output of the FEL, accurate timing of the initial electron injection is necessary.

Table 1 summarizes the main stability requirements for the laser system. Tolerance studies show, that at the electron gun photocathode less than 40fs relative rms phase jitter can be tolerated between laser arrival and RF [3]. A substantial contribution to the phase jitter comes from the drive laser of the photoinjector source.

While oscillators can be synchronized to RF reference signals with very high accuracy (sub-100 fs), maintaining this level through several stages of pulsed amplifier systems and long beam transport paths - often required at accelerator facilities - is challenging.

The aim of this study was to quantify the timing jitter of the two existing drive laser sources at SITF [4-5] and to identify main timing jitter and drift sources. The long term timing drift of the laser system was observed with a fast photodiode and a high bandwidth sampling oscilloscope.

Measurements were also performed at the SwissFEL Injector Test Facility where the electrons are generated by photoemission from a copper cathode inside an RF gun. Timing and correlation studies were based on charge detection operating the gun at the fast rising edge of the Schottky-scan (Figure 3), using consecutive Beam Position Monitors (BPM) downstream of the gun.

Table 1: Laser Requirements

Parameters at the cathode	Required	Unit
Wavelength	~260	nm
Energy/pulse (Cu)	60	μJ
RMS laser spot size	100-270	μm
Energy stability rms	<0.5	%
Pointing stability/beam size	<1	%
Shot to shot timing jitter versus RF reference	40	fs
Pulse length (flat top)	4-10	ps
Rise- and fall-time	700	fs

THE LASER SYSTEMS

The electron source can be driven by two laser systems (Table 2).

Table 2: The Two Drive Lasers' Parameters at the Cathode

Laser/ characteristic	Pulsar (Amplitude Systemes)	Jaguar (TBWP)
Material	Ti:sapphire	Nd:YLF
Mode-locking	Kerr-lens	SESAM
Wavelength	800nm THG 266nm	1047 nm FHG 262nm
Synchronization	FemtoLock	PSI dev.
Amplifiers	CPA, 1 regen, 3 multipass	1 regen
Overall propagation	84 m	30 m
Final pulse shape	Flat top Stacking 4-10 ps	Gaussian fixed 10ps
Amplitude stability	1.2% rms	<1% rms

ISBN 978-3-95450-126-7

BROAD-BAND AMPLIFIER BASED ON TWO-STREAM INSTABILITY*

G. Wang#, V. N. Litvinenko and Y. Jing, BNL, Upton, NY 11973, U.S.A.

Abstract

A broadband FEL amplifier is of great interests for short-pulse generation in FEL technology as well as for novel hadron beam cooling technique, such as CeC. We present our founding of a broadband amplification in 1D FEL dispersion relation based on electron beam with two energy peaks and a strong space charge forces. We connect its origin to the two-stream instability in electron plasma. Assuming a spatially uniform electron beam with double-peak κ-2 velocity distribution, we obtained a close form expression in the 3-D wave vector domain for the electron density variation induced by a point-like perturbation. The solution is then numerically inverse Fourier transformed to the configuration space.

INTRODUCTION

As observed from our previous studies [1], the 1D FEL dispersion relation has two growing modes for electron beam with double-peak energy distribution and sufficiently strong space charge. While one of the solutions has the typical narrow bandwidth of the FEL instability, the other solution has a much wider frequency range for amplification. After properly taking into account the frequency dependence of various parameters such as the Pierce parameter and 1D gain parameter, the mechanism for the wide-band amplification is identified as the two-stream instability, which indeed has a much wider amplification band for electron beam with small energy spread.

While various authors have previously studied the two-stream instability and two-stream FEL[2-5], a self-consistent 3D model to describe the two-stream amplification process for a warm electron beam has not been fully developed, to our knowledge.

In this work, we started from the coupled Poisson-Vlasov equation system and derived an integral equation in the wave vector domain for the electron density variation induced by an arbitrary initial perturbation. Assuming the electrons have double-peak κ-2 velocity distribution, the integral equation reduces to a fourth order differential equation. For a point-like initial density perturbation, the solution has a close form in the wave vector domain, which is then inverse Fourier transformed to the configuration space using numerical method. In the second section, we solve the dispersion relation for an FEL with double-peak Lorentzian energy distribution and show that there is a wide-band growing mode when space charge is sufficiently strong. The growing rate is then compared with that of cold beam two-stream instability. The third section contains our derivation of the equation of motion and its general solution. We solve the initial value problem for a point-like initial perturbation in the fourth sectio and present numerical results of the electron density evolution induced by the perturbation. We summarize our studies in the last n.

* Work supported by Brookhaven Science Associates, LLC under Contract No.DE-AC02-98CH10886 with the U.S. Department of Energy.

#gawang@bnl.gov

A WIDE-BAND GROWING SOLUTION IN FEL DISPERSION RELATION

The 1D FEL dispersion relation reads[6]

$$s=\left(1+is\hat{\Lambda}_p^2\right)D(s), \tag{1}$$

where s is the Laplace transformation-variable of the normalized longitudinal location $\hat{z}\equiv\Gamma z$,

$$\hat{\Lambda}_p\equiv\frac{1}{\Gamma}\left[\frac{4\pi j_0}{\gamma_z^2\gamma I_A}\right]^{1/2}, \tag{2}$$

is the space-charge parameter,

$$\Gamma\equiv\left[\frac{\pi j_0\theta_s^2\omega}{c\gamma_z^2\gamma I_A}\right]^{1/3}, \tag{3}$$

is the 1D FEL gain parameter, $I_A\equiv m_e c^3/e$ is the Alfven current, ω is the radiation frequency, v_z is the longitudinal velocity of electrons, γ_z is the Lorentz parameter for v_z,

$$\hat{\Delta}\equiv-\frac{1}{\Gamma}\left[k_w+\frac{\omega}{c}-\frac{\omega}{v_z}\right] \tag{4}$$

is the normalized detuning parameter, $k_w=2\pi/\lambda_w$ is the undulator's wave number,

$$\rho=\gamma_z^2\Gamma c/\omega \tag{5}$$

is the Pierce parameter. The dispersion integral in eq. (1) is defined as

$$D(s)\equiv\int_{-\infty}^{\infty}d\hat{P}\frac{d\hat{F}\left(\hat{P}\right)}{d\hat{P}}\frac{1}{s+i\left(\hat{P}-\hat{\Delta}\right)}, \tag{6}$$

for any root of eq. (1) with $\mathrm{Re}(s)>0$ to correspond to an exponential growing FEL instability. Taking the energy distribution as

$$\hat{F}\left(\hat{P}\right)=\frac{1}{2\pi\sigma}\left[\frac{1}{1+\left(\hat{P}/\sigma-\xi\right)^2}+\frac{1}{1+\left(\hat{P}/\sigma+\xi\right)^2}\right], \tag{7}$$

and inserting it into eq. (6) yields

$$D(s)=i\frac{\left(s+\sigma-i\hat{\Delta}\right)^2-(\zeta\sigma)^2}{\left[\left(s+\sigma-i\hat{\Delta}\right)^2+(\zeta\sigma)^2\right]^2}, \tag{8}$$

which combines with eq. (1) leads to the following two-stream FEL dispersion relation:

ISBN 978-3-95450-126-7

JLIFE: THE JEFFERSON LAB INTERACTIVE FRONT END FOR THE OPTICAL PROPAGATION CODE*

Anne M. Watson# & Michelle D. Shinn
Jefferson Lab, 12000 Jefferson Ave, Newport News, VA, 23606 U.S.A

Abstract

We present details on a graphical interface for the open source software program Optical Propagation Code, or OPC [1]. This interface, written in Java, allows a user with no knowledge of OPC to create an optical system, with lenses, mirrors, apertures, etc. and the appropriate drifts between them. The Java code creates the appropriate Perl script that serves as the input for OPC. The mode profile is then output at each optical element. The display can be either an intensity profile along the x axis, or as an isometric 3D plot which can be tilted and rotated. These profiles can be saved. Examples of the input and output will be presented.

INTRODUCTION

Since its creation in 2006 to model wave propagation in FEL oscillators, OPC has been used to simulate a wide variety of laser systems. Like most scientific programs, OPC is written such a way that a user interacts with the program using a script they must write themselves. Additionally, the output must then be plotted using a different scripting syntax. For those inexperienced with such coding work, it can be a daunting task, so they choose not to use the program at all. It was our desire to construct a user-friendly piece of software to handle the back-end portion of the optical calculation and present solely the simple forms of input and output. JLIFE, or the Jefferson Lab Interactive Front-End, enables a user to select and configure various optical elements within a web-like form interface. This data is then translated behind the scenes into the appropriate code for use with OPC, as shown in Fig. 1. The resultant graphs showing the beam profile at each element are displayed to the user, and can be modified and saved.

We feel it is important to continue to extend these functions in an open-source (free) manner, since other options such as PARAXIA-Plus [2] or GLAD [3] cost in the thousands of dollars, while OPC is open source. In comparison to these existing programs, JLIFE not only dispenses with the need to construct a script (unlike GLAD) but also includes 3D graphing capabilities (unlike PARAXIA-Plus).

This paper presents details on the construction of the code for JLIFE, along with examples of results generated from using this program.

JAVA INTERFACE

We chose to implement this software in Java for two essential reasons. The primary rationale is that Java is an intrinsically cross-platform language, and thus our program can be run on any operating system that also supports Java. Secondly, Java has native libraries for constructing a Graphical User Interface (GUI) that is adaptable to many sizes of screens and to the look-and-feel for each platform. The back-end portion of code we elected to continue writing in Perl, the same scripting language used by OPC. Perl is a language highly suitable for quick text manipulation, which allowed us to offload memory-heavy in/out operations from Java onto Perl.

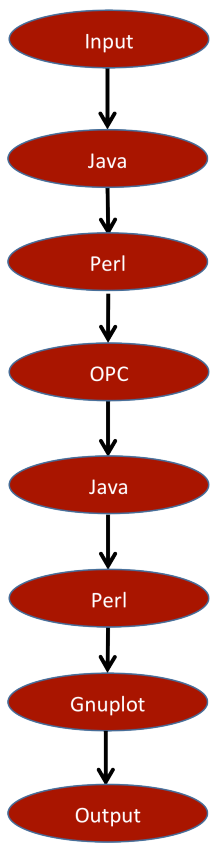

Figure 1: A schematic showing the control flow that JLIFE implements to handle each distinct function.

*Authored by Jefferson Science Associates, LLC and supported by the ONR, the Joint Technology Office, and the DOE under U.S. DOE Contract No. DE-AC05-06OR23177

#awatson@jlab.org

ISBN 978-3-95450-126-7

NUMERICAL INVESTIGATIONS OF TRANSVERSE GRADIENT UNDULATOR BASED NOVEL LIGHT SOURCES *

T. Zhang†, G.L. Wang, H.F. Yao, D. Wang‡, SINAP, Shanghai 201800, China
W.T. Wang, C. Wang, Z.N. Zeng, J.S. Liu, SIOM, Shanghai 201800, China
J.Q. Wang, S.H. Wang, IHEP, Beijing 100049, China

Abstract

With the stat-of-the-art laser technique, the quality of electron beam generated from laser-plasma accelerator (LPA) is now becoming much more better. The natural merits LPA beam, e.g. high peak current, ultra-low emittance and ultra-short bunch length, etc., pave the way to the novel light sources, especially in the realm of developing much compact X-ray light sources, e.g. table-top X-ray free-electron laser, although the radiation power is limited by the rather larger energy spread than conventional LINAC. Luckily, much more power could be extracted by using the undulator with transverse gradient (TGU) when energy spread effect could be compensated. Here we introduce a novel soft x-ray light source driven by LPA based on TGU technique. Meanwhile we present a simple idea on how to achieve much higher rep-rate (e.g.∼100 kHz) storage ring based FELs boosted by TGU.

INTRODUCTION

With the adventure of the world first two hard X-ray free-electron laser — LCLS [1] and SACLA [2], scientists begins to enjoy much more exciting discoveries. However the large scale and huge investment of such kind facilities prevents XFEL from being popular worldwide, especially in the much smaller university laboratories. One of the most important aspects is the rather longer RF linear accelerator, since tens of GeV electron beam is required in the XFEL with the acceleration gradient of tens of MeV per meter.

On the other hand, the laser plasma acceleration technique could generate electron beam with energy of GeV in just centimeter scale [3], which absolutely enlightens the FEL community to build much more compact XFELs by simply replacing the large LINAC with laser plasma accelerator. While the electron beam quality from LPA could not be controlled as ideally as the conventional RF LINAC, it is reported that the LPA could provide electron beam with the energy of $\sim$ GeV [3], normalized transverse emittance of $\sim 0.1\mu$m [4], peak current of several kilo Amperes, bunch length of tens of femtoseconds or shorter, but relative energy spread of several percent level which could limit the maximum FEL output power [5].

Recently, Z. Huang et al. proposed an idea to compensate the energy spread effect in the LPA driven high-gain FELs [6], which reported that by properly transverse dispersing the LPA electron beam, the percent level energy spread in the longitudinal phase space (i.e. $\gamma - t$) could be transformed into the transversal displacement, that means by using undulators with proper transverse gradient the FEL resonant phenomenon could be maintained for electrons with different energies. The essence of TGU application in the high-gain FEL relies on the fact the sacrifice on the transverse current density increases the final extracted FEL power.

Since TGU could be used as the energy spread compensator, in the diffraction-limited storage rings, straight by pass TGU radiator line could be used to generate FELs with high rep-rate [7, 8]. Moreover, we can take the advantage of the rather larger acceptance of TGU to increase the rep-rate by slowly damping. In the following two sections two novel light sources based on TGU is presented and the numerical simulations is mainly focused.

SOFT X-RAY FEL DRIVEN BY LPA AND TGU

The theory of TGU could be simply linked by two equations, i.e.

$$a_u(x) = a_u(1+\alpha x) \quad (1)$$

$$x = \eta\frac{\Delta\gamma}{\gamma} \quad (2)$$

where a_u is the normalized undulator parameter, x is the transverse deviation, α is the transverse field gradient, η is the transverse dispersion, $\frac{\Delta\gamma}{\gamma}$ is the energy deviation. By introducing the FEL resonant equation: $\lambda_s = \lambda_u/\left(2\gamma^2\right)\left(1+a_u^2\right)$, the relationship between $\Delta\gamma/\gamma$ and $\Delta a_u/a_u$ is found as: $\frac{\Delta\gamma}{\gamma} = \frac{a_u^2}{1+a_u^2}\cdot\frac{\Delta a_u}{a_u}$. Then the compromise condition between the field gradient and transverse dispersion is worked out as,

$$\alpha\cdot\eta = \frac{1+a_u^2}{a_u^2} \quad (3)$$

Here we would like to present the numerical simulations of an LPA driven XFEL which equipped with TGU at Shanghai Institute of Optics and Fine Mechanics (SIOM), Chinese Academy of Sciences. The laser plasma accelerator is now under operation at SIOM, electron beam with nearly 1 GeV and energy spread about $\sim 3\%$, peak current of several kA is generated [9]. The next plan is to construct an soft X-ray light source driven by LPA with the name

* Work supported by Major State Basic Research Development Program of China (2011CB808300), and Natural Science Foundation of China (11075199)

† zhangtong@sinap.ac.cn
‡ wangdong@sinap.ac.cn

ISBN 978-3-95450-126-7

LONG-TERM STABLE, LARGE-SCALE, OPTICAL TIMING DISTRIBUTION SYSTEMS WITH SUB-FEMTOSECOND TIMING STABILITY*

M.Y. Peng, P.T. Callahan, A.H. Nejadmalayeri, F.X. Kärtner, MIT, Cambridge, MA 02139, USA
K. Ahmed, S. Valente, M. Xin, F.X. Kärtner, CFEL-DESY, Hamburg, Germany
J.M. Fini, L. Grüner-Nielsen, E. Monberg, M. Yan, OFS Laboratories, Somerset, NJ 08873, USA
P. Battle, T.D. Roberts, AdvR, Inc., Bozeman, MT 59715, USA

Abstract

Sub-fs X-ray pulse generation in kilometre-scale FEL facilities will require sub-fs long-term timing stability between optical sources over kilometer distances. We present here key developments towards a completely fiber-coupled, pulsed optical timing distribution system capable of delivering such stability. First, we developed a novel 1.2-km dispersion-compensated, polarization-maintaining fiber link to eliminate drifts previously induced by polarization mode dispersion. Link stabilization for 16 days showed 0.6 fs RMS timing drift and during a 3-day interval only 0.13 fs drift. Second, we verified that ultralow-noise optical master oscillators for sub-fs timing distribution are available today; the measured jitter for two commercial femtosecond lasers is less than 70 as for frequencies above 1 kHz. Lastly, we fabricated a hybrid-integrated, balanced optical cross-correlator using PPKTP waveguides to eliminate alignment drifts and for future reduction of the link operation power by a factor of 10-100.

INTRODUCTION

Modern X-ray free-electron lasers (FELs) [1,2,3] require timing distribution systems with extremely high timing stability to synchronize RF and optical sources located up to several kilometers apart. Since conventional RF timing systems have already reached a practical limit of about 50-100 fs timing precision for such long distances, next-generation timing systems [4,5] are adopting fiber-optic technology to achieve superior performance with optical signal transport and timing distribution.

Over the past decade, we have been advancing technology for a pulsed optical timing distribution system [5]. Our system consists of a femtosecond mode-locked laser tightly locked to a microwave standard and stabilized fiber links for distributing the pulsed optical timing signal to remote locations. Link stabilization is performed using compact, single-crystal balanced optical cross-correlators (BOC), which are capable of attosecond-level timing resolution. Sub-10-fs system performance over days of operation has been achieved but is limited mainly by polarization mode dispersion (PMD) in standard single-mode fiber.

In the near future, it is necessary to improve timing distribution down to sub-fs precision since current facilities, such as LCLS at Stanford, can already produce X-ray pulses shorter than 10 fs [6] and concepts for sub-fs X-ray pulse generation are in place. Improving upon our previous work, we demonstrate here: 1) timing stabilization of a dispersion-slope-compensated 1.2-km polarization-maintaining (PM) fiber link with sub-fs residual timing drift over 16 days, 2) jitter measurements of two ultralow-noise, commercial femtosecond lasers for sub-100-as timing distribution, and 3) fiber-coupled, hybrid-integrated cross-correlators using periodically-poled $KTiOPO_4$ (PPKTP) waveguides for improved BOC timing sensitivities and overall system efficiency and robustness.

TIMING-STABILIZATION OF A 1.2-KM PM FIBER LINK

Link stabilization is critical for preserving the timing precision of the pulsed optical timing signal after long-distance propagation. Environmental disturbances to the fiber link (e.g. thermal fluctuations, acoustic noise, and vibrations) will cause pulse timing errors at the link output. To stabilize the link, we use a BOC to measure the round-trip link timing error with high timing resolution and correspondingly adjust a variable delay within the link path to compensate for the detected error.

Our previous results with a 300-m stabilized fiber link using standard single-mode fiber showed that PMD limited the link stability to about 10 fs over few days of operation and caused delay jumps as much as 100 fs when the fiber was significantly perturbed [6]. To eliminate PMD-induced drifts, we collaborated with OFS in designing and fabricating a 1.2-km PM link with 3rd-order dispersion-compensation. The PM link consists of 1088 m of standard PM fiber matched to 190 m of custom dispersion-compensating PM fiber (PM-DCF). The PM-DCF has a PANDA-like geometry containing Boron stress rods with 35-μm diameters, a core index profile similar to conventional DCF, and a 2nd and 3rd order dispersion of -104.1 ps/(nm·km) and -0.34 ps/(nm^2·km), respectively, at 1550 nm.

*Work supported by the United States Department of Energy through contract DE-SC0005262, and the Center for Free-Electron Laser Science at Deutsches Elektronen-Synchrotron, Hamburg, a research center of the Helmholtz Association, Germany. S.V. acknowledges support by Italian National Civil Authority (ENAC) and University of L'Aquila through Giuliana Tamburro and Ferdinando Filauro scholarships, respectively.

ISBN 978-3-95450-126-7

PITZ EXPERIENCE ON THE EXPERIMENTAL OPTIMIZATION OF THE RF PHOTO INJECTOR FOR THE EUROPEAN XFEL

M. Krasilnikov[#], F. Stephan, G. Asova[†], H.-J. Grabosch, M. Groß, L. Hakobyan, I. Isaev, Y. Ivanisenko*, L. Jachmann, M. Khojoyan, G. Klemz, W. Köhler, M. Mahgoub, D. Malyutin, M. Nozdrin[§], A. Oppelt, M. Otevrel, B. Petrosyan, S. Rimjaem[‡], A. Shapovalov, G. Vashchenko, S. Weidinger, R. Wenndorff, DESY, Zeuthen, Germany
K. Flöttmann, M. Hoffmann, S. Lederer, H. Schlarb, S. Schreiber, DESY, Hamburg, Germany
I. Templin, I. Will, MBI, Berlin, Germany
V. Paramonov, INR, Moscow, Russia
D. Richter, HZB, Berlin, Germany

Abstract

The Photo Injector Test facility at DESY, Zeuthen site (PITZ), develops high brightness electron sources for modern free electron lasers. A continuous experimental optimization of the L-band photo injector for such FEL facilities like FLASH and the European XFEL has been performed for a wide range of electron bunch charges – from 20 pC to 2 nC – yielding very small emittance values for all charge levels. Experience and results of the experimental optimization will be presented in comparison with beam dynamics simulations. The influence of various parameters onto the photo injector performance will be discussed.

INTRODUCTION

The development of high brightness electron sources is strongly motivated by recent progress in free electron lasers based on the self-amplified spontaneous emission (SASE FELs). RF photo injectors are capable to produce electron beams with very low transverse emittance [1]. Since more than a decade the Photo Injector Test facility at DESY, Zeuthen site (PITZ), develops electron sources for modern FELs like the Free-electron Laser in Hamburg, FLASH [2], and the European X-ray Free-Electron Laser, European XFEL [3]. The stringent requirement on beam emittance for the European XFEL of 0.9 mm mrad at 1 nC bunch charge in the injector was experimentally demonstrated at PITZ [1, 4].

Besides the beam emittance a unique pulse structure has to be supported by the electron sources developed and optimized at PITZ in order to use advantage of the superconducting linac. Trains with up to 600 electron bunches and 1 μs spacing between the pulses of the train have been produced at 10 Hz repetition rate. To realize full specification for the European XFEL the bunch frequency of the photocathode laser has to be increased from 1 to 4.5 MHz. Thus, 27000 bunches per second have to be accelerated.

The pulse train structure yields an advantage for the emittance optimization at low bunch charge. The transverse emittance has been minimized for bunch charges from 0.02 to 2 nC [1, 5].

The paper gives a general overview of the PITZ accelerator and summarizes the results of the rf photo injector experimental optimization at various bunch charge levels. Beam dynamics simulations will be presented for the photo injector of the European XFEL as well as for the PITZ setup.

PITZ ACCELERATOR

A general schematic diagram of the current PITZ setup is shown in Fig. 1. The accelerator consists of a photocathode rf gun, a normal conducting booster cavity and various systems for cathode laser and electron beam diagnostics.

RF Gun

The PITZ gun is a 1.6 cell L-band normal conducting copper rf cavity with a Cs_2Te photocathode. The gun cavity is supplied with main and bucking solenoids for control and mitigation of space charge forces within electron bunches of very high density.

The rf feed of the gun is realized using a 10 MW multibeam klystron [1] which supplies the power via two waveguide arms. A T-combiner is installed in the rf gun vicinity and serves to superpose waves from these two arms to feed the gun cavity.

A phase shifter in one of the waveguides is used to match amplitudes and phases of the mixing waves. The combined wave is fed through a rotationally symmetric coaxial coupler into the rf gun. The rf feed regulation is realized on a FPGA platform based on signals from so-called 10 MW coupler [1] which measures the forward wave after the T combiner and the wave reflected from the gun cavity. The shot-to-shot rms phase jitter is ~0.1 deg, the phase slope within an rf pulse is ~0.1 deg/μs.

mikhail.krasilnikov@desy.de
† currently at INRNE, Sofia, Bulgaria
* currently at PSI, Villigen, Switzerland
§ on leave from JINR, Dubna, Russia
‡ currently at Chang Mai University, Thailand

ISBN 978-3-95450-126-7

BEAM DIAGNOSTICS FOR COHERENT OPTICAL RADIATION INDUCED BY THE MICROBUNCHING INSTABILITY*

Alex H. Lumpkin#, Fermi National Accelerator Laboratory, Batavia, IL 60510, USA

Abstract

The observations of the microbunching instability were initially reported in S-band linacs that used photo-injected beams. However, we now have observations in linacs with thermionic cathode generated beams in the past year at SCSS, SACLA, and APS. A summary of the results is provided which also illustrate the beam diagnostics used.

INTRODUCTION

The generation of the ultra-bright beams required by modern free-electron lasers (FELs) has generally relied on chicane-based bunch compressions that often result in the microbunching instability [1, 2]. Following compression, spectral enhancements extend even into the visible wavelengths through the longitudinal space charge (LSC) impedances. Optical transition radiation (OTR) screens have been extensively used for transverse electron beam size measurements for the bright beams, but the presence of longitudinal microstructures (microbunching) in the electron beam or the leading edge spikes can result in strong, localized coherent enhancements (COTR) that mask the actual beam profile. We now have evidence for the effects in both rf photocathode (PC) gun injected linacs and thermionic-cathode (TC) gun injected linacs. Since the first observations, significant efforts have been made to characterize, model, and mitigate COTR effects on beam diagnostics [3-6]. An update on the state-of-the-art for diagnosing these effects will be given as illustrated by examples at LCLS, SCSS, SACLA, APS, and NLCTA. The most recent microbunching instability workshop was held in Pohang, Korea [7] in May 2013, and the website provides more details in the files for the talks including an extensive overview on observations [8].

INSTABILITY EFFECTS

It should be kept in mind that the modulation is even stronger in the several-micron-period regime where it impacts the effective energy spread and can reduce FELgain. As reference the original description by Saldin, Schneidmiller, and Yurkov [1] provides an analysis of the charge density noise being amplified via LSC impedances with the gain as a function of wavelength as shown in Fig. 1. In this case curve 1 includes energy spread as compared to curve 2 which is for a cold beam. Experimentally, one images the 0.4 to 0.7 μm regime of COTR with our standard CCD cameras in the various linac facilities. Another gain calculation has been given by Huang et al. [2] with maximum gain calculated at about 10 μm under an initial 150 μm period modulation with 8% amplitude.

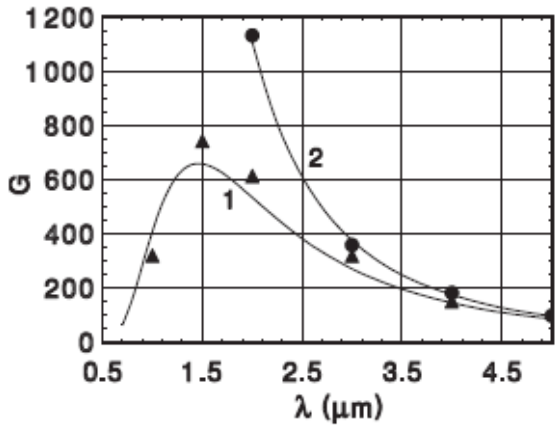

Figure 1: Calculated gain (G) for the microbunching instability versus wavelength from reference [1].

The instability effects were graphically demonstrated in the high energy spectra at LCLS as presented at FEL 10 by J. Welch [9]. The modulation in energy attributed to such microbunching is seen with the laser heater off in Fig. 2a, while it is suppressed with the laser heater on in Fig. 2b. Concomitantly, the observed x-ray spectra for the two cases showed the dramatic simplification of the spectrum with laser heater "on" in Fig. 3.

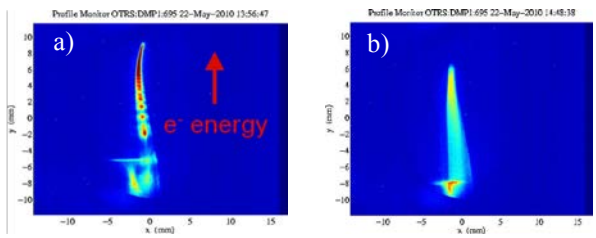

Figure 2: Examples of the LCLS electron beam high energy spectrum a) without and b) with the laser heater active [9].

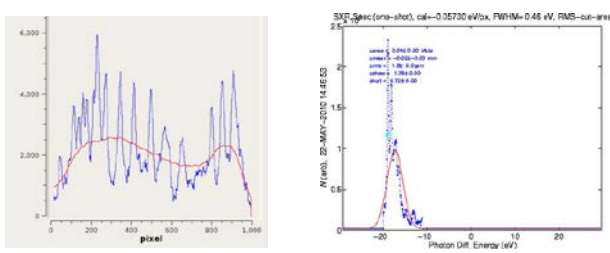

Figure 3: Corresponding x-ray spectra at LCLS for Fig. 2 without (left) and with (right) the laser heater active [9].

lumpkin@fnal.gov

*Work supported under Contract No. DE-AC02-07CH11359 with the United States Department of Energy.

ISBN 978-3-95450-126-7

AN RF DEFLECTING CAVITY BASED SPREADER FOR NEXT GENERATION LIGHT SOURCES*

C. Sun#, L. Doolittle, P.J. Emma, J.Y. Jung, M. Placidi and A. Ratti
Lawrence Berkeley National Laboratory, Berkeley, CA 94720, U.S.A.

Abstract

The Lawrence Berkeley National Laboratory (LBNL) is developing design concepts for a multi-beamline soft X-ray FEL array powered by a superconducting linac with a bunch repetition rate of about one MHz [1]. A beam spreader will transport the electron beam to any FEL line with minimal beam loss at any operational energy and rate. This paper documents a novel system where the use of RF Deflectors (RFD) as fast-switching devices is proposed. The LBNL site-complying spreader scheme can be configured to fit any beam switchyard topology including an array of beamlines symmetrically split at both sides of the linac.

Introduction

Electron bunches supplied by a high-brightness, high-repetition-rate photocathode gun and accelerated in a CW linac to a nominal energy of 2.4-GeV are distributed by a beam spreader into an array of independently configurable FEL beam-lines with nominal bunch rates in the MHz range in each FEL.

Superconducting RF dipole cavities [2] provide vertical deflection for bunches traveling on the crest and at the zero-crossing of the transverse electric field in the cavities (three-way splitting). The emerging trajectories are horizontally bent by two Lambertson magnets and a standard horizontal dipole to create a three-branches takeoff section. The process, applied to each branch, produces the nine lines spreader layout of Figure 1.

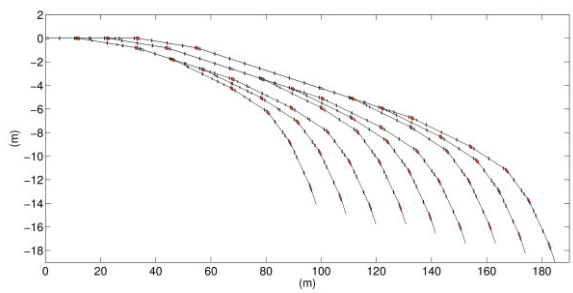

Figure 1 : The 9 FEL lines layout of the NGLS spreader.

The achromatic and isochronous transport lines preserve the beam qualities after a total 36-deg deflection, and provides a 5.56 / 6.23-m separation between the FEL lines within a compact footprint. The Gun-Spreader complex is suitable to deliver photon bunches with equal arrival time at detectors in adjacent lines ("Two-color" X-ray pulse capability) by populating RF buckets with time separation consistent with the beamlines path length.

*Work supported by the Director, Office of Science, of the U.S. Department of Energy under Contract No. DE-AC02-05CH11231
#ccsun@lbl.gov

The Takeoff Section

A novel takeoff scheme evolved from the original one [3] is shown in Figure 2. Bunches arriving at the RFD1 dipole cavity are either vertically deflected by ±1.15-mrad (on crest passage) or travel straight (zero-crossing passage) while two Lambertson septa (LSM) and a conventional dipole (HB) provide horizontal deflections.

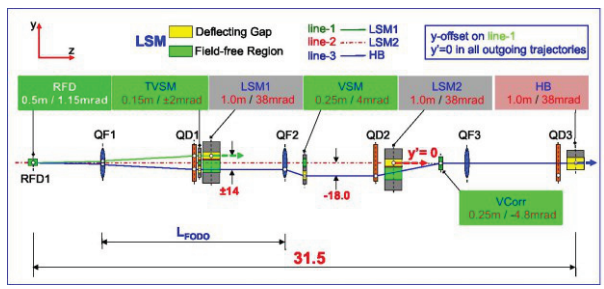

Figure 2 : The RFD takeoff section showing three vertically deflected trajectories horizontally right-bent by two Lambertson and one standard dipole.

The LSM1 Lambertson magnet provides a 38-mrad horizontal deflection to line-1 and transmits undeflected the line-2 and line-3 trajectories in the zero-field channel. The line-2 travels at the zero-crossing phase of the RF deflector and is deflected by the LSM2 septum while the line-3 is eventually deflected by the standard dipole HB. The Lambertson septa are both installed in upright position, differently from what suggested in [3], and are mechanically and magnetically identical. Their design features together with a Poisson's modelization have been described in [3]. The Vertical Septum Magnets TVSM and VSM with the corrector VCorr provide individual vertical steering and slope control. The three split trajectories emerge with no vertical slope so their offsets remain contained and can be compensated anywhere downstream without requiring the use of large correctors. The deflecting elements are imbedded in a 10.87-m long cell, 90-degree phase advance FODO structure.

This module, repeated on each split branch with different orientations, can produce a variety of beam distribution schemes. In the NGLS configuration it generates the nine beamlines spreader scheme of Figure 1. The main takeoff parameters are collected in Table 1 of Ref. [3].

The RF Deflectors (RFD)

The adoption of transverse RF-deflectors allows for bunch repetition rates well above the ~150-kHz limit represented by stripline and ferrite fast kickers. Frequencies lower than 400-MHz are considered in order to limit emittance dilution from spatial chirp for bunches

ISBN 978-3-95450-126-7

PROGRESS IN SRF GUNS*

S. Belomestnykh#, Brookhaven National Laboratory, Upton, NY 11973-5000, USA

Abstract

In the last couple of years great progress has been made in the commissioning and operation of Superconducting RF (SRF) electron beam sources. Both elliptical cavity designs and reentrant cavities have been developed. This paper reviews recent progress in SRF guns.

INTRODUCTION

Application of the superconducting radio frequency technology to photoemission electron injectors is a very active field of research as discussed in recent review articles [1-3]. SRF has advantages over other electron gun technologies (DC or normal conducting RF) in the high duty factor mode of operation, where SRF structures provide higher accelerating gradients. While simulations [4] show that DC and SRF guns have comparable performance with low- and medium-charge bunches, the latter promise to enable generating high-bunch-charge, high-brightness and high-average-current beams for many advanced accelerator applications such as electron-hadron colliders, electron coolers, and free electron lasers. As it was pointed out in [1], SRF guns are expected to play an important role in future linac-driven FEL facilities.

SRF photoemission electron sources are complex devices requiring co-existence of three sophisticated technologies: high quantum efficiency (QE) photocathodes, superconducting RF structures, and high-repetition-rate synchronizable lasers. As a result, progress with developing SRF guns was relatively slow. Only a few years ago SRF gun development efforts began gradual transition from a feasibility demonstration experiments to generating beams for accelerator applications. Recently, several guns generated their first beams and one served as an injector for an FEL at HZDR [5]. For a historical overview of SRF gun development and an in-depth discussions of challenges associated with SRF photoinjectors, I refer readers to previous reviews of the subject [1-3]. In this article I will concentrate on recent progress with SRF guns designed as injectors (SRF photoinjectors) for various applications.

BRIEF SURVEY OF SRF GUNS AND PHOTOCATHODES

Two types of SRF structures are used in photoemission guns: elliptical cavities and quarter-wave / re-entrant resonators. The first guns utilized elliptical cavity geometries, conventional for the high-β SRF cavities. The guns based on elliptical cavities are developed at BNL (USA), HZB (Berlin, Germany), HZDR (Rossendorf, Germany) and Peking University (China). Later on, several guns were designed using a quarter-wave resonator (QWR) approach, which is especially well suited for generating beams with high charge per bunch. The QWRs can be made compact even at long wavelengths thus allowing generation of long electron bunches and minimizing space charge effects and enabling high bunch charge. The guns of this type have been built so far only in the USA for projects at BNL, Naval Postgraduate School (NPS) and University of Wisconsin.

To generate high-intensity and high-average-current beams, one needs high QE photocathodes with a long operational lifetime. Readily available lasers with wavelengths ranging from IR to UV, wide variety of pulse durations and average power of up to several tens of watts enable possible use of many different materials from two classes: metals and semiconductors [6, 7]. Metal photocathodes (Cu, Mg, Pb, Nb) are robust, but have low QE ($<10^{-3}$) and are suitable only for use in the initial phases of an SRF gun development, when high beam intensities / high duty factors are not required. Coating of metal cathodes with a thin (~18 nm) layer of CsBr can increase the QE to $7\cdot10^{-3}$. Superconducting (niobium or lead) photocathodes have been used in small R&D SRF guns as a way to avoid introduction of a special cathode plug and to reduce RF losses.

Semiconductor photocathodes are the preferred option for many projects as they can provide very good QE, 10% and higher. However, these cathodes are very sensitive to contamination and require UHV conditions for operation. The most developed semiconductor photocathodes for SRF gun applications are GaAs(Cs), Cs_2Te, and CsK_2Sb. Gallium arsenide is the only one of the three suitable for producing polarized electrons, but it is the most sensitive to ion back bombardment, requires an extremely good vacuum, and has a short lifetime. Cesium telluride is the most robust and has demonstrated a very long lifetime in an SRF gun at HZDR, but requires the use of UV lasers. This makes it more difficult to use for high bunch charge: more laser power is needed at the same QE than at longer wavelengths, optics and pulse shaping are more difficult as well. Cesium potassium antimonide can be used with green lasers. It demonstrated very good performance in DC guns [8, 9, 10] and holds the world record of average beam current produced from an RF photoinjector [11]. It is the most preferred option for SRF guns at present. A potential alternative is NaK_2Sb, which has a similar to CsK_2Sb production recipe, but proved to be more robust in experiments with a DC gun at Cornell University [12].

Finally, diamond can be used to boost the photoemission current by a factor of ~100 and diamond-amplified photocathodes are very promising for high-charge applications, though still require more R&D. For more details on photocathode materials, I refer readers to the recently published reviews [6, 7].

*Work supported by Brookhaven Science Associates, LLC under Contract No. DE-AC02-98CH10886 with the U.S. DOE.

#sbelomestnykh@bnl.gov

ISBN 978-3-95450-126-7

ELECTRON BEAM LONGITUDINAL PHASE SPACE MANIPULATION BY MEANS OF AN AD-HOC PHOTOINJECTOR LASER PULSE SHAPING*

G. Penco[1#], M. Danailov[1], A. Demidovich[1], D. Castronovo[1], G. De Ninno[1,2], S. Di Mitri[1], W. M. Fawley[1], L. Giannessi[1,3], C. Spezzani[1] and M. Trovo'[1]

[1]Elettra-Sincrotrone Trieste S.C.p.A., Basovizza
[2]University of Nova Gorica, Nova Gorica
[3]ENEA C.R. Frascati, Frascati (Roma)

Abstract

In a seeded FEL machine as FERMI, the interplay between the electrons energy curvature and the seed laser frequency chirp has a relevant impact on the output FEL spectrum. It is therefore crucial controlling and manipulating the electron beam longitudinal phase space at the undulator entrance. In case of very short bunches, i.e. high compression scheme, the longitudinal wakefields generated in the linac induce a positive quadratic curvature in the electrons longitudinal phase space that is hard to compensate by tuning the phase of the main RF sections or the possible high harmonic cavity. At FERMI we have experimentally exploited a longitudinal ramp current distribution at the cathode, obtained with an ad-hoc photoinjector laser pulse shaping, to linearize the longitudinal wakefields in the downstream linac and flatten the electrons energy distribution, as theoretical foreseen in [1]. Longitudinal phase space measurements in this novel configuration are here presented, providing a comparison with the typical longitudinal flat-top profile.

INTRODUCTION

The very high quality of the FEL radiation output relies on the optimization of the high brightness electron beams that represents the medium where the FEL process is stimulated and amplified. Therefore great effort has been spent to produce high peak current (~kA) and low transverse emittance electron beams. In order to have FEL emission at the wavelength λ_0, it is necessary to satisfy the well known resonant condition $\lambda_0 = \frac{\lambda_u}{2\gamma^2}\left(1+\frac{K^2}{2}\right)$, where $K = \frac{eB_u\lambda_u}{2\pi m_e c}$, B_u and λ_u are the magnetic field and period of the undulator, m_e is the electron mass and γ is the electron beam Lorentz factor. As a consequence only electrons with the resonant energy participate to the FEL process, so controlling and eventually manipulating the electrons longitudinal phase space (LPS) has a high priority.

Several elements along the linac contribute in defining the electrons LPS. The first one comes from the linac sections that provide an energy gain E that can be written as $E(t) = \sum_i eV_i \sin\left(\omega_{rf} t + \phi_i\right)$, where t is the bunch internal temporal coordinate, ω_{rf} is the rf frequency, and V_i and ϕ_i are the rf voltage and phase of the i^{th} section. The accelerating sections provide a negative quadratic chirp to the electrons energy curvature. The second contribution is given by the magnetic chicanes that are usually implemented to longitudinally compressed the beam before sending it to the undulator chain. A magnetic chicane has momentum compaction $R_{56}<0$ and without sextupole the second order term $T_{566}\sim -3/2R_{56}$. Thus the magnetic chicane provides a negative quadratic chirp to the LPS. A high harmonic rf cavity is usually implemented to compensate the LPS non linearity introduced by rf sections and chicane, by phasing it close to the maximum decelerating voltage. Another important contribution to the LPS comes from the longitudinal wakefields (LW) generated in the rf sections, that become relevant after the compression. The positive quadratic chirp introduced by the LW is hard to compensate by detuning the phase of the rf sections because of the high order terms in the wake potential function. Moreover, tuning the high harmonic cavity voltage can in principle help but at the cost of jeopardizing the linearity of the compression.

A possible solution has been proposed in [1] and consists in shaping the bunch current profile at the injector exit in order to linearize the LW of the downstream linac sections. The basic assumption is that the output bunch configuration is largely predetermined by the input bunch configuration. The manipulation of the longitudinal density distribution at the beginning of the linac has been proposed as the required additional free parameter. Multi-particles tracking code simulations showed that a linearly ramped current distribution at the injector exit could be well suitable for linearizing the LW generated in the downstream linac sections. In this paper we report the generation of a linearly ramped bunch profile at the FERMI injector, obtained by temporal shaping the photoinjector laser (PIL).

FERMI LAYOUT

The experiment has been performed in the FERMI linac that is routinely used to drive a HGHG seeded soft X-ray FEL [2] and whose layout is sketched in figure 1. The electron beam is generated in a 1.6-cell RF photocathode gun [3] and accelerated up to about 100 MeV by a two-sections linac (L00) and then up to about 320MeV by a four-sections linac (L01).

ISBN 978-3-95450-126-7

PROGRESS IN A PHOTOCATHODE DC GUN AT THE COMPACT ERL

N. Nishimori#, R. Nagai, S. Matsuba, R. Hajima, JAEA, Tokai, Naka, Ibaraki 319-1195, Japan
M. Yamamoto, Y. Honda, T. Miyajima, KEK, Oho, Tsukuba, Ibaraki 305-0801, Japan
H. Iijima, M. Kuriki, Hiroshima University, Higashihiroshima, Hiroshima 739-8530 Japan
M. Kuwahara, Nagoya University, Nagoya464-8603, Japan

Abstract

The next generation light sources such as energy recovery linac (ERL) light sources and X-ray FEL oscillator require high brightness electron gun with megahertz repetition rate. We have developed a DC photoemission gun at JAEA and demonstrated generation of a 500-keV electron beam from the gun. This demonstration was achieved by addressing a discharge problem that leads to vacuum breakdown of the DC gun. The problem is microdischarge at an anode electrode or a vacuum chamber, which is triggered by microparticle transfer or field emission from a cathode electrode. An experimental investigation has revealed that larger acceleration gap optimized to mainly reduce surface electric field of anode electrode results in suppression of the microdischarge events. The gun was transported to the compact ERL (cERL) at KEK. The commissioning of the injector system of the cERL is under way.

INTRODUCTION

Future energy recovery linac (ERL) light sources and megahertz repetition rate X-ray FELs require high-brightness and high-current electron guns capable of delivering an electron beam with emittance lower than 1 mm-mrad and currents up to 100 mA [1]. A DC photoemission gun with a GaAs or alkali photocathode is one of the most promising candidates for such guns, since the high-current beam of 9 mA has been routinely provided from the DC gun at Jefferson Lab FEL [2] and the record high current of 65 mA was recently demonstrated at Cornell photoinjector [3]. Meanwhile, the DC gun operational voltage, which is closely related to brightness of the electron beam [4], has been limited to 350 kV or lower mainly because of the field emission problem since when the first 500-kV DC photoemission gun was proposed in 1991 [5].

We have developed a 500-kV DC gun for ERL light sources in Japan [6] and demonstrated generation of a 500-keV electron beam from a DC photoemission gun [7]. This demonstration was achieved by solving two discharge problems. One is discharge on insulator ceramic surface caused by field emission generated from a central stem electrode. We have employed a segmented insulator with rings to guard the insulator against the field emission [8]. The other problem is discharge between the cathode electrode and the gun vacuum chamber wall including an anode electrode. Those discharge events during HV conditioning almost always accompany gas desorption. This is similar to gas desorption induced microdischarge observed in high voltage insulator system with a large gap [9, 10]. It may occur that microparticles on the anode are propelled to the cathode by explosive bursts due to gas desorption induced discharges and then serve as sources of field emission. Here the microparticles are weakly bound metal particles on the anode or the vacuum chamber wall. In fact we often experienced field emission site suddenly appeared at the cathode electrode during HV conditioning. The field emission starts at voltage much lower than the voltage just we reached by HV conditioning and exponentially increases with voltage. We also found the field emission sites could be removed by simply wiping the cathode electrode with a lint-free tissue after venting the gun chamber with dry nitrogen gas. These observations support our postulation that the sources of the field emission are microparticles transferred from the gun vacuum chamber or the anode by gas desorption induced discharges.

Similar field emission caused by microparticles is observed in high gradient RF cavities. In the process of superconducting RF cavities, high pressure rinsing technique is routinely used to remove residual small particulates [11]. It is however difficult to completely remove those microparticles on the DC gun chamber, because we cannot use the high pressure rinsing technique for a chamber equipped with a massive non evaporable getter (NEG) pumps. We decided to search for a DC gun configuration where microdischarge events are greatly reduced thus leading to suppression of microparticles transfer to the cathode.

In this paper, we study a configuration of gun vacuum chamber appropriate for operation of DC voltage ≥ 500 kV. Experimental results of HV conditioning are presented for different gap lengths. The results are compared in terms of applied voltage as a function of total gas desorption during HV conditioning. We found larger acceleration gap is better for high voltage operation owing to lower surface electric field of the anode electrode. The gun was transported to the compact ERL (cERL) at KEK. Some preliminary results of the commissioning of the cERL injector system are also presented.

DC PHOTOEMISSION GUN AT JAEA

The details of the gun system are described in Refs. [6,7]. A GaAs wafer on a molybdenum puck is used as a photocathode. The wafer is atomic hydrogen cleaned and transferred to the preparation chamber where cesium and oxygen are alternatively applied for negative electron

nishimori.nobuyuki@jaea.go.jp

ISBN 978-3-95450-126-7

FEASIBILITY OF CW AND LP OPERATION OF THE XFEL LINAC

J. Sekutowicz, V. Ayvazyan, J. Branlard, M. Ebert, J. Eschke, T. Feldmann, A. Gössel,
D. Kostin, M. Kudla, F. Mittag, W. Merz, C. Müller, R. Onken, I. Sandvoss, E. Schneidmiller,
A. Sulimov, M. Yurkov, DESY, 22607 Hamburg, Germany
W. Cichalewski, A. Piotrowski, K. Przygoda, TUL, 90-924 Łódz, Poland
W. Jalmuzna, Embedded Integrated Control Systems GmbH, 22525 Hamburg, Germany
K. Czuba, WUT, 00-665 Warsaw, Poland
J. Szewinski, NCBJ, 05-400 Świerk-Otwock, Poland

Abstract

The European XFEL superconducting linac is based on cavities and cryomodules (CM) developed for TESLA linear collider. The XFEL linac will operate nominally in short pulse (sp) mode with 1.3 ms RF pulses (650 µs rise time and 650 µs long bunch train). For 240 ns bunch spacing and 10 Hz RF-pulse repetition rate, up to 27000 bunches per second can be accelerated to 17.5 GeV to generate uniquely high average brilliance photon beams at very short wavelengths [1]. While many experiments can take advantage of full bunch trains, others prefer an increased to several µ-seconds intra-pulse distance between bunches, or short bursts with a kHz repetition rate. For these types of experiments, the high average brilliance can be preserved only with duty factors much larger than that of the currently proposed sp operation.

In this contribution, we discuss progress in the R&D program for future upgrade of the European XFEL linac, namely an operation in the continuous wave (cw) and long pulse (lp) mode, which will allow for more flexibility in the electron and photon beam time structure.

INTRODUCTION

In summer 2011 we began tests with pre-series XFEL cryomodules in order to define limits in the cw and lp operations for the XFEL linac. We conducted up to now, four runs, each approximately one week long, with four pre-series cryomodules. All tested cryomodules differed somewhat from the XFEL series cryomodules, mainly because many cavities they housed were equipped with old type, low heat conduction HOM-coupler feedthroughs and with their thermal connections to the 2-phase helium line. We have presented some of the tests results along with new components needed for these two operation modes (high thermal conduction feedthroughs, beam line absorbers, all superconducting photo-injector, LLRF and new RF-source) in [2, 3, 4 and 5] during last four years.

In short, the goal of our studies is to prove feasibility of the XFEL cw operation at gradients $E_{acc} \leq 7$ MV/m and lp operation at higher E_{acc}, with duty factors (DF) scaled roughly proportional to $(7/E_{acc})^2$. The studies, proposed in 2005/2006, were motivated by the duty factor potential, which can be anticipated for linacs based on the superconducting technology. Unlike XFEL, other short wavelength FELs, proposed or under construction at that time, were based on room temperature technology and thus their DFs are very low, considerably below 0.1%.

For the sp operation, XFEL linac cavities will be fed by pulsed klystrons, which maximum pulse duration is 1.38 ms and thus possible largest nominal DF is 1.38 % at 10 Hz repetition rate. With new operation modes we expect to gain significantly in DF at cost of operation at lower gradients; however this can still allow for very short wavelengths, as it is discussed in [6].

There are technical and practical constraints for the upgraded DF range.

LIMITATIONS FOR DF

Heat Load at 2K (1.8K)

One of technical constraints is the heat load (HL) budget for present type of XFEL cryomodules, which in total (static plus dynamic load) should not exceed 20 W/cryomodule. The limit results from diameter of 2-phase He transport tube and from its approximately 160 m length between feed- and end-cup (12-cryomodule long cryogenic strings in main linac).

Upgrade of the Cryogenic Plant

To keep high quality of electron bunches, as for the present linac configuration and nominal operation, we will need to replace first seventeen cryomodules (136 cavities) with new ones, modified for cw operation at E_{acc} between 11 and 16 MV/m. The new cryomodules will have larger diameter 2-phase helium tube allowing for enhanced HL. Twelve out of seventeen replaced cryomodules can be re-installed at the end of the XFEL main linac (ML). In this scenario, the XFEL linac will consist of 113 cryomodules (904 cavities). Table 1 displays capacity of the present and upgraded cryogenic plant, and the total HL at 2 K and 1.8 K for the 113-cryomodule linac. One should note that the capacity of upgraded cryogenic plant will be similar to that of the existing CEBAF cryogenic refrigerator at JLab.

Table 1: Cryo-plant Capacity and HL for Two Operations

sp operation (2K)		cw/lp operation (1.8K)	
Cap. [W]	HL [W]	Cap. [W]	HL [W]
2450	1175	4980	3320

ISBN 978-3-95450-126-7

DESIGN CONCEPTS FOR A NEXT GENERATION LIGHT SOURCE AT LBNL*

J. N. Corlett#, A. Allezy, D. Arbelaez, K. Baptiste, J. Byrd, C. Daniels, S. De Santis, W. Delp, P. Denes, R. Donahue, L. Doolittle, P. J. Emma, D. Filippetto, J. Floyd, J. Harkins, G. Huang, J.-Y. Jung, D. Li, T. Pui Lou, T. Luo, G. Marcus, M. T. Monroy, H. Nishimura, H. A. Padmore, C. Papadopoulos, C. Pappas, S. Paret, G. Penn, M. Placidi, S. Prestemon, D. Prosnitz, H. Qian, J. Qiang, A. Ratti, M. Reinsch, D. Robin, F. Sannibale, R. W. Schoenlein, C. Serrano, J. Staples, C. Steier, C. Sun, M. Venturini, W. L. Waldron, W. Wan, T. Warwick, R. Wells, R. Wilcox, S. Zimmermann, M. Zolotorev, LBNL, Berkeley, CA, USA
C. Ginsburg, R. Kephart, A. L. Klebaner, T. Peterson, A. Sukhanov, FNAL, Batavia, IL, USA
D. Arenius, G. R. Neil, T. Powers, J. P. Preble, TJNAF, Newport News, VA, USA
C. Adolphsen, K. Bane, Y. Ding, Z. Huang, C. Nantista, C.-K. Ng, H.-D. Nuhn, C. Rivetta, G. Stupakov, SLAC, Stanford, CA, USA

Abstract

The NGLS collaboration is developing design concepts for a multi-beamline soft x-ray FEL array powered by a superconducting linear accelerator, operating with a high bunch repetition rate of approximately 1 MHz. The CW superconducting linear accelerator design is based on developments of TESLA and ILC technology, and is supplied by an injector based on a high-brightness, high-repetition-rate photocathode electron gun. Electron bunches from the linac are distributed by RF deflecting cavities to the array of independently configurable FEL beamlines with nominal bunch rates of ~100 kHz in each FEL, with uniform pulse spacing, and some FELs capable of operating at the full linac bunch rate. Individual FELs may be configured for different modes of operation, including self-seeded and external-laser-seeded, and each may produce high peak and average brightness x-rays with a flexible pulse format, and with pulse durations ranging from femtoseconds and shorter, to hundreds of femtoseconds. In this paper we describe current design concepts, and progress in R&D activities.

FACILITY OVERVIEW

The NGLS concept is an X-ray free-electron laser array powered by a superconducting accelerator capable of delivering electron bunches to a suite of independently configured FEL beamlines. Each beamline, operating simultaneously at a nominal initial repetition rate of 100 kHz, and with potential for MHz operation in some beamlines, will be optimized for specific science needs.

Figure 1 shows a schematic layout of the proposed facility. Most notable among the design features are a high-repetition-rate (MHz), high-brightness electron source, and a superconducting radio-frequency electron linac operating in CW mode that will provide bunches at high rate, high average beam power, and with uniform bunch spacing. These bunches will be distributed via a spreader system to an array of FELs, and each FEL will provide average brightness five or more orders of magnitude higher than existing light sources, and two or more orders of magnitude higher than other planned and under construction light sources. Each FEL will be seeded and feature independently adjustable central wavelength, polarization, photon pulse power, and ultrafast temporal resolution, with some beamlines having control of time-bandwidth trade-off. The high average electron beam power allows the capability of up to ~100 W of average X-ray power per beamline. Flux will vary from ~10^9 to ~10^{12} photons per pulse in the fundamental, depending on the wavelength, pulse duration, and FEL design. Figure 2 shows average brightness for self-seeded FELs, covering different photon energy ranges accessible with different electron beam energies.

A 2.4 GeV beam energy configuration has been reported previously [1], in this paper we also briefly outline capabilities for lower and higher electron beam energies, and corresponding photon energy reach, that could be provided by an initial NGLS and its potential upgrades. Each choice of beam energy retains the basic configuration shown in Fig. 1, and the unique technical capabilities of MHz repetition rate of uniformly spaced bunches, femtosecond pulse duration, ~10 meV FEL output bandwidth. The most critical science capabilities are accessed in the K- and L-edges of the earth-abundant elements, as well as diffraction/scattering in the few to several keV photon energy range. The NGLS approach allows flexibility in staging construction, by adjusting the number of cryomodules and FEL beamlines.

NGLS will provide a suite of unique features compared to existing or planned X-ray light sources, and the facility is being designed to expand capabilities in the most critical needs in X-ray science for imaging, structure determination, and spectroscopy. The facility will enable cinematic imaging of dynamics, reveal the structure of heterogenous systems, and allow for development of novel nonlinear X-ray spectroscopies. The uniform pulse spacing at a high repetition rate will provide unprecedented capabilities, accommodating more diverse and challenging experiments than those enabled by current or other planned sources.

*Work supported by the Director, Office of Science, of the U.S. Department of Energy under Contract No. DE-AC02-05CH11231
#jncorlett@lbl.gov

ISBN 978-3-95450-126-7

SLICE EMITTANCE OPTIMIZATION AT THE SwissFEL INJECTOR TEST FACILITY

Eduard Prat,* Masamitsu Aiba, Simona Bettoni, Bolko Beutner, Marc Guetg,
Rasmus Ischebeck, Sven Reiche, Thomas Schietinger
Paul Scherrer Institut, CH-5232 Villigen PSI, Switzerland

Abstract

Slice emittance measurements with uncompressed beams at the SwissFEL Injector Test Facility have demonstrated emittances for bunch charges between 10 pC and 200 pC well below the tight requirements of the SwissFEL planned at the Paul Scherrer Institute. We present the measurement methods, emittance tuning strategies and results of this effort.

INTRODUCTION

The SwissFEL facility planned at the Paul Scherrer Institute will produce coherent, bright, and short photon pulses covering a wavelength range down to 1 Å, requiring emittances between 0.18 and 0.43 mm mrad for bunch charges between 10 pC and 200 pC. To demonstrate the feasibility of our beam design a test facility of the injector section was built and has been operated since 2010.

The natural length scale along the bunch to analyze beam properties related to the FEL performance is the slippage length, which is in our case about 0.3 µm for a wavelength of 1 Å at 200 pC. Thus longitudinally resolved emittance studies, so called slice emittance measurements, are of great interest and are performed at various machines. Early studies employed slit absorbers in dispersive sections for energy-chirped beams. The typical longitudinal resolution of this approach is of the order picosecond [1]. With transverse deflecting RF-structures, as used at FLASH or LCLS, resolutions on the order of about 10 femtoseconds are possible [2, 3].

We present the methods used for our longitudinally resolved transverse phase-space measurements as well as the optimization techniques applied, followed by the final results.

THE SWISSFEL INJECTOR TEST FACILITY

For details of the SwissFEL Injector Test Facility we refer to [4]. Nominally electron bunches of charges between 10 pC and 200 pC are generated in a CTF3-type 2.6-cell standing-wave S-band RF photoinjector gun using a Ti:Sapphire laser. A longitudinal flat-top profile is approximated by pulse stacking 32 replica. The beam energy at the gun exit is 7.1 MeV. A solenoid close to the gun cavity is used for initial focusing (invariant envelope matching). Additional individually powered windings inside the gun solenoid allow for correction of normal- and skew-quadrupole components.

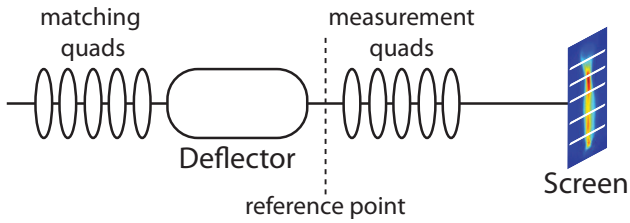

Figure 1: Schematic overview of the setup for slice emittance measurements at the SwissFEL Injector Test Facility.

Four S-band accelerating structures bring the beam energy up to the nominal value of 250 MeV. The structures are operated on-crest to maximize energy gain. Additional solenoid magnets around these structures allow for further control of the transverse optics. After some drift, which is to be used later for an X-band linearizing system and a bunch-compressor chicane, an S-band transverse deflecting cavity is used for longitudinally resolved measurements such as bunch length and slice emittance. The final beam energy is measured by a spectrometer at the beam dump.

SLICE EMITTANCE MEASUREMENTS

Moments of phase-space distributions can be determined by varying the betatronic beam transport between a reference point and a transverse beam profile monitor used for beam size measurements. Specifically we obtain the beam moments $\langle x_0^2 \rangle$, $\langle x_0'^2 \rangle$, and $\langle x_0 x_0' \rangle$ at the reference point from N measured beam sizes σ_i by using the corresponding transport functions R^i and solving the system of equations

$$\sigma_i^2 = {R_{11}^i}^2 \langle x_0^2 \rangle + {R_{12}^i}^2 \langle x_0'^2 \rangle + 2 R_{11}^i R_{12}^i \langle x_0 x_0' \rangle , \quad (1)$$

for $i \in 1, 2, ..., N$. From the measured beam moments the emittance and Twiss parameters can be derived. In principle three different transport functions are sufficient; in practice we use a much larger number of measurements and solve Eq. 1 by a least-square optimization (a detailed description of this procedure can be found in Ref. [5]). The quality and robustness of the measurement can be further increased by a proper choice of the transfer functions R^i, as described, e.g., in Ref. [6].

The above procedure is generic in the sense that it can also be used for slice-emittance measurements in combi-

* eduard.prat@psi.ch

ISBN 978-3-95450-126-7

CORRECTOR RESPONSE BASED ALIGNMENT AT FERMI

Masamitsu Aiba and Michael Böge PSI, Villigen, Switzerland
Davide Castronovo, Simone Di Mitri, Lars Fröhlich and Giulio Gaio
Elettra-Sincrotrone Trieste, Basovizza, Italy

Abstract

The components of a free electron laser (FEL) accelerator generally need to be beam-based aligned in order to meet the design performance. We are developing a new technique, where dipole corrector responses are used instead of orbit difference measurements. When an orbit feedback is running, any change in beam orbit is compensated by the actuators, i.e. the dipole correctors. For example, the spurious dispersion is measured through orbit differences for various beam momenta in the conventional way, while dipole corrector responses are examined in the new method. The advantages are localisation of misalignments, stable measurement as the orbit is kept constant, and automatic averaging and beam jitter filtering by the feedback loop. Furthermore, the method potentially allows us to detect transverse wakefield kicks. A series of machine development shifts to test and establish the method were successfully undertaken at FERMI@Elettra.

INTRODUCTION

The components of an FEL accelerator generally need to be beam-based aligned in order to meet the design performance. For instance, the spurious dispersion needs to be corrected to avoid emittance degradation.

We are developing a new technique, where dipole *corrector responses* are used instead of the conventional orbit difference. When an orbit feedback is running, any change in beam orbit is compensated by the actuators, i.e. the dipole correctors. The advantages of the new approach are localisation of misalignments, stable measurement as the orbit is kept constant, and automatic averaging and beam jitter filtering by the feedback loop.

A particular interest in applying the method to FERMI@Elettra [1], in addition to spurious dispersion measurement and correction, is to detect transverse wakefield kicks from accelerating structures and possibly to mitigate them by optimising the beam orbit.

The results from a series of machine development shifts at FERMI are presented.

FERMI@ELETTRA

FERMI@Elettra is a fourth generation, linac based FEL a schematic layout of which is shown in Fig. 1, and its main parameters are summarized in Table 1. Electron beams are accelerated up to ~1.5 GeV and sent to a current two undulator lines, namely FEL-1 and FEL-2, to generate photon beams, which are finally transported to the experiment beamlines.

Table 1: FERMI@Elettra Operational Parameters

Parameter	FEL-1	FEL-2
Wavelength (nm)	80~20	20~4
e-beam energy (GeV)	0.9~1.5	1.2~1.5
Bunch charge (nC)	0.5	0.5
Peak current (A)	<700	400~600
Bunch length, FWHM (fs)	600	500~700
Norm. emittance, slice (μm)	0.8~1.2	1.0
Energy spread, slice (keV)	150~250	150~250
Repetition rate (Hz)	10/50	10/50

The machine is equipped with a robust orbit feedback [2,3], allowing us to apply the method without any modification.

It is noted that the average iris radius of the accelerating structures of Linac-3 and Linac-4 (see Fig. 1) is only 5 mm. The effect of transverse wakefield was studied [4,5], and it was shown that the projected emittance growth can be significant when the bunch length is long (500 μm, full width) and the misalignments are more than 100 μm in these accelerating structures. Therefore, we need to take into account, in the beam-based alignment, not only the spurious dispersion but also the transverse wakefield.

CORRECTOR RESPONSE BASED ALIGNMENT

Dispersion Source Measurement and Correction

The conventional way of dispersion measurement is to measure orbit differences due to intentionally introduced beam momentum variations. The so-called dispersion free steering (DFS) [6] algorithm is widely used for correction.

Misalignments of accelerator components generate spurious dispersion and it propagates downstream. Therefore, even when a section of the machine is perfectly aligned, the dispersion measured with the conventional way is finite because of upstream dispersion sources. Moreover, it may vary when a modification is made upstream.

On the other hand, when an orbit feedback is kept running, the corrector response is zero in a perfectly aligned section in principle, and it is constant with upstream modifications.

ISBN 978-3-95450-126-7

DARK CURRENT TRANSPORT AND COLLIMATION STUDIES FOR SwissFEL

S. Bettoni, P. Craievich, M. Pedrozzi, S. Reiche, L. Stingelin, PSI, Villigen, Switzerland

Abstract

In all accelerating cavities a non negligible background of electrons can be generated by field emission (dark current), transported and further accelerated along the machine. The RF photoinjector guns, since operated at gradients also exceeding 100 MV/m, are critical sources of dark current. In nominal conditions a large fraction of this current is lost all along the machine, because of the phase mismatch at the entrance of the RF structures, a large mismatch of the optics and the energy acceptance limitations of the dispersive sections. In spite of this filtering a non negligible portion of unwanted charge can be transported and accelerated, therefore a careful estimate of the propagation is necessary to minimize radiation damages of the components and the activation of the machine. This paper describes the generation and the transport of dark current from the SwissFEL photo injector. The analysis is based on numerical simulations and experimental measurements performed at the SwissFEL Injector Test Facility (SITF). The model has been used to analyze the effect on the dark current transport of a low energy collimation system upstream the first travelling wave accelerating structure. A plate with several apertures has been installed in the SITF to benchmark the simulations and to verify the impact of the wakefields on the nominal beam.

THE DARK CURRENT ISSUE

The dark current in RF guns, due to the very high surface field they can reach, may be a very severe problem for the electronics sitting in the tunnel and the machine activation. A large fraction of this charge is typically lost in the low energy part upstream the first accelerating cavity. In spite of this, also if only a small fraction of the dark current is further transported downstream the accelerator, may be critical because lost at higher energy. The critical points in SwissFEL will be the two bunch compressors at 355 MeV and 2.1 GeV, the energy collimator, the septum and the undulators up to 5.8 GeV. To mitigate this problem we investigated the possibility of installing a collimator in the low energy region upstream the first accelerating cavity, where the charge can be lost in a controlled way and at low energy (maximum 7.1 MeV).

In theory all the accelerating cavities are sources of dark current, but we restricted our studies on the charge emitted by the gun, because simulations and measurements in the past indicated that for SwissFEL the other structures will not significantly contribute to the dark current due to the mismatch in the energy with the focusing optics[1].

THE SIMULATIONS

The emission of electrons from a surface with an electric field is a well known phenomenon, described by the Fowler-Nordheim equation:

$$I = A_e \cdot 1.54E-06 \cdot 10^{4.52\phi^{-0.5}} \frac{\beta_0^{\,2} E^2}{\phi} \exp\left(-\frac{6.53E9\phi^{1.5}}{\beta_0 E}\right) \quad (1)$$

where A_e is the effective emitting area in m^2, ϕ is the work function of the material in eV, E is the macroscopic electric field on the surface in V/m and β_0 takes into account the field enhancement factor due to the microscopic structures of the surface. The latter parameter depends not only on the material but also on the details of the surface cleaning and roughness. For polished copper in literature we found values from 30 up to more than 80 [2].

Differently than what done in the past [1], without loosing in generality, we developed a 1D emission model along the gun aperture, considering the cylindrical symmetry of the low energy area (RF structure and surrounding solenoid). We assume that the charge is emitted from the line which defines the profile of the gun and, only to visualize the final results, we mirror the particle distributions with respect to the axis of symmetry. This and the fact that we can neglect the space charge allow running a meaningful simulation of the SwissFEL Injector Test Facility (SITF) [3], 22.9 m long, in less than 15 minutes on a single core machine. To describe the field experienced by the particles we used the 3D field map of the RF gun to take into account the transverse components of the off-axis field. For each longitudinal position on the gun aperture the radius and the field are defined for a starting time, and, using Eq. (1) we calculate the emitted charge from each point. For any other time step we multiply the values of the field map with a sine function to consider the time dependence of the emitted charge in one RF period. In the SwissFEL gun the maximum emission is from the cathode plane and from the points close to the cell restrictions, as shown in Fig. 1.

To consider the filling time of the gun we weighted the maximum amplitude in one RF period with a function taking into account the increase of the peak field per period versus time. The contribution to the transported dark current is less for smaller surface fields, not only because of Eq. (1), but also because the electrons emitted at lower fields are differently accelerated from the gun on and over focused by the solenoid. To introduce this effect we excluded the possibility of directly tracking the particles generated all along the 2 μs long RF pulse, because of the high number of particles we should consider. Due to the ratio between the filling time (805 ns) and the RF period (333 ps), in fact, to simulate the charges generated at peak fields above 80% we should

ISBN 978-3-95450-126-7

SIMULATIONS OF A CORRUGATED BEAM PIPE FOR THE CHIRP COMPENSATION IN SWISSFEL

S. Bettoni, P. Craievich, M. Pedrozzi, S. Reiche, PSI, Villigen, Switzerland

Abstract

In short wavelength FEL designs, bunch compression is obtained by making the beam passing through a magnetic chicane with an energy chirp typically of a percent level. At SwissFEL, before injection into the undulator it is foreseen to remove the residual chirp using the wakes in the C-band accelerating structures of the linac. This scheme works well for the hard X-ray undulator line, which includes the largest accumulation of wakefields, but it leaves a residual chirp in the other undulator line for the soft X-ray beam line, midway in the main linac. Another possibility to remove the residual chirp consists in using the longitudinal wakefields generated by a corrugated beam pipe, as recently proposed by G. Stupakov et al. Before planning a dechirper section in a FEL, an experimental verification of the analytical formulae describing the wakefields is crucial. The SwissFEL injector test facility (SITF) fulfils all the necessary criteria to perform such a proof of principle. We are investigating the technical implementation to perform an experiment in SITF in the second half of 2014. In this paper we present the tracking studies performed to optimize the experiment layout.

INTRODUCTION

In the SwissFEL design two undulator lines are foreseen: Aramis to produce hard X-rays (wavelengths from 1 to 7 Angstrom) and Athos for the soft X-rays (wavelengths from 7 to 70 Angstrom) [1]. The bunch will be compressed up to a factor 150 by means of two compression stages. This process leaves a bunch energy chirp, which has to be removed before the lasing process in the undulator lines. For Aramis the wakes generated by the C-band structures in the main linac are enough to cancel it, whereas for Athos, midway in the main linac, they are not sufficient. A possible solution to this problem would be to use the longitudinal wakes generated by a corrugated beam surface or dechirper, as recently proposed by Stupakov and Bane for NGLS [2]. This idea is very attractive for all short wavelength FELs and several labs are interested to include it in their designs. In the PAL design the use of the corrugated beam pipe has been studied [3] and some experiments have been already performed [4]. A reasonable set of parameters for a possible experiment to verify the validity of the theoretical formulae which describe the wakefield in a corrugated beam pipe have been identified by NGLS and published in summer 2012 [5]:

- Bunch charge > 150 pC;
- Transverse slice emittance < 3 μm;
- A tuneable bunch length in the 4 ps to 8 ps FWHM range;
- A sub-ps resolution RF deflector;
- Energy resolution < 0.05%;
- Space to install the corrugated beam pipe (requested 1 m at least).

The SwissFEL Injector Test Facility [6] fulfils all these conditions and an experiment is planned for the second half of 2014 in the shadow of the U15 prototype undulator test [7].

We optimized the bunch properties, the machine operating point and the geometry of the dechirper we plan to install on the undulator by doing tracking studies to maximize the effect of the energy chirp compensation by the dechirper.

The Longitudinal Wakefields

The longitudinal point-charge wake function generated by a corrugated beam pipe *w(s)* is given by [2]:

$$w(s) \approx \frac{Z_0 c}{\pi a^2} H(s) \cos\left(2\pi/\lambda\, s\right) \tag{1}$$

where Z_0, c are the free space impedance, the vacuum speed of light and $H(s)$ is the unit step function. The other parameters define the geometry of the corrugation, with reference to Fig. 1.

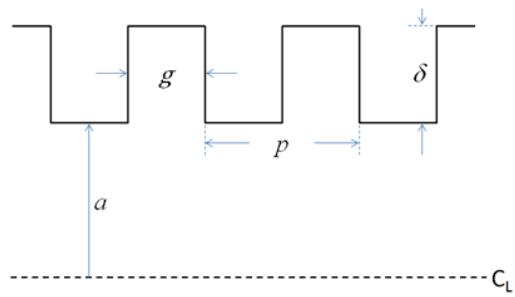

Figure 1: Schematic view of the corrugated beam pipe geometry [5].

The wavelength of the *w(s)* function is defined by the geometry of the corrugation and the semi-aperture as:

$$\lambda \equiv 2\pi \sqrt{\frac{a\delta g}{2p}} \tag{2}$$

The expression in Eq. (1) is valid only under the following assumptions:

- $\delta,\ p << a$
- $\delta \geq p$ (3)

The effect of the wake on the beam, given by the convolution of the bunch temporal profile and *w(s)*, is maximized if the bunch length σ_z is smaller than the wakefield wavelength, i.e. if the condition

ISBN 978-3-95450-126-7

SwissFEL INJECTOR DESIGN: AN AUTOMATIC PROCEDURE

S. Bettoni, M. Pedrozzi, S. Reiche, PSI, Villigen, Switzerland

Abstract

The first section of FEL injectors driven by photocathodes RF guns is dominated by space charge effects due to the low beam energy and the high charge density. An optimization of several parameters such as the emittance and the mismatch along the bunch has to be carried out in order to optimize the final performances of the machine. We focus on the design optimizations of the SwissFEL injector driven by the new PSI RF gun. This device, presently under construction at PSI, is planned to be installed at the end of 2013 in the SwissFEL Injector Test Facility (SITF) to be tested. Due to the number of variables and constraints influencing the beam properties, we developed a code to automatically perform such an optimization. We used this code to optimize the 200 pC operating point of SwissFEL and to fine tune other charge configurations down to 10 pC. With this optimization we obtained a noticeable reduction of the slice emittance with the new PSI gun compared to the CTF2 gun, presently installed in the SITF and on which the old lattice optimization was based. The same code with minor modifications has been successfully applied to the facility.

THE AUTOMATIC OPTIMIZER

The optimization code is based on a Matlab function [1] used to iteratively run a space charge tracking code, in our case Astra [2]. The steps of the function are:

1. The input file is written with given starting parameters (lattice, initial electrons phase space, RF and magnet parameters);
2. The job is submitted to a computer cluster;
3. A sub-function checks if the job finished to run and at this moment the figure of merit (FOM) is calculated;
4. A new input file is generated based on the results of the previous simulation;
5. The job is submitted to the cluster.

These points are repeated until the FOM variation is smaller than a user defined tolerance. The code finds a solution for a typical case of three variables in about 20 iterations and in less than hundred for six or seven variables cases. Each iteration with 5000 particles takes about 5 minutes on the PSI computer cluster running with 8 cores. In maximum about 8 hours we can therefore have a solution. In our case the Matlab function *fminsearch*, based on the derivative-free method, is driving the optimization, but it can be substituted by any Matlab minimizing function or by a user defined algorithm. In the next section the application of this optimizer to the SwissFEL injector is presented.

THE SWISSFEL OPTIMIZATION

The SwissFEL photoinjector is based on a 3 GHz RF gun pulsed by a UV laser (266.7 nm wavelength) on a copper cathode. The photoelectrons are accelerated by two S-band cavities up to about 130 MeV energy, before entering the laser heater and being further accelerated to ~330 MeV and compressed [1]. All the optimizations presented in this paper are run up to the exit of the fourth structure at energy of about 250 MeV (to be well out of the space charge regime) with the laser heater off except when the emittance preservation is checked in this line and beyond.

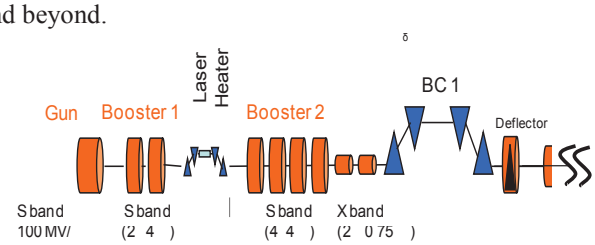

Figure 1: SwissFEL schematic layout [1].

The final slice emittance at the first undulator entrance downstream the main linac strongly depends on the final emittance at the end of the injector (less than 10% difference for the optimized case [1]). In this space charge dominated regime the emittance is influenced by several parameters. The most effective ones are acting at the lowest beam energy between the gun and the first accelerating cavity (E<8 MeV), where we can obtain 30% emittance variation with less than 1% change, so a careful optimization is mandatory [3].

The first parameter, which is fixed during the optimization, is the gun phase, determined by minimizing the energy spread. This is another fundamental quantity for the final beam quality and, with fixed gun geometry and gradient, it depends only on the phase.

Defined in this way the gun phase, the final injector emittance depends strongly on the strength of the solenoid at the gun exit, the laser pulse shape both in longitudinal (fixed by the final current at the entrance of BC1) and in the transverse direction, and the position of the first accelerating cavity. The dependence on the gradient, phase and magnetic field of the first accelerating structure and the corresponding solenoid around it is weaker. In a multivariable problem it is extremely important to restrict the number of variables as much as possible, to ease the convergence of the algorithm and to avoid being trapped in a local minimum. Because of this in the first step of the optimization we varied only the strength of the gun solenoid, the transverse size of the laser, and the position of the first accelerating cavity. Only after a good point has been found, we include the other variables in the optimizer to refine the result.

ISBN 978-3-95450-126-7

RF DESIGN APPROACH FOR AN NGLS LINAC*

J. M. Byrd, J. Corlett, L. Doolittle, P. Emma, A. Ratti#, M. Venturini, R. P. Wells, LBNL, Berkeley, CA, U.S.A.
C. Ginsburg, R. Kephart, T. Peterson, A. Sukhanov, FNAL, Batavia, IL, U.S.A.
D. Arenius, S. Benson, D. Douglas, A. Hutton, G. Neil, W. Oren, G. Williams, JLab, Newport News, VA, U.S.A.
C. Adolphsen, C. Nantista, SLAC, Menlo Park, CA, U.S.A.

Abstract

The Next Generation Light Source (NGLS) is a design concept for a multi-beamline soft X-ray FEL array powered by a superconducting linear accelerator, operating in CW mode with evenly spaced bunches at approximately a 1 MHz repetition rate. This paper describes the concepts under development for a linac based on minimal modifications to the design and technology of the International Linear Collider technology in order to leverage the ILC community's extensive investment in R&D and infrastructure development. Particular emphasis is given here to high loaded-Q operation and microphonics control, as well as high reliability and operational up time.

NGLS LINAC OVERVIEW

The NGLS uses a single-pass, continuous-wave (CW), superconducting, high-brightness electron linac to provide high-repetition-rate beam to multiple FELs. The NGLS main parameters are presented elsewhere in this Proceedings [1].

The linac has four sections of accelerating cryomodules, separated by other elements: a laser heater, a 3rd harmonic linearizer system (also a series of cryomodules operating at a higher harmonic frequency) and two bunch compressors. The linac is shown in Fig. 1.

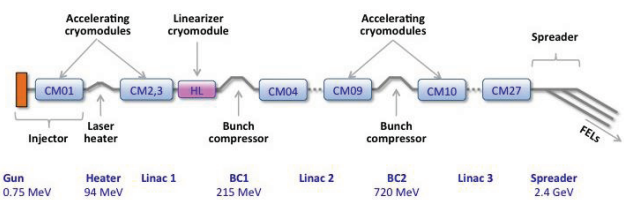

Figure 1: NGLS linac schematic layout.

LINAC RF DESIGN

RF Parameters

The choice of SCRF cavity frequency for NGLS is ultimately driven by the need to minimize development cost by taking advantage of existing proven technology that meets the needs of the NGLS. We plan to take advantage of the extensive worldwide investments in TESLA/ILC/XFEL technology; this sets most of the RF parameters for the linac, when combined with the desire to run at a high loaded Q to minimize RF source costs. Table 1 summarizes the main RF parameters.

Table 1: Main RF Parameters

RF frequency	1300	MHz
Operating temperature	1.8	K
Average operating grad.	12-20	MV/m
Average Q_0 per CM	$2x10^{10}$	
Cavity length	1.038	m
R/Q	1036	Ohm
Coarse tuner range	600	kHz
Fine tuner range	2	kHz
Lorentz detuning	1.5	$Hz/(MV/m)^2$
Number of cav. per CM	8	
Peak detune allowance	15	Hz
Q_{ext}	$3.2x10^7$	
Min. RF power per cavity	5.4	kW
Total cavity dynamic load	12.5	W
Total CM dynamic load	100	W

CAVITY AND CRYOMODULE DESIGN

Cavity Considerations

The differences in operating ILC-like cavities in CW mode go beyond the need for increased heat rejection. The emphasis on resonance control moves from coping with the hammer-like effect of pulsed Lorentz forces, to minimizing the impact of microphonics-induced frequency shifts due to mechanical vibrations. For the NGLS cavities the most important factor is to operate at a high loaded Q, which results in reduced power consumption. This goal is realized by successful control of microphonics. We have chosen to allow for a 15 Hz peak detuning from microphonic effects without having to de-rate the cavity field due to limited RF source power. This choice corresponds to a loaded Q of ~3.2 $x10^7$ and has a direct impact on the requirements for the RF plant. A smaller allowance for microphonics would result in significant cost savings but could compromise reliability. We are therefore monitoring progress in the community to identify the most reasonable compromise.

Tuners, Couplers and HOM Dampers

Resonance control is particularly important because we want to operate at high loaded Q and therefore we

*Work supported by the Director, Office of Science, of the U.S. Department of Energy under Contract No. DE-AC02-05CH11231.
#aratti@lbl.gov

ISBN 978-3-95450-126-7

SUPERCONDUCTING LINAC DESIGN CONCEPTS FOR A NEXT GENERATION LIGHT SOURCE AT LBNL*

J.N. Corlett#, J. Byrd, L. Doolittle, P.J. Emma, A. Ratti, F. Sannibale, M. Venturini, R. Wells, S. Zimmermann, LBNL, Berkeley, CA, USA
C.M. Ginsburg, R.D. Kephart, A.L. Klebaner, T.J. Peterson, A.I. Sukhanov, FNAL, Batavia, IL, USA
D. Arenius, G.R. Neil, T. Powers, J.P. Preble, TJNAF, Newport News, VA, USA
C. Adolphsen, C.D. Nantista, SLAC, Stanford, CA, USA

Abstract

The NGLS collaboration is developing design concepts for a multi-beamline soft X-ray FEL array powered by a superconducting linear accelerator, operating in CW mode, with a high bunch repetition rate of approximately 1 MHz [1]. The superconducting linear accelerator design concept is based on existing TESLA and ILC technology, to be developed for this CW application in a light source. We outline design options and preferred approaches to the linac.

NGLS OVERVIEW

Recent advances in X-ray FELs are extending the reach of photon science, and concurrently superconducting RF technologies have developed the ability to deliver high average power electron beams. There is now significant interest in increasing the average power of X-ray lasers, and in response to this need the NGLS (Next Generation Light Source) concept has been developed for an X-ray free-electron laser array powered by a superconducting accelerator capable of delivering electron bunches to a suite of independently configured FEL beamlines [1]. Each beamline, operating simultaneously at a nominal initial repetition rate of 100 kHz, and with potential for MHz operation in some beamlines, will be optimized for specific science needs.

Most notable among the design features are a high-repetition-rate (MHz), high-brightness electron source, and a superconducting radio-frequency (SCRF) electron linac operating in CW mode that will provide bunches at high rate, high average beam power, and with uniform bunch spacing. Choices for beam energy and pulse repetition rates are motivated by the science needs for soft X-ray laser pulses, and FEL technology, and necessitate the adoption of CW SCRF technology for the linac.

The linac will accept electron bunches from the injector, providing acceleration and bunch compression, before directing the beam to the spreader for distribution into the separate FEL undulator lines. Bunches from the linac will be distributed via a spreader system to an array of FELs, and each FEL may provide average brightness five or more orders of magnitude higher than existing light sources, and two or more orders of magnitude higher than other planned and under construction light sources. The high average electron beam power allows the capability of up to ~100 W of average X-ray power per beamline.

NGLS LINAC APPROACH

The CW SCRF linac will provide a "backbone" for delivering high-brightness and high-repetition-rate electron beams to an array of independent FELs. The machine design concept (see Figure 1) is for a maximum bunch charge of 300 pC and nominal 1 MHz repetition rate (i.e., an average current of 300 μA), and with upgrade paths consistent with a range of lower bunch charge at increased rate while maintaining average current. A variety of bunch time structures may be accommodated by the injector and linac, and our conceptual design allows flexibility to accommodate the desired science scope. The nominal electron beam energy of 2.4 GeV has been chosen so as to be able to produce tunable FELs which together cover an operating range from 100 eV and up to 1.2 keV photon energy in the fundamental, and 6 keV and beyond in harmonics. Table 1 shows linac and cryosystems parameters for this configuration. An alternate, low cost configuration with a 1.2 GeV linac has also been studied, which could produce a photon energy range of 50 – 720 eV in the fundamental – still accessing the K- and L-edges of the most abundant elements. Upgrade options include adding cryomodules to the main linac to increase beam energy, and a 3.5 GeV linac could extend the X-ray reach to 5 keV in the fundamental (with limited tuning range), and higher electron beam energies providing harder X-rays (5 GeV reaches the 10 keV range). For the highest energies additional cryomodules may be placed in a spreader arm dedicated to the hardest X-ray FELs, with soft X-ray capabilities provided by the better-matched lower energy beam.

The NGLS linac design is currently based on the use of TESLA-type cavities, and ILC cryomodule design developed for CW operation, including use of discrete cryomodules with warm/cold transitions at each end. The NGLS approach to the CW superconducting linac will be to maximize use of existing expertise, designs, infrastructure, and industrialization. Engineering optimizations of existing components and systems can enhance performance and reliability over today's designs, and will be needed to meet NGLS requirements, reduce costs, and deliver a reliable and cost-effective CW SCRF electron linac.

*Work supported by the Director, Office of Science, of the U.S. Department of Energy under Contract No. DE-AC02-05CH11231
#jncorlett@lbl.gov

ISBN 978-3-95450-126-7

TRANSVERSE DEFLECTING STRUCTURES FOR BUNCH LENGTH AND SLICE EMITTANCE MEASUREMENTS ON SwissFEL

P. Craievich, R. Ischebeck, F. Loehl, G.L. Orlandi, E. Prat, PSI, Villigen, Switzerland

Abstract

The SwissFEL project, under development at the Paul Scherrer Institut, will produce FEL radiation in a wavelength range from 0.1 nm to 7 nm. The facility consists of an S-band RF-gun and booster, and a C-band main linac which accelerates the beam up to 5.8 GeV. Two magnetic chicanes will compress the beam between 2 fs rms and 25 fs rms depending on the operation mode. The bunch length and slice parameters will be measured after the first bunch compressor (330 MeV) by using an S-band transverse deflecting structure (TDS). A C-band TDS will be employed to measure the longitudinal parameters of the beam just upstream of the undulator beam line (5.8 GeV). With the designed transverse beam optics, an integrated deflecting voltage of 70 MV is required in order to achieve a longitudinal resolution on a femtosecond scale. In this paper we present the TDS measurement systems to be used at SwissFEL, with a particular emphasis on the new C-band device, including hardware, lattice layout and beam optics.

INTRODUCTION

Complete characterization of the beam phase space by means of measurements of the bunch length and of the transverse slice emittance are important tasks for commissioning and optimization of SwissFEL [1]. A Transverse Deflecting Structure (TDS), such as an iris loaded wave guide or multi cell standing wave structures, is a powerful tool to reach this aim. Two TDS measurements systems will be positioned at two points in the linac: the first one (TDS-1) at 330 MeV (low energy region), after the first bunch compressor (BC1), the second (TDS-2) at the linac end (high energy region), before the upstream of the undulators. Figure 1 shows the layout of the BC1 and injector diagnostic sections where the TDS-1 is indicated. The TDS-1 will operate in a vertical streaking mode to allow measurements of the horizontal slice emittance and bunch length. This will allow the efficiency of the first compression to be estimated. Beam slice emittance will be investigated by a multi-quadrupole scan technique combined with the TDS. By means of the TDS, the beam is vertically streaked and a multi-quadrupole scan is performed only in the horizontal direction, with the constraint of keeping the vertical beam size constant over the whole scan. For this purpose five quadrupoles are foreseen to be placed downstream of the TDS. Reconstruction of the longitudinal phase space will be performed by means of the spectrometer line.

The second measurement system based on TDS is foreseen at the linac-end and with a beam mean energy between 2.1 and 5.8 GeV. Figure 2 shows the layout of the linac-end, Aramis energy collimator and diagnostic section and, as in the injector diagnostic section, electron beam will be vertically streaked and a multi-quadrupole scan will be performed in order to measure the slice emittance. The longitudinal phase space will be measured in the Aramis collimator before the undulator line. Two standard operational modes are foreseen for the SwissFEL at 200 pC and 10 pC for the long and short pulse options, respectively. Tables1 and 2 contain the beam and optical parameters for both long and short pulse options that have been used for the calculations in the following sections.

Table 1: Beam and optical parameters involved in the streaking process at TDS-1 diagnostic sections for both pulse length options.

Parameter	Sy.	Long	Short	Unit
Beam energy	E	330	330	MeV
β@TDS	β_d	30	30	m
β@screen	β_s	$\sim$5	$\sim$5	m
Bunch length	σ_t	290	220	fs
Emittance	$\gamma\varepsilon_y$	0.30	0.11	μrad

Table 2: Beam and optical parameters involved in the streaking process at TDS-2 diagnostic sections for both pulse length options. HR is high resolution option.

Parameter	Sy.	Long	Short	HR	Unit
Beam energy	E	5.8	5.8	2.1	GeV
β@TDS	β_d	30	30	70	m
β@screen	β_s	$\sim$25	$\sim$25	$\sim$5	m
Bunch length	σ_t	25	2	2	fs
Emittance	$\gamma\varepsilon_y$	0.43	0.18	0.18	μrad

The measurement of the transverse slice emittance requires short portions of the bunch length to be resolved at the screen after the bunch is streaked. In general, the TDS measurement strategy at SwissFEL consists in resolving the beam profile with at least 10 slices. As this will be non-critical for TDS-1, most of the TDS-2 measurements will also be achieved with the nominal beta function at the TDS and the nominal operational beam energy of SwissFEL. However, towards the shortest bunch lengths, the maximum deflecting voltage of actual deflecting structures imposes limitations on the achievable resolution. The most challenging case is the short pulse operational mode with beam energy of 5.8 GeV and a nominal rms bunch length of 2 fs. This value corresponds to the TDS-2 resolution limit with nominal beam parameters. In order to provide a reasonable "sliced beam parameter measurement" in

ISBN 978-3-95450-126-7

BEAM DIAGNOSTICS REQUIREMENTS FOR THE NEXT GENERATION LIGHT SOURCE*

S. De Santis#, J. Byrd, J. Corlett, P. J. Emma, D. Filippetto, M. Placidi, H. Qian,
F. Sannibale LBNL, Berkeley, CA 94720, USA

Abstract

The Next Generation Light Source (NGLS) project, in its standard configuration, consists of a 2.4 GeV superconducting linac accelerating sub-1 μm normalized emittance bunches used to produce high intensity soft X-ray short pulses from multiple FEL beamlines. The 1 MHz bunch repetition rate, and the consequent high beam power, present special challenges, but also opportunities, in the design of the various electron beam diagnostic devices. The wide range of beam characteristics, from the photoinjector to the undulators, require the adoption of different diagnostics optimized to each machine section and to the specific application of each individual measurement. In this paper we present our plans for the NGLS beam diagnostics, discussing the special requirements and challenges.

INTRODUCTION

The design concepts for the NGLS, a proposed fourth generation light source, have been described in [1-2]. Low-emittance bunches are generated at a high repetition rate, accelerated in a superconducting linac while being shortened by bunch compressors, and fed to various FEL beamlines by an RF-based spreader for the production of ultra-short soft X-ray pulses. The delivery of bunches with appropriate characteristics for the generation of such pulses relies on the accurate measurements of a number of beam parameters (Tab. 1) throughout the machine.

Table 1: Electron Beam Parameters

Final Beam Energy (GeV)	E_f	2.4
Bunch Charge (pC)	Q_b	300
Bunch Length (fs)	σ_t	2900-170
Bunch Transverse Size (μm)	σ_x, σ_y	100's-40
Normalized Emittance (μm)	ε_N	1
Relative Energy Spread (%)	σ_E	1-0.05
Beam Power (kW)	P_{beam}	720
RF Frequency (GHz)	f_{RF}	1.3
Bunch Repetition Rate (MHz)	f_{rep}	1

*Work supported by the U.S. Department of Energy under Contract No. DE-AC02-05CH11231.
#sdesantis@lbl.gov

The high bunch repetition rate and consequent elevated beam power are a distinctive feature of the NGLS which present special challenges from the point of view of the beam diagnostics, not usually encountered in linear accelerators, but on the other hand offer unique opportunities as it will be described in the following sections.

The type of beam measurements that need to be performed can be subdivided in three main categories:

- Bunch-by-bunch measurements.
- Sampled beam measurements.
- Measurements for machine commissioning/set-up.

These categories will be described in the following sections, with the individual measurements belonging to each one and the devices we plan to use.

BUNCH-BY-BUNCH MEASUREMENTS

Measurements belonging to this category need to be performed on every single bunch and have to be minimally invasive therefore. These are the measurements used for the trajectory control, feedback systems, timing measurements provided to users. Additionally, bunch-by-bunch charge measurements can be used as part of the machine protection system, although in this case the single bunch resolution level is not necessary, but it is sufficient to perform such measurement averaged over a adequately short time window, which for a 1 MHz bunch repetition rate can be of the order of

Beam Trajectory

The transverse position of each bunch is measured all along the linac. The target requirement for the trajectory control is to maintain an RMS transverse stability below 5% of the beam transverse dimensions. This means that the position monitors have to measure the bunch position with a resolution of 10 μm or better. We plan to use stripline BPM's derived from the ones we have designed for the Advanced Photoinjector Experiment currently in use [3]. With a 300 pC bunch charge in our standard 1.5" ID circular beampipe the readout electronics currently developed can easily achieve the required resolution in a single-bunch measurement. The shorted stripline design allows to install the BPM's in a compact fashion together with the quadrupoles.

Although a simpler button BPM could achieve the same resolution at full charge, we have chosen striplines with their larger coupling impedance in order to be able to satisfy the resolution requirement even with a reduced

ISBN 978-3-95450-126-7

STATUS OF THE MANUFACTURING PROCESS FOR THE SWISSFEL C-BAND ACCELERATING STRUCTURES

Urs Ellenberger, Ludwig Paly, Heinrich Blumer, Charles Zumbach, Florian Loehl, Markus Bopp, Hansrudolf Fitze, Paul Scherrer Institut, 5232 Villigen PSI, Switzerland

Abstract

For the SwissFEL project a total of 104 C-band (5,712 GHz) accelerating structures are needed. After developing and radio frequency (RF) testing of several short structures (0.5m), three 2meter prototypes have been produced successfully in-house. Avoiding any RF-tuning after fabrication, a high precision machining of the components is necessary. Special procedures were developed and handling equipment was built in order to maintain the accuracy during stacking and vacuum brazing of the parts for the C-band structures. This paper summarizes the manufacturing techniques and the mechanical test results.

INTRODUCTION AND OVERVIEW

The linear accelerator (LINAC) of the SwissFEL consists of 104 C-band structures each of 2m length. They are aligned along a row of 300m and are used to accelereate an electron bunch to an energy of 5.8 GeV before the lasing process is initiated in the subsequent undulator section.

The manufacturing of C-band structures has to conform to stringent requirements to minimize cost and to achieve a stable process for an economical industrial series production over years:

- Target precision of one single copper cell of +/- 2 µm with a surface roughness R_a of 25 nm
- After brazing all individual volumes of the 108 copper cells match the specified klystron frequency (5'712 MHz) and the nominal phase advance of 120°
- Perpendicularity of less than 50 µm before and after vacuum brazing of 108 copper cells and of two J-couplers to produce one 2m C-band structure
- Therefore no additional tuning of each individual cell and iteratively measure its frequency would be required after brazing

Encouraged by the results of test structures [1] we have developed, built and improved the equipment necessary to produce the 2m C-band structures to meet the requirements as summarized above. In this paper we report on the procedures and handling equipment of the manufacturing process and on the mechanical test results to meet the stringent requirements. The results of RF and power testing of the first 2m C-band structures are reported in a companion paper of this conference.

MANUFACTURING

The manufacturing process of a copper cell is summarized in [1] when building short test structures. In this paper we describe in more detail how we have proceeded to achieve the precision required to meet the stringent specifications of the C-band LINAC.

Machining

The copper for the C-band cells is oxygen free, high-conductivity and forged in three-dimensions. Because of the forging-process we have a homogenous distribution of only small pores (not detectable with ultrasonic probes), a stress-free and inherently stable material due to the additional heat-treatment (forging) with a rather large grain size of about 400 µm. To achieve the precision required per cup the stress-free material is mandatory even if chip formation is less favourably for large grain size. On the other hand this is related to large grain boundaries which are less prone to breakdowns in high high-voltage RF fields (28 MV/m at 5'712 MHz).

The raw-cut copper pieces are first pre-turned on a conventional and numerical controlled lathe to a precision of about 10 µm. The finish of the cups to a precision of +/- 2 µm is performed on a sturdy and pneumatically stabilized slanted bed lathe (Hembrug) as depicted in figure 1. A defined sequence of cuts (each cut prepares the next one) with poly- and mono-crystalline diamond (PCD, MCD) tools is required in a temperature and humidity controlled machining compartment of the lathe.

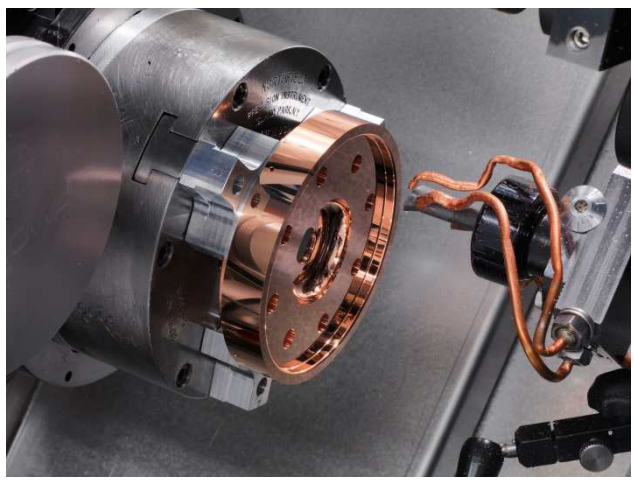

Figure 1: Copper cup in chuck of slant bed lathe after machining with monocrystalline tool.

For this purpose and for the blowing air for machining the copper we use ambient air of the temperature-controlled and air-conditioned room (18.50°C +/- 0.1°C at less than 50% relative humidity and oil-free). With this we finally reach a measured precision of +/- 2 µm on the copper cups. Heat input on the copper cups is mainly caused by the edge of the turning diamond tool. Due to temperature fluctuations during the day while two people

ISBN 978-3-95450-126-7

OPTIMIZATION OF DIELECTRIC LOADED METAL WAVEGUIDES FOR ACCELERATION OF ELECTRON BUNCHES USING SHORT THZ PULSES *

A. Fallahi †, F. X. Kärtner, CFEL-DESY, Hamburg, Germany
L. J. Wong, A. Sell, RLE-MIT, Cambridge, USA

Abstract

The last decade has witnessed extensive research efforts to reduce the size of charged particle accelerators to achieve compact devices for providing relativistic particles. To this end, various methods such as laser plasma and dielectric wakefield acceleration are investigated and their pros and cons are studied. With the advent of efficient THz generation techniques based on optical rectification, THz waveguides are also considered to be proper candidates for compact accelerators. Sofar, the proposed schemes toward high power THz generation are capable of producing short pulses, which dictates the study of particle acceleration in the pulsed regime rather than continuous-wave regime. Therefore, THz waveguides are more suitable than cavities for the considered purpose. Consequently, various effects such as group velocity mismatch and group velocity dispersion start to influence the acceleration scenario and impose limits on the maximum energy gain from the pulse. In this contribution, we investigate electron bunch acceleration and compression in dielectrically loaded metal waveguides for the THz wavelength range and present design methodologies to optimize their performance.

INTRODUCTION

Linear accelerators are the major tools for providing relativistic particles [1]. Linear colliders for high-energy physics, high-power proton linacs for advanced neutron sources, small linacs for medical applications, free electron lasers for small wavelength sources, and high frequency power generators are examples of devices in which accelerators play significant roles. The current research on linacs focuses on new performance levels with better beam quality and lower power requirements. Acceleration of a particle using a high frequency beam is one of the potential ways to enhance the performance of the particle accelerators. The main concept of this technique is exposing an electron bunch to a traveling beam with a properly selected phase and beam spatial profile, and consequently accelerate the electrons using the electric and magnetic fields of the propagating beam. The optimum operating wavelength of the accelerator has been often a topic of elaborate discussions in the community. On one side, the available efficient sources limit the operation wavelengths to specific ranges and on the other the amount of charge needed for the application of interest and the overall efficiency of the device give priorities to other wavelength ranges. Linear accelerators in radio frequency (RF) range has been widely studied and matured in the last century, owing to the availability of high power RF klystrons [2]. By the emergence of high power lasers and the techniques in ultrafast optics, research on laser-plasma acceleration received substantial attention [3]. The RF regime often leads to devices with large dimensions whereas the laser acceleration exhibits acceleration in very small sizes with very limited aptitude in terms of charge amount. In this regard, high power short THz pulses available from optical rectification [4, 5] show strong potentials for realizing compact accelerators with large charge capacities compared to optical counterparts [6, 7].

This paper focuses on the design and implementation of a scheme in which electrons are accelerated by a THz beam. For this purpose, a THz waveguide is designed considering the required specifications for the electron acceleration and the beam requirements. Subsequently, the interaction between the electron and the guided beam is investigated. The pros and cons of THz acceleration of an electron bunch is examined based on the theoretical simulations. In the following sections, the step by step analysis and optimization is presented with the goal of achieving an optimal performing THz accelerator.

DIELECTRIC LOADED METAL WAVEGUIDES

To accelerate charged particles using an electromagnetic wave a longitudinal electric field is always required for transferring energy to the electrons. One approach to realize such an acceleration gradient is coupling the electromagnetic radiation into a waveguide. The phase velocity of the wave is synchronized with the velocity of the electron beam, which is always less than the speed of light or in case of relativistic beams is very close to it. However, the phase velocities of electromagnetic waves in empty uniform waveguides always exceed the speed of light in vacuum. Therefore, this parameter must be slowed down to the particle velocity to achieve considerable acceleration. This can be accomplished by loading waveguides with dielectrics as is done in linear accelerators based on dielectric loaded metal waveguide [8].

Consequently, the structure to analyze is a multilayer dielectric-loaded metallic waveguide (Fig. 1) and the goal of the analysis is evaluating the propagation constants of the modes and the acceleration properties of the waveg-

* Work is supported by DARPA under contract N66001-11-1-4192 and the Center for Free-Electron Laser Science, DESY Hamburg
† arya.fallahi@cfel.de

ISBN 978-3-95450-126-7

THE PHOTOCATHODE LASER SYSTEM FOR THE APEX HIGH REPETITION RATE PHOTOINJECTOR*

D, Filippetto†, L. Doolittle, G. Huang, G. Marcus, H. Qian, F. Sannibale
LBNL, Berkeley, CA 94720, U.S.A.

Abstract

The APEX photoinjector has been built and commissioned at LBNL. A CW-RF Gun accelerates electron bunches to 750 keV with MHz repetition rate. High quantum efficiency photocathodes are being tested with the help of a load lock system, with different work functions. The photocathode drive laser is thus conceived to provide up to 50 nJ per pulse in the UV and 250 nJ per pulse in the green at 1 MHz, with transverse and longitudinal shaping (flat top, 60 ps FWHM). A transfer line of about 12 meters has been designed and optimized to optimize position jitters. Remote control of repetition rate, energy and position have been implemented on the system, together with offline and online diagnostic for beam monitoring. Here we present the laser system setup as well as the first measurements on longitudinal pulse shaping and jitter characterization.

INTRODUCTION

The Next Generation Light Source (NGLS) is an high repetition rate Soft X-ray Free Electron Laser recently proposed at LBNL. It is conceived as a seeded machine, delivering to the user end stations fully coherent X-ray pulses at MHz repetition rate, with pulse duration ranging from 100 down to the single femtosecond [1]. The unprecedented average brightness will open the way to a series of new experiments and new techniques in all the fields of natural sciences, from chemistry to biology, to material science and condensed matter.

Among the various challenging aspects of the machine, the development of the photoinjector is of great importance as it directly impacts the FEL performances (and strongly affects the total cost). An R&D effort on high repetition rate photoinjectors has lead LBNL to the design and construction of the Advanced Photoinjector Experiment (APEX), a CW normal conducting electron gun, operating at 186 MHz. The accelerating electric field is 20 MV/m and the electron beam is accelerated to 750 keV energy in a 4 cm gap. The beam properties are then measured in the subsequent diagnostic beam line [2].

A load-lock system allows cathode replacement without exposing them to air. This feature, together with a vacuum pressure in the low 10^{-11}torr, makes APEX a perfect candidate for testing high quantum efficiency photocathode materials in rf environment, where surface contamination is a concern (e.g. multi-alkali [5]). The photocathode drive laser needs to be able to produce MHz pulses at different wavelengths (from 532 nm down to 213 nm) for cathode physics, with enough energy per pulse to produce the hundreds of pC needed by the NGLS, and with longitudinal and transverse pulse shape optimized for electron beam dynamics. The 12 meters transport line takes the pulses to the final laser table where most of the diagnostic for pulse shape, energy and position is hosted. In what follows we give a detailed description of the different laser subsystems.

* Work supported by the Director of the Office of Science of the US Department of Energy under Contract no. DEAC02-05CH11231
† dfilippetto@lbl.gov

THE LASER SYSTEM

The fiber laser oscillator and amplification stage were provided by the Lawrence Livermore National Laboratory (LLNL), in november 2010. The Yb-doped fiber oscillator is pumped with a 980 nm CW diode, producing output pulses at 37.14 MHz, with ∼mW output power around 1030-1070 nm. The mode locking is achieved via nonlinear polarization rotation in the fiber, and the dispersion is controlled by the presence of a grating pair in the cavity. A chain of 4 pre-amplifiers gets the seed from the oscillator. After the first two pre-amplifiers, the repetition rate is decreased to 1 MHz by a acousto-optic kicker (AOM), driven by a 2 W 100 MHz pulsed rf signal synchronous with the oscillator. The AOM's rise and fall time are at the 20-30 ns level. A 100 m fiber is then used to stretch the pulse to around 100 ps, the bandwidth around 1064 nm is selected by an interferometric filter, and then sent in the last 2 preamplifiers and the final amplifier. The laser energy at the end of the chain is around 1.5 μJ, but it lowers down to 0.8 after re-compression with a grating pair. A KDP pockels cell (PC) is inserted at this point together with a half wave plate and a polarizing beam splitter, and it is used for low repetition rate operations (from 10 KHz down to 1 Hz). The HV power supply for the PC produces 3 KV pulses with 5 ns duration, in order to efficiently separate pulses. Despite its low non-linearity, KDP has been chosen to maximize the PC extinction rate. The final pulse, with a FWHM duration of 700 fs (Fig. 1), is used for second (SHG) and fourth (4HG) harmonic generation. A 3 mm non critically phase matched LBO crystal was used for SHG. The crystal is heated to 160 deg, and produces 270 mW output energy at 530 nm. The green pulse is then used in 4HG to get 50 mW UV in a 1.75 mm BBO crystal, via type I phase matching.

Laser Longitudinal Shaping

One of the laser requirements for the NGLS is a 60 ps longitudinally flat top beam. This is required for op-

ISBN 978-3-95450-126-7

SwissFEL CATHODE LOAD-LOCK SYSTEM

R. Ganter, M. Bopp, R. Gaiffi, T. Le Quang, M. Schaer, T. Schietinger, L. Schulz, L. Stingelin, A. Trisorio, M. Pedrozzi, PSI, Villigen, Switzerland

Abstract

The SwissFEL electron source is an RF photo-injector in which the photo-cathode plug can be exchanged. Without load-lock, the cathode exchange takes about one week and cathode surface gets contaminated in the atmosphere during installation, leading to unpredictable quantum efficiency (QE) fluctuations. This motivated the construction of a load lock system to prepare and insert cathodes in the photo-injector. This load-lock system gives the possibility to prepare the cathode surface with methods like annealing. The QE can be checked and the plug can be inserted in the gun without breaking vacuum. This system will eventually give the possibility to use semiconductor cathodes like Cs_2Te. The system is described and first experience with its use is reported. A preparation procedure is proposed to obtain QE above 5.10^{-5} over 6 months

LOAD-LOCK SYSTEM DESCRIPTION

The SwissFEL injector Test Facility [1] is currently operated with an RF photoinjector from CERN (CTF3 Gun – 10 Hz repetition rate [2]). The backplane of this gun, has a hole where a cathode plug can be inserted (Fig. 1 Top). The future SwissFEL gun, allowing 100 Hz operation rate, will also be compatible with such cathode. A cathode plug can be exchanged without breaking the vacuum thanks to a load lock system. Such load-lock system has been recently developed together with Ferrovac [3] and commissioned at the SwissFEL injector test facility (Fig. 2 and 3). With a load-lock chamber the cathode exchange becomes much faster since no venting of the gun is necessary. Only half a day, including RF conditioning of the new cathode, is required per exchange (tested on Cu_17).

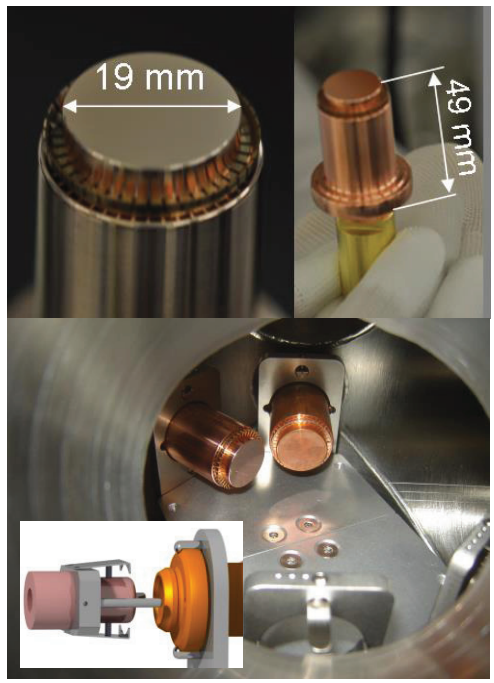

Figure 1: SwissFEL gun cathode plug with RF contact (Top). Grabbing system and storage carrousel (bottom)

The load-lock system consists in fact of three chambers (Fig. 2):

- the preparation chamber where cathodes can be cleaned, annealed and where the quantum efficiency (QE) can be checked.
- the vacuum suitcase where cathode plugs can be loaded from preparation chamber and transported to the gun.

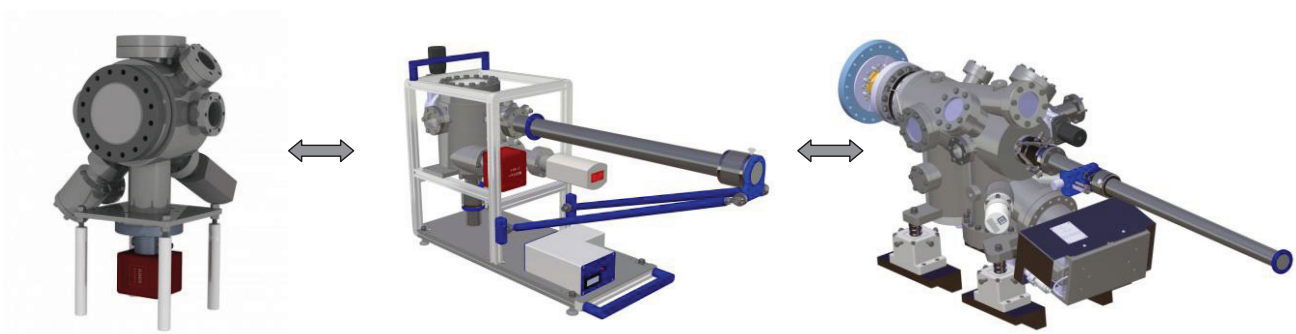

Figure 2 : Cathode plugs go first through the preparation chamber (left), are then transported via the vacuum suitcase (center) into the Load-lock chamber (right).

ISBN 978-3-95450-126-7

STATUS OF SwissFEL UNDULATOR LINES

R. Ganter, M. Aiba, H.-H. Braun, M. Calvi, P. Heimgartner, H. Joehri, G. Janzi, R. Kobler, F. Loehl, M. Negrazus, E. Prat, L. Patthey, S. Reiche, S. Sanfilippo, U. Schaer, T. Schmidt, L. Schulz, V. Vrankovic, J. Wickstroem, PSI, Villigen, Switzerland

Abstract

SwissFEL [1] will start operation with the so-called Aramis FEL line which lases in the hard X-ray wavelength range from 1 to 7 Angstroem. First photons are foreseen for the end of 2016. In this first phase of the project only the transfer line (a dog-leg section) to the soft X-ray line will be assembled. The soft X-ray undulator line, Athos, will be completed at a later stage after 2018. The civil construction of SwissFEL has started in spring 2013 and will be completed by December 2014. Aramis line has 12 undulator segments but can host up to 20 segments. Tests of an undulator prototype have been recently completed and are described in a companion paper [2]. The layout and the design status of components are presented.

LAYOUT ARAMIS LINE & TRANSFER LINE

The overall layout of SwissFEL is shown in Fig. 1. In order to tune the FEL wavelength of Aramis between 1 and 7 Angstroem, the electron beam energy can be varied between 2.1 and 5.8 GeV. This is achieved with Linac 3 which either accelerates or decelerates the beam. This enables the energy at the extraction point towards Athos (end of Linac 2) to stay always constant and equal to 3 GeV. The Aramis line (Fig. 3) has 20 half FODO period of 4.75 m length that is to say a total length of 95 m for a maximum saturation length around 50 m (Fig. 2). This additional length in Aramis allows installation of more segments in case the electron beam quality is worse than expected but it also reserves space in the building for a future integration of an X band deflecting cavity downstream undulators like recently built at LCLS [3]. The Aramis line is located in a single floor building (Fig. 4) and most of the electronic infrastructure is situated in the gallery beside the tunnel. The vacuum tank of the in-vacuum undulator will be assembled in the SwissFEL building (see U15 assembly area in Fig. 4) just after the final magnet optimization which is done in the insertion device laboratory (ID lab in Fig. 4). The transport of undulators to their final destination is done thanks to an air cushion vehicle because of small tunnel height and in order to limit mechanical shocks.

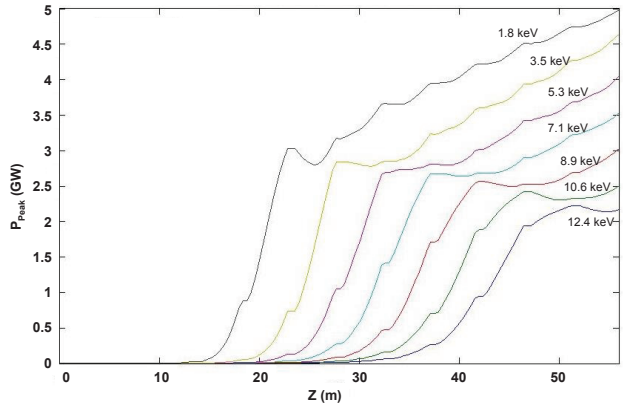

Figure 2: Genesis simulation of FEL power growth for the nominal design parameters of SwissFEL: 200 pC; 3 kA; 0.45 µm slice emittance.

At the end of the undulator line, electrons are bent vertically down towards a 240 tons beam dump shielding. Such massive beam dump can absorb 288 µC/h allowing the area situated 5 m above to stay a public zone [4]. The base plate for the beam dump is already poured on construction site (Fig. 5).

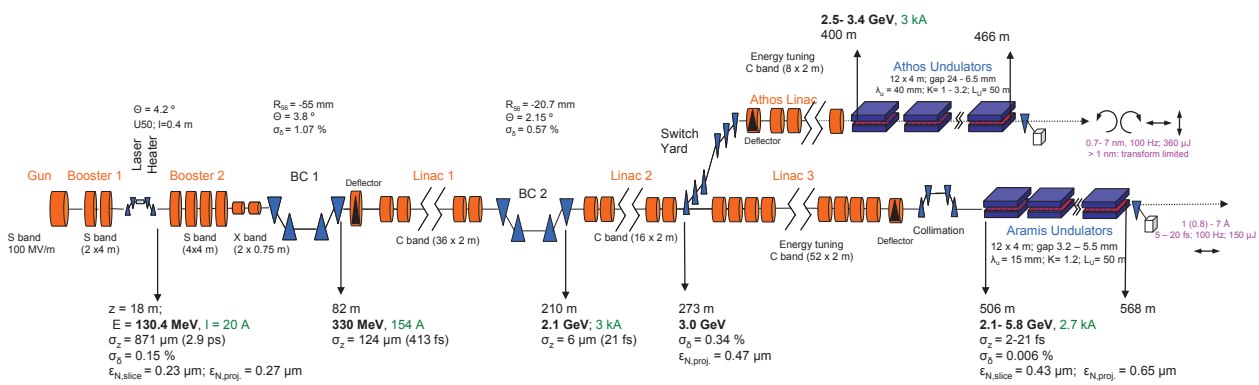

Figure 1: Layout of SwissFEL with the hard X-ray FEL line Aramis and the future Athos line to be built after 2018 (some parameters are just indicative and only valid for a specific mode of operation).

ISBN 978-3-95450-126-7

DISPERSION BASED BEAM TILT CORRECTION

Marc W. Guetg*, Bolko Beutner, Eduard Prat, Sven Reiche
Paul Scherrer Institut, CH-5232 Villigen PSI, Switzerland

Abstract

In Free Electron Lasers (FEL), a transverse centroid misalignment of longitudinal slices in an electron bunch reduces the effective overlap between radiation field and electron bunch and therefore the FEL performance. The dominant sources of slice misalignments for FELs are the incoherent and coherent synchrotron radiation within bunch compressors as well as transverse wake fields in the accelerating cavities. This is of particular importance for overcompression which is required for one of the key operation modes for the SwissFEL planned at the Paul Scherrer Institute.

The centroid shift is corrected using corrector magnets in dispersive sections, e.g. the bunch compressors. First and second order corrections are achieved by pairs of sextupole and quadrupole magnets in the horizontal plane while skew quadrupoles correct to first order in the vertical plane. Simulations and measurements at the SwissFEL Injector Test Facility are done to investigate the proposed correction scheme for SwissFEL. This paper presents the methods and results obtained.

INTRODUCTION

FELs need high-current low-emittance (ε) beams to lase. The slice emittance $\varepsilon_{\text{slice}}$ is of special importance. But the projected emittance $\varepsilon_{\text{proj}}$ influences the gain as well, since the effective overlap between electrons and radiation field is decreased.

Measurements of the slice parameter are more difficult since streaking is required. If projected and slice parameters are similar the operation of any accelerator is simplified.

SwissFEL

The SwissFEL injector will use an S-band gun followed by 6 S-band cavities (with a laser heater after the first two) and 2 X-band cavities followed by a bunch compressor BC ($R_{56} = -55.1$ mm) with 330 MeV nominal beam energy for operation [1, 2, 3]. The injector is followed by a C-Band linac bringing the beam up to 2.1 GeV and the second BC ($R_{56} \geq -22.5$ mm) compressing up to 3 kA. The final C-Band linac boosts the energy up to 5.8 GeV and is followed by an energy collimator with variable R_{56} (nominally at zero).

With the exception of the laser heater all magnetic chicanes are symmetric and horizontal, and all of them contain a pair of quadrupole, skew quadrupole and sextupole magnets each to correct for the centroid shifts.

For longitudinal diagnostic there is a transverse deflection cavity (TDC) (50 cm up to 4.9 MV) after the first BC as well as the BC quadrupoles and skew quadrupoles to streak the beam.

A schematic overview in Fig. 1 shows the setup. Since SwissFEL is not yet built all results concerning SwissFEL are obtained by simulation using elegant [4].

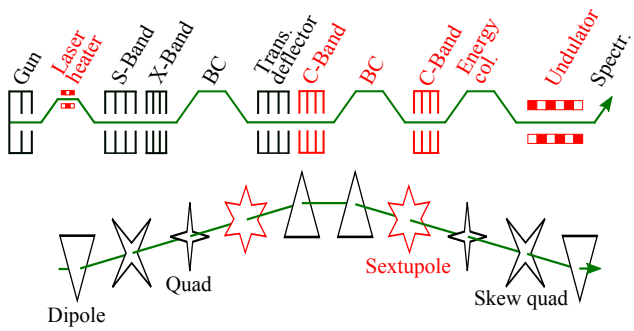

Figure 1: Schematic drawing of SwissFEL. SITF consists only of the black elements. The lower part is a more detailed sketch of the bunch compressors. The green arrow corresponds to the electron beam.

SwissFEL Injector Test Facility

The SwissFEL Injector Test Facility (SITF) implements the injector of the future SwissFEL facility. It is built for testing components and beam parameters for SwissFEL.

The SITF consists of an S-band gun, four S-band and one X-band cavities for acceleration up to 270 MeV on-crest. We reduced the energy to 180 MeV due to off-crest acceleration and linearisation of the longitudinal phase space. SITF has the same longitudinal diagnostic options as described for SwissFEL.

There are no sextupoles installed at the SITF. The black elements in Fig. 1 show the SITF setup. The SITF beam line setup was used for measurements as well as simulations [5].

BEAM DYNAMICS

We use the statistical definition of the emittance ε_{rms} for simulations and for measurements Gaussian fits are used to obtain the beam sizes. It has been shown that both methods are equivalent in our case (mostly Gaussian beams). The variable ε denotes projected and normalized emittance.

* marc.guetg@psi.ch

ISBN 978-3-95450-126-7

STATUS OF THE EU-XFEL LASER HEATER

M. Hamberg*, V. Ziemann, Uppsala University, Uppsala, Sweden

Abstract

We describe the technical layout and the status of the laser heater system for the EuXFEL. The laser heater is needed to increase the momentum spread of the electron beam to prevent micro-bunching instabilities in the linac.

INTRODUCTION

The electron beam for the EuXFEL [1], is generated in a photo cathode and has such a small momentum spread, that the beam is susceptible to space-charge driven instabilities in the linear accelerator. This problem can be alleviated by increasing the momentum spread of the electron beam in a controlled way. This is done in the laser heater where a laser beam is superimposed to the electron beam that passes through an undulator magnet. If tuned to resonance the transversely oscillating electrons acquire a momentum modulation that is smeared out in a chicane resulting in increased incoherent momentum spread [2-3].

The laser heater consists of several key parts such as the laser system providing the photons, an optical table with optical elements for controlling and shaping the laser beam, a vacuum system for transporting the photons down to the electron interaction point, additional optical tables for control, adjustment and readout of the laser beam, OTR-screens and BPM for overlap adjustments and a compact undulator (see Figure 1).

The laser heater for the XFEL is built up as an in kind contribution from Sweden. We report of the current status and technical layout of the project.

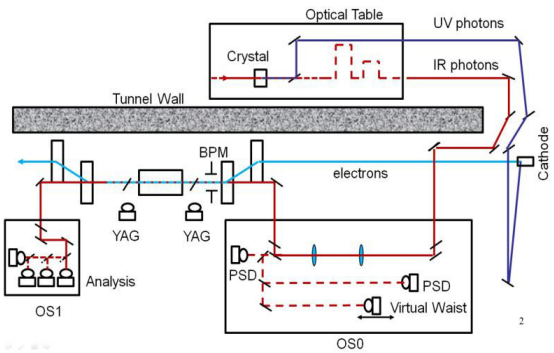

Figure 1: Schematical overview of the laser heater. The IR-laser starts on the optical tables at level 5, continues down a vertical shaft, enter the accelerator tunnel at level 7. The beam is focused, analysed and stabilized on a large optical table before it continous through the interaction region in the undulator and out on a small optical table for analysis.

*mathias.hamberg@physics.uu.se

LASER PREPARATION

The laser system is designed and built up at the Max-Born Institute (MBI). The working concept is to use a part of the Nd:YAG laser beam with a wavelength of 1064 nm that is quadrupled in frequency to generate the ultra-violet photons for the photo-cathode electron gun. Deriving the laser-heater photons directly from the gun-laser ensures temporal locking of the electrons and laser throughout the full pulse train of up to 2700, 20 ps pulses with 4.5 MHz repetition rate and the pulsetrains coming at 10 Hz. Moreover the pulse length of laser and electron bunch are matched. Regarding the available pulse energy at XFEL the required output is 50 μJ and a nominal usage of 5 μJ is foreseen.

ON THE LASER TABLE

Since both laser pulse and electrons stem from the same initial laser oscillator, they have a stable relative temporal relation and we need to provide means to fine adjust the arrival time of the laser pulse in two stages. 1) nano seconds (1-10 ns), static delay line. 2) pico seconds (1-1000 ps), remotely controlled translation stage. These two delay stages are shown as the two bumps on the laser table in the upper right in Fig. 1.

The origin of the arrival time difference is because both laser pulses actually co-propagate for a long way until they reach the accelerator where the UV pulse is propagating upstream towards the laser gun and the IR pulse for the laser heater is propagating downstream to the laser heater chicane. To avoid strong divergence due to diffraction limitation the laser is in an early stage magnified up to ~ 3 mm FWHM.

LASER TRANSPORT VACUUM SYSTEM

The IR pulses have to be transported from the laser room situated outside the accelerator tunnel (as depicted in Fig. 1) out and down to the optical station 0 (OS0). The total length of the optical beam line will be approximately 50 m and there are 5 mirrors required to guide the laser light to the optical table close to the undulator. Because of the significant distance between the laser room and the undulator, temperature variations can cause convection and fluctuating refractive indices that will disturb the laser beam. It was therefore decided to use an evacuated laser beam pipe.

For the laser transport vacuum system we will use mobile turbo-pump stations to reach initial low pressure that is then maintained by ion pumps. This will reduce the wear on the bearings of the turbo-pumps and will especially limit the vibration level that might disturb the mirrors which are attached to the vacuum beam pipe. Furthermore, thanks to the rather good vacuum, effects

ISBN 978-3-95450-126-7

DESIGN FOR A FAST, XFEL-QUALITY WIRE SCANNER

M. Harrison*, R. Agustsson, T. Hodgetts, A. Murokh, M. Ruelas, P. S. Chang
RadiaBeam Technologies, Santa Monica, CA 90404, USA

Abstract

RadiaBeam Technologies has designed and manufactured a new wire scanner for high-speed emittance measurements of XFEL-type beams of energy 139 MeV. Using three 25-micron thick tungsten wires, this wire scanner measures vertical and horizontal beam size as well as transverse spatial correlation in one pass. The intensity of the beam at a wire position is determined from emitted bremsstrahlung photons as measured by a BGO scintillator system. The wires are transported on a two-ended support structure moved by a ball-screw linear stage. The double-ended structure reduces vibrations in the wire holder, and the two-bellows design negates the effects of air pressure on the motion. The expected minimum beam size measurable by this system is on the order of 10 microns with 0.1-micron accuracy. To achieve this, new algorithms are presented that reduce the effect of the non-zero thickness of the wire on the wire scan output. In addition, novel calculations are presented for determining the elliptical geometric parameters (vertical and horizontal beam size and correlation, or alternatively, the axis lengths and rotation) of the beam from the wire scanner measurements.

WIRE SCANNER OPERATION

The prototype RadiaBeam wire scanner (see Fig. 1) operates by moving three tungsten wires transversely across the electron beam. When the beam impacts the wire, the interaction generates a pulse of bremsstrahlung photons in the 10 MeV range that emerges in a narrow cone around the downstream beam. These photons are absorbed and measured by a bismuth germanium oxide (BGO) scintillator system to measure the total energy of the gamma pulse. This total energy is proportional to the integrated intensity of the beam at the location of the wire. The beam widths measured by horizontal, vertical, and 45-degree wires allow for the determination of the beam widths and other transverse geometric properties.

MECHANICAL DESIGN

Tungsten Wire

Tungsten wire was chosen for its high tensile strength (to ease installation by hand), high melting point (to withstand the high energy beam), and short radiation length due to its high mass number and density (to generate a larger number of photons). The high tensile strength of tungsten also allows for a higher tension in the wire to reduce sag and raise the fundamental mode of vibration above that of any nearby vibration sources like the linear motor. The three wires are angled 45 degrees from each other, resulting in a vertical, diagonal, and horizontal wire assembly that will be sufficient to reconstruct the transverse profile of an elliptical beam.

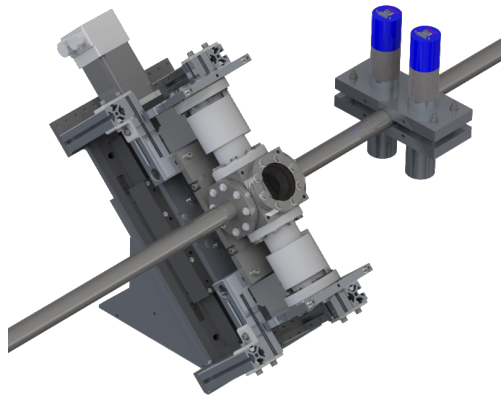

Figure 1: Complete wire scanner structure.

Ceramic Wire Holder

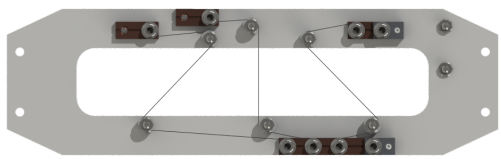

Figure 2: Wire holder.

The wire holder (shown in Fig. 2) was manufactured from alumina to counter problems with wire breakage due to RF heating experienced in wire scanners at CERN [1] and SLAC [2]. The insulating material also allows for monitoring of the wires through their electrical resistance. Each tungsten wire is connected to an SMA feedthrough on the lower end flange to allow an ohmmeter to check the wire integrity. An increase in resistance indicates the wire is heating up and possibly stretching. An open circuit indicates the wire has broken.

The aperture in the wire holder allows for a maximum 25-mm width beam to pass through. The wires are spaced such that, even with a maximum-sized beam, only one wire will interact with the beam at once, thus preventing bremsstrahlung photons from more than one wire being detected from a single beam pulse.

Vacuum Chamber Design

The wire holder is supported at both ends by plates fastened to the end flanges. These end flanges are connected

* harrison@radiabeam.com

ISBN 978-3-95450-126-7

DEVELOPMENT OF PHOTOCATHODE RF-GUN AT PAL

J. Hong*, J.-H. Han, S.-J. Park, H.-S Kang, Y.-J. Park, Y.-W. Parc,
PAL, Pohang, Kyungbuk 790-784, Korea
I.S. Ko, POSTECH, Pohang, Kyungbuk 790-784, Korea

Abstract

We are developing two types of S-band photocathode RF-guns for the X-ray free electron laser (XFEL) at Pohang Accelerator Laboratory (PAL). One is a 1.6-cell RF-gun with a dual side coupler and two pumping ports. This RF-gun is similar to the earlier guns developed at PAL. The other one is a 1.5-cell RF-gun with a coaxial coupler and a cathode preparation system. This RF-gun is similar to the DESY-type L-band RF-gun. We have designed and fabricated two types of RF-guns. In this paper we introduce and compare two different RF-guns.

INTRODUCTION

Pohang Accelerator Laboratory X-ray Free Electron Laser (PAL XFEL) is now under construction [1]. PAL XFEL is the 4th-generation light source based on the self amplified spontaneous emission (SASE) scheme. There will be a hard X-ray (0.1nm) beamline with self-seeding scheme with 10 GeV electron beam. There is a 3 GeV branch also to make 1 nm soft X-ray radiation.

A photocathode RF-gun has been studied as an electron source with low emittance for future accelerators. The RF-gun for PAL XFEL is required to provide electron beams with their emittance better than 0.5 mm-mrad (projected normalized rms) at beam charge of 200 pC and its repetition rate of 60 Hz. Since 2005, we have concentrated in development of a photocathode RF-gun. The photocathode RF-guns developed at PAL are based on S-band RF-gun [2, 3]. From 2010 to 2011 the 4-hole Type RF-gun (Old-gun) was successfully fabricated and finished its low-power test [4]. After that, Old-gun was installed and tested at the gun test facility (GTF) at PAL. In this test, we have several problems in the GTF [5]. During the measurement, we could not perfectly care of the laser system and the temperature cooling system. The shape of UV laser looks like ellipse and the pulse power of UV laser was so unstable. And the laser power was too small. At the GTF, the horizontal (x) emittance are doubled as compared with the vertical (y) emittance. The difference between the horizontal and the vertical emittance was caused by the difference size of the transverse UV laser. Large values of emittances and its errors are possibly caused by the instability of the whole system. In the middle of 2012, Old-gun had been installed at the ITF. After that, the ITF is operated for various beam experiments and devices testings for the successful construction of PAL XFEL. However, there are some RF-gun problems such as dark current, electric discharges, and difficulty of gun align. To avoid the problems of Old-gun, we have designed two kinds of RF-gun. One is the upgrade version of 4-hole Type RF-gun (GUN-I) and another is the Coaxial Type RF-gun (GUN-II) [6].

* npwinner@postech.ac.kr

PHOTOCATHODE RF-GUN

GUN-I

A upgrade version of RF-gun with dual-side-coupler and two pumping ports has been designed. The design has been optimized to allow good performance and simple fabrication. The features incorporated into GUN-I are as follows:

- Dual feed coupler&Two pumping ports: To minimize high-order fields
- Field probes
- Fixed cathode: Simply Fabrication
- Long beam tube
- Large coupling iris radius&Short coupling iris length: To increase 0 and π-mode separation
- Elliptical iris: To reduce the surface E-field
- Rounded cell edge: To increase the quality factor, To decrease the thermal stress
- Modified Cooling channels: To be uniform the RF-heating

The three dimensional drawing of GUN-I is shown in Fig. 1. The manufacture of GUN-I, including the machining, brazing, cold test and tuning has been finished. The RF-parameters after cold test are: the operating frequency (π-mode) of 2856 MHz, the mode separation of 16.8 MHz, the quality factor of 13800, the coupling coefficient of 1.43, the field balance of 1.02, which match the parameters in RF-design. After cold test, GUN-I was successfully installed and conditioned at the ITF for PAL XFEL. The measured amplitude data of the full cell probe was collected using a low-level RF (LLRF) system.

Figure 2 shows the forward, the reflected, and probe RF-powers collected by the LLRF. Here the forward power is about 1 MW. GUN-I has operated with a maximum field gradient of 120 MV/m and has achieved a maximum beam energy of up to 5.6 MeV for a 30° laser injection phase. We have measured the transverse emittance using a quadrupole scan technique at the ITF. The lowest measured transverse emittances are $\epsilon_x = 0.67$ mm-mrad and $\epsilon_y = 0.73$ mm-mrad up to now. This experiment was performed with the condition of a 140-MeV beam energy, a solenoid current

ISBN 978-3-95450-126-7

CONDITIONING STATUS OF THE FIRST XFEL GUN AT PITZ

I. Isaev*, P. Boonpornprasert†, J. Good, M. Groß, L. Hakobyan, M. Khojoyan, G. Kourkafas, W. Köhler, M. Krasilnikov, D. Malyutin, B. Marchetti, R. Martin, M. Nozdrin‡, A. Oppelt, M. Otevrel, G. Pathak§, B. Petrosyan, A. Shapovalov, F. Stephan, G. Vashchenko, R. Wenndorff, L. Jachmann, DESY, 15738 Zeuthen, Germany
G. Asova, INRNE BAS, 1784 Sofia, Bulgaria
D. Richter, HZB, 12489 Berlin, Germany
S. Rimjaem, Chang Mai University, 50200 Chiang Mai, Thailand

Abstract

The paper describes the recent results of conditioning and dark current measurements for the photocathode RF gun at the photoinjector test facility at DESY, Zeuthen site (PITZ). The aim of PITZ is to develop and operate an optimized photo injector for free electron lasers and linear accelerators which require high quality beams. In order to get high gradients in the RF gun extensive conditioning is required. A data analysis of the conditioning process is based on data saved by a Data Acquisition system (DAQ). Conditioning results of the first gun cavity for the XFEL is presented. The events which occurred during the conditioning are briefly described.

INTRODUCTION AND OVERVIEW

The photo injector test facility at DESY, Zeuthen site (PITZ) has been built for the development, testing and optimization of high brightness electron sources for FELs like FLASH and the European XFEL.

The 1.6 cell normal conducting (copper) cavity with the Cs_2Te photocathode serves as an electron source at PITZ for its subsequent application at superconducting linac based FELs. Several gun prototypes were conditioned and characterized at PITZ and successfully operated at FLASH. Recently the first gun (Gun 4.3) for the European XFEL [1] was conditioned in Zeuthen as well.

The gun life cycle includes following stages: production (fabrication) → tuning → dry-ice cleaning → RF conditioning → characterization.

Conditioning was done from the end of spring to the middle of summer 2013. The main goal of the conditioning was to reach 6 MW peak power in the gun at a 650 μs RF pulse length and a 10 Hz repetition rate. This corresponds to the average RF power of 39 kW. The gun was conditioned and tested together with the upgraded RF waveguide distribution system, which close to the gun is similar to the one to be installed at the European XFEL. The previous setup of two 5-MW vacuum windows was replaced by one of the 10-MW THALES [2] vacuum windows which was installed downstream the 10-MW directional coupler for power measurements and low level RF control.

* igor.isaev@desy.de
† On leave from Chang Mai University, 50200 Chiang Mai, Thailand
‡ On leave from JINR, 141980 Dubna, Russia
§ On leave from Hamburg University, 20148 Hamburg, Germany

ISBN 978-3-95450-126-7

The gun was built in 2012 and later the new RF cathode spring design was applied. Afterwards the gun was dry-ice cleaned [3]. On the 18th of March 2013 the gun was installed in the PITZ tunnel and RF conditioning was performed from the 10^{th} of April to the 15^{th} of July 2013. A Molybdenum (Mo) cathode plug was inserted during the RF conditioning instead of the Cs_2Te cathode plug, used for photoelectron production, in order to prevent destruction of the Cs_2Te coating on the cathode surface. This coating is very sensitive to the vacuum pressure. Also effects like the field emission of electrons from rough surface, multipacting or sparks can damage it. In the case of such events, the gun interlock system (IL) [4] consisting of different detectors will switch off the RF feed to the gun.

The gun conditioning setup consisting of a 10-MW klystron, an upgraded RF waveguide distribution system, a 10-MW THALES vacuum window, directional couplers, Ion Getter vacuum Pumps (IGP) and Pressure Gages (PG), photomultipliers (PMT) and electron detectors (e-det) located around the gun coupler is presented in Fig. 1.

CONDITIONING PROGRAM AND DATA ANALYSIS

The main goal of the conditioning process is the cleaning of the in-vacuum surfaces to get rid of residual contamination from previous production and cleaning steps. This process is accompanied by the increased vacuum pressure level at the beginning of the conditioning. The vacuum pressure later decreases, but single vacuum spikes happened up to the end of the conditioning. The vacuum activity is a normal conditioning behavior and means that the conditioning process as long as there is no leak in the vacuum system.

The applied conditioning procedure is based on the conditioning requirement of the THALES window includes following principles:

- RF pulse length: 10 – 650 μs.
- RF power increase in steps of max 0.2 MW every 15 min for each new RF pulse length.
- Vacuum pressure must be below 10^{-7} mbar.
- In the case of significant vacuum events or other trips:
  - restart with the shortest RF pulse length (10 μs).
  - increase the pulse length in reasonable steps.
- Initially, the RF gun solenoid is off.

PROJECT OF THE SHORT PULSE FACILITY AT KAERI*

N. Vinokurov#, S. V. Miginsky, Budker INP SB RAS, Novosibirsk, Russia and KAERI, Daejon, Republic of Korea
S. Bae, B. Gudkov, B. Han, K. H. Jang, Y. U. Jeong, H. W. Kim, K. Lee, J. Mun, S. H. Park, G. I. Shim, KAERI, Daejon, Republic of Korea

Abstract

A low-energy electron accelerator with subpicosecond electron bunches is under construction at the Korea Atomic Energy Research Institute (KAERI). It will serve as a user facility for high-energy ultrafast electron diffraction and synchronized high-power terahertz pulse and short x-ray pulse generation. The accelerator consists of an RF gun with a photocathode and 20-MeV linac. The bunching of an accelerated beam is achieved in a ninety-degree achromatic bend. After that, a fast kicker deflects some of the bunches to the target for x-ray generation, and other bunches come to the terahertz radiator (undulator or multifoil). Bunches from the RF gun are also planned for use in ultrafast electron diffraction. Some details of the design, current status of the project, and future plans are described.

INTRODUCTION

The availability of subpicosecond electron bunches makes possible a variety of new experimental techniques, including the generation of ultra short radiation pulses, time-resolved pump-probe experiments, and ultrafast electron diffraction. The main aim of the project of the short-pulse facility in KAERI is to provide tools for experiments with subpicosecond time resolution and high-power terahertz pulses.

LOW ENERGY PART

The standard way of preparing short electron bunches is the use of a radiofrequency (RF) gun with a photocathode, illuminated by picosecond laser pulses. The best example of such a gun is used in an x-ray free electron laser LCLS (USA) [1]. The RF gun in our project differs from it in two features.

1. It has a coaxial input coupler, which provides the axial symmetry of the accelerating field.
2. The input power is 5 MW, which is 50% that of LCLS. Correspondingly, the accelerating field is 30% less. Therefore, more relaxed tolerances for the inner copper surface treatment are expected.

To obtain short bunches with high enough electric charge, it is necessary to compress the bunches at high

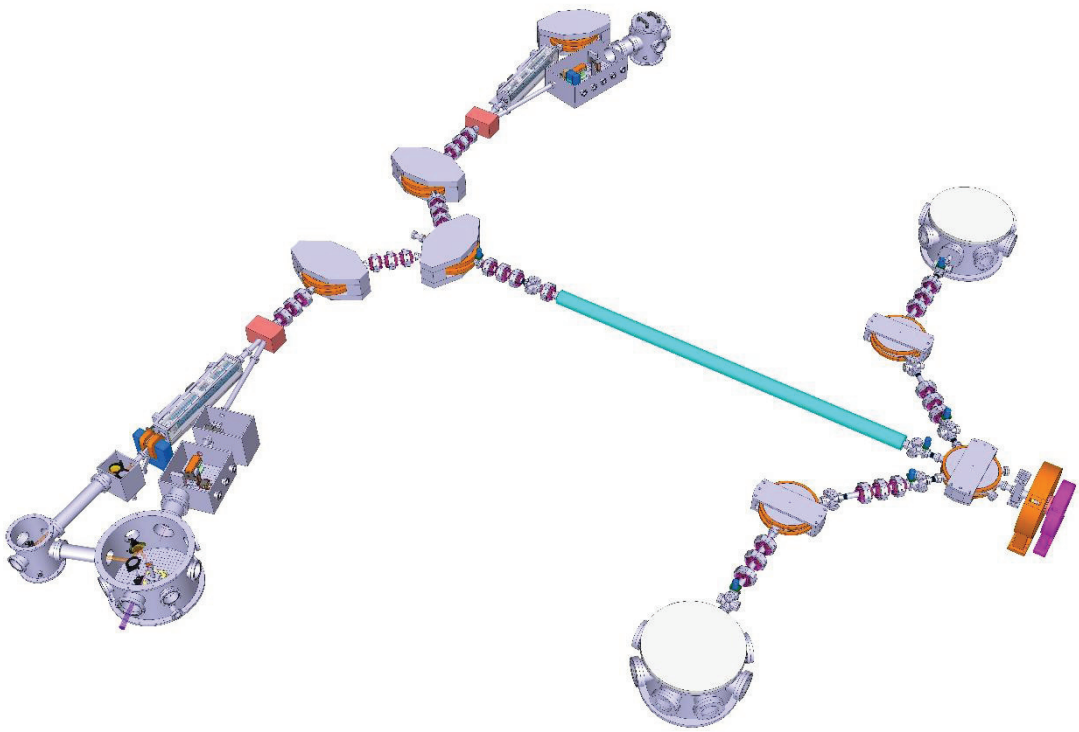

Figure 1: Scheme of a short-bunch accelerator and beamlines.

*Work supported by the WCI Program of NRF of Korea (NRF Grant Number: WCI 2011-001) and the RFBR Grant 11-02-91320-SIG_a.
#nikolay.vinokurov@gmail.com

ISBN 978-3-95450-126-7

THE COMMISSIONING OF TESS: AN EXPERIMENTAL FACILITY FOR MEASURING THE ELECTRON ENERGY DISTRIBUTION FROM PHOTOCATHODES

L.B. Jones*, R.J. Cash, B.D. Fell, K.J. Middleman, T.C.Q. Noakes & B.L. Militsyn
STFC Daresbury Laboratory, ASTeC & the Cockcroft Institute, Warrington WA4 4AD, UK

H.E. Scheibler, D.V. Gorshkov & A.S. Terekhov
Institute of Semiconductor Physics, SB RAS, Novosibirsk 630090, Russia

Abstract

ASTeC have developed an instrument to measure the *transverse energy* (ε_{tr}) of electrons emitted from photocathode sources. The instrument ('*TESS*' for *transverse energy spread spectrometer*) is connected to our GaAs photocathode preparation facility (PPF) which is capable of producing photocathodes with quantum efficiencies (*Q.E.*) up to 20 % at 635 nm [1, 2]. TESS is currently being used to study the emission properties of these photocathodes.

The methodology is based on extracting a fA–scale electron beam from a small area of a photocathode source, and allowing it to expand under the influence of its transverse energy component while in flight between the electron source and a detector. Images of the electron emission footprint are analysed to measure the transverse energy distribution curve (TEDC), and the mean transverse energy extracted (MTE) from this.

TESS is compatible with a number of different light sources, so can support measurements on various photocathode materials from the metal and semiconductor families. The system includes a piezo–electric leak valve allowing precision gas dosing to control the degradation state of the photocathode, and therefore its *Q.E.*. The system also supports cathode cooling to LN_2 temperature at 77 K.

The system has been commissioned recently, in collaboration with the Institute of Semiconductor Physics (ISP) at Novosibirsk. We present this TESS commissioning data for photoelectron emission from a GaAs photocathode.

INTRODUCTION

The development of high–performance accelerator drivers for light sources based on Free–Electron Lasers requires technology which delivers a high–brightness electron beam for reasons that are well–documented [3]. Electron beam brightness in an accelerator is fundamentally limited by injector brightness, and this is itself limited by the source beam emittance or the *intrinsic emittance* of the cathode source. Electron beam brightness will be increased significantly by reducing the longitudinal and transverse energy spread in the emitted electrons, thereby creating a *cold beam*.

* lee.jones@stfc.ac.uk

For a bound electron, the component of electron momentum which is parallel to the surface translates into its transverse momentum component on photoemission. This transverse momentum component is directly related to transverse electron energy, and is measurable as the beam emittance at some distance from the source. When using GaAs photocathodes, the upper limit on transverse electron energy is determined by the illumination wavelength, the level of electron affinity and the photocathode temperature. The profile of the measured TEDC itself depends on various elastic and inelastic electron scattering processes at the photocathode–vacuum interface, which are themselves dependent on several factors such as surface roughness, surface diffraction, material structure/crystallinity etc.

The ability to measure this transverse energy, and to make direct comparisons between photocathodes which have been prepared in different ways is therefore a key enabling step towards increasing electron beam brightness.

We have constructed TESS to measure the transverse energy of photoemitted electrons through analysis of the beam footprint recorded after propagation over a known drift distance, with the emission footprint being directly coupled to the source emittance.

TRANSVERSE ENERGY MEASUREMENT

Early published work (circa 1972) suggested that the angular emission cone for photoelectrons from GaAs is small, though later work appeared to imply the opposite [4]. Applying angle–resolved photoelectron spectroscopy to measure this angular distribution for GaAs is challenging as the angular distribution is affected by the specific geometry of the vacuum chamber and experiment itself, so will vary in each installation. Further recent work indicates that GaAs does indeed have a narrow emission cone with a half–angle of only 15 ° relative to the surface normal [5].

However, it is not possible to decouple the effects of an electron's transverse energy component from its emission angle when considering only its transverse displacement in the emission plane from the point of emission. Consequently, data from TESS includes a contribution from the angular emission, and values returned from a TESS measurement are upper limits on the mean transverse energy.

ISBN 978-3-95450-126-7

THE MAX IV LINAC AS X-RAY FEL INJECTOR: COMPARISON OF TWO COMPRESSION SCHEMES

O. Karlberg*, F. Curbis, S. Thorin, S. Werin, MAX-lab / Lund University, Sweden

Abstract

The MAX IV linac will be used for injections and top up of two storage rings and at the same time provide high brightness pulses to a short pulse facility (SPF) and in a second phase an X-ray FEL. Compression in the linac is done in two double achromats which implies a positive R56 unlike the commonly used chicane compressor scheme with negative R56. Compression using the achromat scheme requires the electron bunch to be accelerated on a falling RF slope resulting in an energy chirp that longitudinal wakefields will boost along the linac. This permits a stronger compression.

In this proceeding we will present how the longitudinal wakefields interact with the bunch compression in the double achromat scheme, compared with the chicane compression case. Focus is brought on how the unique MAX IV linac lattice is fully capable to cope with the high demands of an FEL injector. The charge related electron beam jitter in both set-ups will also be investigated.

INTRODUCTION

The new synchrotron facility at MAX IV laboratory [1] is now being constructed in Lund (Sweden). A 300 m long S-band linac, equipped with two guns, will serve as injector for two storage rings and drive a SPF using 3 GeV high brightness pulses to generate short spontaneous X-ray pulses. The linac layout is illustrated in Fig 1. As a second development stage of the facility an X-ray FEL is considered [2].

Double Achromat Compression Scheme

Two double achromats, BC1 at 260 MeV and BC2 at 3 GeV, serve as bunch compressors (BCs) in the linac. More precisely, one achromat structure consists of four bending magnets, a sextupole and a series of quadrupoles forming an arc, see Fig 1. The double achromat scheme gives a positive R56 and consequently the electrons must be accelerated on a falling RF voltage slope to achieve compression. Since the R56 is fixed to 3.2 cm in BC1 and 2.6 cm in BC2, the compression factor is tuned by changing the off-crest RF phase. The BCs in the MAX IV linac are self-linearizing in the longitudinal phase space since they both have a positive T566, which in the achromat case act linearizing while ordinary chicanes have opposite sign on R56 and T566 perturbing the linearization. To compensate for possible over-linearization and to minimize second order dispersion at the end of the BCs, a sextupole is used in the middle of each achromat structure [3].

Longitudinal Wakefields

When a charged particle bunch passes through a geometric varying structure, such as an RF cavity, it will induce wakefields that can act back on the particles and lead to beam instabilities. Only short ranged wakefields i.e. wakes generated by and acting up on particles within the same bunch, are considered in this article since the time between each electron bunch during MAX IV linac operation is sufficient to attenuate all long range wakes. Wakefields affect both the longitudinal and transverse beam dynamics, additional discussion about the transverse wakes in the MAX IV linac can be found in [4]; however it is the longitudinal wakes that are of interest here since they influence the compression. More precisely, the longitudinal wakefields affect the energy spread of the pulse since the particles in the back of the bunch lose energy from the wake generated by the particles in the head. In this way, the wakes will either enhance (achromat scheme) or reduce (chicane scheme) the energy chirp already obtained from the RF slope which is used to vary the compression.

COMPARISON OF COMPRESSOR SCHEMES, TWO CASES

Two compression schemes for the MAX IV linac were set up and compared using Elegant [5]; the original lattice including the double achromats versus a lattice using chicane compressors. Figure 2 illustrates the two setups. The dipole magnets in each BC are identical for both layouts

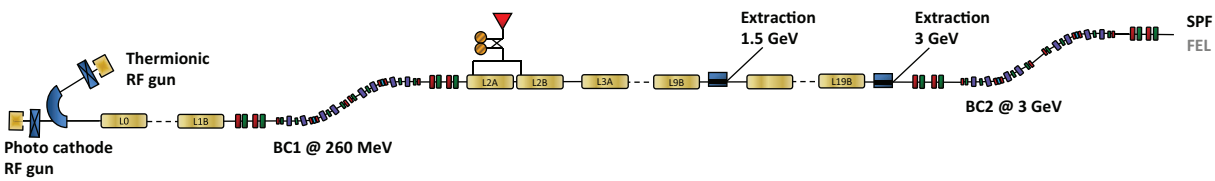

Figure 1: The MAX IV linac layout

* olivia.karlberg@maxlab.lu.se

ISBN 978-3-95450-126-7

BEAM DYNAMICS OPTIMIZATION FOR THE HIGH BRIGHTNESS PITZ PHOTO INJECTOR USING 3D ELLIPSOIDAL CATHODE LASER PULSES*

M. Khojoyan#, M. Krasilnikov, F. Stephan, G. Vashchenko DESY, 15738 Zeuthen, Germany

Abstract

The Photo Injector Test facility at DESY, Zeuthen Site (PITZ) is one of the leading producers of high brightness electron beams for linac based Free Electron Lasers (FELs) with a specific focus on the requirements of FLASH and the European XFEL. The main activities at PITZ are devoted to the detailed characterization and optimization of electron sources yielding to an extremely small transverse beam emittance. The cathode laser pulse shaping is considered as one of the key issues for the high brightness photo injector. Beam dynamics simulations show that the injector performance could be further improved by replacing the typical cylindrically shaped PITZ bunches by uniformly filled 3D ellipsoidal shaped electron beams. A set of numerical simulations were performed to study the beam dynamics of uniformly filled 3D ellipsoidal bunches with 1 nC charge in order to find an optimum PITZ machine setup which will yield the best transverse emittance. Simulation results comparing both options of cylindrical and 3D ellipsoidal beams are also presented and discussed.

INTRODUCTION

The X-ray free electron lasers (XFELs) require excellent electron beam quality in terms of high peak current, small transverse emittance and energy spread. Production of such high quality beams is obligatory to perform a single pass beam transport through hundreds of meters long undulators with a gap size of a few millimetres. The ideal beam distribution for the best transverse and longitudinal bunch compression is a three-dimensional uniformly filled ellipsoid, in which the space charge force fields inside the bunch are linear [1]. Such distributions, also called 3D Kapchinskij and Vladimirskij distribution [2], will allow a full emittance compensation scheme [3] with proper arrangement of the beam optics. One possibility to create such beams is to use a uniform ellipsoid photocathode laser pulse [4], which is a challenging task due to the difficulty of simultaneous spatiotemporal control of the photon distribution at the photocathodes.

Recently many investigations have been carried out into creation of quasi ellipsoidal electron bunches relying on the beam expansion due to strong longitudinal / transverse space charge forces. In the first case, (longitudinal beam expansion, also called blow up regime) the studies were performed for a pancake shape (transverse bunch size much bigger compared to longitudinal one) electron beams initialized from an ultra-short (~30 fs) laser pulse [5]. As the formation of the ellipsoidal beam shape is also sensitive to the radial laser profile the idea was further improved later on by the suggestion of using a surface charge density with a "half-circle" radial profile [6]. In the second case, (transverse beam expansion) a "cigar-like" beam (longitudinal size much bigger compared to transverse one) with a parabolic longitudinal profile was applied by using a very small (~30 μm) transverse laser spot size on the cathode. An electron beam with quasi ellipsoidal shape was formed after the emission due to strong space charge driven transverse expansion [7]. In the former cases the transverse emittance is limited by the thermal emittance which is comparably high due to a big laser spot size on the cathode. The latter case could cause difficulties to transport ultralow charge (0.1-1pC) beams and to measure the beam properties though a nanometer transverse emittance out of such investigations (measurements and simulations) was reported.

The Photo Injector Test facility at DESY, Zeuthen Site (PITZ) is well-known for developing of high brightness electron sources for linac based, single pass multi user FEL facilities such as Free electron LASer in Hamburg (FLASH) and the European XFEL. The PITZ facility was already utilized to establish the injector requirements of the high quality electron beam for the European XFEL [8]. A schematic layout of the current PITZ beamline is shown in Fig. 1. The electron bunches are created in an L-band RF gun cavity using a Cs_2Te cathode and accelerated up to ~6.2 MeV energy. Typically electron beams with 1 nC charge are formed with a longitudinally flat-top and transversely radial homogenous photo-cathode laser profile. The RF gun is surrounded by two solenoids: main and bucking. The main solenoid is used for the transverse beam focusing, while the bucking solenoid is meant to compensate the remaining longitudinal magnetic field at the cathode. The transverse emittance of the 25 MeV electron beam (after post acceleration through the booster cavity) along the linac is measured by the emittance measurement systems (EMSY), using a single slit scan technique [9]. Additionally, there are many diagnostics devices available for full characterization of high brightness electron beams. More detailed description of the PITZ setup can be found elsewhere [10]. Recent measurements of the transverse emittance for different bunch charges yielded worldwide record low values where the photocathode laser with a flat-top temporal profile was used to create the electron bunches [11]. To further improve the electron beam quality, a 3D ellipsoidal photocathode laser system

*The work is funded by the German Federal Ministry of education and Research, project 05K10CHE "Development and experimental test of a laser system producing quasi 3D ellipsoidal laser pulses".

#martin.khojoyan@desy.de

ISBN 978-3-95450-126-7

DEVELOPMENT OF A PHOTO CATHODE LASER SYSTEM FOR QUASI ELLIPSOIDAL BUNCHES AT PITZ*

M. Krasilnikov#, M. Khojoyan, F. Stephan, DESY Zeuthen, Zeuthen, Germany
A. Andrianov, E. Gacheva, E. Khazanov, S. Mironov,
A. Poteomkin, V. Zelenogorsky, IAP/RAS, Nizhny Novgorod, Russia
E. Syresin, JINR, Dubna, Moscow Region, Russia

Abstract

Cathode laser pulse shaping is one of the key issues for high brightness photo injector optimization. A flat-top temporal profile of the cylindrical pulses reduces significantly the transverse emittance of space charge dominated beams. As a next step towards further improvement in photo injector performance 3D pulse shaping is considered. An ellipsoid with uniform photon density is the goal of studies in the frame of a Joint German-Russian Research Group, including the Institute of Applied Physics (Nizhny Novgorod), Joint Institute of Nuclear Research (Dubna) and the Photo Injector Test facility at DESY, Zeuthen site (PITZ). The major purpose of the project is the development of a laser system capable of producing 3D quasi ellipsoidal bunches and supporting a bunch train structure close to the European XFEL specifications. The laser pulse shaping is realized using the spatial light modulator technique. Laser pulse shape diagnostics based on a cross-correlator is under development as well. Experimental tests of the new laser system with electron beam production are planned at PITZ. First results on the quasi ellipsoidal laser pulse shaping will be reported.

INTRODUCTION

3D shaping of photocathode laser pulses is considered as a next step for further optimization of high brightness photo injectors. Beam dynamics simulations have demonstrated a significant reduction of transverse emittance of electron bunched produced by applying 3D ellipsoidal laser pulses to the rf photo gun [1, 2]. A laser system capable to produce quasi 3D ellipsoidal UV pulses is under development at the Institute of Applied Physics (Nizhny Novgorod, Russia). The Photo Injector Test facility at DESY, Zeuthen site (PITZ) develops high brightness electron sources for modern Free Electron Lasers (FELs) and is intended to be at the site for experimental tests of this system with electron beam production.

The laser system consists of a two-channel fiber laser, a diode pumped Yb:KGW disk amplifier, a 3D pulse shaper and frequency conversion crystals for second and fourth harmonics generation. A scanning cross-correlator system was developed and built to measure spatial and temporal distributions of the laser pulses.

The fiber laser oscillator generates 150 fs pulses at 45 MHz repetition rate. It includes a fiber pulse stretcher, a preamplifier and a system for pulse train (macropulse) formation. A piezoceramic cylinder inside the optical fiber coil of the oscillator is used for precise tuning of the pulse timing to the rf phase of the rf gun. The fiber laser output is splitted into two channels – working and diagnostics. Each channel is supplied with a powerful fiber amplifier. The working channel is used for further amplification, 3D pulse formation and frequency conversion. The diagnostics channel is used to measure the spatial and temporal characteristics of the pulses generated in the working channel. A high speed delay line is implemented in the second channel in order to realize a high precision 3D pulse shape diagnostics. Each channel is supplied with an optical compressor based on a diffraction grating which allows varying the pulse duration within wide range from 200 fs to 100 ps. The compressor of the diagnostic channel is always tuned to the maximum compression down to 200 fs.

The output of the working channel is further amplified by a diode pumped multipass Yb:KGW disc amplifier. 3D shaped pulses are converted into second and fourth harmonics by nonlinear crystals and imaged via the transport beam line onto the photocathode. A splitter before the transport beam line redirects a fraction of the pulse to a cross-correlator.

The paper presents experimental studies performed with different components of the photocathode laser system.

FIBER LASER OSCILLATOR

The fiber laser oscillator has two channels: the channel 1 (CH1) is used for diagnostic of the output laser pulses and channel 2 (CH2) is the working one. Each channel has its own optical compressor with diffraction grating. Linear chirped pulses have ~100 ps duration at the entrance of compressors. The spectra of both channels are centered at 1030 nm and have a width of $\Delta\lambda(FWHM)$=11 nm. A typical spectrum measured at the fiber oscillator output is shown in Fig. 1 (green curve). The optical compressors are based on diffraction gratings with 1200 lines/mm and are capable to compress pulses in each channel down to 200 fs. The maximum average power of the diagnostic and the working channels are P(CH1)=0.912 W and P(CH2)=0.554 W respectively. The pulse train frequency is 1 MHz for each channel and, therefore, the micropulse energies are W(CH1)=0.912 μJ

* The work is funded by the German Federal Ministry of education and Research, project 05K10CHE "Development and experimental test of a laser system for producing quasi 3D ellipsoidal laser pulses".
# mikhail.krasilnikov@desy.de

ISBN 978-3-95450-126-7

THE ULTRASHORT BEAM LINAC SYSTEM AND PROPOSED COHERENT THZ RADIATION SOURCES AT NSRRC

W.K. Lau, N.Y. Huang, A.P. Lee, NSRRC, Hsinchu, Taiwan.
Z.Y. Wei, Department of Engineering and System Science, NTHU, Hsinchu, Taiwan

Abstract

The NSRRC ultrashort beam facility is a few tens MeV linac system for generation of GHz-repetition-rate femtosecond electron pulses. The electron source for this linac system is a 2998 MHz, thermionic cathode rf gun with on-axis coupled rf structure in which the longitudinal electric field profile is trimmed to optimize the electron distribution in longitudinal phase space. Bunch compression will be done in the rf linac during the early stage of beam acceleration by velocity bunching. With this femtosecond electron beam, generation of broadband coherent THz synchrotron radiations from bending magnet and narrow-band coherent radiation from undulator are being studied.

INTRODUCTION

High power THz radiations found interesting applications in studying the dynamical processes of various materials. Free electron lasers and other coherent spontaneous emission sources are good candidates to produce high power THz radiations [1]. Coherent emission of spontaneous radiations from a bunch of N_e electrons is possible as long as its bunch length is much shorter than the radiation wavelengths of interest [1-3]. Depending on the bunch form factor, the power of coherent spontaneous radiations can be $\sim N_e^2$ times higher than that from a single electron. In cooperated with proper bunch compression scheme, the thermionic rf gun injectors allow the possibility to produce femtosecond electron pulses at relatively low beam energy. They are very well suited for the production of coherent radiations in THz range. Sucessful generation of coherent transition radiations (CTR) with the SUNSHINE and SURIYA facilties are good examples [4,5]. Similar system is under construction in Tohoku University, Japan [6].

A few tens MeV ultrashort beam linac system is under construction at NSRRC to produce GHz-repetition-rate sub-100 fs electron pulses. A thermionic cathode rf gun will be used to generate electron bunches with optimal time-energy correlation for bunch compression in the rf linac via velocity bunching [7-9]. Since on-axis coupled structure (OCS) rf gun shows better performance over previous design and has the advantage that it allows precision tuning of gun cavity microwave properties [10,11], it is now under consideration at NSRRC to employ such rf gun in our system. In this report, the design of this new rf gun will be discussed. The effectiveness of velocity bunching in the rf linac with new rf gun parameters expected from this OCS rf gun are re-examined. We can expect that this high repetition-rate ultrashort electron beam will be available in the near future, we now looked into the possibilities to generate broadband coherent synchrotron radiation (CSR) from bending magnet as well as narrow-band coherent THz radiations from undulators (CUR) for material studies with THz spectroscopy.

THE 30 MEV ULTRASHORT BEAM LINAC SYSTEM

This 2998 MHz thermionic cathode rf gun linac system is designed to produce thousands of sub-100 fs electron pulses of few tens pC bunch charge in each of the 10 Hz, ~1 μsec macropulses. Bunch compression scheme employed in this system rely mainly on velocity bunching in the rf linac. Beam selection is done by an energy filter in an alpha magnet at linac upstream. Space charge dynamics in the system is being studied with PARMELA [12] and GPT [13].

The 2998MHz RF Gun with On-axis Coupled Structure

Starting from circuit analysis and 2D SUPERFISH calculations, we determined preliminarily the inner dimensions of the OCS rf gun cavity (Fig. 1). The cathode assembly is located on the side-wall of the half-cell which is on the left-hand side of Fig.1. Microwave power is fed into the full-cell of the gun cavity and coupled to the half-cell through an on-axis coupling cell (the middle-cell).

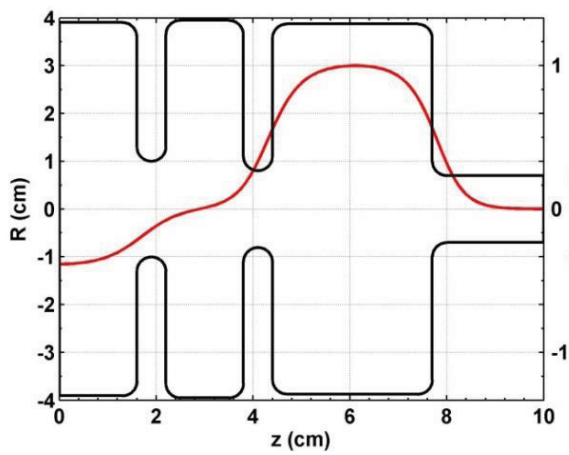

Figure 1: Geometry of the NSRRC 2998 MHz OCS rf gun. The red line is the relative amplitude of the longitudinal component of the rf electric field along the cavity axis when it is operated at π/2-mode.

Main parameters of the rf gun operating mode (π/2-mode) are listed in Table 1. It is worth noting that we decided to adjust the field ratio (i.e. full-cell to half-cell) to 2.5 for

ISBN 978-3-95450-126-7

SHIMMING STRATEGY FOR THE PHASE SHIFTERS USED IN THE EUROPEAN XFEL

Yufeng Yang[+], Yuhui Li[*], Huihua Lu[+], Frederik Wolff-Fabris[*] and Joachim Pflueger[*]
[*]European XFEL, Notkestrasse 85, 22607 Hamburg, Germany
[+]Institute of High Energy Physics in China, 19B Yuquanlu Road, 100049 Beijing, China

Abstract

The undulator systems of the European XFEL need a total of 91 Phase Shifters. The 1st field integral of these devices must not exceed 0.004 T.mm for working gaps > 16mm. For smaller gaps it is slightly released. In spite of the highly magnetically symmetric design and considerable effort such as the selection and sorting of the magnets small 1st field integral errors cannot be excluded. In this paper a strategy is studied to correct small gap dependent kicking errors as expected for the phase shifters of the XFEL.EU by using shims of different geometries and sizes.

It is found, that small gap dependent kicking errors can be well corrected for using this method. This is a systematic effort to provide effective fast tuning methods, which can be applied for the mass production.

The meaning of shim signatures will be explained in this paper. The method is demonstrated by RADIA simulations.

INTRODUCTION

Gap adjustable undulators are used in the European XFEL for the easy control of wavelength. A phase shifter is needed in between adjacent undulators to match the ponderomotive phase between electron microbunches and the laser field. The undulator systems of the European XFEL need a total of 91 phase shifters [1]. In order to avoid any steering errors induced by phase shifters, the first field integral of these devices must not exceed 0.004 T.mm for working gaps larger than 16mm, which is a tight specification. In spite of the highly magnetically symmetric design [2] and considerable construction effort such as the selection and sorting of the magnets remaining small first field integral errors cannot be excluded. The XFEL.EU Phase shifters use a similar magnetic and mechanic design as the undulators for the European XFEL: The height and the tilt of the poles are adjustable [3-4]. However there might still be small residual field integral errors. Therefore an additional tuning tool is needed. By placing small pieces of iron shims on magnets or poles a small 1st integral to the phase shifter field can be induced. The 1st field integrals induced by the shims are uncorrelated to the field integrals by pole height tuning. Therefore applying shims enriches the tuning capability to compensate field integral errors and therefore can be very useful for the phase shifter tuning.

For the production of 91 devices a fast and effective tuning procedure is needed. This paper addresses on this issue and gives first results of RADIA simulations [5].

According to the experiences from the phase shifter prototypes built for the European XFEL [2] the gap dependent field integral errors demonstrate irregular curve with one or more knee points which increase the shimming challenge. Numerical simulations of shims of different geometry using RADIA [5] were performed. The strategy is similar to the method used for the undulators, which is to calculate a combination of several shims whose total contribution matches the gap dependence of an observed error. For this objective, two basic assumptions are made:

1. Linearity principle: The contribution of a shim is proportional to its thickness.

2. Superposition principle: The contribution of a combination of several shims equals to the sum of the individual shims.

First the definition for the so called shimming signature is given: It is the contribution to the gap dependent kicking of a shim of unit thickness. Based on the shimming signature and the two assumptions above one can find a combination of several shims by decomposing the target gap dependence error into a linear combination of known signatures. Two algorithms have been proposed in Ref. [6]. One is an analytical solution: Here the first step is polynomial fitting the signature of each shim as a function of gap to n^{th} order:

$$S_1 = s_{11}g + s_{12}g^2 + s_{13}g^3 + \cdots + s_{1n}g^n, \qquad (1)$$

where g is the gap and s_{ij} is the coefficient of the j^{th} order of the i^{th} type of shim. The second step is polynomial fitting the field integral error of a Phase Shifter to n^{th} order:

$$E = e_1g + e_2g^2 + e_3g^3 + \cdots + e_ng^n. \qquad (2)$$

Where e_i is the i^{th} fitting coefficient. The *nth* order fitting needs a combination of n shims. Suppose each shim has different thickness d a system of linear equations is given:

$$\begin{pmatrix} s_{11} & s_{12} & \cdots & s_{1n} \\ s_{21} & s_{22} & \cdots & s_{2n} \\ \cdots & \cdots & \cdots & \cdots \\ s_{n1} & s_{n2} & \cdots & s_{nn} \end{pmatrix} \begin{pmatrix} d_1 \\ d_2 \\ \cdots \\ d_n \end{pmatrix} = \begin{pmatrix} e_1 \\ e_2 \\ \cdots \\ e_n \end{pmatrix}, \qquad (3)$$

If the matrix S can be inverted the thickness of each shim can be determined.

The second method is based on a trial and error using a large number of trials/ simulations: Several shims whose signatures are known are randomly selected with random thickness. The contribution of each combination is evaluated and compared with the error to be corrected. The combination which gives the best fit is selected for solution. The first method gives analytical solutions, which are mathematically correct but not always useful in practice requiring sometimes thick shims. The second is

ISBN 978-3-95450-126-7

STATUS OF THE SWISSFEL C-BAND LINEAR ACCELERATOR

F. Loehl, J. Alex, H. Blumer, M. Bopp, H. Braun, A. Citterio, U. Ellenberger, H. Fitze,
H. Joehri, T. Kleeb, L. Paly, J. Raguin, L. Schulz, R. Zennaro,
Paul Scherrer Institut, Villigen PSI, Switzerland

Abstract

This paper summarizes the status of the linear accelerator (linac) of the Swiss free-electron laser SwissFEL. The linac will be based on C-band technology and will use solid-state modulators and a novel type of C-band accelerating structures which has been designed at PSI. Initial test results of first 2 m long structures will be presented together with measurements performed with the first BOC-type pulse compressors. Furthermore, we will present first results of a water cooling system for the accelerating structures and the pulse compressors.

INTRODUCTION

The SwissFEL [1] is an x-ray free-electron laser that is currently under construction at Paul Scherrer Institut in Switzerland. A schematic layout of the facility is depicted in Fig. 1. In an initial phase, the project includes the main accelerator and a hard x-ray line called Aramis. A soft x-ray line, Athos, can be added at a later stage. The facility will operate at a repetition rate of 100 Hz and uses an S-band photo-injector to generate an ultra-bright electron beam that is accelerated to a beam energy of about 380 MeV in S-band structures. After the first magnetic bunch compressor chicane, the beam enters the main linac, which is based on C-band technology. The linac is divided into three segments. Linac 1 accelerates the beam to an energy of 2.1 GeV after which the beam is compressed in a second magnetic bunch compressor chicane. Linac 2 boosts the energy to 3 GeV. At this point, a switch-yard will be installed to allow distributing two electron bunches that are accelerated within a single RF pulse - spaced by 28 ns in time - to Aramis and Athos. After this switch yard, linac 3 accelerates the beam to its maximum energy of 5.8 GeV. Finally, the beam enters an around 60 m long undulator with a period of 15 mm in which x-ray radiation ranging from 0.1 to 0.7 nm is generated.

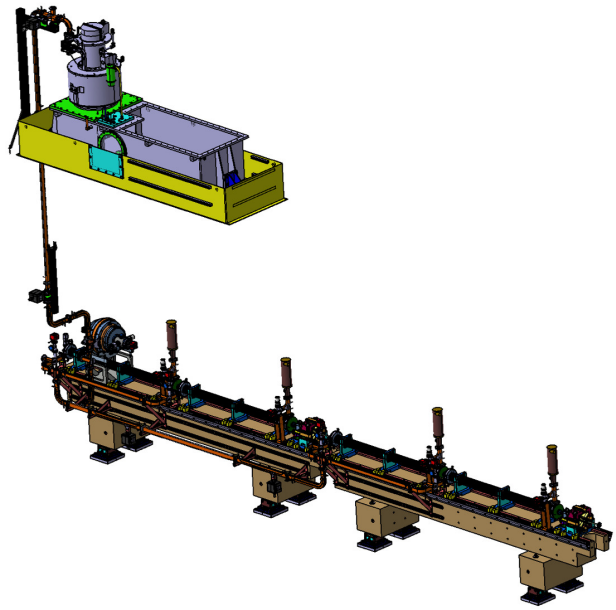

Figure 2: Layout of a linac module consisting out of the RF source (modulator not shown), the waveguide network, a BOC-type pulse compressor, and four 2 m long C-band structures.

C-BAND LINAC MODULE

The C-band linac consists out of 26 linac modules each of which comprises an RF source, a waveguide network, a barrel-open cavity (BOC) type pulse compressor, and four 2 m long accelerating structures. A schematic of a linac module is shown in Fig. 2. The RF source is placed in the technical gallerie on top of the accelerator, shielded by a concrete ceiling of 1.5 m thickness. The accelerating structures and the RF pulse compressor are installed on two granite girders, and the design is made in such a way

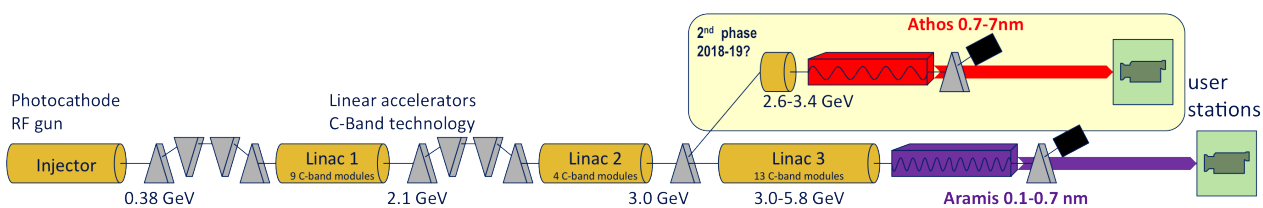

Figure 1: Schematic layout of the SwissFEL facility. It consists of an S-band injector, a C-band linear accelerator, and two undulator lines. The hard x-ray line Aramis will be built in the first project phase and in a second project phase the soft x-ray line Athos can be added.

ISBN 978-3-95450-126-7

TRANSVERSE EMITTANCE MEASUREMENT BY SLIT-SCAN METHOD FOR AN SRF PHOTO INJECTOR

P. Lu, H. Vennekate, HZDR & TU Dresden, Germany
A. Arnold, P. Michel, P. Murcek, J. Teichert, R. Xiang, HZDR, Germany

Abstract

New measurements of the transverse emittance for a Superconducting Radio Frequency (SRF) gun are conducted with slit-scan method. This contribution introduces the experimental setup, a detailed algorithm and first measurement results. The algorithm proves effective of handling irregular images while the phase space measurement is performed with high resolution. The measured values are around 1-2 πmm·mrad. The results are compared with ASTRA simulations and quad-scan measurement, followed with analysis about the measurement accuracy.

INTRODUCTION

An SRF-gun with a 3½-cell cavity has been built up and in commission at Helmholtz-Zentrum Dresden-Rossendorf (HZDR) since 2007. This SRF photo injector is designed to provide an electron beam with the energy of 9.5 MeV and the bunch charge of 1 nC. With different operation modes, it is planned to be use for the infrared free-electron lasers (FELs)[1] and the inverse Compton backscattering research at the radiation source ELBE (Electron Linac with high Brilliance and low Emittance). As a recent performance of the SRF gun, a 3.3 MeV, 30 pC (400 μA) and 1.6 ps rms bunch length beam has been created to generate the FEL radiation with 50 μm wave length [2].

Transverse emittance plays a significant role on the high bunch charge beam transport. Emittance measurements using solenoid\quadrupole scans and a multi-slits mask have been developed at ELBE [3] and were conducted with the SRF gun [4]. The solenoid\ quadrupole scan method does not measure the phase space distribution, while the multi-slits mask method has the difficulty of data overlap between its slits. To solve these problems is the motivation of developing a slit-scan measurement system.

The distinctive feature of this beam diagnostics work is a automatic and universal image processing method with a high tolerance for noises.

EXPERIMENTAL SETUP

The emittance is measured 2.6 m downstream from the photo cathode, where a 1.5 mm thick tungsten mask with a 0.1 mm wide slit samples the beam. The sampled beamlet is emittance dominated. After about 77 cm of drift, the spread beamlet is recorded by a 45° YAG screen and a CCD camera. If the slit scans all over the beam section, then the complete phase space can be recorded. Fig. 1. illustrates the entire measurement setup.

A labview program is created to control automatically the measurement and computation. For both parts the user-operation time is in seconds but the processing time is around 5 minutes.

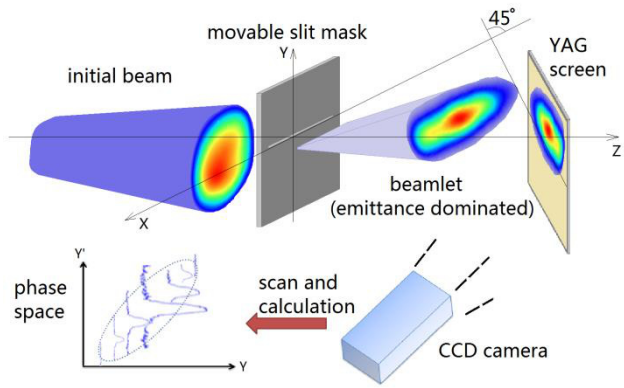

Figure 1: Experimental setup of the slit-scan emittance measurement for the SRF gun at HZDR.

DATA PROCESSING

Normally, beamlet images from the YAG screen cannot be used directly to obtain the angle distribution. Inevitable background and noisy pixels are common problems [5][6]. In Ref. [5] a Gaussian fit is performed to select the Region Of Interest (ROI), data outside of this area indicates the background and data inside is denoised by an iterative procedure. In Ref. [6] the background is from images of beam-off states. And then the filtering for isolated noises is performed to get a final image.

In our case, a universal and automatic image processing is necessary for the hundreds of images recorded for each measurement. The three main difficulties are listed below and illustrated in Fig. 2.

- Multi-peak beamlet image.
- Weak beamlet signal at the edge of a beam.
- Multi-pixel noises.

For the multi-peak and weak signal cases, universal fittings are usually not accurate enough. And a lot of multi-pixel noises will survive the filtering.

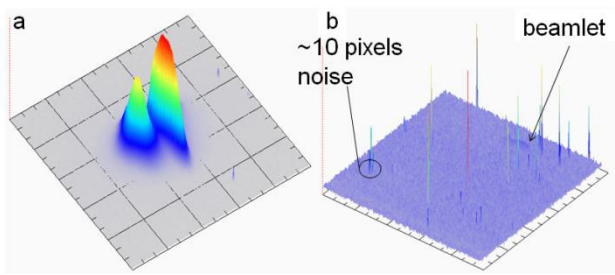

Figure 2: Special cases of beamlet images. (a) multi-peak case. (b) weak-signal case and multi-pixel noise.

ISBN 978-3-95450-126-7

INITIAL STREAK CAMERA MEASUREMENTS OF THE S-BAND LINAC BEAM FOR THE UNIVERSITY OF HAWAI`I FEL OSCILLATOR*

A.H. Lumpkin, Fermi National Accelerator Laboratory, Batavia, IL 60510 USA
M.R. Hadmack, J.M.D. Kowalcyzk, E.B. Szarmes, and J.M.J. Madey
University of Hawai`i at Mānoa, Department of Physics and Astronomy, Honolulu, HI,USA

Abstract

Experiments with a Hamamatsu C5680 dual-sweep streak camera have been performed on the Mark V Free-electron Laser (FEL) oscillator linac beams at the University of Hawai`i. The bunch length and phase of the e-beam were evaluated throughout the macropulse duration via both optical transition radiation and coherent spontaneous harmonic radiation sources. Bunch lengths of 3-5 ps FWHM and phase slews of 7 ps over 2 μs are reported under lasing conditions.

INTRODUCTION

The S-band linac driven Mark V Free-electron Laser Oscillator (FELO) at the University of Hawai`i operates in the mid-IR at electron beam energies of 40-45 MeV with a four microsecond macropulse length [1]. Recently investigations of the electron beam micropulse bunch length and phase as a function of macropulse time became of interest for potentially optimizing the FELO performance. These studies involved the utilization of a Hamamatsu C5680 streak camera with dual sweep capabilities, depending on the vertical sweep and horizontal sweep units installed, and the transport of optical transition radiation (OTR) generated at an upstream Cu mirror, and of coherent spontaneous harmonic radiation (CSHR) [2] generated in the undulator to the streak camera location outside of the linac tunnel. Both a fast single sweep vertical unit and a synchroscan unit tuned to 119.0 MHz were used. Initial results include measurements of the individual CSHR (on the FEL7th harmonic at 652 nm) micropulse bunch lengths, the CSHR signal intensity variation along macropulse time, and a detected phase slew of 7 ps over the last 2.4 μs of the macropulse. Complementary OTR measurements were also evaluated and will be presented.

FACILITY ASPECTS

The UH Mark V linac with thermionic microwave rf gun, one S-band normal conducting accelerator, and beamline is schematically shown in Fig. 1. The S-band accelerating section provided 40- to 45-MeV beams before the diagnostics chicane. Micropulse charges of 40 pC were used typically with an rf macropulse duration of ~4 us. The macropulse repetition rate was 5 Hz.

The experimental conditions provided several challenges between the broadband OTR source which is quite weak with only 46 pC in a single micropulse, but quite strong if integrated over 4 μs (but heats up the screen) and the CSHR which was 1000 times stronger and narrowband at a harmonic of the 4.5-μm FEL fundamental. The 119.0 MHz synchroscan unit was phase-locked to the 24th subharmonic of the micropulse repetition rate. The OTR and CSHR pulse length and phase were measured with the Hamamatsu UV-visible C5680 streak camera system. The camera was a demo from Hamamatsu, and the synchroscan unit was on loan from Argonne National Laboratory. The synchroscan streak camera allowed tracking of the relative phase within the macropulse of sets of micropulses to about 200 fs. The OTR and CSHR were transported 7 m using mirrors and lenses to an optical enclosure (including a photodiode and the streak camera) located outside of the accelerator tunnel.

Table 1: Summary of Electron Beam Properties During Run

Parameter	Units	Values
Bunch charge	pC	46
Energy	MeV	40-45
Bunch length, (FWHM)	ps	2-5
Macropulse Length	μs	4

lumpkin@fnal.gov
'Work supported under Contract No. DE-AC02-07CH11359 with the United States Department of Energy and work at UH supported by United States Department of Homeland Security grant number 20120-DN-077-AR1045-02.

ISBN 978-3-95450-126-7

ANALYSIS AND MEASUREMENT OF FOCUSING EFFECTS IN A TRAVELING WAVE LINEAR ACCELERATOR

H. Maesaka, T. Asaka, H. Ego, T. Hara, T. Inagaki, T. Sakurai, K. Togawa, H. Tanaka, Y. Otake
RIKEN SPring-8 Center, Kouto, Sayo, Hyogo, Japan

Abstract

For a recent precise linear accelerator, such as an x-ray free electron laser facility, the beam orbit and the beam envelope should be properly calculated from the beam dynamics model of a traveling wave accelerating structure (TWA). In order to check the validity of the dynamics model of a TWA proposed so far, we compared a calculated beam orbit with an observed one in the C-band TWA section in SACLA. Although the beam orbit in the crest acceleration part was appropriately reproduced by the TWA model, the orbit in the off-crest acceleration part did not agree with the model calculation. We found out that the discrepancy came from a quadrupole field in the coupler cell of the TWA. The strength of the quadrupole field in the coupler was estimated by a three-dimensional rf simulation and the transverse dynamics model of a TWA was modified based on the simulation result. Consequently, the beam orbit was appropriately reproduced by the new model.

INTRODUCTION

The electron beam dynamics in recent precise electron linear accelerators, such as x-ray free electron lasers (XFEL), should be appropriately understood in order to predict the beam envelope and the beam orbit. In the XFEL facility, SACLA, for example, the beam energy is often changed to adjust the photon energy requested by an XFEL user. In such a case, the beam envelope in the undulator section should be calculated instantly and accurately for the transverse phase space matching to maximize the XFEL intensity.

For the precise calculation of transverse beam parameters in the accelerator section, in particular, the transverse dynamics model of a traveling wave accelerating structure (TWA) is important. The beam dynamics model of a TWA has been already proposed and such a model includes the effects of acceleration damping and edge focusing [1]. Therefore, this model has been applied to the TWA in SACLA and the beam envelope and the beam orbit have been calculated in various operation tools. In order to evaluate the validity of the dynamics model of a TWA, we compared a calculated beam orbit with an observed orbit in the C-band choke-mode accelerator section [2] in SACLA. An electron beam was slightly kicked by a corrector dipole magnet and the orbit distortion was observed by rf cavity beam position monitors (RF-BPM) [3]. Then, the calculated orbit based on the TWA model was compared with the observed orbit.

In this article, the transverse dynamics model of a TWA believed so far is summarized and the comparison between RF-BPM data and the calculation is discussed. Since the data implies that a TWA has a quadrupole focusing effect at an off-crest acceleration phase, this effect is estimated by using a three-dimensional rf electromagnetic field simulator. Finally, we propose a modified dynamics model of a TWA and we demonstrate that the modified model appropriately reproduce the beam orbit.

#maesaka@spring8.or.jp

BEAM DYNAMICS IN A TRAVELING WAVE LINEAR ACCELERATOR

In an ordinary transverse beam dynamics model of a TWA [1], following two effects are taken into account.

- Acceleration damping.
- Monopole focus at each end.

Therefore, we briefly introduce these effects in this section. Although a TWA has a ponderomotive focusing effect [4] due to the periodic component of the acceleration electric field, this effect is negligibly small for a high energy electron beam more than 100 MeV. Accordingly, we do not consider the ponderomotive focusing effect.

Hereafter, the direction of an electron beam is set to z axis, and the derivative of the transverse beam position x with respect to z is defined to be x'. The Lorentz factor is written by γ, and β is defined as $\beta = \sqrt{1-\gamma^{-2}}$.

Acceleration Damping

When an electron beam is accelerated, the longitudinal momentum is increased while the transverse momentum is conserved. Thus, x' is decreased and hence the beam emittance is damped. If the acceleration gradient is constant, the transfer matrix of this damping effect (M_{ACC}) can be written as [1],

$$M_{\mathrm{ACC}} = \begin{pmatrix} 1 & \dfrac{\beta_0\gamma_0}{\gamma'\cos\theta}\ln\dfrac{\gamma_1+\beta_1\gamma_1}{\gamma_0+\beta_0\gamma_0} \\ 0 & \dfrac{\beta_0\gamma_0}{\beta_1\gamma_1} \end{pmatrix}. \quad (1)$$

Here, β_0 and γ_0 (β_1 and γ_1) are Lorentz factors before (after) acceleration, γ' is the derivative of the Lorentz factor with respect to z, and θ is the rf phase of the beam with respect to the crest acceleration phase. The derivative of the Lorentz factor γ' can be represented by

$$\gamma' = \frac{eE_0}{m_e c^2},$$

ISBN 978-3-95450-126-7

FIRST RESULTS OF A LONGITUDINAL PHASE SPACE TOMOGRAPHY AT PITZ

D. Malyutin*, M. Gross, I. Isaev, M. Khojoyan, G. Kourkafas, M. Krasilnikov, B. Marchetti, F. Stephan, G. Vashchenko, DESY, 15738 Zeuthen, Germany

Abstract

The Photo Injector Test facility at DESY, Zeuthen Site (PITZ), was established as a test stand of the electron source for FLASH and the European X-ray Free Electron Laser (XFEL). One of the tasks at PITZ is the detailed characterization of longitudinal properties of the produced electron bunches.

The measurements of the electron bunch longitudinal phase space can be done by tomographic methods using measurements of the momentum spectra by varying the electron bunch energy chirp. At PITZ the energy chirp of the electron bunch can be changed by varying the RF phase of the accelerating structure downstream the gun. The resulting momentum distribution can be measured in a dispersive section installed downstream the accelerating structure.

The idea of the measurement and the tomographic reconstruction technique is described in this paper. The setup and first measurement results of the bunch longitudinal phase space measurements using the tomographic technique for several electron bunch charges, including 20 pC, 100 pC and 1 nC, are presented as well.

INTRODUCTION

High brilliance photon sources like high gain Free Electron Lasers (FELs) have strong requirements on the electron beam quality used for the production of photon beam. This implies: small transverse beam emittance, high peak current and small energy spread [1]. To satisfy these requirements the electron bunch must be well prepared already in the injector part of the accelerator, i.e. at the electron source.

The Photo Injector Test facility at DESY, Zeuthen Site (PITZ) was built as a test stand for the electron source for FLASH and the European XFEL [2]. A normal conducting L-band 1.6-cell copper gun cavity with a Cs_2Te photocathode generates about 7 MeV electron bunches with ~20 ps bunch length FWHM and up to several nC charge. Then the electrons are further accelerated by an accelerating structure to an energy of up to about 27 MeV. Downstream the accelerating structure the PITZ beamline consists of various diagnostic devices for detailed measurements of the electron beam properties. Characterization of the electron bunch transverse phase space at PITZ is mainly done by a slit scan technique [3]. For electron bunch length measurements and longitudinal phase space measurements a streak camera system was used in the last years in the straight section and in dispersive sections, respectively [4]. A recently installed RF deflector is expected to provide a much better time resolution and new possibilities to study the bunch longitudinal properties compared to the streak camera [5] in the near future. Besides the measurements with the RF deflector or with the streak camera, the electron bunch longitudinal phase space can also be measured using a tomographic technique [6]. Measuring the momentum distribution for different RF phases of the accelerating structure, the longitudinal phase space can be restored applying tomographic reconstruction to the measured distributions. From the restored phase space the slice energy spread, the time-energy correlation and the beam current distribution can be extracted. In contrary to a measurement with the RF deflector, this method is a multi-shot technique as the set of momentum distributions cannot be measured at once.

The current PITZ beamline schematic layout is shown in Fig. 1. The main components of the PITZ setup are a photocathode laser system, an RF photo-electron gun surrounded by a main and a bucking solenoid, an accelerating structure – cut disk structure (CDS) which is also called booster cavity, three dipole spectrometers – one in the low energy section downstream the gun (Low Energy Dispersive Arm – LEDA), a second one in the high energy section downstream the booster (the first High Energy Dispersive Arm – HEDA1) and a third one in the end of the PITZ beamline (the second High Energy Dispersive Arm – HEDA2), three Emittance Measurement Stations (EMSYs), a transverse deflecting structure (TDS) and a phase space tomography module (PST).

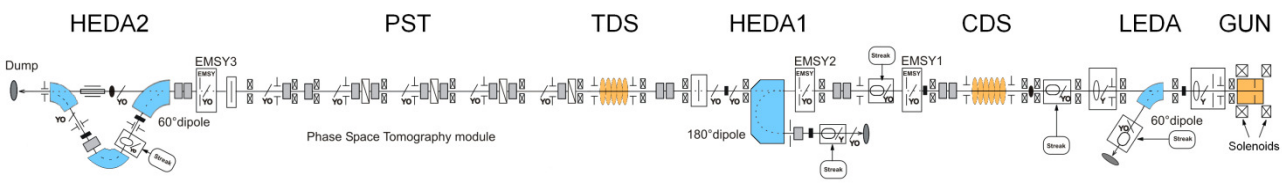

Figure 1: PITZ beamline schematic layout. The beam propagates from right to left.

*dmitriy.malyutin@desy.de

ISBN 978-3-95450-126-7

ELECTRIC FIELD DEPENDENCE OF PHOTOEMISSION FROM N- AND P-TYPE SI CRYSTALS

S. Mingels*, B. Bornmann, D. Lützenkirchen-Hecht, G. Müller
University of Wuppertal, Faculty C – Physics, Gaußstr. 20, 42119 Wuppertal, Germany
C. Langer, C. Prommesberger, R. Schreiner
Regensburg University of Applied Sciences, Faculty of Microsystems Technology, Seybothstr. 2, 93053 Regensburg, Germany

Abstract

The performance of free electron lasers depends on the brilliance of the electron source. Nowadays photocathodes (e.g. Cs_2Te) are used despite of their high emittance. To develop robust and more brilliant cathodes we have built up an UHV system which enables systematic photoemission (PE) measurements with a tunable pulsed laser (hν) at high electric fields (E). First results on Au and Ag crystals revealed only low quantum efficiency (QE) due to fast electron relaxation. Hence, we have started QE(hν,E) investigations on n- and p-Si wafers. Resonant PE was observed above as well as below the work function Φ, which can be assigned to optical transitions in the electronic band structure or explained by thermally excited states at the bottom of the conduction band. As expected, only low QE values were achieved even for n-Si probably due to surface oxide. Moreover, a significant rise of the QE peaks above Φ were obtained for n-Si at E > 8 MV/m but limited by the occurrence of parasitic field emission from dust particles.

INTRODUCTION

High brightness electron sources are crucial for large FELs [1] like LCLS or XFEL with intense beams or novel compact x-ray lasers where coherent synchrotron radiation is generated by means of the ion cores in a single crystal [2]. State of the art Cs_2Te photoemission (PE) cathodes provide high peak currents up to 50 A in short (~20 ps) pulses [3]. However, their brightness is limited by the thermal emittance, which results from the kinetic surplus energy and transverse momentum. Recently, a geometric mean emittance of 0.70 mm mrad for a bunch charge of 1 nC was achieved with Cs_2Te at PITZ [4]. Moreover, alkali-based photocathodes require extreme vacuum < 10^{-8} Pa for sufficient lifetime of high quantum efficiency (QE).

An attractive alternative to generate highly brilliant electron beams from more robust cathodes is photo-induced field emission (PFE) which might combine fast switching of PE with the low emittance of field emission (FE) [5]. In order to find a suitable PFE material, we have recently set up an UHV apparatus with electron spectrometer in adjustable triode configuration which is designed for high electric field E as well as tunable laser illumination of the cathode [6]. First PFE measurements were performed on Si tip arrays in dc mode, i.e. with an old Auger electron spectrometer and a green laser. As next step, a ns-pulsed laser tunable over a wide range (0.54 – 5.90 eV) was installed, which enables indirect but prevents direct spectroscopy of the PFE electrons. Au and Ag crystals yielded only moderate QE(5.8 eV,18 MV/m) = 9×10-5 [7] due to fast electron relaxation in the highly populated conduction band. Therefore, we have started to investigate the PFE of slightly doped semiconductors, e.g. flat n-Si(111) and p-Si(100) crystals.

EXPERIMENTAL

The actual PFE measurement apparatus is shown in figure 1. The vacuum system consists of a load-lock and a main chamber with a base pressure of 10^{-5} Pa and 10^{-7} Pa, respectively. The load-lock contains a transport system for cathode and gates and a ion sputtering system for in-situ cleaning, and a gate valve enables quick sample exchange [6]. The main chamber contains a triode system, which consists of a cathode, a gate, and a spectrometer. Figure 2 shows the rotatable excentric cathode holder opposite to the electron extractor gate in detail. The cathode holder is mounted on a linear piezo drive by which the gap distance d_{gap} can be set with µm resolution. The support rod can be retracted over 40 mm for cathode and gate exchange. The mesh gate is fixed to a truncated hollow cone support system (2.6 mm inner and 3.0 mm

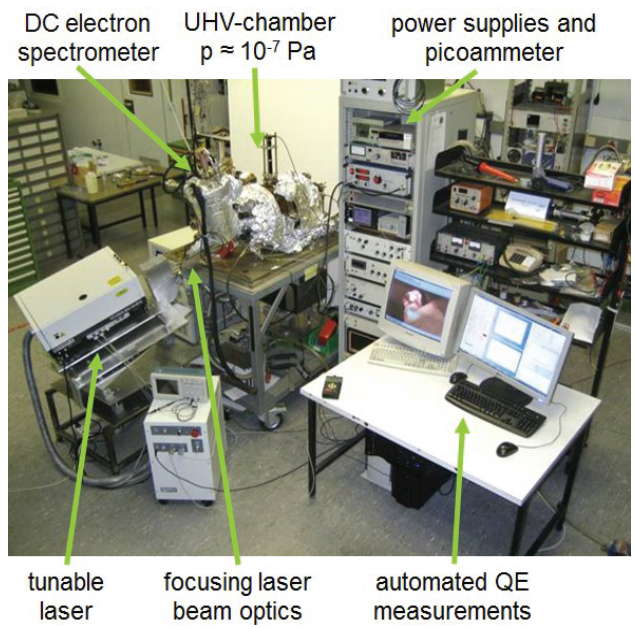

Figure 1: Photo of the PFE measurement apparatus.

*s.mingels@uni-wuppertal.de

ISBN 978-3-95450-126-7

NUMERICAL STUDY ON ELECTRON BEAM PROPERTIES IN TRIODE TYPE THERMIONIC RF GUN

K. Mishima, K. Torgasin, K. Masuda, M. Inukai, K. Okumura, H. Negm, M. Omer,
K. Yoshida, H. Zen, T. Kii, H. Ohgaki
Institute of Advanced Energy, Kyoto University, Gokasho, Uji, Kyoto, 611-0011, Japan

Abstract

The KU-FEL(Kyoto University- Free Electron Laser) facility uses a thermionic 4.5 cell S-band RF gun for electron beam generation. The main disadvantage of using a thermionic RF gun is the back-bombardment effect, which causes energy drop in the macro pulse. A modification of the thermionic RF gun to a triode type RF gun shall reduce the back-bombardment power and enlarge the macro pulse duration.

In this work we report the results of numerical studies of operational parameters depending on electron beam properties for a triode type thermionic RF.

INTRODUCTION

A 4.5 cell thermionic RF gun is used as the injector for oscillator type MIR-FEL facility (KU-FEL: Kyoto University Free Electron Laser) at Institute of Advanced Energy, Kyoto University. As compared with photocathode RF gun a thermionic RF gun has advantage of compact and economic structure, easy operation and high averaged current. The disadvantage however is the occurrence of back-bombardment effect. Thereby some electrons are getting into the decelerating phase of the driving RF wave and are accelerated back into the cathode. The back streaming electrons heat up the cathode additionally and the current rises as the consequence. The ramped current leads to limitation of the macro pulse duration. In order to solve this problem and to obtain electron beam of high brightness with long macro pulse duration, which is essential for oscillator type FEL, we are developing what we call a triode type thermionic RF gun [1]. For it an additional small coaxial cavity (triode cavity, hereafter) which serves as a control grid should be attached to the currently used thermionic RF gun. The triode cavity has a separate from the 4.5 cell gun power supply with amplitude and phase controlled with respect to those driving the gun main cavities. Figure 1 shows schematic drawing for the triode RF gun system, where the triode cavity is integrated into the main thermionic RF gun. The thermionic cathode material is located on the inner rode of the triode cavity. The triode cavity geometry and corresponding cavity voltage and cathode emmition current were designed for reduction of back-bombardment power by more than 80% [2].

The triode cavity was designed and fabricated, such that experimental proof-of-concept is planned for near future [3].

COAXIAL CAVITY DESIGN

Figure 2 shows a cross sectional view and a photograph of the triode cavity. An accessible structure with a demountable aperture as shown in the future has an advantage of being able to align and to measure the cathode position.

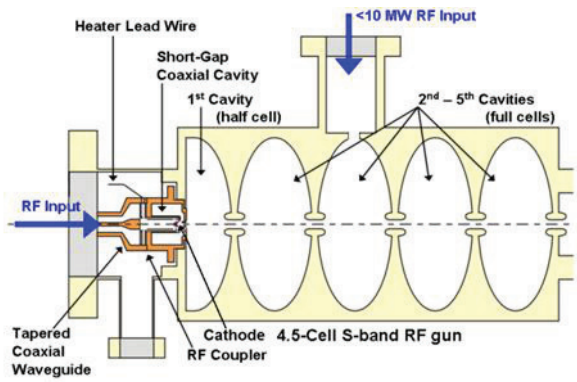

Figure 1: Triode type thermionic RF gun consisting of a small coaxial cavity and the 4.5 cell thermionic RF gun.

The cavity has a stub and spacer tuning system for resonance frequency adjustment. The stub tuning changes the resonance for 15 MHz per each mm stub length. The spacer tuning allows a wider tuning range of resonance by 256 MHz each mm of stub width, while it changes the gap length between the cathode and the aperture as well and might affect the beam focusing as a consequence (see Fig. 3).

The parameters which can be controlled for the operation of the triode cavity are following: The cathode emission J_c by means of the cathode temperature, the triode cathode cavity V_c, and the RF phase difference between triode cavity and main gun cavities φ by means of the input RF amplitude and phase control. Prior to testing the triode system we want to investigate suitable operational conditions which give optimal beam properties like emittance $\varepsilon_{r,n}$ and peak current I_{peak} for minimal power of back streaming electrons P_{back}.

ISBN 978-3-95450-126-7

R&D TOWARDS A DELTA-TYPE UNDULATOR FOR THE LCLS*

H.-D. Nuhn ,#S. Anderson, G. Bowden, Y. Ding, G. Gassner, Z. Huang, E.M. Kraft, Y. Levashov, F. Peters, F.E. Reese, J.J. Welch, Z. Wolf, J. Wu
SLAC National Accelerator Laboratory, Menlo Park, CA 94025, U.S.A
A.B. Temnykh, LEPP-CHESS Laboratory, Cornell University, Ithaca, NY, 14853, U.S.A

Abstract

The LCLS generates linearly polarized, intense, high brightness x-ray pulses from planar fixed-gap undulators. While the fixed-gap design supports a very successful and tightly controlled alignment concept, it provides only limited taper capability (up to 1% through canted pole and horizontal position adjustability) and lacks polarization control. The latter is of great importance for soft x-ray experiments. A new compact out-of-vacuum undulator design (Delta), based on a 30-cm-long in-vacuum prototype at Cornell University, is being developed and tested to add those missing properties to the LCLS undulator line. Tuning Delta undulators within tight, FEL type tolerances is a challenge due to the fact that the magnetic axis and the magnet blocks are not easily accessible for measurements and tuning in the fully assembled state. An R&D project is underway to install a 3.2-m long out-of-vacuum device in place of the last LCLS undulator, to provide controllable levels of polarized radiation and to develop measurement and tuning techniques to achieve x-ray FEL type tolerances. Presently, the installation of the device is scheduled for August 2014.

INTRODUCTION

The Linac Coherent Light Source (LCLS) has been delivering intense ultra-short x-ray beams to international users at the SLAC National Accelerator Laboratory (SLAC) since 2009 [1]. These x-ray beams are generated with fixed, canted gap hybrid permanent magnet undulators [2]. The design supports a very successful and tightly controlled alignment concept [3]. The canted poles, in connection with remote controlled undulator displacement, provide limited taper capability (up to 1% through canted pole and horizontal position adjustability). The LCLS undulator, so far, lacks full range K adjustability and polarization control. The latter is of great importance for soft x-ray experiments.

THE DELTA UNDULATOR

SLAC is developing a 3.2-m-long out-of-vacuum version of the Delta undulator to add polarisation control to the LCLS. The Delta undulator, which is a compact adjustable-phase device, was first developed at Cornell University [4] as a 0.3-m-long in-vacuum prototype. The SLAC version employs a vacuum beam pipe in order to keep the overall transverse size sufficiently small to allow it to replace an existing LCLS undulator segment. The Cornell prototype demonstrated that the concept produces an undulator with the required properties. The main parameters of the LCLS Delta undulator are listed in Table 1. As with the Cornell prototype, the core of the undulator consists of four parallel longitudinal structures (rows) that support arrays of magnet blocks, such that the pole tips of the magnet blocks on opposing rows face each other to form two crossed pure permanent magnet undulators. The undulators are designed in an anti-symmetric pole arrangement. The end pole design uses a 3-pole retraction technique [5]. Longitudinal position of each row can be remotely controlled. By setting the z-positions (phases) of the 4 rows, the degree of polarisation and the radiation wavelength (or on-axis magnetic field strength) can be controlled. The capabilities are similar to that of an APPLE device.

Table 1: LCLS Delta System Properties

Device Length	3.2	m
Operational K Parameter Range	0 – 3.37	
Period Length	32	mm
Gap Height	6.6	mm
Number of Magnet Rows	4	
Number of Magnet Blocks per Row	391	
Row Motion Range	±17	mm

CHALLENGES

Challenges that are introduced by the LCLS Delta design include (1) tighter (FEL-type) K reproducibility, phase shake and field integral tolerances; (2) increased mechanical reproducibility issues due to the 10 times longer device length; (3) incorporation of a vacuum chamber and (4) high precision magnetic field measurement of the fully assembled device.

Undulator Tolerances

One of development goals of the Delta undulator is to make it capable of functioning as segment in an x-ray FEL. The main requirement of x-ray FEL undulator segments is that they all operate at or can be fine tuned to the same resonant wavelength. Once installed, it is quite difficult to measure the resonant wavelength of each undulator segment to sufficient precision. It is essential that row position encoder readings can reliably predict undulator K values with an accuracy of $\Delta K/K<3\times10^{-4}$.

* Work was supported by U.S. Department of Energy, Office of Basic Energy Sciences, under Contract DE-AC02-76SF00515. A.B. Temnykh is supported U.S. National Science Foundation awards DMR-0807731 and DMR-DMR-0936384.

nuhn@slac.stanford.edu

ISBN 978-3-95450-126-7

UNDULATORS FOR FREE ELECTRON LASERS

C. W. Ostenfeld, M. N. Pedersen
Danfysik A/S Taastrup, Denmark

Abstract

Danfysik has produced insertion devices for the FEL community for almost 10 years. In this paper, we describe two recent undulator deliveries: a 2.8 m undulator for the FELIX free electron laser, and a 4.5 m device for the FLARE project, both at Radboud University in Nijmegen, in the Netherlands.

The device for FELIX is a 2.8 m PPM device, with a peak field of 0.483 T, and a minimum gap of 22 mm. The device for FLARE, is a 4.5 m hybrid device, with special poles, which allow for double focusing.

For both devices,we describe the magnetic modelling, and the magnetic performance.

INTRODUCTION

Danfysik[1] has the ability to deliver all types of insertion devices, including in-vacuum devices, out of vacuum devices, and Apple-II type devices[2,3]. In this short paper, we describe the latest FEL undulators deliveries, this time to Radboud University, in Nijmegen, where 2 undulators have been delivered.

FLARE PROJECT

The FLARE facility[4] is a new light source capable of generating powerful pulsed light in the THz range, between 300 GHz, and 3 THz.

Danfysik received the order to design and build a 110 mm period double-focussing undulator. The main specifications are summarized in Table 1.

Table 1: FLARE Undulator Specifications

Period length	**110 mm**
Number of full-size periods	40
# poles, including end poles	80+2
K_{RMS}	3.45
Effective field	0.475 T
Minimum clear gap	24 mm
Field flatness (x<10 mm)	+1.0 %
Undulator type	Hybrid
Magnet block type	SmCo

Magnetic Design

The undulator was modeled both in RADIA[5] and in Vectorfields OPERA. RADIA was used to get the end termination correct, whereas Vectorfields OPERA was used to double-check central field performance, and demagnetization losses. To achieve the specified double focusing action, we designed a small groove into all of the pole. In this way, we achieved a field increase of 1.0 % at 10 mm.

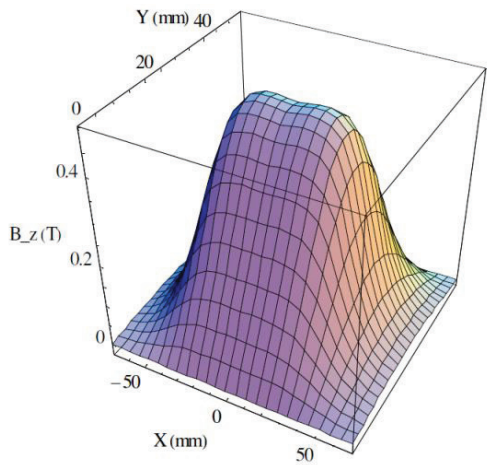

Figure 1: Magnetic field profile on the median plane of the undulator.

Magnetic Results and Shimming

The magnet blocks were delivered by Vacuumschmelze and were well within the limits specified by Danfysik. In particular, the spread in the magnitude of the magnetic moment was mostly within ± 0.5%. This minimized the time necessary for shimming.

The field integral contributions of the horizontally magnetized magnets were all measured individually with the flip coil. The magnets were then installed on the girders, in a sequence determined by the field integral, thus minimizing different accumulated field errors, using a competitive cost-function scheme.

The device was shimmed mostly by magnetic pole displacements, to optimize the electron orbit at all gaps.

ISBN 978-3-95450-126-7

300 MM ELECTROMAGNET WIGGLER FOR ELBE

C. W. Ostenfeld, M. N. Pedersen, Danfysik A/S Taastrup, Denmark

Abstract

In the past two years, a number of insertion devices have been designed, assembled and tested at Danfysik. They are used for a variety of applications at free electron lasers and synchrotron radiation facilities. In this paper, we describe the 300 mm electromagnetic wiggler, to be used at HZDR Dresden

INTRODUCTION

Danfysik[1] has the ability to deliver all types of insertion devices, including in-vacuum devices, out of vacuum devices, and Apple-II type devices[2,3]. In this short paper, we describe the latest electromagnetic wiggler delivery, this time to Helmholtz-Zentrum Rossendorf, in Dresden.

MAGNETIC DESIGN AND RESULTS

Danfysik received the order to design and build a 300 mm period, fixed-gap, electromagnetic wiggler. This wiggler will serve as a source of narrow-band THz radiation in the 100 μm to 10 mm range[4]. It will be operated with electron beams of 15 to 40 MeV, with beam currents up to 1.6 mA.

Magnetic Design

The wiggler was modeled both in RADIA[5] and in Vectorfields OPERA. RADIA was used to get the end termination correct, whereas Vectorfields OPERA was used to double-check the iron losses to make sure we had sufficient current. The field in the pole was approaching 1.9 T, so we felt quite confident that a minimum K_{RMS} of 7.5 could be reached. To achieve the specified double focusing action, we designed a small groove into all of the poles, except the thin end poles. In this way, we achieved a field increase of 0.2 % at 20 mm.

Due to the harsh demands for electron trajectory straightness, the wiggler is powered by 5 independent power supplies, such that the two end poles can be controlled independently, at the entrance and exit, while the central poles are on a common supply. The magnet power supplies are all built by Danfysik, and are summarized in Table 2.

For this projet, it was crucial that the magnetic pole centers were periodic, including the end pole pieces. This required careful optimization of the end sections, where there was

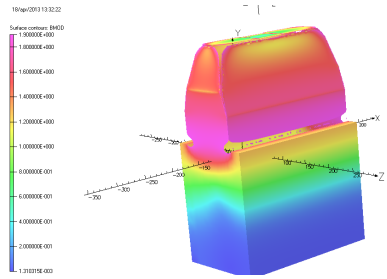

Figure 1: Modelling of a central pole using Vectorfields OPERA. The field is shown up to 1.9 T.

Table 1: Electromagnet Wiggler Specifications

Period Length	300 mm
Number of full-size periods	8
# poles, including end poles	16+2
K_{RMS}	7.76
Peak field	0.38 T
Minimum clear gap	102 mm
Field flatness	+0.2 %

Table 2: Summary of Magnet Power Supplies

	MPS type	**Quantity**	**Stability**	**Max. Current**
Central poles	854	1	10 ppm	625 A
Large end poles	854	2	10 ppm	235 A
Small end poles	9100	2	10 ppm	200 A

Magnetic Cycling

It was crucial to determine a “washing” procedure, before any fine tuning of the trajectory was possible. This is summarized in Table 2. After this was determined, the fine tuning of the trajectory was quite effective. The washing sequence was: wash End-1 pole (end at set current), wash End-5 pole (end at set current), wash End-2 pole (end at set current), wash End-4 pole (end at set current) and then wash main poles (end at set current).

ISBN 978-3-95450-126-7

GENERATION OF ULTRAFAST, HIGH-BRIGHTNESS ELECTRON BEAMS*

Jangho Park#, Hans Bluem John Rathke, Tom Schultheiss, and Alan M. M. Todd
Advanced Energy Systems, Inc., Medford, New York 11727

Abstract

The production and preservation of ultrafast, high-brightness electron beams is a major R&D challenge for free electron laser (FEL) and ultrafast electron diffraction (UED) because transverse and longitudinal space charge forces drive emittance dilution and bunch lengthening in such beams. Several approaches, such as velocity bunching and magnetic compression, have been considered to solve this problem but each has drawbacks. We present a concept that uses radial bunch compression in an X-band photocathode radio frequency electron gun. By compensating for the path length differential with a curved cathode in an extremely high acceleration gradient cavity, we have demonstrated numerically the possibility of achieving more than an order of magnitude increase in beam brightness over existing electron guns. The initial thermo-structural analysis and mechanical conceptual design of this electron source are presented.

INTRODUCTION

Ultrafast high-brightness electron beams are desired as injectors for many accelerator-driven facilities such as light sources, including free-electron lasers (FEL), and medical applications. Brightness is the holy grail of most light sources and brighter, short-pulse electron injectors are to be prized where there are no downstream transport consequences of the short bunches such as microbunching instabilities that can result from transport interactions with the energy modulations induced by the longitudinal space charge (LSC) forces in the bunches. Beam brightness is also of value in medical applications including monochromatic X-ray sources utilizing Compton back-scattering that can result in reduced dose with higher resolution images, and also tomographic imaging systems. Additionally, these sources find direct application in advanced accelerators like the plasma wake-field accelerator (PWFA) and ultrafast electron diffraction (UED) [1]. Plasma accelerators promise orders-of magnitude increases in accelerating gradient to greater than 100 GeV/m and could lead to very compact and economical systems for those many accelerator applications that require high particle energies. Ultrafast diffraction techniques, which provide information about atomic-scale molecular structure, are critical to chemists and material scientist in their research and development activities.

In the generation of ultrafast, high-brightness electron beams, space-charge forces play a fundamental role in emittance dilution and bunch lengthening within the gun and subsequent emittance compensation drift. In order to generate and preserve the beam brightness, transverse and longitudinal space charge effects have to be precisely managed. Several different approaches have been reported and are being actively pursued within the worldwide accelerator community. These include various velocity bunching and magnetic compression techniques. However, each option suffers drawbacks that must be overcome in order to deliver a compact and economic ultrafast, high-brightness source.

In recent years, due to a better understanding and improved control of the propagation dynamics in the non-relativistic electron guns used to date for high-brightness electron source, sub-picosecond level temporal structures have been achieved. In order to develop an improved ultrafast high-brightness electron source, we have proposed a scheme that compensates for path length differences by using a curved cathode [2] to introduce radial compression that compensates for geometric bunch lengthening effects when coupled with extremely high acceleration gradient that minimizes the impact of space-charge forces. AES patented cathode rear feeding coaxial coupling also eliminates contributions to transverse emittance from non-axisymmetric modes [3]. We show that combining these two effects is feasible and does indeed deliver a more compact, economic, ultrafast high-brightness electron beam for various applications such as FEL and advanced accelerator injector and UED.

CAVITY DESIGN

For a high-aspect-ratio (short bunch length) electron bunch, the asymptotic bunch length due to the space charge forces of a uniformly accelerated bunch, ignoring the drive laser duration and assuming prompt response from a copper cathode where the laser spot radius (R) is kept constant, is expressed by:

$$\Delta t_{sc}(\infty) = \frac{mc^2}{e}\frac{Q}{\pi R^2 \varepsilon_0 c E^2}. \qquad (1)$$

Here, bunch lengthening due to space charge is inversely proportion to the square of the bunch radius (R) and the square of the accelerating field (E). Bunch length stretches due to the longer path lengths of the outer particles compared to electrons emitted closer to the axis. Bunch lengthening due to geometrical effects is proportional to the square of the beam radius.

Use of a coaxial waveguide feeding the front of the gun cavity has the drawback that radial space for electron beam emission and drive laser insertion is relatively small from the previous cavity design [4]. We have completed

* This work was supported by the U.S. Department of Energy, under Contract No. DE-SC0009556.
#jangho_park@mail.aesys.net

ISBN 978-3-95450-126-7

DEVELOPMENTS OF A HIGH-AVERAGE-CURRENT THERMIONIC RF GUN FOR ERLS AND FELS*

J. Park#, H. Rathke, T. Schultheiss, A.M.M. Todd
Advanced Energy Systems, Medford, NY 11763, USA

Abstract

The development of a high-average-current thermionic RF gun with the required beam performance for lasing would provide significant cost of ownership and reliability gains for high-average-power energy recovery linac (ERL) and free electron laser (FEL) devices. The beam for these applications requires high quality and high performance, specifically: low transverse emittance, short pulse duration and high average current. We are developing a gridded thermionic cathode embedded in a copper one-and-half cell UHF cavity to generate the electron beam. The fundamental RF and higher harmonics are combined on the grid and a gated DC voltage controls the beam emission from the cathode. Simulations indicate that short pulse ~ 10 psec, < 1 MeV electron beams with low-emittance ~ 15 mm-mrad at currents ≥ 100 mA can be generated. The elimination of sensitive photocathodes and their drive laser systems would provide significant capital cost saving, improved reliability and uptime due to increased robustness and hence operating and lifecycle cost savings as well. We will present the gun design and performance simulations and the progress achieved to date in optimizing the device.

INTRODUCTIONS

In order to develop high-average power IR free electron laser (FEL) and energy recovery linac (ERL), high brightness, high-average-current electron beam is required. There are several approaches to generate high-average-current electron beam. One example is JLAB's GaAs DC photocathode gun that makes high average current, high brightness electron beam sources for the development of 100 mA class injectors for ERLs and FELs [1-2]. Photocathode guns are employed in the majority of FELs and are capable of generating short, high-quality, and high-charge electron bunches However, photocathodes have some drawbacks when operated at high-average power values due to excessive cathode heating, short cathode lifetimes, and high-average power drive laser requirements. Thermionic cathodes have demonstrated long lifetime operation high-peak-current densities without the need of drive lasers. Several FELs have used thermionic gun technology, however, these guns generate bunches at a subharmonic of the linac frequency and cannot be used for high-average-power IR FELs because of their low repetition rates.

To resolve this issue, AES, here, proposed a thermionic rf gun with gridded cathode driven with harmonics of the main linac rf frequency. When the grid is negatively biased with respect to the cathode, emission is restricted to a small portion of the RF phase [3], thereby generating short bunches at a repetition rate equal to the gun rf frequency.

CAVITY DESIGN

The proposed gun cavity is shown in Figure 1(a). The thermionic cathode is hollowed slightly from the body of a 700-MHz RF cavity. Fields from the RF cavity slightly decrease into the gridded cathode gap, reaching a nonzero value at the cathode surface. After injecting RF power at the 3rd and 5th harmonics of the fundamental cavity frequency into the gridded cathode gap, the longitudinal electric field at the cathode surface takes the superposition of those mentioned fields could control the beam emission. Figure 1(b) shows the fundamental field prof

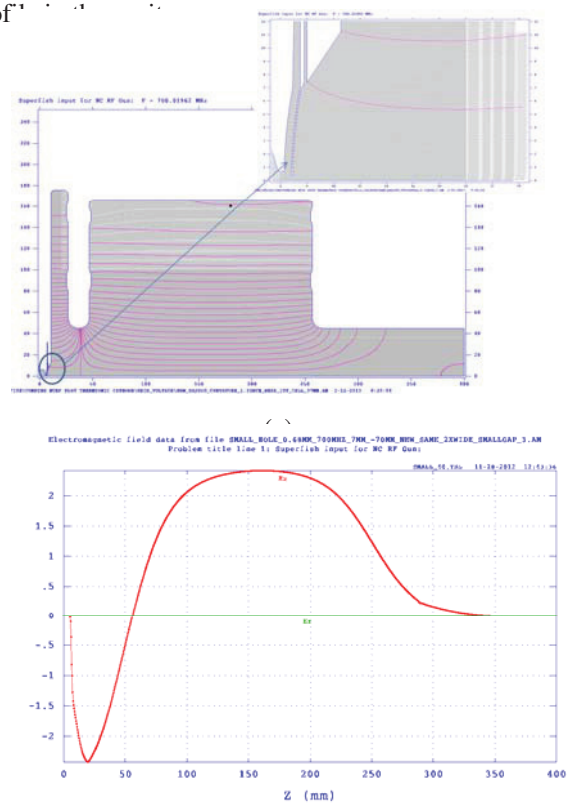

(b)

Figure 1: (a) Thermionic rf gun cavity with grid control mesh in the cathode region and (b) fundamental field profile of the cavity.

Various grid spacing and cavity length have visited to get optimized cavity design. The resulted cavity design

* This work was supported by ONR under Contract No. N00014-10-C-0191.
#jangho_park@mail.aesys.net

ISBN 978-3-95450-126-7

SIMULATION OF A PHOTOCATHODE-BASED MICROTRON USING A PIC CODE

Sunjeong Park, Eun-San Kim, KNU, Daegu, Korea
Kyu-Ha Jang, Seong Hee Park, Young Uk Jeong, KAERI, Daejeon, Korea
Nikolay A. Vinokurov, KAERI, Daejeon, Korea & BINP, Novosibrisk, Russia

Abstract

Korea Atomic Energy Research Institute (KAERI) has used a microtron accelerator based on a thermionic cathode for operating a compact terahertz (THz) free-electron laser (FEL). We would like to develop a photo-cathode-based microtron for generating high-peak (~ 100 A) and ultrashort (~ 1 ps) as an electron source for generating intense and ultrashort THz pulses. It is necessary to analyze precisely the electron beam dynamics in a microtron, especially, the relation between the RF phase in a microtron cavity and laser input time for adapting the photocathode to a microtron. Hence, we conduct computer simulation with a 3D PIC-code to find those optimized conditions for the photocathode-based microtron with the beam energy of ~7 MeV and bunch charge of ~ 100 pC with a bunch duration of 1 ps.

INTRODUCTION

Terahertz (THz) rays have been drawing attention because of their peculiarities which are different from visible ray or x-ray. Most interesting characteristic is that they can penetrate various substances but they are much less harmful than X-rays. And THz is known as a fingerprint spectral range for identifying molecules. So THz technology is promising for medical imaging and security inspection. However, this range is known as 'terahertz gap' because it is difficult to generate broadband THz ray with high power [1]. Recently, Nikolay Vinokurov proposed an efficient way of generating ultrashort THz pulses by sub-picosecond relativistic electron bunches passing through a multi-foil cone radiator [2]. The multi-foil cone radiator can improve the generation efficiency proportional to the number of foils than usual single-foil coherent transition radiation source. These THz-rays can be achieved by using multi-foil cone radiator which the coherent transition radiation is generated when sub-picosecond bunches are passing through the thin multi-foil. Microtron can accelerate the electron beam to get those ranges of energy. The microtron is the device that accelerates electrons with circular orbit due to Lorentz force under a constant magnetic field. The electrons are accelerated in the RF cavity, so the arrival time of electron beam and the RF field for accelerating in the RF cavity should be synchronized. It has not only relatively low cost but also quite small size for accelerating the electrons so it is suitable for compact THz Radiator [3, 4, 5].

SYNCHRONICITY AND PHASE STABILITY CONDITIONS

In the microtron, the electrons must have exactly same phase of electric field for acceleration that supplied from magnetron to gain the energy. For the start, the period of first orbit should be an integer multiple of period of RF to inject the acceleration phase. Also, the electrons which energy is increased at the acceleration field have larger orbit and the arriving time for the acceleration is longer than previous one. Therefore to inject appropriate phase of acceleration the gap between the two orbits must be an integer multiple of period of RF. This is called as synchronization condition and according to those conditions the orbit of first period (T_1) is given by $T_1 = 2\pi m_0\gamma_1 /eB$ and the difference between two periods of each orbit (ΔT) are given as $\Delta T = T_{n+1} - T_n = 2\pi m_0 \Delta\gamma_g /eB$, where B is strength of magnetic field, γ_1 is energy of electrons at the first orbit and $\Delta\gamma_g$ is energy gain at the RF cavity.

The more energy electrons get the period last longer, and then the range of stable phase of RF voltage is under the native slope. We can find the range of stable phase for acceleration of the electron beam by calculating the transfer matrix. At the accelerating cavity, the phase of the electrons is not changed because the velocity of them is close to the velocity of light, but the energy of the electrons is changed due to the RF. On the other hand, the energy of electrons is same at anywhere except RF cavity since there is no electric field but a uniform magnetic field. Then the transfer matrix can be calculated as shown below by applying those relations.

$$R = \begin{bmatrix} 1 & -\frac{2\pi\ell}{\Delta E} \\ 0 & 1 \end{bmatrix} \begin{bmatrix} 1 & 0 \\ -\Delta E \tan\phi_s & 1 \end{bmatrix} = \begin{bmatrix} 1+2\pi\ell/\tan\phi_s & -\frac{2\pi\ell}{\Delta E} \\ -\Delta E \tan\phi_s & 1 \end{bmatrix}$$

To find the stable condition of the trajectory of electrons beam, eigenvalue and determinant of transfer matrix should be used. According to those qualifications, the stable condition is -2< Trace R <2, in other words the condition can be written as $-2 < \pi\ell\tan\phi_s < 0$. At this time the RF acceleration phase for stability is $-\tan^{-1}(2/\pi\ell) < \phi_s < 0$, then we can find the stable region of RF phase of fundamental mode, $-32.5 < \phi_s < 0$. It is natural that the phase oscillations are bigger when the ϕ_s approaches the boundary of the stable region. Therefore, the

ISBN 978-3-95450-126-7

STATUS OF THE UNDULATOR SYSTEMS FOR THE EUROPEAN X-RAY FREE ELECTRON LASER

J. Pflueger, M. Bagha-Shanjani, K. Berndgen, A. Beckmann, P. Biermordt, G. Deron, U. Englisch, S. Karabekyan, B. Ketenoglu, M. Knoll, Y. Li, F. Wolff-Fabris, M. Yakopov
European XFEL, Hamburg, Germany

Abstract

For the European X-ray Free Electron Laser (XFEL.EU) three undulator systems with a net magnetic length of 455 meters are planned, employing 91 undulator segments each 5m long. They are gap variable and use planar hybrid undulator technology. Their production has started in March 2012 using the technology and methods developed during the prototyping phase. An overview over the production and representative results are given.

INTRODUCTION

The European XFEL is currently under construction [1]. It uses the principle of Self-Amplified-Spontaneous-Emission, (SASE) [2, 3]. Three undulator systems will be built: SASE1 and SASE2 will operate mainly in the hard X-ray regime from 0.04 to 0.2 nm. SASE3 will be operated in the soft X-ray regime from 0.4 to 5.2 nm. Parameters are given in Table 1 below.

Table 1: Parameters of the XFEL.EU Undulator Systems

	SASE1/2	SASE3
λ_0 [mm]	40	68
Operational Gap Range [mm]	10-20	10-25
K-Range	3.9–1.65	9.0-4
Radiation Wavelength Range [nm]		
@ 17.5 GeV	0.147-0.040	1.22-0.27
@ 14.0 GeV	0.230-0.063	1.90-0.42
@ 8.5 GeV	0.625-0.171	5.17-1.15
# of Segments	35	21
System Length [m]	213.5	128.1

SASE FELs need long undulator systems: SASE1/2 will use each 35 segments of 40mm period length (U40). Including the intersections each has a total length of 215 m. SASE3 requires 21 segments of 68mm period length (U68), resulting in a total length of 128 m. In total, 91 undulator segments, 70 U40s and 21 U68s are needed.

Due to the short radiation wavelengths, the magnetic fields of the EXFEL undulator segments need to fulfil demanding specifications in order to provide longitudinal phase synchronization and transverse overlap over the whole length of an undulator system. Since the undulators are gap-tuneable the specifications must be fulfilled over the whole operational gap range [4]. Production started in early 2012. The EXFEL time schedule requires all undulator segments to be finished by the end of 2014. An overview over the production in industry and the tuning methods applied at XFEL.EU is given.

HARDWARE & PRODUCTION ASPECTS

The mechanical design of the XFEL undulator segments was the result of a synergetic collaborative effort for the insertion devices for PETRAIII at DESY [5] on one side and for the XFEL.EU undulator segments on the other. There is a common basis for key technologies such as motion control, mechanical design, magnetic design, magnetic tuning and measurement techniques.

Mechanical Design

For the large number of undulator segments for the XFEL.EU strict standardization is essential to simplify the design effort and allow for an economic production and maintenance. As a consequence there is only one standard mechanical support system for both the U40 and U68. It is designed to meets all requirements, specifically it withstands magnetic forces for the U68 and simultaneously fulfils the higher accuracy requirements for the U40. There is a standard interface on the girder surfaces towards the gap side. Different magnet structures, using his interface can be attached via clamps. In Fig. 1 an undulator segment for SASE1 equipped with a U40 structure is shown. The same AlMg alloy for both the girders and the non-magnetic support structure is used to minimize thermal deformation and increase thermal stability. More details are given in [6].

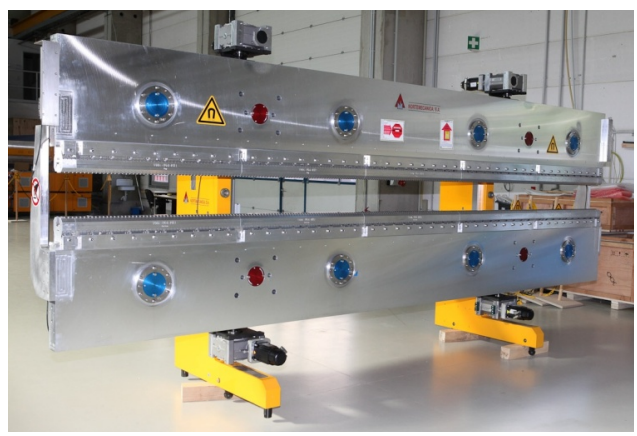

Figure 1: Undulator Segment for SASE1 with λ_0=40mm.

Motion Control System

Each undulator segment uses four individual servo motors to drive the gap. There are no coupling gears and drive shafts. Synchronization is done electronically by a

ISBN 978-3-95450-126-7

STATUS OF THE PLANAR UNDULATOR APPLIED IN HUST THz-FEL OSCILLATOR

B. Qin*, L. Yang, X.L. Liu, K.F. Liu, J. Yang, P. Tan, Y.Q. Xiong, X. Lei, Y.B. Wang
State Key Laboratory of Advanced Electromagnetic Engineering and Technology
Huazhong University of Science and Technology, Wuhan 430074, Hubei, China

Abstract

To fulfill the physical requirement of a 50-100 μm Free Electron Laser (FEL) oscillator, design considerations of a planar undulator are described. Some technical issues, including the tolerances study, the beam match, the field measurement setup and the influence on the magnetic field by the waveguide are discussed as well.

INTRODUCTION

In the past decade, terahertz (THz) science and technology has been developed rapidly. In applications of real-time imaging, security inspection, materials and biomedicals, high power compact THz sources with Watt level average power are demanded[1], which is beyond capability of traditional THz sources.

A prototype compact terahertz FEL oscillator was proposed at Huazhong University of Science and Technology (HUST), which is designed to generate $50-100\mu m$ coherent radiation with 1 MW level peak power[2]. The conceptual design is shown in Fig. 1, with the main design parameters listed in Table 1. We choose a thermionic electron gun with an independently tunable cell (ITC) as the electron beam source for simplicity, with output energy around 2MeV[3]. A S-band linac with traveling wave structure will accelerate the beam to range of 6 MeV to 14 MeV, that covers the energy from 8.1 to 11.7 MeV. The macro pulse duration $5\mu s$ is long enough for the power build up process which is around $1\mu s$. A symmetrical near-concentric optical cavity is formed by two gold-coated copper toroid mirrors, with the cavity length of 2.93m. A planar undulator with a moderate K is adopted. This paper mainly describes the physical parameters determination and technical aspect of the undulator.

Table 1: Parameters of the THz FEL Oscillator.

Beam energy	8.1-11.7 MeV
Radiation wavelength,λ_r	50 - 100 μm
Bunch charge	$\geq$ 200pC
Bunch length (FWHM),σ_s	5-10ps
Energy spread (FWHM)	0.3%
Normalized Emmittance,ϵ_n	$15\pi mm\cdot mrad$
RF	2856 MHz
Macro pulse duration	4-6 μs
Repetition rate	10-200Hz
Number of the full strength period,N_u	30
Undulator period,λ_u	32 mm
Undulator parameter,K	1.0-1.25
Optical cavity length	2.93m
Peak power	0.5-1 MW

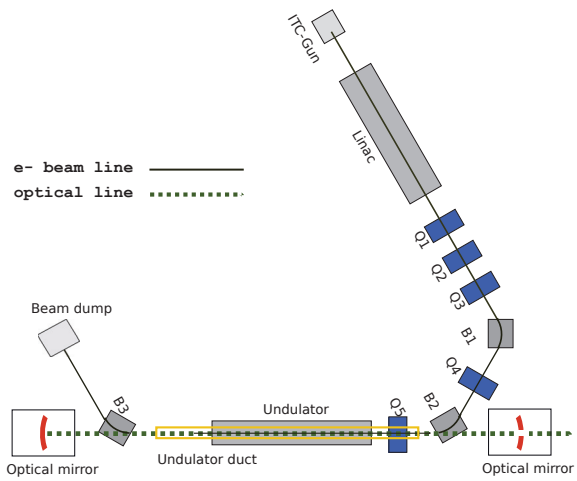

Figure 1: Schematic view of HUST THz-FEL oscillator.

DETERMINATION OF PARAMETERS

The evaluation of the FEL performance, including the gain, the saturated power and the saturation time is performed using 1D linear theory, and finally determined the undulator parameters based on the specification of the electron beam [2]. In the low gain FEL oscillator, the power build up process is non-linear and difficult to be described analytically. But the saturation time can be estimated with an analytical method[1]. The round-trip number m can be derived from the approximated exponential growth of the power build up $P_{sat} = P_0 \cdot (1 + G_{net})^m$, where $G_{net} = G_{max} - G_{loss}$ is the net round-trip gain with round-trip loss rate G_{loss} due to internal and transmission losses in the optical resonator.

$$m = \ln(P_{sat}/P_0)/\ln(1+G_{net}) = \ln n/\ln(1+G_{net}) \quad (1)$$

To achieve possible higher undulator peak field, the vertical aperture of the waveguide duct is 10mm, and the minimum gap size of the undulator $g = 16mm$. For a reasonable ratio $g/\lambda_u = 0.5$, the undulator period length $\lambda_u = 32mm$ is determined.

K is investigated from 1.0 to 1.5, and K_{max}=1.25 is determined. Compared to K=1.0, the gain is increased 35%, leading to 30% decrease of the saturation time and 20% increase of the saturation power. $K > 1.25$ brings insignifi-

* bin.qin@mail.hust.edu.cn

ISBN 978-3-95450-126-7

HIGH AVERAGE BRIGHTNESS PHOTOCATHODE DEVELOPMENT FOR FEL APPLICATIONS

T. Rao, I. Ben-Zvi, J. Skaritka, E. Wang, BNL, Upton, NY 11973, USA

Abstract

Two load-lock chambers have been built to transport and insert multialkali cathodes in SRF guns operating at 704 MHz and 112 MHz. In this paper, we will describe the design of the load-lock chambers, transfer mechanisms, Change in QE in one of the transfer chambers and the removal of used cathode from the substrate using excimer laser.

INTRODUCTION

There has been considerable interest in generating high average current, low emittance and high brightness electron beams for a number of accelerator applications. Recent studies have shown cesium potassium antimonide to be a robust photocathode capable of producing high peak and average currents. Typically, this cathode is fabricated in a UHV system attached to the gun. However, for some applications, the fabrication site has to be physically removed from the gun location and the cathode has to be transferred between the two sites in UHV load lock chambers. Such a detachable load-lock system should meet the constraints imposed by the fabrication chamber, gun as well as the transport system. We discuss below the constraints faced in two different SRF guns, the design of detachable load-lock systems for these guns, QE evolution in a storage chamber in one of the transport systems. In addition, in some designs, the cathode insertion section does not lend itself to cathode removal by thermal processes. An alternate mechanism, cathode removal by excimer laser is also presented

Load-Lock chamber for 112 MHz SRF gun

112 MHz, SRF, quarter wave resonator gun was built to provide electron beams to increase the luminosity of the Relativistic Heavy Ion Beam (RHIC) at BNL by coherent electron cooling[1]. The constraints for inserting the cathode into this gun are a) particulate free insertion to preserve the Q of the SRF cavity b) breakdown-free operation in field gradients > 20 MV/m and c) thermal isolation from the cavity wall. Figure 1 shows a drawing of the insertion device. The load-lock chamber with the magazine supporting 4 cathode pucks is shown in Fig. 2. The vacuum in this chamber is maintained by a 25 l/s ion pump and a 400 l/s NEG pump. The magazine can store up to 5 cathodes reducing the down time for cathode exchange, once the load-lock is in place.

Prior to fabricating the cathode, the substrate can be heated up to 400 C by irradiating the Mo substrate puck with a 5 W CW laser operating at 532 nm. The maximum achievable temperature is dictated by the absorption coefficient of the material of the puck and the optical arrangement.

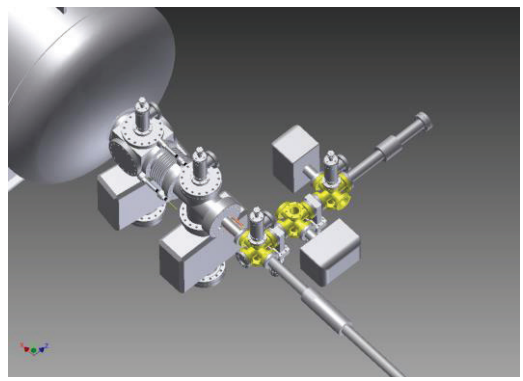

Figure 1: Schematic of the detachable load-lock system for 112 MHz SRF gun. The manipulator in the bottom right quadrant transfers the cathode from the load-lock chamber at the top right quadrant to the gun in the top left quadrant.

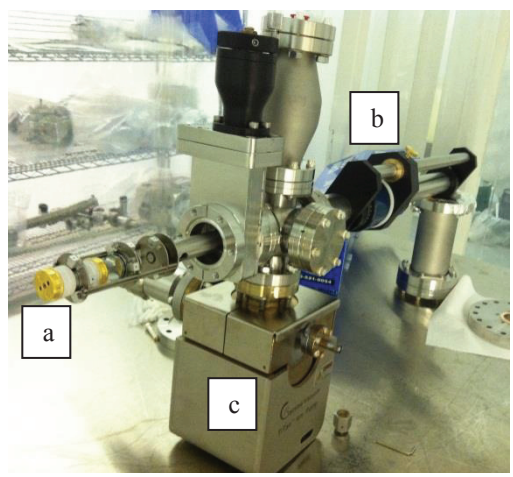

Figure 2: Photograph of the load-lock chamber with the magazine (a) in the foreground. Two sets of pucks are mounted on the magazine. (b) is manipulator and (c) is the pumping plenum.

Figure 3 shows the temperature ramp-up and -down of the Mo puck. The laser heating has several advantages over the normally used resistive heating: a) only the puck is heated, b) temperature of surrounding vacuum chamber is minimally changed reducing the gas load in the system significantly, c) both heating and cooling are very fast, and d) the heat source is external to the system hence changes and modification can be made to it without altering the system. Since most photoinjector facilities already have a laser in place, the high cost associated with the laser is not a significant concern.

ISBN 978-3-95450-126-7

SHORT SASE-FEL PULSES AT FLASH*

J. Rönsch-Schulenburg†, E. Hass, A. Kuhl, T. Plath, M. Rehders, J. Rossbach,
Hamburg University & CFEL, Hamburg, Germany
G. Brenner, C. Gerth, U. Mavric, H. Schlarb, E. Schneidmiller, S. Schreiber, B. Steffen, M. Yan,
M. Yurkov, DESY, Hamburg, Germany

Abstract

FLASH is a high-gain free-electron laser (FEL) in the soft x-ray range. This paper discusses the generation of very short FEL pulses in the Self-Amplified Spontaneous Emission (SASE) - mode without an external seeding signal. In the optimal case a SASE-FEL can be operated in the so-called single-spike mode. At FLASH a new photo-injector laser has been commissioned, which allows the generation of shorter bunches with low bunch charge directly at the photo-cathode. This shorter injector laser reduces the required bunch compression for short pulses and thus allows a stable SASE performance with shorter pulses. First SASE performance using the new injector laser has been demonstrated and electron bunch and FEL radiation properties have been measured. These measurements are presented and next steps towards single spike operation are discussed.

MOTIVATION

The users of free-electron lasers (FELs) show a rising interest in very short vacuum ultraviolet (VUV), extreme ultraviolet (XUV) and X-ray pulses to study ultra-fast processes in different areas of science. Several schemes to achieve such short bunches have been proposed. In order to produce radiation pulses of a few femtoseconds at FELs like FLASH, the most robust method is to create an electron bunch, which is in the most extreme case as short as one longitudinal optical mode. The electron bunch length (σ_b) has to fulfill the condition $\sigma_b \leq 2\pi L_{coop}$ [1, 2], with L_{coop} the cooperation length. These so-called single spike SASE pulses [1, 2] attract the interest of several FEL facilities [3, 4, 5]. Such a single spike SASE pulse is bandwidth limited, longitudinally coherent and compared to other concepts (e.g. seeding) no long background signal disturbs the signal. The usage of short pulses also prevents damage of the studied object, since most applications of short pulses do not rely on a high photon count [6]. A single spike operation at FLASH [7, 8] requires an electron bunch with a duration of a few fs and to mitigate space charge forces, a bunch charge of about 20 pC is required. First beam dynamics studies have been performed [9] to estimate the required parameters.

* This project has been supported by BMBF under contract 05K10GU2 & FS FLASH 301
† juliane.roensch@desy.de

NEW INJECTOR LASER

The standard photo injector laser used at FLASH has an rms duration of 6.5 ps. To reach a bunch duration of about 3 fs a compression by more than a factor 2000 (as shown in Table 1) would be required. Such a strong compression would lead to strong instabilities in the machine caused by small phase fluctuations. A reduced photo injector laser pulse duration would help to relax the RF tolerances which scale linear with the compression factor. Thus a shorter injector laser pulse duration is required. Due to the usage of the lower bunch charge this reduction of the bunch length at the injector is possible. Therefore a new photo injector laser with sub-picosecond pulse duration in combination with a stretcher is used to optimize the initial bunch length. The commissioning of the new laser system are described in detail in [10]. Details about the synchronization of the laser system can be found in [11].

Table 1: Required Compression Depending on Injector Laser Pulse Duration and Aiming Bunch Duration

	typical FLASH operation	single spike operation	single spike operation
injector laser pulse duration	15.3 ps (FWHM)	15.3 ps (FWHM)	1-3 ps (FWHM)
bunch charge	0.08-1 nC	20 pC	20 pC
rms bunch duration	30-200 fs	3 fs	3 fs
compression	220 - 32.5	**2200**	**140 - 430**
FEL pulse duration	30-200 fs (FWHM)	3 fs (FWHM)	3 fs (FWHM)

To judge the performance of the new short pulse injector laser the charge stability was measured in comparison to the standard injector laser in September 2012. In these measurements the short pulse laser and the standard injector laser showed a comparable charge stability. The short pulse injector laser beam line was designed such that the beam was collimated in both BBOs crystals. For the first SASE with the new injector, which was performed in January 2013 and is discussed in the next section, a different setup was used. Here the beam was focused into both BBO crystals. This setup was used to achieve a sufficiently high conversion efficiency, but unfortunately it increased also the instability by more than a factor of two. For future applications the beam line is modified for high conversion efficiency and high stability at the same time.

ISBN 978-3-95450-126-7

TRANSPORT OF TERAHERTZ-WAVE COHERENT SYNCHROTRON RADIATION WITH A FREE-ELECTRON LASER BEAMLINE AT LEBRA

N. Sei#, H. Ogawa, Research Institute of Instrumentation Frontier, National Institute of Advanced Industrial Science and Technology, 1-1-1 Umezono, Tsukuba, Ibaraki 305-8568, Japan

T. Sakai, K. Hayakawa, T. Tanaka, Y. Hayakawa, K. Nakao, K. Nogami, M. Inagaki, Laboratory for Electron Beam Research and Application, Nihon University, 7-24-1 Narashinodai, Funabashi, 274-8501, Japan

Abstract

Nihon University and National Institute of Advanced Industrial Science and Technology have jointly developed terahertz-wave coherent synchrotron radiation (CSR) at Laboratory for Electron Beam Research and Application (LEBRA) in Nihon University. We have already observed intense terahertz-wave radiation from a bending magnet located above an undulator, and confirmed it to be CSR. To avoid a damage caused by ionizing radiation, we worked on transporting the CSR to an experimental room, which was next to the accelerator room across a shield wall, using an infrared free-electron laser beamline. The CSR power of the vertically polarized component was approximately 40 nJ per macropulse at frequencies of 0.09-0.17 THz.

INTRODUCTION

Because an electron beam of a linac in a free-electron laser (FEL) facility must have a short bunch length and a high charge to realize the FEL lasing, it is suitable for generating intense coherent radiation in the terahertz (THz) region. Although there are various THz-wave sources using such an electron beam [1-3], coherent synchrotron radiation (CSR) hardly affects the electron beam [4]. It can be developed without degrading performance of an FEL. Therefore, Nihon University and National Institute of Advanced Industrial Science and Technology have jointly developed intense THz-wave CSR at Laboratory for Electron Beam Research and Application (LEBRA) in Nihon University. We have already observed an intense CSR using an S-band linac at LEBRA and reported the performance of the CSR [5]. However, there is high-flux ionizing radiation due to the electron beam loss around a bending magnet in which the intense CSR is generated. When the CSR is used for a sample with a detector near the bending magnet, the ionizing radiation may spoil the sample and the detector. In order to use the CSR in various experiments, it is necessary to transport it to a safe place for ionizing radiation. Then, we transported the CSR to the experimental room, which was next to the accelerator room across a shield wall, using an infrared FEL beamline. We could obtain a CSR beam whose intensity was approximately one-tenth of that around a bending magnet. In this article, the transport of the CSR using the infrared FEL beamline and characteristics of the CSR transported to the experimental room are reported.

#Corresponding author. sei.n@aist.go.jp

FEL BEAMLINE AT LEBRA

An infrared FEL has been developed with the S-band linac at LEBRA [6]. Because the frequency of the buncher and accelerator tubes is 2856 MHz, the electron beam is bunched in 350 ps intervals. The macropulse duration determined by the flat-top pulse width of the 20 MW klystron output power is 20 μs. Then, there are approximately 57 thousand micropulses in a macropulse. The electron-beam energy can be adjusted from 30 to 125 MeV, and the charge in a micropulse is up to approximately 30 pC in full-bunch mode. The electron beam accelerated by the linac is guided to an FEL undulator line by two 45 degree bending magnets. After passing a 2.4 m planar undulator, it is removed from the FEL undulator line by a 45 degree bending magnet and loses its energy in a beam dump. The spontaneous emission of the undulator is accumulated by two metal concave mirrors which are installed in a 6.72 m optical cavity, and it is amplified by an interaction with the electron beam in the undulator. Fundamental FELs oscillate at wavelengths of 1–6 μm. The FEL beam, which is translated through a hole coupling in the upstream mirror, is converted to a parallel beam with 30 mm diameter by aspherical mirrors. Using the infrared FEL beamline which has 4 flat mirrors in the accelerator room, it is transferred to the experimental room.

GENERATION OF CSR

In a normal operation of FEL experiments, the electron bunch is compressed from 3 to 1 ps by a magnetic compressor using the two 45 degree bending magnets at the FEL undulator beamline [7]. However, there is no optical beam port to extract CSR at the downstream 45 degree bending magnet. Then, we used an optical beam port at the second 45 degree bending magnet which was located above the undulator. Although the CSR was emitted along the electron-beam orbit in the bending magnet chamber with the inner height of 24 mm, its solid angle which incident on a transfer pipe (diameter, 20 mm; length, 265 mm) was only 65 mrad. The CSR passed

ISBN 978-3-95450-126-7

DESIGN OPTIMIZATION OF 100 KV DC GUN WEHNELT ELECTRODE FOR FEL LINAC AT LEBRA

T. Sakai#, T. Tanaka, K. Hayawaka, Y. Hayakawa, K. Nakao, K. Nogami, M. Inagaki,
Laboratory for Electron Beam Research and Application, Nihon University, Chiba, Japan

Abstract

The electron gun wehnelt employed in the FEL linac at Nihon University was originally designed for extraction of the long duration macropulse beam with a peak current of 200 mA. Since 2011, the electron gun system has equipped with the high-speed gridpulser, which has made it possible to extract the burst beam with a higher peak current. A computer simulation of the burst beam extraction with the present gun wehnelt design showed a large divergence of the beam at the first magnetic lens in the injector line. Calculation with an improved wehnelt design adjusted for the burst mode beam extraction has suggested a possibility of achieving smaller divergence and approximately 20% reduction of the beam emittance.

INTRODUCTION

The 125-MeV electron linac at the Laboratory for Electron Beam Research and Application (LEBRA) in Nihon University has been used for generation of the near infrared FEL and the quasi-monochromatic Parametric X-rays. In addition, the THz beam generated in a bending magnet became available in the FEL experimental rooms in 2012 by transporting along the FEL optical beam line [1]. Since 2011, the electron gun system for the LEBRA linac has been capable of operation in three different modes of the beam extraction i.e., the full bunch mode, the burst mode, and the superimposed mode of the former two modes [2][3][4]. The electron gun wehnelt electrode was originally designed for use in the full bunch mode operation; no upgrade in the wehnelt electrode has been made for optimization of the beam focusing in the superimposed/burst mode operation. The beam trace simulation for the present geometry of the wehnelt suggested that the emittance of the beam extracted in the superimposed/burst modes was considerably increased due to the strong space charge effect resulted from a high peak extraction current. This paper reports on the result of a design simulation made to optimize the shape of the wehnelt for the superimposed/burst beam operation modes.

LEBRA 100 KV DC ELECTRON GUN

Electron Gun Specifications

The present electron gun has been used since 2000 when the design of the wehnelt electrode was changed to get an optimum beam extraction property for the beam extraction current of 200 mA with the CPI EIMAC Y-646B cathode [5], which was introduced in place of Y-646E cathode [6][7]. The cross-sectional drawing of the electron gun is shown in Figure 1. The parameters of the electron gun and Y-646B cathode are shown in Table 1. The anode plate has a flat surface.

The Kentech high-speed gridpulser was installed in the gun high voltage terminal in 2011, which made it possible to extract a train of short beam pulses with 0.7 ns FWHM at a peak current of several amperes. Simultaneous or exclusive use of the high-speed gridpulser and the normal gridpulser allows extraction of the electron beam in three different modes i.e., the full bunch mode, the burst mode, and the superimposed mode of the former two modes. Since the wehnelt electrode of the gun was designed for operation at the full bunch mode, the beam transparency and the acceleration efficiency in the linac is very low in the superimposed/burst mode operations where the peak extracted beam current is more than 10 times higher.

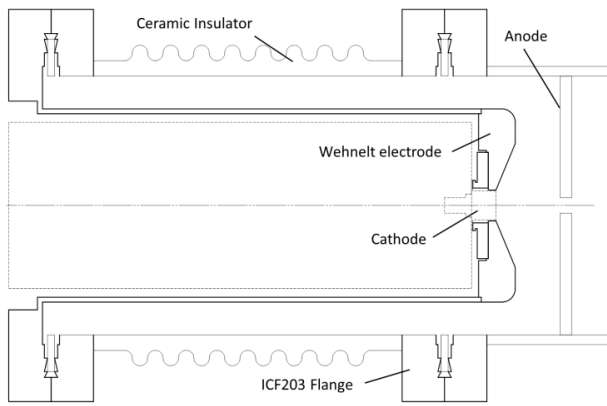

Figure 1: Present LEBRA 100 kV DC electron gun system. The focus effect is suppressed by the shallow slope of the wehnelt around the cathode. The anode plate has a flat surface.

Table 1: Electron Gun Specifications

Electron sources	EIMAC Y-646B
Cathode area	0.5 cm^2
Cathode filament voltage	6.0 V
Cathode filament current	1.3 A
Cathode voltage	-100 kV
Macropulse width	50 μs
Macropulse current	200 mA
Cathode to anode distance	30 mm
Gridpulse voltage	53 ~ 63 V
Grid bias voltage	53 V

#sakai@lebra.nihon-u.ac.jp

ISBN 978-3-95450-126-7

INJECTOR DESIGN STUDIES FOR NGLS*

C.F. Papadopoulos†, F. Sannibale, P.J. Emma, D. Filippetto, H. Qian, M. Venturini, R. Wells
Lawrence Berkeley National Laboratory, Berkeley, CA, USA

Abstract

The APEX project at LBNL is developing an electron injector to operate a high repetition rate x-ray FEL. The injector is based on the VHF gun, a high-brightness, high-repetition-rate photocathode electron gun presently under test at LBNL. The design of the injector is particularly critical because it has to take the relatively low energy beam from the VHF gun, accelerate it at more relativistic energies while simultaneously preserving high-brightness and performing longitudinal compression. The present status of the APEX injector design studies is presented.

INTRODUCTION

The Next Generation Light Source (NGLS) [1] concept is an array of multiple FEL beamlines, each capable of operating at high repetition rates ($>$ 100 kHz) simultaneously with the other beamlines. In order to achieve this, the repetition rate requirements on the linac and injector are of the order of 1 MHz, requiring continuous wave (CW) operation of the machine. As part of the R&D effort for NGLS, the Advanced Photoinjector Experiment (APEX) is currently under commissioning at LBNL, in order to demonstrate the feasibility of a high repetition rate photoinjector, satisfying all the machine requirements of NGLS.

Both the NGLS and APEX injectors are based on a normal conducting electron source cavity, operating at the VHF band (186 MHz) and in CW mode. The beam dynamics implications of this novel (for FEL injectors) mode of operation have been described elsewhere [2], and in this paper we will describe the current status of simulations for APEX, based on initial energy measurements of the electron beam. Start-to-end simulations of the full NGLS machine are reported elsewhere in these proceedings [3].

THE APEX BEAMLINE

A schematic of the APEX beamline is shown in Fig. 1. The beamline consists of 1 normal conducting electron gun cavity at 186 MHz, 3 focusing solenoid magnets and 1 bucking coil, 1 single cell buncher cavity at 1.3 GHz and 3 7-cell accelerating cavities. The nominal final energy at the exit of the APEX injector can be as high as 30 MeV, but due to RF focusing of the beam, in the optimized case the energy is typically lower than 15-20 MeV.

The low energy ($<$ 750 keV) part of the beamline is identical to the current design for NGLS, with 1 MHz rep. rate, while the higher energy part is similar, with standing wave accelerating cavities at 1.3 GHz. The main difference is that due to space and shielding limitations in the current location of APEX, there are only 3 normal conducting cavities instead of the superconducting TESLA-like cavities that would support CW operation at energy higher than 750 keV, as required by the NGLS design. The buncher and accelerating cavities will operate in pulsed mode instead, although the current design of the buncher includes the cooling required for CW operation. Additionally, studies are under way to optimize the coupler design for the buncher and accelerating section, to be reported on a later publication. Although some RF design considerations change for superconducting cavities, the single bunch beam dynamics are expected to be similar in the 2 cases.

The VHF gun has a load-lock system installed that can accommodate different cathodes, and the one assumed in the simulations is based on Cs_2Te, with an intrinsic emittance coefficient conservatively estimated to be 1 mm-mrad/mm [4]. The combination of laser power available at 1 MHz rep. rate [5] and high quantum efficiency of the photocathode allow for bunch charges $>$ 500 pC, but beam dynamics considerations in the start-to-end simulations set the design bunch charge to 300 pC.

The energy out of the electron gun has the design value of 750 keV, corresponding to a peak RF gradient at the cathode of 19.5 MV/m, but during initial commissioning and operations this specification was exceeded and the energy was measured to be 800 keV, corresponding to peak gradient of 21.3 MV/m. This higher gradient is expected to improve the beam quality [6], as discussed later.

INJECTOR OPTIMIZATION

In the case of the injector, there are 2 main processes related to beam dynamics. First is the longitudinal compression of the beam, either by setting the phase of the buncher cavity at zero crossing (-90 deg. from peak acceleration) or by dephasing the accelerating cavities. This is required in the case of high repetition rate injectors, as the initial bunch length at the cathode is higher than pulsed guns with higher peak gradients [2]. The other important process is the well known emittance compensation [7] that minimizes the projected emittance of the beam, removing the correlated emittance growth due to linear space charge.

The parameters available for the combined optimization of these 2 processes are the gun phase, solenoid strengths[1] and phase and gradient of the 1.3 GHz cavities. The gradient of the gun is put to the maximum value possible, as increasing it is expected to always improve the beam brightness[2]. In addition, 2 knobs related to laser shaping are

* This work was supported by the Director of the Office of Science of the US Department of Energy under Contract no. DEAC02-05CH11231
† Corresponding author:cpapadopoulos@lbl.gov

[1] the strength of the bucking coil behind the cathode is set to cancel the magnetic field of the first focusing solenoid on the cathode and hence it is not an independent variable

[2] Higher gradient is also associated with increased dark current, but in the current work we are focusing on beam dynamics

ISBN 978-3-95450-126-7

A COAXIALLY COUPLED DEFLECTING-ACCELERATING MODE CAVITY SYSTEM FOR PHASE-SPACE EXCHANGE (PSEX)

Young-Min Shin, Philippe Regis-Guy Piot, Accelerator Physics Center (APC), FNAL, Batavia, IL 60510, USA and Department of Physics, Northern Illinois University, Dekalb, IL, 60115, USA
Jang-Ho Park, Alan Todd, Advanced Energy Systems (AES) Inc, Medford, New York 11763, USA
Michael Church, Accelerator Physics Center (APC), FNAL, Batavia, IL 60510, USA

Abstract

The phase space manipulation of bunched beams offers a wide range of flexibility in beam dynamics control for advanced accelerator application. In particular, the capability of exchanging the transverse and longitudinal phase spaces enables to switch the transverse and horizontal emittance or shaping the charge distribution of an electron bunch to improve acceleration gradient and transformer ratio in beam-driven accelerators. A deflecting mode cavity has been used as the most integral element in the beam control scheme as imposing a kick on particles transferred between the two phase planes. In practice, the presence of the RF element with a finite length, however, induces thick lens effect limiting the phase-space exchange (PSEX) performance based off a thin lens model. Extending the idea from [A. Zholents PAC 11], we proposed momentum compensation technique using a single accelerating mode cavity coaxially coupled with the deflecting mode one. This paper describes the composite 3.9 GHz system and presents design analysis, including tracking and particle-in-cell (PIC) simulations, and layout of feasible experiment at the Advanced Superconducting Test Area (ASTA) of Fermilab.

INTRODUCTION

Optimization of the six dimensional phase-space volume is essential to high-quality electron beam applications and the next generation of advanced accelerators. Emittance compensation of electron gun phase space with solenoidal coils [1, 2] is one such example of phase space manipulation. Here, the emittance compensation solenoid is used to align the transverse phase ellipses of the each longitudinal beam slice in the bunch to minimize the transverse emittance. Many other approaches to the modification of phase-space have been demonstrated for different applications. Phase-space manipulation of beam lines was initially considered as a means of increasing the luminosity at the collision point in B-factories [3] and to improve the performance of free-electron laser (FEL) based light sources [4] and single-pass FELs [5].

Deflecting cavities are being used for a number of accelerator applications that include particle-species separation [6], beam distribution [7], longitudinal phase space characterization [8, 9] and phase space manipulation [10]. One application, manipulation between the transverse and longitudinal phase space, has opened up new opportunities [3 – 5] and the development of single-shot, longitudinal phase space (LPS) diagnostics [8]. In order to manipulate and control 6-D electron beam phase-space, transverse and longitudinal effects have to be carefully considered. Several approaches are under development around the world including emittance exchangers (EEX) [3, 4, 5, 10] and single-shot longitudinal phase space (LPS) diagnostics [8, 9]. However, each approach has drawbacks that must be overcome to deliver the requirements of the different applications.

The first beam line proposed for EEX consisted of a simple four-dipole chicane and an RF deflecting cavity [4]. While easy to implement, the resultant emittance exchange is not complete. An improved EEX beam line using two identical doglegs was later demonstrated [5], and while this beam line does provide full emittance exchange, it does not consider thick-lens effects. These effects result in a longitudinal accelerating term in the deflecting cavity which is generally undesirable. Instead, we proposed a simple method for achieving phase space exchange (PSEX) where the emittances as well as the coordinates are exchanged – that is to say we map x to z, x' to δ, z to x, and δ to x'. This approach uses a 5-cell deflecting cavity and a single-cell fundamental mode cavity in two identical doglegs dispersive section [11 – 13].

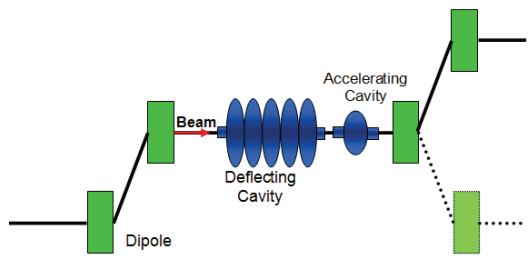

Figure 1: Proposed phase-space exchange experiment using a hybrid deflecting-accelerating radio-frequency cavity in the dispersive region of two identical doglegs (a four dipole-magnet chicane). The longitudinal energy gain in the deflecting cavity can be canceled by using the TM_{010} fundamental mode cavity.

THEORETICAL BACKGROUND

The simplest PSEX beam-line, shown in Figure 1, consists of a 3.9 GHz 5-cell horizontal deflecting cavity, operating in the TM_{110} mode, flanked by two identical horizontally dispersive sections arranged as “doglegs". The system can be arranged as the standard double-

ISBN 978-3-95450-126-7

DESIGN ANALYSIS AND HIGH POWER RF TEST OF A 3.9 GHZ 5-CELL DEFLECTING-MODE CAVITY IN A CRYOGENIC OPERATION

[1, 2]Young-Min Shin, and [2]Michael Church
[1]Department of Physics, Northern Illinois University, Dekalb, IL, 60115, USA
[2]Accelerator Physics Center (APC), FNAL, Batavia, IL 60510, USA

Abstract

A deflecting mode cavity is the integral element for six-dimensional phase-space beam control in bunch compressors and emittance transformers at high energy beam test facilities. RF performance of a high-Q device is, however, highly sensitive to operational conditions, in particular in a cryo-cooling environment. Using analytic calculations and RF simulations, we examined cavity parameters and deflecting characteristics of $TM_{110,p}$ mode of a 5 cell resonator in a LN_2-cryostat, which has long been used at the Fermilab A0 Photoinjector (A0PI). The sensitivity analysis indicated that the cavity could lose 30 – 40 % of deflecting force due to defective input power coupling accompanying non-uniform field distribution across the cells with 40 ~ 50 MeV electron beam and 70 – 80 kW klystron power. Vacuum-cryomodules of the 5 cell cavity are planned to be installed at the Fermilab Advanced Superconducting Test Accelerator (ASTA) facility. Comprehensive modeling analysis integrated with multi-physics simulation tools showed that RF loading of 1 ms can cause a ~ 5 °K maximum temperature increase, corresponding to a ~ 4.3 μm/ms deformation and a 1.32 MHz/K maximum frequency shift. The frequency deviation resulting from a RF-pulse loading will need to be included in design process of a high-Q deflecting mode cavity.

INTRODUCTION

Over the past decade, a multi-cell deflecting (TM_{110}) mode cavity has been employed for phase-space manipulation tests of high brightness beams [1 – 6] at the Fermilab A0 photoinjector (A0PI), and extended applications are currently scheduled at the ASTA user facility (> 50 MeV). Despite the past successful experimental results, the cavity demonstrated a limited RF performance during liquid nitrogen (LN_2) operation, which did not reach the theoretically predicted gradient. The designed cavity has been fully examined with theoretical calculations, based on the Panofsky-Wenzel theorem, using an integrated modeling tool with a comprehensive system analysis capacity to solve complex thermodynamics and the mechanical stress of the multi-cell. This paper discusses the cryogenic RF performance of the 5-cell deflecting mode cavity with numerical modeling analysis. It also presents up-to-date test simulation results of an integrated thermo-stress analysis modeling tool on the deflecting cavity vacuum-cryomodule and low power RF-test results of warm (room-temp, 297 K) and cold (LN_2-temp, 80K) cavities.

SYSTEM DESCRIPTION

At the Fermilab A0PI, the deflecting mode cavity has been used for various beam optics experiments. As shown in Fig. 1, the cavity was designed with 5 cells to maximize kick strength and powered with a 50 kW (peak), S-band (3.9 GHz) klystron. The RF power was coupled into the cavity through the high power TEM-mode coaxial coupler that was built in the liquid nitrogen (LN_2) vessel. The coupler design includes a temperature gradient from cryogenic temperature (80K) of a LN_2-ambient cavity to room temperature of an input waveguide. As the emittance exchange only requires modest fields and short pulse lengths, the TM_{110} mode cavity was constructed out of oxygen-free, high conductivity (OFHC) copper [7]. A higher Q_0 was required than what was achievable at room temperature with the OFHC copper. We see that Q_0 is proportional to the square root of the copper's bulk conductivity. A Q_0 2.4 times greater was achieved by simply incorporating a LN_2 cryogenic jacket into the design.

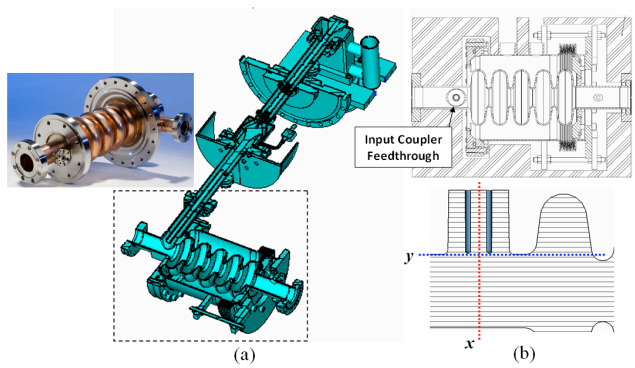

Figure 1: (a) 3D solid model of a 5-cell deflecting mode cryomodule (inset: photo of a 5 cell, courtesy of Timothy W. Koeth[14]) (b) top: engineering drawing; bottom: simulation model with position (x, y) of coaxial antenna.

The system is designed with the LN_2 vessel because the conductivity of normal conducting copper is increased 6 times from 5.8×10^7 $\Omega^{-1}m^{-1}$ at room temperature to 3.5×10^8 $\Omega^{-1}m^{-1}$ at 80 K, which doubles the cavity Q. As shown in Fig. 1(b), the cryo-vessel was designed with three frequency tuning screws, attached to the chamber-outside body at one end and the flange, brazed with the beam pipe at the other end, across the flexible bellows. The tuners push the flange against the body and the mechanical pressure is transferred to the cavity through the beam pipe so the structural distortion by the tuner induces frequency

ISBN 978-3-95450-126-7

IN SITU CHARACTERIZATION OF ALKALI ANTIMONIDE PHOTOCATHODES*

J. Smedley, K. Attenkofer, S. G. Schubert, BNL, Upton, NY 11973, USA
H. A. Padmore, J. Wong, LBNL, Berkeley, CA 94720, USA
J. Xie, M. Demarteau, ANL, Argonne, IL 60439, USA
M. Ruiz-Oses, I. Ben-Zvi, X. Liang, E. M. Muller, Stony Brook University, Stony Brook, NY 11794, USA
A. Woll, Cornell University, Ithaca, NY 14850, USA

Abstract

Alkali antimonide photocathodes are a prime candidate for use in high-brightness photoinjectors of free electron lasers and 4th generation light sources. These materials have complex growth kinetics - many methods exist for forming the compounds, each photocathode having different grain size, roughness, and crystalline texture. These parameters impact the performance of the cathodes, including quantum efficiency (QE), intrinsic emittance and lifetime. In situ analysis of the growth of these materials has allowed investigation of correlations between the growth parameters and the resulting cathode performance. This work explores the relationship between the crystallinity of the initial antimony film and the roughness of the final cathode.

Two growth methods are compared – a "traditional" recipe which uses a crystalline initial antimony film and a "yo-yo" process which builds the cathode through an iterative process using sub-crystalline antimony layers. The traditional method provides exemplary QE (7.5% @ 532 nm), but an exceptionally rough surface. The "yo-yo" produces a somewhat lower final QE (4.9% @ 532 nm) but a much smoother surface, as observed by grazing incidence small angle x-ray scattering (GISAXS).

INTRODUCTION

While they provide high QE for visible light, and high average current operation in injectors [1-3], there is reason for significant concern that the intrinsic emittance of photoinjectors relying on alkali antimonide photocathodes may be impacted by the surface roughness of the cathode film [4]. Traditional growth methods have resulted in films that are very rough; atomic force microscopy (AFM) yields a 25 nm rms roughness (50% of the total film thickness) over a 100 nm spatial period [5]. This will particularly impact high-gradient injectors; an intrinsic emittance in excess of 1 μm/mm is expected from this surface for a 20 MV/m emission field.

We have developed tools to understand the formation of these materials, both structurally and chemically, with the goal of altering the growth to produce cathodes with less roughness, better stoichometry, and larger crystal grains. The in situ techniques being used are x-ray diffraction (XRD), grazing incidence small angle x-ray scattering (GISAXS) and x-ray reflection (XRR). These tools enable determination of the crystal form of the cathode at each phase of growth, the film thickness and roughness, the texture and grain size of the film, and the presence of "imperfectly reacted" material. This work has been carried out at the National Synchrotron Light Source (NSLS) using beamline X21 and at the Cornell High Energy Synchrotron Source (CHESS) using beamline G3.

Here we focus on two cathodes; one grown using our typical "High QE" process, and a second grown with a "yo-yo" process that begins with an antimony layer that is not thick enough to have crystallized prior to the first layer of potassium being deposited. The rationale for this approach arises from the observed growth kinetics of the compound – the initial crystalline antimony layer is fully dissolved by the addition of potassium prior to forming an antimonide. The large variation in lattice constants likely leads to the formation of the observed rough surface structure, as the alkali initially diffuses along Sb grain boundaries and pushes the material apart, forming the observed nano-pillar structure [5]. By eliminating the crystalline Sb phase, we hope to prevent this roughening.

EXPERIMENT

In the interest of space, the growth chamber with in situ x-ray analysis is described elsewhere [6]. The cathodes were grown in a UHV chamber, with a typical operating pressure of 0.2 nTorr. Residual gas analysis confirms that the partial pressures of reactive gases (H_2O, CO) were better than 0.05 nTorr. Silicon [100] wafers 1x2 cm^2 were used as substrates; these were exposed to HF prior to installation, and baked to 500 C for an hour prior to growth. Once the substrate has cooled to 160 C, a further cleaning of the substrate is achieved by an initial potassium evaporation – XRR measurements confirm that this K does not remain resident on the surface, however the QE of cathodes grown is significantly improved by this initial step. Antimony is evaporated from PtSb beads; alkali-Bi sources from Alvatech are used to supply Potassium and Cesium. Deposition is sequential, with Sb evaporated, then K, then Cs, all at ~0.2 Å/s. The QE is observed during K and Cs evaporation, and the deposition is halted when the QE reaches a plateau. The "traditional" cathode is a multi-layer growth on a single substrate, with the first cathode "baked off" (substrate raised to 500 C for 10 min) prior to the growth of a second.

1st Layer	Temp	QE	2nd Layer	Temp	QE
15 nm Sb	100		15 nm Sb	125	
62 nm K	125	0.14	60 nm K	125	0.37
118 nm Cs	125	4.1	120 nm Cs	125	7.5

ISBN 978-3-95450-126-7

ANALYTICAL AND NUMERICAL ANALYSIS OF ELECTRON TRAJECTORIES IN A 3-D UNDULATOR MAGNETIC FIELD*

N.V. Smolyakov#, S.I. Tomin, NRC Kurchatov Institute, Moscow, Russia
G. Geloni, European XFEL GmbH, Hamburg, Germany

Abstract

It is well-known that an electron trajectory in an undulator is influenced by the magnetic field focusing properties (both horizontal and vertical). Approximate solutions of the equations of motion for electrons in a 3-dimensional magnetic field, which describes these focusing properties, are usually found, in literature, by means of averaging over the short-length oscillations. At variance, the equations of motion can be solved numerically, for example by applying the Runge-Kutta algorithm. It is shown in this paper that there are cases where the numerically computed trajectories, which can be considered, for our purposes, as exact, differ considerably from the corresponding approximate solutions obtained through the averaging method. This means that the undulator field influence on the electron trajectory is complicated and that approximations found in literature should be used with extreme care.

INTRODUCTION

As far as we know, horizontal and vertical focal lengths of an undulator were first calculated in [1]. In a planar undulator with infinitely wide magnetic poles and hence without horizontal focusing, the vertical focusing was analysed in [2, 3]. In [4, 5] trajectories in the presence of focusing undulator magnetic field were calculated up to the lowest order in the initial positions and angles of the electrons. Some general relations dealing with undulator focal lengths were derived in [6 – 8]. Long-length-scale anharmonic betatron motion of electrons in very long undulators was studied in [9]. All these studies were carried out within the following limits: the focusing effects were calculated averaging over the undulator period and only terms, which are linear in the electron initial positions and angles, were taken into account.

In this paper we discuss the limits of this approximation when one needs to calculate the electron trajectory with high accuracy. Consider, for example, the line width of FEL radiation, which is related to the dimensionless Pierce parameter ρ. It has typical values for XFELs of the order of 10^{-4}. Since an accuracy of the fundamental wavelength is about $\Delta\lambda/\lambda \le \rho$, the requirement on the accuracy for the undulator deflection parameter K is very strict, $\Delta K \approx 10^{-4}$. The expression for the phase of spontaneous radiation in the general case [10] gives the following relation for K, see Fig. 1:

$$\frac{K^2}{2} = \frac{\gamma^2}{\lambda_u}\int_0^{\lambda_u} \beta_x^2(z)dz\,. \qquad (1)$$

Here λ_u is an undulator period, γ is an electron reduced energy, β_x is its reduced horizontal velocity, being of the order of K/γ. It can be derived from (1) that the necessary accuracy for β_x is of the order of $\Delta\beta_x \approx \Delta K/\gamma \approx 3\cdot 10^{-9}$. It is doubtful whether known analytical (approximate) solutions for trajectories, obtained with the averaging method, provide so high accuracy. In fact, we will show in this article that they should be used with extreme care.

TRAJECTORY EQUATIONS IN 3-D FIELD

We model the three-dimensional magnetic field by the following expressions which satisfy Maxwell equations:

$$B_x(x,y,z) = -\frac{k_x}{k_y}B_0\sin(k_x x)\sinh(k_y y)\sin(k_z z)\,, \qquad (2)$$

$$B_y(x,y,z) = B_0\cos(k_x x)\cosh(k_y y)\sin(k_z z)\,, \qquad (3)$$

$$B_z(x,y,z) = \frac{k_z}{k_y}B_0\cos(k_x x)\sinh(k_y y)\cos(k_z z)\,. \qquad (4)$$

Here $k_x = 1/a$, $k_z = 2\pi/\lambda_u$, $k_y = \sqrt{k_x^2 + k_z^2}$, λ_u is the undulator period length. The linear parameter a gives the field non-uniformity along X-axis and is of the order of the width of the undulator poles.

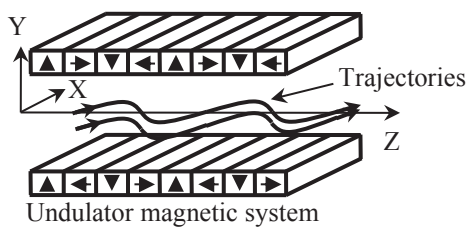

Figure 1: Sketch of a permanent magnet undulator.

We will use the exact equations for trajectory [11]:

$$x'' = -q\sqrt{1+x'^2+y'^2}\left\{(1+x'^2)B_y - y'B_z - x'y'B_x\right\}, \qquad (5)$$

$$y'' = q\sqrt{1+x'^2+y'^2}\left\{(1+y'^2)B_x - x'B_z - x'y'B_y\right\}. \qquad (6)$$

Here β and γ are the electron reduced velocity and energy respectively, $q = e/(mc^2\beta\gamma)$ and an apostrophe indicates a derivative with respect to z.

A computer code was written, which solves the systems of Eqs. (2) – (6) by using the Runge-Kutta algorithm.

*This work was partially supported by the Russian Federation program "Physics with Accelerators and Reactors in West Europe (except CERN)" and by BMBF-Project 05K12GU2.
smolyakovnv@mail.ru

ISBN 978-3-95450-126-7

DESIGN OF A COLLIMATION SYSTEM FOR THE NEXT GENERATION LIGHT SOURCE AT LBNL*

C. Steier†, P. Emma, H. Nishimura, C. Papadopoulos,
H. Qian, F. Sannibale, C. Sun, LBNL, Berkeley, CA 94720, USA

Abstract

The planned Next Generation Light Source at LBNL is designed to deliver MHz repetition rate electron beams to an array of free electron lasers. Because of the high beam power approaching one MW in such a facility, effective beam collimation is extremely important to minimize radiation damage, prevent quenches of superconducting cavities, limit dose rates outside of the accelerator tunnel and prevent equipment damage. We describe the conceptual design of a collimation system, including detailed simulations to verify its effectiveness.

INTRODUCTION

A collimation system is necessary to safely contain the beam halo in high power cw accelerators. The beam halo can be produced by many sources, including dark current from the RF gun or from the accelerating modules, scattering off of residual gas particles, Touschek scattering within the bunches, and several other smaller effects. If not collimated safely, this beam halo can damage undulators, cause Bremsstrahlung co-axial with the photon beams, cause quenches in superconducting cavities and can activate the components of the facility. Collimating the beam halo at the lowest possible beam energy, which means as near as possible to the various sources, is important as this reduces the overall radiation levels in the machine. In addition to the continuous removal of the beam halo, the collimation system must also provide protection against misteered beam or element failure scenarios without being damaged itself.

Collimation Strategy and System Layout

The plan for the NGLS is to make use of a distributed collimation system, roughly similar to the approach that has been used successfully at FLASH [1]. In the injector, in addition to collimation of large transverse amplitude particles, a dark current kicker will remove most of the dark current bunches. The next stage consists of multiple (energy) collimators in the middle of each of the bunch compressors as well as the laser heater chicane to achieve collimation at the lowest beam energy feasible. The post-linac collimation removes the beam halo particles in a transverse collimation section with approximately 90 degree phase advance between each set of horizontal and vertical collimators (two of each). Finally there is another energy collimation section that makes use of the dispersion at the beginning of each of the spreader arcs. The geometry of the spreader allows to keep any particle showers after the collimators away from the photon production sections, similar to top-off collimation at 3rd generation light sources [2]. Figure 1 shows the conceptual collimator layout for the NGLS.

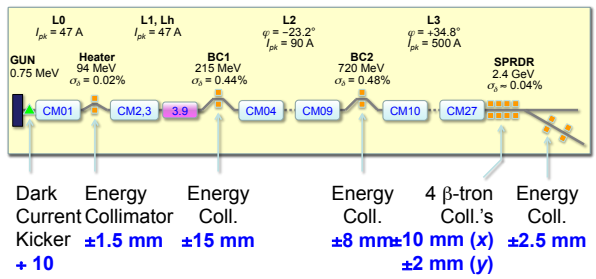

Figure 1: Schematic layout of NGLS injector, linac, bunch compressors, and undulators with collimator locations and settings.

DARK CURRENT TRANSPORT

Dark current from the gun usually is the major source of beam halo. This is expected to be true at NGLS, since gradients for the s/c cavities are relatively low (15 MV/m), where dark-current-free cavities have been demonstrated. To study the effectiveness of the conceptual NGLS collimation system, simulation techniques similar to FLASH, XFEL [1] and LCLS [3] have been employed. The dark current model has been calibrated with data from the APEX test facility. It is expected that APEX dark current will be improved over time, so this is a conservative starting point for the collimation design. The dark current emission is then simulated in ASTRA [4].

The distribution has a very large energy spread and some of the particles spill into subsequent linac buckets. We simulate about 250,000 macroparticles at the cathode, of which about 50,000 survive to the end of the injector at about 90 MeV. The predicted loss rates (compare Fig. 2) in the injector cryomodule for the most conservative dark current model appear to have little safety margin compared to conservative quench thresholds for superconducting cavities without a dark current kicker. So the kicker is now considered part of the baseline.

Dark Current Deflector

The dark current produced at the gun is quasi continuous with the rf-frequency of the gun as repetition rate

* This work is supported by the Director, Office of Science, Office of Basic Energy Sciences, of the U.S. Department of Energy under Contract No. DE-AC02-05CH11231.

† CSteier@lbl.gov

ISBN 978-3-95450-126-7

THE MAX IV LINAC AND FIRST DESIGN FOR AN UPGRADE TO 5 GeV TO DRIVE AN X-RAY FEL

S. Thorin, F. Curbis, N. Cutic, M. Eriksson, O. Karlberg, F. Lindau,
A. Mak, E. Mansten, S. Werin, MAX-lab, Lund, Sweden

Abstract

The installation of the MAX IV linear accelerator is in full progress, and commissioning is planned to start in the second quarter of 2014. The 3 GeV linac will be used as a full energy injector for the two storage rings, and as a high brightness driver for a Short Pulse linac light source. The linac has been deigned to also handle the high demands of an FEL injector. The long term strategic plan for the MAX IV laboratory includes an extension of the linac to 5 GeV and an X-ray FEL.

In this paper we present the both design concept and status of the MAX IV linac along with parameters of the 3 GeV high quality electron pulses. We also present the first design and simulation results of the upgrade to a 5 GeV X-ray FEL driver.

BACKGROUND

The MAX IV facility [1], successor of the MAX-lab accelerators at Lund University, Sweden, was already in the initial plans around year 2000 drawn with the idea that the facility could be extended with a FEL in a later stage. Since then the X-ray FELs LCLS [2] and SACLA [3] have been put into operation as well as the UV machines FLASH [4] and Fermi [5]. The European XFEL [6], the SwissFEL [7] and the PAL-XFEL [8] are currently being constructed, indicating the development of the photon science scene worldwide. The MAX IV facility includes a linear accelerator followed by a short pulse linac light source (SPF) and two storage rings at 3 and 1.5 GeV. The facility is right now being constructed with the installation of the linac structures (up to 3 GeV), waveguides and magnetic systems almost completed (August 2013).

The MAX IV laboratory strategy includes a plan for an extension of the facility with an X-ray FEL starting by a conceptual design in near future, followed by a technical design and a tentative operation in 2021. No funding is at the moment available.

MAX IV LINAC DESIGN CONCEPT

For injection and top up to the storage rings a thermionic gun with a pulse train chopper system is used. In high brightness mode we use a 1.6 cell photo cathode gun capable of producing an emittance of 0.4 mm mrad at a charge of 100 pC [9]. The gun will be operated together with a kHz Ti:sapphire laser at 263 nm. The same laser will be used for timing and synchronisation of the whole accelerator.

The acceleration is done in 39 warm S-band linac sections together with 18 RF units, each consisting of a 35 MW klystron and a solid state modulator. The Klystrons are operated at the lower power of 25 MW which reduces the operational cost and gives a total redundancy in energy of 0.6 GeV. The RF power will be doubled with a SLED

The three first RF units are driven individually by a low level rf system, and the main drive line for the remaining 15 RF units is controlled by extracting power from the last of these LLRF stages. The RF phase can be set individually in the first three stages and power can be set individually for all RF units. The MDL is situated inside the linac tunnel and is attached to the linac in such a way that it will follow the length variations of the linac and help keep the phases stable.

The lattice in the main linac is made with few magnets for simplicity and reduction of vibration sensitivity. Matching is done before each bunch compressor, and the beam is focused with one triplet before each injection extraction point. This means that only 6 quads are used through the whole main linac, about 200 m. This restrictive use of quads leads to a simple, stable and cost effective lattice, that is easy to operate and tune.

The beam is kicked out for injection into the storage rings at 1.5 and 3 GeV. Bunch compression is done in double achromats at 260 MeV and at full energy, 3 GeV, after extraction to the storage ring. A schematic view of the layout can be seen in Figure 1. BC2 is not only used for bunch compression, but also works as a beam distributor for a few beamlines. This is done by letting all electrons pass through the first achromat, and then chose where, in a long transport, to extract the bunch in the second, compressing achromat.The second exit is used for the Short Pulse facility in the current MAX IV plan. The first exit achromat would be used to lead the beam into the linac extension for a possible FEL.

Self Linearising Bunch Compressors

The two magnetic double achromats used as bunch compressors in the MAX IV linac has a positive R56 unlike the commonly used magnetic chicane which has a negative R56. The energy chirp needed for compression is done by accelerating the electrons on the falling slope of the RF voltage. Both types of bunch compressors naturally have a positive T566 and in the case of a BC with positive R56 this has a linearising effect on the longitudinal phase space. We can thus choose the optical parameters in the achromat to get optimal linearisation without needing to have a harmonic linac for this purpose [10].

ISBN 978-3-95450-126-7

CHALLENGES FOR DETECTION OF HIGHLY INTENSE FEL RADIATION: PHOTON BEAM DIAGNOSTICS AT FLASH1 AND FLASH2

K. Tiedtke*, M. Braune, G. Brenner, S. Dziarzhytski, B. Faatz, J. Feldhaus, B. Keitel, H. Kühn, M. Kuhlmann, E. Plönjes, A. A. Sorokin, R. Treusch, DESY, Hamburg, Germany

Abstract

Photon beam diagnostics play an essential role for tuning free-electron lasers (FEL) and delivering the requested beam properties to the users. An overview of the FLASH1 and FLASH2 photon diagnostic devices will be presented with emphasis on the new pulse resolving intensity monitor covering an extended energy range.

INTRODUCTION

In spite of the evident progress in the development of FEL facilities, the characterization of important FEL photon beam parameters during FEL commissioning and user experiments is still a great challenge. In particular, pulse-resolved photon beam characterization is essential for most user experiments, but the unique properties of FEL radiation such as extremely high peak powers and short pulse lengths makes the shot-to-shot monitoring of important parameters very difficult. Therefore, sophisticated concepts have been developed and used at FLASH1 in order to measure radiation pulse intensity, beam position and spectral as well as temporal distribution - always coping with the highly demanding requirements of user experiments as well as machine operation. Here, an overview on the photon diagnostic devices operating at FLASH1 and planned for FLASH2 (see [1] and referendes therein) will be presented, with emphasis on pulse resolving intensity and energy detectors based on photoionization of rare gases.

LAYOUT OF THE PHOTON DIAGNOSTIC SECTION

On its way from the source to the user endstations the FEL radiation passes through a set of photon diagnostics and beam manipulation tools, such as a set of four gas-monitor detectors (GMD) for intensity and beam position determination, an attenuation system based on gas absorption, a set of filters and a fast shutter [2]. Downstream of the undulators a set of photon diagnostics is installed mainly for use by operators during setup of SASE. The FEL beam passes two diagnostic units equipped with apertures and Ce:YAG screens for visualization of the XUV radiation. Centering the FEL beam with respect to these apertures ensures an accurate propagation of the photon beam across all beamlines towards the experiments. For fast intensity measurements an MCP tool [3] and one of the GMD detector pairs (see below) are located in front of the beam distribution system, as well as a grating spectrometer and a detector system based on photo-electron and -ion spectroscopy (OPIS) for online determination of the spectrum in parallel to the user experiments.

At the same time, most user experiments need online information about important photon beam parameters, such as intensity, spectral distribution, and temporal structure. Furthermore, due to the stochastic nature of the SASE process and the resulting pulse-to-pulse fluctuations of the FLASH photon beam, photon diagnostics need to be capable of resolving each individual pulse within a pulse train. This requires diagnostic tools which operate in parallel to the experiments in a non-destructive way, i.e. not blocking the beam for the experiments behind.

Monitoring of the Spectral Distribution

Some user experiments require knowledge of the spectral distribution of the individual FEL pulses to interpret their data, but may not want to use the plane-grating-monochromator (PG) beamline at FLASH, because of temporal broadening of the pulse or a reduction of photon flux. Three options have been developed and are available to users for this purpose, an online photoionization spectrometer (OPIS) located in the photon diagnostic section, a mobile compact spectrometer which can be setup at the endstation or behind user experiments, and a variable-line-spacing (VLS) grating spectrometer integrated into the FLASH BL beamline branch. The latter will not be provided for FLASH2, since the short wavelength end of the FLASH2 range requires shallow incidence angles of 1° for the beam distribuion optics to avoid damage of the coatings and would finally require extreme long and hardly available gratings.

Online photoionization spectrometer The wavelength measurement with the online photoionization spectrometer is based on photoionization processes of gas phase targets like rare gases and small molecules e.g. N_2 and O_2 [4, 5, 6]. Therefore it is in principle not limited in the wavelength range. For wavelength determination the relevant quantities of the ionization process are the binding energies and photoionization cross sections which are well known from literature. Typical target gas pressures are in the range of 10^{-7} hPa which allows a photon transmission to the user experiment of essentially 100 %. The OPIS device (see Fig. 1) comprises a set of time-of-flight spectrometers for detection of photo-ions and photo-electrons, respectively. Measuring the detector signals by means of fast digitizers recording traces of full bunch trains it is possible to have a monitor for micro bunch resolved determination of the spectral distribution. The ion spectrometer is used to measure the intensities of different charge

* kai.tiedtke@desy.de

ISBN 978-3-95450-126-7

SPECTROSCOPY SYSTEM FOR LCLS PHOTOCATHODES*

P.M. Stefan, T. Vecchione#, A. Brachmann, SLAC National Accelerator Laboratory, Menlo Park, CA 94025, U.S.A.

Abstract

Photocathode reliability is important from an operational standpoint. Unfortunately LCLS copper photocathodes have not always been reliable. Some have operated well for long periods of time while others have required continual maintenance. It is believed that the observed variations in quantum efficiency, emittance and lifetimes are inherently surface related, corresponding to changes in composition or morphology. The RF Electron-gun Cathode, Electron Surface Spectrometer, or RECESS, system has been commissioned to study this by making essential measurements that could not be obtained otherwise. These involve photocathode surface chemical characterization. The system is designed to use a combination of angle-resolved ultraviolet and x-ray photoelectron spectroscopy and is capable of either stand-alone operation or interoperability with a beam line at SSRL. Here we report on the first commissioning spectra and the direction of the project going forward.

INTRODUCTION

Cu photocathodes used at SLAC have operational lifetimes that vary from tens of thousands of hours down to single-digit hours. This variation is difficult to predict, due to a lack of understanding of either the emitting surfaces or the vacuum environments in which they operate. Increasingly, evidence suggests that the optimum surfaces are not atomically clean but rather are coated by layers that alter the material's work function. These coatings may come from vacuum interactions or may be residual from fabrication steps. In either case the variations in quantum efficiency, emittance, and lifetimes are thought to result from changes in surface composition and morphology, analogous to other photoemissive systems. Understanding photocathode performance is increasingly dependent on surface science models and techniques.

Unfortunately the design of the LCLS RF gun makes it difficult to study photocathodes in-situ. It is not possible to deposit fresh surfaces or to use plasma or sputtering-based cleaning techniques for surface preparation. Furthermore no techniques exist that can infer chemical information from electrons accelerated to MeV levels. Therefore separate experiments are being carried out in a dedicated surface science system to make essential measurements that could not be obtained otherwise, in order to aid in accurately predicting photocathode performance. The RECESS (RF Electron-gun Cathode, Electron Surface Spectrometer) surface science system was designed specifically to study LCLS photocathodes and is currently configured for ultraviolet or x-ray photoelectron spectroscopy (Figs. 1,2).

*Work supported by US DOE contract DE-AC02-76SF00515.
#tvecchio@slac.stanford.edu

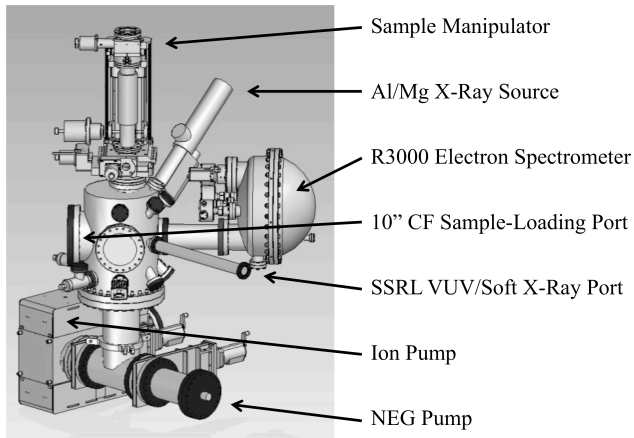

Figure 1: RECESS system configured for operating on a beam line at SSRL.

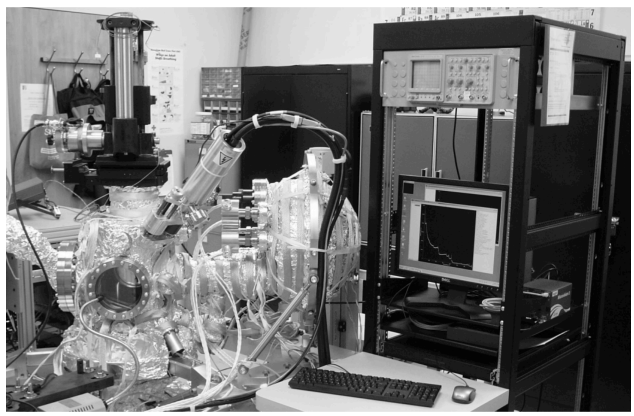

Figure 2: Photo of RECESS system configured for stand-alone operation.

LCLS photocathodes are fabricated from high-purity copper. First they undergo a dry hydrogen braze at 950 °C followed by diamond fly-cutting to a surface roughness < 10 nm rms. Then they are vacuum fired at 650 °C for 24 hours, welded to their base flange, and then vacuum fired again at 550 °C for another 24 hours. Once the photocathodes are installed, RF processing occurs until the desired RF conditions are achieved without breakdown. Typical operating conditions in a S-band (2856 MHz) RF gun are 1.5 µs RF pulses at 120 Hz with 10 MW of input power. This creates accelerating gradients > 100 MV/m at the photocathode. A 1.6 ps laser pulse of 10-20 µJ at 253 nm generates a 5.5 MeV beam at between 100-200 pC. These numbers illustrate that the operating photocathode environment is not a typical UHV environment. Because of this care must be taken to connect the results obtained in the RECESS system to those projected to occur in the gun.

ISBN 978-3-95450-126-7

QUANTUM EFFICIENCY AND TRANSVERSE MOMENTUM FROM METALS *

T. Vecchione#, D. Dowell, SLAC National Accelerator Laboratory, Menlo Park, CA 94025, U.S.A.
W. Wan, J. Feng, H. A. Padmore, LBNL, Berkeley, CA 94720, U.S.A.

Abstract

QE and transverse momentum are key parameters limiting the achievable brightness of FELs. Despite the importance, little data is available to substantiate current models. Expressions for each and experimental confirmation of each expression with respect to excess energy are presented. Novel instrumentation and analysis techniques developed are described.

INTRODUCTION

FELs are the next generation in high brightness accelerator based light sources. Because FEL brightness is ultimately limited by the quantum efficiency and transverse momentum of photocathodes confirmed expressions for each are important.

SINGLE CRYSTAL THEORY

The Sommerfeld model describes electronic states in metals. It has two components. The first is that electrons are bound by uniform potential and have kinetic energy measured with respect to it. The resulting density of states is constant. The second is that occupational probability is governed by Fermi-Dirac statistics with the chemical potential μ defined by the energy of the maximum occupied state at zero temperature. This gives an exponentially decaying occupational probability to states above the work function, ϕ.

The Spicer model identifies steps in photoemission. In the first step electrons absorb photons such that their momentum is increased normal to the surface only. Justification is given by observing that even in this case few states have sufficient momentum to escape. In the second step electrons diffuse to the surface where they escape in the third step based on their momentum. The surface barrier is treated as a well such that the bottom of the valence band is μ+ϕ below the vacuum level. Photoexcited electrons traversing the barrier lose energy equal to μ+ϕ-ħω in the direction normal to the surface. The probabilities associated with steps one and two are assumed to be represented by a constant S_{12} such that $0 \le S_{12} \le 1$. The probability associated with step three is given by the charge emitted per unit time per unit area assuming all electrons are ideally photoexcited divided by the current density normally incident on the surface.

Quantum Efficiency

QE is the number of emitted electrons per incident photon. The combination of Sommerfeld and Spicer models produces an expression for QE, Eqn. 1. A consequence of the Fermi-Dirac distribution is that there is photoemission even when ħω<ϕ. When ħω-ϕ>>kT Eqn. 1. reduces to the Fowler-Dubridge equation.

$$QE = S_{12}\left(\frac{Li_2\left[-Exp\left[\frac{e}{kT}\left(\hbar\omega-\phi\right)\right]\right]}{Li_2\left[-Exp\left[\frac{e}{kT}\mu\right]\right]}\right) \quad (1)$$

The differential of the emitted current density, dJ/dr, expressed in external cylindrical coordinates and normalized to unity at p_r=0 gives the transverse momentum distribution, Eqn. 2.

$$\frac{dJ_r}{dJ_0} = \frac{Li_1\left[-Exp\left[\frac{e}{kT}\left(\hbar\omega-\phi\right)-\frac{1}{2mkT}\left(\frac{mc}{1000}\right)^2 p_r^2\right]\right]}{Li_1\left[-Exp\left[\frac{e}{kT}\left(\hbar\omega-\phi\right)\right]\right]} \quad (2)$$

The polylogarithm functions used here are defined by Eqn. 3.

$$Li_n\left[z\right] = \frac{\left(-1\right)^{n-1}}{\left(n-2\right)!}\int_0^1 \frac{1}{t} Log\left[t\right]^{n-2} Log\left[1-zt\right]dt \quad (3)$$

RMS Transverse Momentum

The combination of Sommerfeld and Spicer models produces an expression for RMS transverse momentum ε_x, Eqn. 4, including a √2 to convert to Cartesian coordinates.

$$\varepsilon_x = 1000\sqrt{\frac{kT}{mc^2}}\sqrt{\frac{Li_3\left[-Exp\left[\frac{e}{kT}\left(\hbar\omega-\phi\right)\right]\right]}{Li_2\left[-Exp\left[\frac{e}{kT}\left(\hbar\omega-\phi\right)\right]\right]}} \quad (4)$$

The RMS transverse momentum is non-zero even when ħω<ϕ. In the limit of ħω=0 and ϕ<<kT, Eqn. 4 equals the RMS transverse momentum of thermal emission. In the limit of ħω-ϕ>>kT Eqn. 4 reduces to the Dowell equation.

METHODS

Sample Preparation

10 nm thin films of aluminum were deposited onto doped silicon. The substrates were first dipped in hydrofluoric acid and then flashed in vacuum. Next films were deposited at room temperature using a DC sputter gun. A quartz crystal monitor measured the rates. Chamber pressures were 1-2x10^{-10} torr. Finally H_20 and O_2 were used to oxidize the films.

*Work supported by US DOE contracts DE-AC02-05CH11231, KC0407-ALSJNT-I0013, and DE-SC000571.
#tvecchio@slac.stanford.edu

ISBN 978-3-95450-126-7

SLAC RF GUN PHOTOCATHODE TEST FACILITY*

T. Vecchione#, A. Brachmann, J. Corbett, M.J. Ferreira, S. Gilevich, E.N. Jongewaard, H. Loos, J.C. Sheppard, S.P. Weathersby, F. Zhou, SLAC National Accelerator Laboratory, Menlo Park, CA 94025, U.S.A.

Abstract

A RF gun photocathode test facility has been commissioned at SLAC. The facility consists of a S-band gun, high power RF, a UV drive laser and beam diagnostics. Here we report on the capabilities of the facility demonstrated during commissioning. Currently the facility is being used to study in-situ laser processing of copper photocathodes. In the future the facility will be used to study fundamental gun and photocathode performance limitations and enhancement strategies. Eventually it is envisioned to integrate a load lock and plug into the gun enabling the evaluation of high performance surface sensitive semiconductor photocathodes and the incorporation of ex-situ surface science analytical techniques.

INTRODUCTION

The Accelerator Structure Test Area (ASTA) at SLAC has been reconfigured to study RF gun photocathode performance. The 1.2 m thick concrete vault now contains a replica of the first 1.4 m of the LCLS injector, including the spare LCLS gun. The motivation for this is that LCLS operations have previously suffered from unexpected variations in photocathode quantum efficiency, emittance, and lifetimes. As a result a program was initiated to develop robust procedures for photocathode exchange and in-situ surface processing. The immediate goal is to demonstrate reliability. By performing these experiments in a dedicated test facility regular LCLS operations are not affected.

Photocathode Processing

LCLS photocathodes (Fig. 1) are fabricated from high-purity copper. The recipe varies but normally they first undergo a dry hydrogen braze at 950 °C followed by a diamond fly-cut to a final surface roughness < 10 nm RMS. Then they are vacuum fired at 650 °C for 24 hours, welded to their base flange, and then vacuum fired again for another 24 hours at 550 °C. Once the photocathodes are installed, RF processing occurs until full power operation is achieved without breakdown. At this point the QE of a given photocathode can vary from $1x10^{-6}$ (low) to $6x10^{-5}$ (high) under nominal operating conditions. To increase QE in-situ techniques such as laser-processing and RF plasma cleaning are being developed.

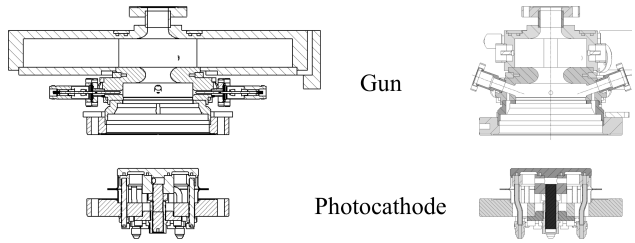

Figure 1: Cross-sections of LCSL photocathode and gun.

INSTRUMENTATION

Gun

The LCLS gun (Fig. 2) is a 1.6 cell racetrack shaped cavity with symmetrical RF feeds and field probes. Field gradients of 115 MV/m can generate greater than 3 nC pulses at 6 MeV. Gun performance in ASTA however is intentionally limited to hundreds of pC at 5.5 MeV. The gun is bakeable to 150 °C and can achieve $4x10^{-10}$ torr vacuum in operation. The gun assembly includes a solenoid, bucking coil, and transverse correctors. The ASTA installation also includes UV transport, RF waveguide and diagnostics (Fig. 3).

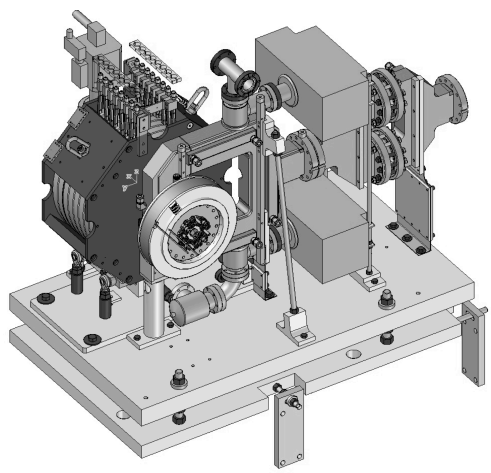

Figure 2: Gun assembly.

*Work supported by US DOE contract DE-AC02-76SF00515.
#tvecchio@slac.stanford.edu

ISBN 978-3-95450-126-7

HIGH BRIGHTNESS ELECTRON BEAMS FROM A MULTI-FILAMENTARY NIOBIUM-TIN PHOTOCATHODE

F. Ardana-Lamas*, C. Vicario, F. Le Pimpec, A. Anghel and C. P. Hauri*,
SwissFEL, Paul Scherrer Institut, 5232 Villigen-PSI, Switzerland
*also at Ecole Polytechnique Federale de Lausanne, 1015 Lausanne, Switzerland

Abstract

High-brightness electron sources are of fundamental interest for particle accelerators and modern free electron lasers. Inspired by the micro-structure of field emitter arrays [1,2] we report on a new type of metallic photo-cathode consisting of thousands of Nb3Sn micro-columns. With this metallic photocathode we could demonstrate quantum efficiencies up to 0.5% under stable operation [3,4]. Preliminary emittance measurements on a 50 keV table-top electron gun are presented.

INTRODUCTION

SwissFEL is aiming for a low-emittance electron linear accelerator with a photo-electron gun based on a conventional, flat copper cathode. Since modern electron accelerators have shown capable to provide low emittance beams up to GeV energy, the generation of a low-emittance electron beam at the gun is essential. In principle, well polished technical metallic photocathodes are well suited since they provide fastest response time upon laser excitation and lowest electron beam emittance. They are furthermore less sensitive to vacuum conditions than the semiconductor (SC) type cathodes. Unfortunately, metallic cathodes suffer from a lower quantum efficiency (QE) than SC type electron emitters, which is a drawback for high charge extraction since larger laser spot size and higher laser energy need to be applied to reach an equivalent charge without risking ablation damage on the cathode. An enlargement of the electron-emitting surface on the cathode goes naturally along with an increase in electron beam emittance ($\varepsilon \propto \sigma_{laser}$). The aim of our investigation was to find a metallic photocathode which withstands higher laser fluence and providing larger quantum efficiencies while keeping the advantages of metal photocathodes.

Here we report on the electron emission of a metallic-composite, multi-filamentary wire as potential candidate for a brilliant electron source. The micro-structured wire (Fig. 1) contains about 14'000 metallic filaments, each of them with a 2-5 µm diameter, grouped in bundles and embedded in a bronze matrix. A pure copper jacket and a tantalum ring keep the filament bundles together. The wire has been etched and reacted. The reacted wires contain the low-T_c superconductor Nb_3Sn while the non-reacted filaments are of pure Nb. Both the non-reacted and reacted wires have been investigated as electron emitters [3,4]. Although there is no structural difference between the two, the reacted ones are interesting in view of their superconducting properties at 4.2 K. In this paper the cathode is operated only at room temperature.

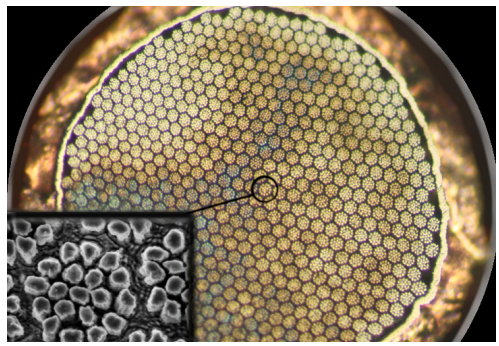

Figure 1: Multi-filament cathode (overall diameter 0.8 mm) with bundles of niobium filaments. The Nb filaments are arranged in bundles, one of which is shown in the close-up view (SEM picture). The cathode wire has a total of 14326 filaments, grouped in 754 bundles of 19 filaments each, (picture from [3]).

EXPERIMENTAL SETUP

The wire cathode has been implemented in a table-top 50 keV high-voltage pulser, as shown in Fig. 2. The high-voltage pulses have a rise/fall time of 1ns and a time jitter of approximately 200 ps from pulse to pulse. The applied electric field at the cathode tip is up to 15 MV/m.

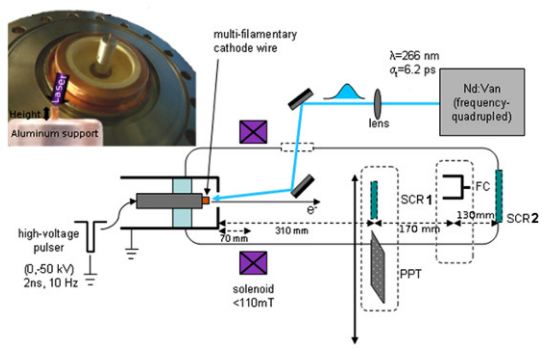

Figure 2: Experimental setup with the Nd:Van laser used to drive the electron emission process on the multifilament wire, located in the pulser. The electron beam properties are measured by a pepperpot (PPT), two YAG screens (SCR1,SCR2) and a Faraday cup (FC). The 2 ns, 50 kV pulser is used to accelerate the electron bunch from the cathode towards the anode at 10 Hz repetition rate, (picture from [4]).

ISBN 978-3-95450-126-7

PHOTOCATHODE LASER WAVELENGTH-TUNING FOR THERMAL EMITTANCE AND QUANTUM EFFICIENCY STUDIES

C. Vicario, S. Bettoni, B. Beutner, M. Csatari Divall, E. Prat, T. Schietinger, A. Trisorio,
Paul Scherrer Institute, 5232 Villigen PSI, Switzerland
C. P. Hauri, Ecole Polytechnique Federale de Lausanne, 1015 Lausanne, Switzerland and
Paul Scherrer Institute, 5232 Villigen PSI, Switzerland

Abstract

The SwissFEL compact accelerator design is based on extremely low emittance electron beam from an RF photoinjector. Proper temporal and spatial shaping of the photocathode drive laser is employed to reduce the space charge emittance contribution. However, the ultimate limit for the beam quality is the thermal emittance, which depends on the excess energy of the emitted photoelectrons. By varying the photocathode laser wavelength it is possible to reduce the thermal emittance. For this purpose, we applied a tunable Ti:sapphire laser and an optical parametric amplifier which allow to scan the wavelength between 250 and 305 nm. The system permits to study the thermal emittance and the quantum efficiency evolution as function of the laser wavelength for the copper photocathode in the RF gun of the SwissFEL injector test facility. The results are presented and discussed.

INTRODUCTION AND MOTIVATIONS

The Paul Scherrer Institute (PSI) is building an X-ray Free Electron Laser (FEL) user facility, which aims to deliver ultrashort coherent photon pulses with wavelengths ranging between 0.1 and 0.7 nm by the year 2017 [1]. For cost and space reasons the driving accelerator is foreseen with relatively modest final energy, thus calling for very low emittance. In preparation of SwissFEL, PSI is commissioning a 250 MeV photo-injector (SITF), which intends to demonstrate the generation of high-brightness electron beams and serves as a realistic test bed for crucial components for SwissFEL [2].

Modern linear accelerators demonstrated that it is feasible to preserve the electron beam emittance throughout acceleration. It becomes therefore important to generate the electron bunch at the source with the lowest possible emittance. Its growth due to the linear space charge forces is effectively counteracted by emittance compensation scheme. The photocathode drive lasers employ typically spatial and temporal pulse shaping in order to compensate the emittance dilution due to nonlinear space charge effect. Therefore the thermal or intrinsic emittance becomes a realistic limit for the beam quality. This parameter is a measure of the temperature of the electrons emitted from the cathode and it depends on the excess of energy of the photoelectrons in vacuum. Thermal emittance is function of the cathode material and surface quality, the accelerating electric field and laser wavelength.

The value of the intrinsic emittance is linked directly to the quantum efficiency (QE) of the photocathode (number of emitted electrons per incident photons). In the presented work we characterize the intrinsic emittance and the QE in RF gun while varying the laser wavelength. Similar studies are reported for photocathodes in DC gun [3]. The intrinsic emittance, ε_{in} can be written as [4]:

$$\varepsilon_{in}(\omega) = \sigma_L \sqrt{\frac{\hbar\omega - \Phi_{eff}}{3mc^2}} \quad (1)$$

with ω the laser wavelength, $\hbar\omega$ the photon energy, σ_L the rms laser spot size and Φ_{eff} the effective work function of the copper cathode including the Schottky effect. The Schottky term accounts for the reduction of potential barrier due to the applied electric field on the cathode surface. The total emittance can be reduced by adapting the laser photon energy to the net work function of the cathode. A decrease in quantum efficiency (QE) is expected when the laser photon energy approaches the effective work function. The QE can be expressed as [4]:

$$QE(\omega) \approx K \cdot \left(\hbar\omega - \Phi_{eff}\right)^2 \quad (2)$$

K takes into account the reflection of the laser at the cathode surface and the probability of the emission process. From equations 1 and 2 it is clear that lower ε_{in} can be obtained at the price of also lower QE.

For the design of high brightness accelerator a trade-off between the maximum acceptable intrinsic emittance and the quantum efficiency need to be established. The lower QE calls for higher energy and more complex drive laser with consequent worsening of system stability and ability control the photon beam tridimensional shape.

EXPERIMENTAL SETUP

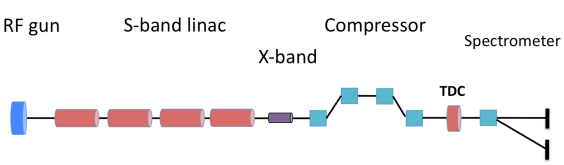

Figure 1: Layout of the swissFEL injector test facility.

The presented studies were conducted at the SwissFEL Injector Test Facility. The machine is based on a 3 GHz RF gun driven by a deep-UV laser on a copper cathode. The layout is depicted in Figure 1 and more details can be

ISBN 978-3-95450-126-7

HIGH-FIELD LASER-BASED TERAHERTZ SOURCE FOR SWISSFEL

C. Vicario, B. Monoszlai and C. Ruchert, Paul Scherrer Institute, 5232 Villigen PSI, Switzerland
C. P. Hauri, Ecole Polytechnique Federale de Lausanne, 1015 Lausanne, Switzerland and Paul Scherrer Institute, 5232 Villigen PSI, Switzerland

Abstract

We present efficient laser-driven THz generation by optical rectification in various organic materials yielding transient fields up to 150 MV/m, 0.5 Tesla and energy per pulse up to 45 μJ. The generated spectra extend over the entire THz gap (0.1-10 THz). Manipulation of the absolute phase by dispersion control is demonstrated for 5-octave spanning, single-cycle pulses. The presented source will be applied to the future SwissFEL as Xray photon temporal diagnostics and for pump-and-probe experiments.

INTRODUCTION

THz radiation located between the optical and the microwave frequency region known as terahertz gap (0.1-10 THz) is well suited to explore fundamental physical phenomena and to drive applications in condensed matter, chemistry, medicine and biology [1]. Few MV/cm THz electric transients and tesla magnetic fields open new opportunities to study ultrafast magnetization dynamics, collective effects and charged particle manipulations [2]. High-peak THz sources are required at X-ray free electron laser facilities, such as SwissFEL, for novel pump and probe experiments as well as for the temporal characterization of the Xray pulse on the femtosecond time scale [3]. The generation of few-cycle fields exceeding 1 MV/cm in the THz gap has remained challenging. To access high field in the full THz gap we recently developed a compact and powerful laser-driven THz source based on nonlinear organic crystals. The radiation is generated by optical rectification in organic salt material such as DAST, OH1 and DSTMS. The optical rectification in these nonlinear materials permits the realization of extremely intense and phase-stable THz transient [4-6]. These organic crystals provide in fact low THz absorption and the highest susceptibility for optical rectification. Moreover, velocity matching between laser pump and THz radiation is achieved in a collinear geometry for pump wavelengths between 1.35 and 1.5 μm. THz radiation is emitted collinearly to the pump with excellent focusing characteristics which is key feature to achieve the highest peak field. Spectra covering the full THz gap become accessible for femtosecond laser pump and sufficiently thin crystal supporting this bandwidth. The crystals can be anti-reflection coated for maximum optical rectification efficiency, and, as we show in the experiment, their damage threshold for femtosecond pulses is in excess of 160 GW/cm^2

THZ GENERATION AND CHARACTERIZATION

In the experimental setup a TW-class Ti:Sa at 100 Hz, producing 60 fs FWHM pulses is used to drive a white-light continuum optical parametric amplifier (OPA). The multi-mJ OPA delivers 70 fs transform-limited infrared pulses to pump the organic crystal for THz generation.

In order to prevent organic crystal damage while using the maximum available pump flux, large crystals with up to 10 mm aperture at a nominal thickness of 0.5 mm are utilized. The THz beam is emitted collinearly to the pump and is tightly focused for the realization of the highest field. The THz temporal shape is measured by electro-optical sampling (EOS). The EOS gives direct access to the THz the absolute electric field and the spectral content. The electro-optical spectral sensitivity for our electro-optical setup decreases above 5 THz. Higher frequencies are measured by means of Michelson interferometer equipped with THz sensitive detectors.

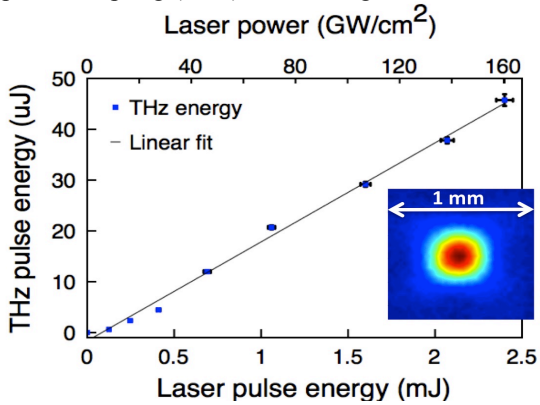

Figure 1: THz pulse energy as function of the pump fluence. Inset, 360 μm FWHM terahertz spot achieved at the waist.

Energy Conversion and Focal Spot

Absolute energy measurements are carried out by means of a calibrated Golay cell. The transverse beam profile is recorded with a bolometer un-cooled camera having a pixel size of 23.5 microns. In Figure 1 the THz pulse energy generated in a 0.5 mm thick DAST crystal with an aperture of 8 mm is shown as function of the infrared laser energy and power density. Maximum THz pulse energy of 45 μJ is reached when the crystal is pumped OPA pulse energy of 2.4 mJ (at 160 GW/cm^2). The highest pump-to-THz energy conversion is about 2% corresponding to photon conversion efficiency larger than 220%. Furthermore remarkable is the shot-to-shot THz

ISBN 978-3-95450-126-7

NEW CONCEPT FOR THE SwissFEL GUN LASER

A. Trisorio, M. Divall, C. Vicario and C. P. Hauri
SwissFEL, Paul Scherrer Institut, Villigen, Switzerland
A. Courjaud, Amplitude Systèmes, Pessac, France

Abstract

We report on a new concept for the gun laser system of the future hard and soft x-ray SASE FEL (SwissFEL) at the Paul Scherrer Institute and present first experimental verifications. The system consists of a hybrid Yb fiber and solid state Yb:CaF_2 amplifier. The laser performance, such as energy stability, timing jitter, double pulse operation, temporal and spatial pulse shape of the ultra-violet laser pulses match the SwissFEL requirements. The mature and stable direct diode pumping technology and an optimized design allow for high reliability, long lifetime and lower maintenance cost compared to the widely used Ti:sapphire laser systems.

INTRODUCTION

The operation of SwissFEL puts very stringent constrains on the gun laser system. First the parameters, such as energy stability, timing jitter, double pulse operation, flat top temporal and spatial pulse shape of the ultra-violet (UV) laser pulses (see Tab. 1) used to generate the photo-electrons are challenging even for the state of the art laser technologies.

Table 1: Gun Laser Characteristics for SwissFEL

Laser specifications	
Maximum pulse energy on cathode	60 µJ
Central wavelength	250-300 nm
Bandwidth (FWHM)	1-2 nm
Pulse repetition rate	100 Hz
Double-pulse operation	yes
Delay between double pulses	50 ns
Laser spot size on cathode (rms) (10 pC/ 200 pC)	0.1 / 0.27 mm
Minimum pulse rise-time	< 0.7 ps
Pulse duration (FWHM)	3-10 ps
Longitudinal intensity profile	various
Transverse intensity profile	Uniform
Laser-to-RF phase jitter on cathode (rms)\	<100 fs
UV pulse energy fluctuation	<0.5% rms
Pointing stability on cathode (relative to laser diameter)	<1% ptp

Second, the laser system must be extremely stable, reliable and its maintenance cost as low as possible. In this perspective, we prospected for alternative technologies to the well known, commonly used but costly Ti:sapphire (Ti:Sa) laser systems [1]. Here we show that a hybrid Yb fiber and solid state Yb:CaF2 amplifier system can be a very interesting approach. This gain medium [2] allows the production of sub-500 fs, high fidelity, high stability, high energy pulses in the infrared and in the ultra-violet with low timing jitter. The system profits of the mature, stable direct diode pumping technology and optimized design. It delivers the two high-energy, shaped UV pulses separated by 28 ns to produce the photo-electrons, a short IR probe (<80 fs FWHM) to temporally characterize those pulses and the two stretched IR pulses (50 ps FWHM) necessary for the laser heater.

LASER SYSTEM

The choice of the laser system gain medium and architecture has a direct impact on its final performance and reliability. The Yb:CaF_2 have all desired properties for the production of high energy, UV femtosecond pulses. Moreover by keeping the laser architecture simple and compact the system reliability is improved.

Yb:CaF2 Crystal

The use of calcium fluoride with ytterbium doping (Yb:CaF_2) as an active laser medium for CW systems started in 2004 [3]. Its very interesting properties for laser amplification led to developments for short-pulse, high energy laser system up to the TW-scale [4].

- Yb:CaF_2 crystal exhibit a very broad and smooth emission band. The material is able to emit in the 1020-1060 nm spectral range allowing the generation of sub-500 fs pulses.
- The crystal absorption cross section exhibits a pronounced and narrow band peak at 980 nm as can be seen in figure 1. This point is of particular interest since it allows direct pumping with CW infrared diode modules developed for telecom applications.
- The material fluorescence lifetime of 2.4 ms and the thermal conductivity of 4.9 $W.m^{-1}.K^{-1}$ are well suited to the design of high power lasers. The first one is crucial, since it permits high energy storage in regenerative amplifier cavities leading to high energy pulses. The later permits CW pumping with high average power while avoiding detrimental thermal effects.

ISBN 978-3-95450-126-7

A FEMTOSECOND RESOLUTION ELECTRO-OPTIC DIAGNOSTIC USING A NANOSECOND-PULSE LASER

David Alan Walsh, William Allan Gillespie, University of Dundee, Nethergate, Dundee, Scotland
Steven Jamison, STFC Daresbury Laboratory & Cockcroft Institute, Daresbury, UK

Abstract

Electro-optic diagnostics with a target time resolution of 20fs RMS, and with intrinsically improved stability and reliability, are being developed. The new system is based on explicit temporal measurement of an electro-optically upconverted pulse, following interaction of the bunch with a quasi-CW probe pulse. The electro-optic effect generates an "optical-replica" of the longitudinal charge distribution from the narrow-bandwidth probe, simultaneously up-converting the bunch spectrum to optical frequencies. By using Frequency Resolved Optical Gating (FROG), an extension of autocorrelation, the optical replica can then be characterised on a femtosecond time scale. This scheme therefore bypasses the requirement for unreliable femtosecond laser systems. The high pulse energy required for single-shot pulse measurement via FROG will be produced through optical parametric amplification of the optical-replica pulses. The complete system will be based on a single nanosecond-pulse laser – resulting in a reliable system with greatly relaxed timing requirements.

INTRODUCTION

Electro-optic (EO) techniques have for some time held the promise of high time resolution non-destructive bunch longitudinal profile diagnostics. A range of EO diagnostic systems has been developed and demonstrated, such as Spectral Decoding [1], Spatial Encoding [2], Temporal Decoding [3], and Spectral Upconversion [4], although all have the same underlying physical principle of encoding the temporal or spectral information of the bunch profile into an optical signal via the second order non-linear (EO) interaction. Despite the large number of demonstrations of EO diagnostic concepts, there are only a very limited number of examples of EO diagnostics being integrated into operational accelerator diagnostic systems [5-7]. This can at least partially be attributed to the increasing demands for the time resolution, now reaching down to the sub 10 fs level for FELs, which remain beyond state-of-the-art EO systems. Where lower, demonstrated, time resolutions are acceptable, there is also a significant barrier to operational implementation due to the complexity and reliability of the ultrafast laser systems that have until now been necessary.

Here we describe the development of a new variant of EO diagnostic, which we term 'Electro-Optic Transposition' (EOT) [8], that has the potential for both high time resolution and robust implementation. The system requires no ultrafast lasers and can be based on narrowband nanosecond lasers that have reached a mature level of 'industrial' reliability. The development described here relates to the laser system and optical characterisation. For higher time resolution, a parallel improvement in EO materials is also required, and while not described here this is the subject of a separate research project in our group.

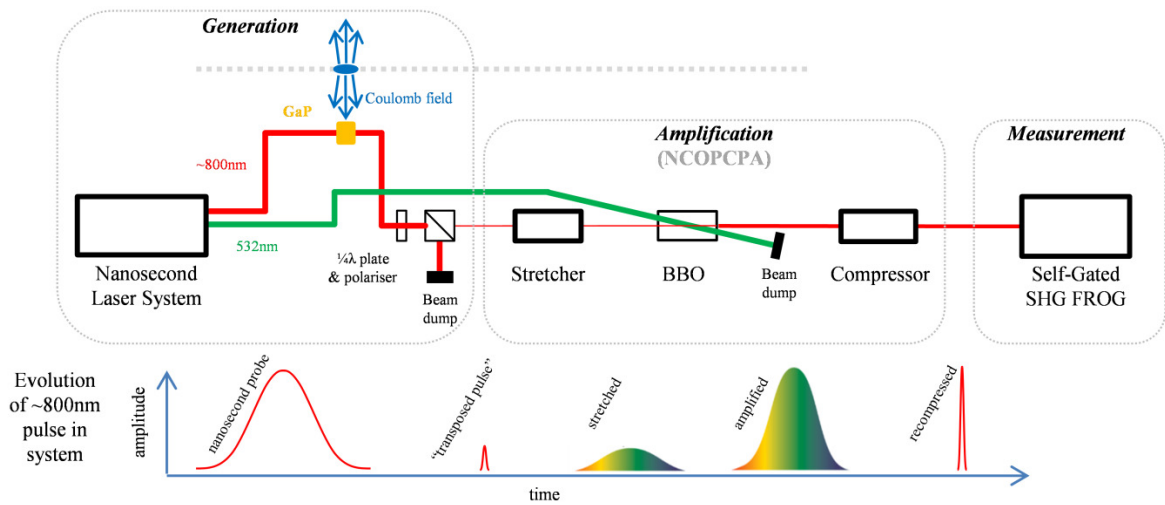

Figure 1: Schematic of the electro-optic transposition system. The system can be considered as 3 separate stages: generation of the optical probe and subsequent up-converted signal pulse; amplification of the signal pulse to a level that can be characterised, and finally measurement of the signal to reveal its temporal structure.

ISBN 978-3-95450-126-7

FEL R&D WITHIN LA³NET*

C.P. Welsch#, Cockcroft Institute and The University of Liverpool, UK
on behalf of the LA³NET Consortium

Abstract

The detailed diagnostics of the shortest beam pulses in free-electron lasers still pose significant challenges to beam instrumentation. Electro-optical methods are a promising approach for the non-intercepting measurement of electron bunches with a time resolution of better than 50 fs, but suitable optical materials need to be better understood and carefully studied. In addition, adequate timing systems with stability in the femtosecond regime based on mode-locked fibre laser optical clocks, and actively length-stabilised optical fibre distribution require further investigation. These important problems are being addressed within the broader EU-funded LA³NET project by an international consortium of research centres, universities, and industry partners. This contribution gives an overview of the wider LA³NET project and results from initial studies in both areas. It also describes the events that LA³NET will organize.

INTRODUCTION

Lasers will make an increasingly important contribution to the characterization of many complex particle beams necessary for optimising FEL operation by means of laser-based beam diagnostics methods. As the limits of performance of conventional radiofrequency particle accelerators are reached new methods for particle acceleration and beam optimization are needed. Lasers will also play a key role in the development of accelerators by improving the generation of high brightness electron and exotic ion beams and through increasing the acceleration gradient.

The LA³NET network [1] is built around 17 early stage researchers working on dedicated projects to research and develop a complete spectrum of laser-based applications for accelerators. The network presently consists of an international consortium of more than 30 partner organizations including universities, research centres and private companies working in this field. This will provide a cross-sector interdisciplinary environment for beyond state-of-the-art research and researcher training while developing links and new collaborations.

FEL RESEARCH

Research within LA³NET is distributed in five different work packages: Laser-based particle sources, laser-driven particle beam acceleration, lasers for beam instrumentation, system integration and lasers and photon detector technology. Although each fellow works on an independent research project, there are many links between work packages. The following sections describe research being carried out by consortium Members University of Dundee and STFC in the UK to which LA3NET contributes

EO Bunch Temporal Profile Monitor

Detailed temporal diagnostics of the shortest electron beam bunches in free-electron lasers pose some of the most significant challenges in accelerator beam instrumentation. Electro-optical (EO) methods are a promising approach for the single-shot non-intercepting measurement of electron bunches with a time resolution of better than 50 fs, but new, more reliable methods of measurement require to be developed, and suitable electro-optical materials need to be better understood and carefully studied. These aspects are currently under study in a collaboration between the University of Dundee and STFC Daresbury Laboratory, and is partially supported through the EU-funded LA³NET project [1].

Current techniques, developed over the last decade by the Dundee-Daresbury Group, are based on either spectral or temporal decoding of the Coulomb field of ultra-relativistic electron beams. The former technique is limited to beam bunches around 1 ps [2], while the latter requires ultra-short-pulse lasers that are expensive and potentially unreliable, making them unsuitable for turn-key accelerator control systems. The Group is currently working with the CERN compact linear collider (CLIC) project, with the intention of measuring the 150 fs CLIC main beam bunches to an accuracy of 15-20 fs, and using relatively simple laser systems, which is better than the current state-of-the-art for such measurements.

This work is also of pivotal importance for future advanced light sources, free-electron lasers and laser plasma wakefield accelerators, all of which share the characteristic of few-femtosecond (and shorter) electron bunches. There is therefore a pressing requirement to devise methods of measuring and optimising such very short electron bunch profiles, which will ultimately extend to the attosecond regime.

All of these techniques rely on the generation of a faithful 'optical replica' of the Coulomb field of the beam. This is generated by a process termed 'spectral upshifting' or 'pulse carving', whereby the Terahertz pulse representing the transverse Coulomb field is upshifted to an optical frequency via sum and difference frequency mixing in a suitable optical detector material placed adjacent to (but not traversed by) the electron beam. This is currently achieved using thin inorganic electro-optic crystals such as GaP and ZnTe, but the optical bandwidth of these materials (a few THz) renders them inefficient at very short bunch lengths, partly due to the onset of transverse optical phonon resonances [3]. Since 2011 the Dundee Group have been investigating a range of

*Work supported by the EU under contract PITN-GA-2011-289191.
c.p.welsch@liverpool.ac.uk
ISBN 978-3-95450-126-7

DARK CURRENT MEASUREMENTS AT THE ROSSENDORF SRF GUN*

R. Xiang#, A. Arnold, P. Murcek, J. Teichert, HZDR, Dresden, Germany
V. Volkov, BINP, Novosibirsk, Russia
P. Lu, H. Vennekate, HZDR & Technische Universität Dresden, Germany
R. Barday, T. Kamps, HZB, Berlin, Germany

Abstract

The injector plays a significant role in accelerator facilities for FEL sources, electron colliders and Thomson backscattering sources [1-3]. During the operation of an electron gun, the dark current creates significant background to the accelerator users. In this work, we used the existing beam line to study the dark current from the SRF gun at HZDR. The dark current emitted from the niobium cavity and the Cs_2Te photocathode was separately measured. A multi-peaked energy spectrum for the dark current has been observed.

INTRODUCTION

Recently, superconducting RF photoinjectors (SRF gun) draw a lot of attention because of its continuous-wave (CW) operation, low emittance and potential application for polarized beam generation [4]. The ELBE SRF gun under the cooperation of HZDR, BESSY, DESY and MBI has been successfully commissioned [5] and firstly operated for the ELBE IR-FEL [6]. It is operated with the gradient up to 6 MV/m at CW mode or with 8 MV/m at macro pulse mode. With a Cs_2Te photocathode driven by the 13 MHz UV laser the ELBE SRF gun has produced the photocurrent beam up to 0.5 mA.

During the operation of the gun, the dark current can induce beam loss, increase the risk of damages to accelerator components, and raise additional background for users [7]. Especially for SRF guns and superconducting accelerators, the dark current increases the rf power consuming and the heat load for the liquid helium system.

EXPERIMENTAL SETUP

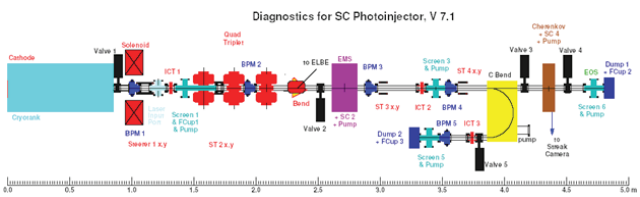

Figure 1: The diagnostic beam line for SRF gun. [8]

*Work supported by the European Community-Research Infrastructure Activity under the FP7 program (EuCARD, contract number 227579), as well as the support of the German Federal Ministry of Education and Research grant 05 ES4BR1/8.
#r.xiang@hzdr.de

The diagnostic beam line was designed and built in 2007 by HZB [8], schematically shown in figure 1. Behind the exit of the gun a solenoid locates, followed by the laser input port and a Faraday cup. A group of quadrupole triplet is used to optimize the beam before the dipole to ELBE dogleg beamline. Several beam position monitors (BPM) and steerers (ST) are used to guide the beam, and six screen stations to view the beam spot. The 180° dipole (C-bend) is installed for energy and energy spread measurement.

FIELD EMISSION IN THE CAVITY

The field emission from the inner wall of the niobium cavity and from the photocathode builds up the dark current. For the ELBE SRF gun it is possible to detect separately the field emission from the niobium cavity and that from photocathode.

Field Distribution in the Cavity

In Figure 2, the cavity shape of ELBE SRF gun is shown on top. The distribution of the surface electric field on the cavity wall and the field on the axis are presented along the cavity axis z at the bottom. The solid red line is the surface electric field of the cavity with cathode, the blue dashed line presents the surface field for the same cavity without cathode, and the black dots show the acceleration field E_z along the axis z.

Obviously the existing of a cathode does not change the field distribution in the TESLA cells or the maximum field in the half cell. It is worthy to note that the peak field in the half-cell located at the edge of the cathode hole, where the peak field reaches 20 MV/m, i.e. about 123 % of the peak field on axis E_{max} 16.2 MV/m.

From the surface field distribution, possible emission sources can be found at the rim of cathode hole, the cavity iris and the half-cell back wall. If one compares the surface field and axis acceleration field distribution, logically the field emission around the cathode hole is the main part of the dark current, where the field emitted electrons can be accelerated forward together with the photo electrons by the electric field. The other field emitted electrons are not synchronized well to the rf field. However, these electrons can hit the cavity wall leading to more helium consummation, or bombard the cathode layer degrading the photocathode quality.

ISBN 978-3-95450-126-7

TOWARDS ZEPTOSECOND-SCALE PULSES FROM X-RAY FREE-ELECTRON LASERS

D.J. Dunning, N.R. Thompson, ASTeC, STFC Daresbury Laboratory and Cockcroft Institute, UK
B.W.J. McNeil, Department of Physics, SUPA, University of Strathclyde, Glasgow, UK

Abstract

The short wavelength and high peak power of the present generation of free-electron lasers (FELs) opens the possibility of ultra-short pulses even surpassing the present (tens to hundreds of attoseconds) capabilities of other light sources - but only if x-ray FELs can be made to generate pulses consisting of just a few optical cycles. For hard x-ray operation ($\lesssim$0.1nm), this corresponds to durations of approximately a single attosecond, and below into the zeptosecond scale. This talk will describe a novel method [1] to generate trains of few-cycle pulses, at GW peak powers, from existing x-ray FEL facilities by using a relatively short 'afterburner'. Such pulses would enhance research opportunity in atomic dynamics and push capability towards the investigation of electronic-nuclear and nuclear dynamics. The corresponding multi-colour spectral output, with a bandwidth envelope increased by up to two orders of magnitudes over SASE, also has potential applications.

INTRODUCTION

The motivation for generating short pulses of light is to study and influence ultra-fast dynamic processes. To do this, radiation pulses on a shorter scale than the dynamics involved are required. The timescales of different processes have been described by Krausz and Ivanov [2]: Atomic motion on molecular scales occurs at femtosecond (10^{-15} s) to picosecond (10^{-12} s) scales, electron motion in outer shells of atoms takes place on tens to hundreds of attoseconds, and electron motion in inner shells of atoms is expected to occur around the scale of a single attosecond (10^{-18} s). At faster scales still are nuclear dynamics, which are predicted to occur at zeptosecond (10^{-21} s) time scales .

The record for the shortest pulse of light has seen a progression from approximately 10 ps in the 1960s to around 67 attoseconds generated recently by Chang et al. [3]—a development of approximately five orders of magnitude in five decades. As noted by Corkum et al. [4, 5], it is particularly relevant to consider the way in which this frontier progressed. The duration of a pulse of light is its wavelength, λ_r multiplied by the number of optical cycles, N, divided by the speed of light. Initially progress was made in conventional lasers operating at approximately a fixed wavelength ($\lambda_r \approx$600 nm), by reducing the number of optical cycles. This continued until, in the mid 1980s, pulses of only a few cycles could be generated (corresponding to a few fs), then could proceed little more.

It took a transformative step—high harmonic generation (HHG) [2, 4, 5], for progress to continue by (in very simple terms) reducing the wavelength of the generated light. This technology allowed pulses in the attosecond scale to be generated for the first time, and now reaches just under a hundred attoseconds.

It seems that a further step to shorter wavelength is now required to progress to significantly shorter pulses. Proposals are being developed outlining how future progress in HHG might achieve this [6]. Alternatively, x-ray free-electron lasers (FELs) (reviewed in several recent papers [7–9]) presently surpass HHG sources in terms of shortest wavelength by approximately two orders of magnitude, and it is this property which first suggests FELs as a promising candidate for progressing to shorter radiation pulses than are available today.

SHORT-PULSE POTENTIAL OF FREE-ELECTRON LASERS

The free-electron laser in fact has two particular advantages which give it potential for pushing the frontier of short pulse generation. The first, as described in the previous section, is short wavelength. Recent new FEL facilities (LCLS [10] commissioned in 2009, and SACLA [11] commissioned in 2011) have extended FEL operation down to approximately 0.1 nm. Assuming that pulses of only a few optical cycles could be attained, this would correspond to pulse durations of approximately a single attosecond—approximately two orders of magnitude shorter than present HHG sources, and four orders of magnitude beyond conventional lasers.

Of course x-ray sources other than FELs have been available for many years, however the peak powers are insufficient to deliver a significant number of photons within an attosecond timescale. It is the high peak power of the free-electron laser (exceeding synchrotrons - the next highest intensity source of x-rays - by approximately 9 orders of magnitude) which gives it potential to push the frontier of ultra-short pulse generation. A hard x-ray FEL typically generating approximately 20 GW peak power, corresonds to 10^{25} photons/second. For a pulse duration of a single attosecond this would correspond to 10^7 photons per pulse.

The challenge for reaching the very shortest pulses from FELs - as described in the following sections - will be to minimise the number of cycles per pulse.

STANDARD OPERATING MODE OF A HARD X-RAY FEL - SASE

Present hard x-ray FELs normally operate in the high-gain amplifier mode generating self-amplified spontaneous emission (SASE) (as described by Bonifacio et al. [12]),

ISBN 978-3-95450-126-7

NEW SCHEME TO GENERATE A MULTI-TERAWATT AND ATTOSECOND X-RAY PULSE IN XFELS

T. Tanaka*
RIKEN SPring-8 Center, Koto 1-1-1, Sayo, Hyogo 679-5148, Japan

Abstract

A new scheme to upgrade the source performance of X-ray free electron lasers (XFELs) is proposed, which effectively compresses the radiation pulse, i.e., shortens the pulse width and enhances the peak power of radiation, by inducing a periodic current enhancement with a long-wavelength laser and applying a temporal shift between the X-ray and electron beams. Calculations show that a 10-keV X-ray pulse with the peak power of 6.6 TW and pulse width of 50 asec can be generated by applying this scheme to the SACLA XFEL facility.

INTRODUCTION

In order to investigate unknown phenomena with a photon beam, its size should be as small as possible both in space and time: its focal size should be ideally smaller than the typical dimension of the target, and its pulse width should be shorter than the typical time scale for the target to change. It should be noted, however, that the focal size and pulse width can never be smaller than the wavelength because of the uncertainty of light. This puts a lower limit on the focal size and pulse width of any kind of lasers.

In the long-wavelength region such as the optical and infrared regions, a focal size and pulse width that are close to these theoretical minima have been already achieved with the state-of-the-art laser technologies. In other words, optical lasers with the focal size less than 1 μm and the pulse width of around several femtoseconds are readily available. On the other hand, the situation is completely different in XFELs having wavelengths four orders of magnitude shorter than the optical lasers: the attainable focal size and pulse width are 50 nm and several femtoseconds, respectively, being far from the theoretical minima, i.e., 0.1 nm and several hundreds of zeptoseconds. It is worth noting that the focal size has been reduced step by step by means of improving the x-ray optics, and possibly will go down to several nm in the near future. On the other hand, there have been no means to compress the XFEL pulse corresponding to the laser pulse compression scheme in the long-wavelength regions. Instead, a number of proposals have been made [1]-[6] to shorten the pulse width at the expense of the reduction of the effective charge contributing to lasing, in which shorting the pulse width does not necessarily mean the enhancement of the peak laser power.

In order to deal with the issue, a novel scheme has been recently proposed [7], in which the XFEL pulse is effectively compressed: the pulse width is shortened and the laser peak power is enhanced as well. In this paper, the principle of the new scheme is introduced and several calculation results to quantify the laser performance are presented.

PRINCIPLE OF OPERATION

The principle of operation is first explained. Figure 1 shows the schematic diagram of the accelerator layout to apply the proposed pulse compression scheme.

In addition to ordinary components for XFELs, two extra elements are installed before the undulator section, which generates an electron beam having a special bunch structure to realize the bunch compression scheme.

The first one is the slotted foil that has been originally proposed for shortening the XFEL pulse [1] and demonstrated in LCLS. The metal foil installed int the bunch compressor (BC) scatters the electrons and spoils the beam emittance, and thus suppresses the lasing region in the bunch. Because of the strong correlation between the longitudinal coordinate s and horizontal coordinate x at the BC section, lasing is suppressed in the corresponding head and tail of the bunch and thus the XFEL pulse width can be controlled. Note that its function in our scheme is to set a defined temporal window of lasing and define the lasing domain in the electron bunch.

The second one is the E-SASE (enhanced SASE) section in which an optical laser (E-SASE laser) with a wavelength of λ_E is injected synchronously with the electron bunch to a long-period undulator whose fundamental wavelength equals λ_E. In the following dispersive section, the energy modulation is converted to the density modulation with the pitch of λ_E and thus a comb-like current distribution is created in the electron bunch.

After the two processes described above, the current distribution is give as

$$I(s) = [I_u(s) + I_o(s)]E(s),$$

where $I_u(s)$ and $I_o(s)$ denote the current distributions just after the BC section. The former refers to the electrons that are scattered by the foil and do not contribute to lasing and the latter to the electrons that are scattered and do not contribute to lasing. The horizontal beam size at the BC section depends on the energy chirp for the bunch compression and other intrinsic factors such as the beam emittance, betatron function and energy spread. If the latter effect is negligible compared to the former one, $I_o(s)$ is expected to have a rectangular profile. In reality, there exists a fringe region at the boundary between $I_o(s)$ and $I_u(s)$ because of

* ztanaka@spring8.or.jp

ISBN 978-3-95450-126-7

LONGITUDINAL COHERENCE IN AN FEL WITH A REDUCED LEVEL OF SHOT NOISE

Vitaliy Goryashko*, Volker Ziemann
Uppsala University, Sweden

Abstract

For a planar free electron laser (FEL) configuration we study self-amplified coherent spontaneous emission driven by a gradient of the bunch current in the presence of different levels of noise in bunches. We calculate the probability density distribution of the maximum power of the radiation pulses for different levels of shot noise. It turns out that the temporal coherence quickly increases as the noise level reduces. We also show that the FEL based on coherent spontaneous emission produces almost Fourier transform limited pulses and the time-bandwidth product is mainly determined by the bunch length and the interaction distance in an undulator. We also propose a scheme that permits the formation of electron bunches with a reduced level of noise and a high gradient of the current at the bunch tail to enhance coherent spontaneous emission. The presented scheme uses effects of noise reduction and controlled microbunching instability and consists of a laser heater, a bunch compressor, and a shot noise suppression section. The noise factor and microbunching gain of the overall proposed scheme with and without laser heater are estimated.

INTRODUCTION

Longitudinal (temporal) coherence of free-electron lasers (FELs) is important for a number of applications like coherent scattering, time-resolved spectroscopy, nonlinear science. Most existing short wavelength FELs are operated as single pass amplifiers so that the coherence of FEL output strongly depends on the coherence of an effective input signal. The latter can be a gradient of density or velocity modulations in electron bunches, or an external electromagnetic signal. In SASE FELs the gradient of electron density is caused by shot noise so that shot noise in electron bunches plays a role of an ultra-wide band effective seed. But shot noise has a random nature and as a result the output of SASE FEL is stochastic and presented by a series of random superradiant spikes with a large variation of intensities [1]. In order to mitigate this drawback and reach longitudinal coherence, a number of techniques like seeding with external quantum lasers, self-seeding and high-brightness SASE FELs [2] based on bunch-radiation manipulations were proposed. The idea of seeding techniques is to achieve the dominance of an initial coherent signal over an incoherent one at the FEL start-up. The input signal-to-noise ratio along with the FEL process define the longitudinal coherence at the output.

In order to reach high coherence with external seeding schemes, the energy of an external seed laser up to several millijoules [3] is typically required. That is achievable by commercially available quantum lasers. But the capability of seeding with a high repetition rate is questionable. For example, for FELs based on superconducting technology like the European XFEL, the energy of a quantum laser has to be of the order of kJ per second. This implies a laser system that is well beyond the existing state-of-the-art lasers. Then, it is beneficial to reduce an incoherent signal at the FEL start-up and correspondingly reduce the required coherent seed power. As we mentioned, the main contribution to the incoherent effective input signal comes from shot noise, so the latter must be suppressed.

To mitigate the shot noise effect several techniques have been proposed and FELs with a reduced level of shot noise are under active study [4, 5, 6]. At the same time, to the authors' knowledge only a linear theory of such FELs have been published. The problem to what extent the bunch noise has to be suppressed in order to obtain well-determined radiation pulses requires further studies and we address this question in our paper.

We study how the coherence of an effective input signal affects the FEL output coherence on the example of an FEL having an essential level of coherent spontaneous emission (CSE) and different levels of shot noise. Recall that the total spontaneous radiated power at wavenumber k is

$$P_{\text{spontaneous}}(k) = Q_b P_{\text{und}}(k) + Q_b^2 |F(k)|^2 P_{\text{und}}(k), \quad (1)$$

where the first term is the contribution from shot noise whereas the second one is that from coherent spontaneous emission. Here, Q_b is the number of electrons in a bunch, $P_{\text{und}}(k)$ is the power emitted by a single electron in an undulator, $F(k)$ is the bunch form-factor (Fourier transform of the longitudinal electron density) that at given wavelength depends on the bunch length and the gradient of the bunch current. By changing the level of shot noise one modifies the first term in (1) and changes the coherence of the FEL output radiadion.

SELF-AMPLIFIED COHERENT SPONTANEOUS EMISSION

We analyse the properties of an FEL with a reduced level of shot noise using a 1D approximation for the electron bunch but still consider the longitudinal discreteness of the electrons and employ a non-averaged FEL model [7], [8]. The dependence of the bunch current and excited radiation field on the transverse coordinates is ignored in this approach. However, the 3D effects are taken into account in a phenomenological way by using an effective value of

* vitaliy.goryashko@physics.uu.se; vitgor06@gmail.com

ISBN 978-3-95450-126-7

SUPER-RADIANT LINAC-BASED THz SOURCES IN 2013

M. Gensch, HZDR, Dresden, Germany

Abstract

These proceedings shall give an overview over the rapidly growing number of super-radiant linac-based THz sources which have been developed and designed over the past 13 years following the seminal pilot experiment at the Jefferson lab energy recovery linac in 2001 [1]. More than 20 super-radiant THz facilities already exist or are planned worldwide and are listed together with a set of fundamental parameters in the appendix of this paper.

INTRODUCTION

Super-radiant THz sources are a relatively new class of accelerator-based photon sources. They became only technically feasible in the early 2000´s when accelerator technology had evolved to a stage where highly charged electron bunches could be compressed to the sub mm regime. A relativistic electron bunch prepared in that way allows generating coherent THz bursts during one single path through a radiator of synchrotron radiation. This generation principle leads to systematically different properties than that of the other already class of accelerator based coherent THz radiation namely that of the low gain THz free electron lasers (for details see [2] and references therein). In short, this corresponds to three key parameters which can be much more flexibly chosen in the design of these facilities: *(i) spectral bandwidth (ii) repetition rate (iii) carrier envelope phase stability*. In particular the latter property is of large importance in modern ultra-fast science experiments which aim at elucidating transient or magnetic field-driven dynamics (for timely review on such experiments see [3]). The particular interest of the ultra-fast community in super-radiant THz sources lies in their enormous scalability both in repetition rate and pulse energy. This stems from the fact that the conversion of electron energy into THz pulse energy can be done in the absence of any media. Recent trends as reported on the FEL13 conference were: firstly the emergence of many new facilities and facility proposals. Secondly, the development of new source concepts that go beyond the classical radiators such as coherent transition radiators, bending magnets or undulators and thirdly the combination of super-radiant THz sources with synchronized fs probes such as fs X-ray or fs laser pulses that allow elucidating dynamics on sub THz cycle timescales. A future challenge discussed on FEL13 is here the synchronization of such sources on sub THz cycle timescales. On approach which achieves few fs-level synchronization is shown in figure 1, where a super-radiant THz undulator pulse has been sampled sequentially by fs X-ray pulses [4]. In this case THz pulse and fs X-ray pulse are intrinsically synchronized because they are generated by the same electron bunch.

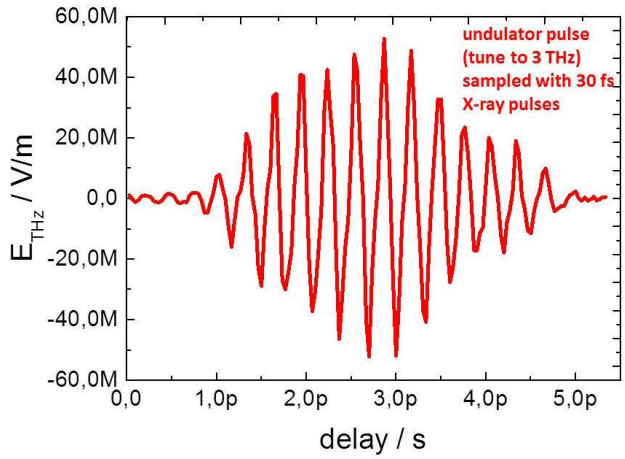

Figure 1: 3 THz pulse from the super-radiant THz undulator at FLASH sampled by the intrinsically synchronized fs X-ray pulses from the same electron bunch [4, 5].

ACKNOWLEDGMENT

A.Perucchi (FERMI), B.Schmidt, N.Stojanovic, M.V. Yurkov (DESY), A.S. Fisher (SLAC), J. Park (PAL), W.v.Zande (Radboud Univ. Nijmegen), B. Redlich (FELIX), W. Schoellkopf (FHI), G.P. Williams, M.Klopf (Jlab), M. Nasse (KIT), S. Huang (Peking Univ.), G.L.Carr (BNL), S. Winnerl, J. Teichert (HZDR), Y.U. Joeng (KAERI), R. Kuroda (AIST), W.B. Colson (NPS), Y. Kim (Idaho State University), M. Surman (ASTEC), P. Weightman (Univ. Liverpool), B.Qin (Huazhong Univ. of Sci. and Technol.), W.K.Lau (NSRRC) for helping to assemble this overview.

REFERENCES

[1] G.L. Carr et. al., “High power terahertz radiation from relativistic electrons”, Nature 420 (2001), 153.

[2] G.P. Williams, “Filling the THz gap – high power sources and applications”, Rep. Prog. Phys. 69 (2006), 301.

[3] T. Kampfrath, K.A. Nelson, K. Tanaka, “Resonant and nonresonant control over matter and light by intense terahertz transients”, Nature Photon. 7 (2013), 680.

[4] U. Frühling et. al., “THz-field-driven X-ray-streak camera”, Nature Photon. 3 (2009), 523.

[5] M. Foerst et. al., “THz control in correlated electron solids” in Terahertz Spectroscopy and Imaging, 1 Springer Series in Optical Sciences 171, Springer Verlag, Berlin Heidelberg 2012.

ISBN 978-3-95450-126-7

INTENSE EMISSION OF SMITH-PURCELL RADIATION AT THE FUNDAMENTAL FREQUENCY FROM A GRATING EQUIPPED WITH SIDEWALLS

J.T. Donohue, Centre d'Etudes Nucléaires de Bordeaux-Gradignan, Université Bordeaux 1, CNRS/IN2P3, BP 120, 33175 Gradignan, France
J. Gardelle, P. Modin, CEA, CESTA, F-33114 Le Barp, France

Abstract

The two-dimensional theory of the Smith-Purcell free-electron laser predicts that coherent Smith-Purcell radiation can occur only at harmonics of the frequency of the evanescent wave that is resonant with the beam. Particle-in-cell simulations have shown that in a three-dimensional context, where the lamellar grating has sidewalls, coherent Smith-Purcell radiation can be copiously emitted at the fundamental frequency, for a well-defined range of beam energy. An experiment at microwave frequencies has confirmed this prediction. The power output is considerably greater than for the previously observed emission at the second harmonic, in agreement with three-dimensional simulations. The dependence of frequency on beam energy and emission angle is also in good agreement with three-dimensional theory and simulations. Provided that a reduction in scale can be achieved, a path is open to coherent Smith-Purcell radiation at Terahertz frequencies.

INTRODUCTION

Radiation emitted by an electron passing over a diffraction grating was observed long ago by Smith and Purcell [1], and the idea of using this effect in a free-electron laser (FEL) has been proposed by numerous authors [2, 3, 4, 5, 6]. Renewed interest in the Smith-Purcell (SP) FEL followed the analysis of the dispersion relation for lamellar gratings by Andrews and Brau (AB) [7]. This relation links the axial wave number k to the frequency ω of the evanescent surface that propagates along the grating. They pointed out that the interaction between an initially continuous electron beam and this evanescent wave could lead to bunching at the frequency of the wave, giving rise to what they called coherent SP radiation. Such bunching would increase the intensity of the SP radiation, and by its periodicity, constrain the frequency of the radiation to be a multiple of the frequency of the evanescent wave. However, that frequency was necessarily inferior to the minimum allowed frequency, as determined by the well-known SP relation,

$$\lambda = \frac{c}{f} = \frac{L}{|n|}\left(\frac{1}{\beta} - \cos\theta\right), \qquad (1)$$

where λ denotes the wavelength of the radiation of frequency f produced at angle θ with respect to the beam direction, L is the period, c is the speed of light, β is the electron's relative axial velocity, and the integer n is the order of diffraction. However, if the bunching were strong enough, it might contain harmonics whose frequencies are SP allowed. Under these circumstances, monochromatic radiation at these frequencies would be observed at the angles corresponding to Eq. (1). The evanescent wave was expected to escape from the ends of the grating, according to AB. Using an approach based on finding singularities of the reflection matrix, Kumar and Kim [8] obtained results similar to those of AB. Simulations using the particle-in-cell code "MAGIC" [9] performed by two of us [10] and by Dazhi Li and collaborators [11] supported the AB scenario. A common aspect of all these works was that the analysis was two-dimensional (2-D), i.e., the electromagnetic fields did not depend on the coordinate parallel to the grating's grooves.

Although theory and simulations predicted emission of radiation at the second and perhaps higher harmonics of the evanescent wave, experimental confirmation was obtained only recently [12]. This was a demonstration experiment in the microwave domain, and used a wide (10 cm) flat and intense (180A) electron beam to produce bunching at 4.6 GHz, and radiation at 9.2 GHz. The ratio of radiated power to beam power was approximately 0.15%. A follow-up experiment used a very narrow slit to reduce the current and found that a start current of approximately 20 A/m was needed to achieve gain [13].

GRATINGS WITH SIDEWALLS

An experiment had previously used gratings equipped with conducting sidewalls at the ends of the grooves [14]. Two of the present authors presented a generalization of the AB 2-D dispersion relation to 3-D for a grating with sidewalls [15]. In this study, the sidewalls rise infinitely high above the grating. In practice, of course, they rise only a small distance above the top of the grating. However, if the evanescent height of the wave is less than the sidewall height, the approximation of an infinite wall is valid. A number of measurements with a signal analyzer of the grating used in our experiments confirmed the predictions of the theory, as did 3-D simulations performed with "MAGIC". Li and collaborators had also performed simulations for sidewall with gratings [16].

ISBN 978-3-95450-126-7

3-D THEORY OF A HIGH GAIN FREE-ELECTRON LASER BASED ON A TRANSVERSE GRADIENT UNDULATOR

Panagiotis Baxevanis, Yuantao Ding, Zhirong Huang and Ronald Ruth
SLAC National Accelerator Laboratory, Menlo Park, CA 94025, USA

Abstract

The performance of a free-electron laser (FEL) depends significantly on the various parameters of the driving electron beam. In particular, a large energy spread in the beam results in a substantial reduction of the FEL gain, an effect which is especially relevant when one considers FELs driven by plasma accelerators or storage rings. For such cases, one possible solution is to use a transverse gradient undulator (TGU). In this concept, the energy spread problem is mitigated by properly dispersing the electron beam and introducing a linear, transverse field dependence in the undulator. This paper presents a self-consistent theoretical analysis of a TGU-based high gain FEL, taking into account three-dimensional (3-D) effects and beam size variations along the undulator. The results of our theory compare favorably with simulation and are used in fast optimization studies of various X-ray FEL configurations.

INTRODUCTION

In recent years, the free-electron laser (FEL) has demonstrated its value as a tunable source of intense, coherent X-rays. In order to achieve the desired quality for the output radiation, a high-brightness electron beam is required to drive the machine. Electron beams from laser-plasma accelerators (LPAs) and ultimate storage rings (USRs) are characterized by low emittance and (in the case of the former) very high peak current, which would make them attractive for FEL applications. Unfortunately, they also have a relatively large energy spread, which poses a problem as far as their use in FELs is concerned. That is because a large spread in the energy of the electrons translates into a significant spread in the resonant wavelength, exceeding the FEL bandwidth. In this paper, we focus on one proposed solution, namely the transverse gradient undulator (TGU). The latter is an undulator with canted magnetic poles, so that its vertical field has a linear dependence upon the horizontal position x. Using a suitable dispersive element, one can also introduce a linear correlation of the electron energy with x. By properly selecting the parameters involved, one can ensure that electrons with higher than nominal energy are dispersed towards the higher-field region in such a way that the variation in the resonant frequency is minimized.

Originally conceived as a way to increase the energy acceptance of low gain (oscillator) FELs ([1]-[2]), the TGU has recently been considered in the context of its possible application in high gain devices. In particular, Ref. [3] developed a 1-D theoretical model and examined 3-D effects through simulation. Here, we present a theoretical description of a TGU-based FEL in the framework of the Vlasov-Maxwell formalism, including 3-D effects due to the transverse electron beam size and emittance. Starting from the single particle equations of motion, a self-consistent equation for the amplitude of the radiation is derived using the Vlasov-Maxwell equations. Whenever applicable, we show how a simple solution can be obtained in terms of the eigenmodes of the system.

THEORY

Single Particle Motion

In our analysis, we assume that the magnetic field of the TGU is given by

$$\begin{aligned} B_{ux} &= B_0 \frac{\alpha}{k_u} \sinh(k_u y) \sin(k_u z) \\ B_{uy} &= B_0 (1+\alpha x) \cosh(k_u y) \sin(k_u z) \\ B_{uz} &= B_0 (1+\alpha x) \sinh(k_u y) \cos(k_u z) \,, \end{aligned} \tag{1}$$

where $k_u = 2\pi/\lambda_u$ (λ_u is the undulator period), B_0 is the peak on-axis field and α is the transverse field gradient, which can be related to the cant angle of the undulator poles. This magnetic field satisfies Maxwell's equations and reduces to the field of a standard, flat-pole undulator for $\alpha \to 0$. As we have already mentioned, the object of the TGU is to mitigate the negative impact of a large energy spread in the electron beam by significantly reducing the resulting spread in the resonant wavelength. In order to achieve this, the beam is dispersed in the x-direction so that the horizontal position of an electron is linearly correlated to its energy γmc^2 according to $x = \eta\delta$, where $\delta = \gamma/\gamma_0 - 1$ is the energy deviation and $\gamma_0 mc^2$ is the average electron energy. On the other hand, the introduction of the constant field gradient α leads to a linear x-dependence of the undulator parameter K, i.e. $K = K_0(1+\alpha x)$, where $K_0 = eB_0/(mck_u)$ is its on-axis value (e is the electron charge). By selecting the dispersion function η as

$$\eta = \frac{2 + K_0^2}{\alpha K_0^2} \,, \tag{2}$$

the resonant condition $\lambda_r = \lambda_u(1 + K^2/2)/(2\gamma^2)$ is now satisfied by all the electrons in the beam (up to linear order in x).

For a detailed derivation of the single particle equations of motion, we refer to [4]. Here, we merely quote the main results. As far as the transverse dynamics is concerned, the TGU is characterized by a horizontal focusing strength

ISBN 978-3-95450-126-7

FREE ELECTRON LASERS IN 2013

J. Blau#, K. Cohn, W. B. Colson and R. Vigil
Physics Department, Naval Postgraduate School, Monterey CA 93943 USA

Abstract

Thirty-seven years after the first operation of the free electron laser (FEL) at Stanford University, there continue to be many important experiments, proposed experiments, and user facilities around the world. Properties of FELs operating in the infrared, visible, UV, and X-ray wavelength regimes are tabulated and discussed.

List of FELs in 2013

The following tables list existing (Table 1) and proposed (Tables 2, 3) relativistic free electron lasers (FELs) in 2013. The 1st column lists a location or institution, and the FEL's name in parentheses. References are listed in Tables 4 and 5; another useful reference is http://sbfel3.ucsb.edu/www/vl_fel.html.

The 2nd column of each table lists the operating wavelength λ, or wavelength range. The longer wavelength FELs are listed at the top and the shorter wavelength FELs at the bottom of each table. The large range of operating wavelengths, seven orders of magnitude, indicates the flexible design characteristics of the FEL mechanism.

In the 3rd column, t_b is the electron bunch duration (FWHM) at the beginning of the undulator, and ranges from almost CW to short sub-picosecond time scales. The expected optical pulse length in an FEL oscillator can be several times shorter or longer than the electron bunch depending on the optical cavity Q, the FEL desynchronism and gain. The optical pulse can be many times shorter in a high-gain FEL amplifier. Also, if the FEL is in an electron storage-ring, the optical pulse is typically much shorter than the electron bunch. Most FEL oscillators produce an optical spectrum that is Fourier transform limited by the optical pulse length.

The electron beam kinetic energy E and peak current I are listed in the 4th and 5th columns, respectively. The next three columns list the number of undulator periods N, the undulator wavelength λ_0, and the rms undulator parameter $K=eB\lambda_0/2\pi mc^2$ (cgs units), where e is the electron charge magnitude, B is the rms undulator field strength, m is the electron mass, and c is the speed of light. For an FEL klystron undulator, there are multiple undulator sections as listed in the N-column; for example 2x7. Some undulators used for harmonic generation have multiple sections with varying N, λ_0, and K values as shown. Some FELs operate at a range of wavelengths by varying the undulator gap as indicated in the table by a range of values for K. The FEL resonance condition, $\lambda = \lambda_0(1+K^2)/2\gamma^2$, relates the fundamental wavelength λ to K, λ_0, and the electron beam energy $E=(\gamma-1)mc^2$, where γ is the relativistic Lorentz factor. Some FELs achieve shorter wavelengths by using coherent harmonic generation (CHG), high-gain harmonic generation (HGHG), or echo-enabled harmonic generation (EEHG).

The last column lists the accelerator types and FEL types, using the abbreviations listed after Table 3.

The FEL optical power is determined by the fraction of the electron beam energy extracted and the pulse repetition frequency. For a conventional FEL oscillator in steady state, the extraction can be estimated as 1/(2N); for a high-gain FEL amplifier, the extraction at saturation can be substantially greater. In a storage ring FEL, the extraction at saturation is substantially less than this estimate and depends on ring properties.

In an FEL oscillator, the optical mode that best couples to the electron beam in an undulator of length $L=N\lambda_0$ has a Rayleigh length $z_0 \approx L/12^{1/2}$ and has a fundamental mode waist radius $w_0 \approx (z_0\lambda/\pi)^{1/2}$. An FEL typically has more than 90% of its power in the fundamental mode.

At the 2013 FEL Conference, there were three new lasings reported worldwide: an HGHG VUV/soft X-ray FEL at FERMI in Trieste (FERMI-2), an EEHG UV FEL at SINAP in Shanghai (SDUV-FEL), and a super-radiant THz FEL at ELBE in Dresden (TELBE). Progress continues on many other existing and proposed FELs, including several large X-ray FEL facilities around the world.

ACKNOWLEDGMENTS

The authors are grateful for support from ONR and the HEL-JTO.

#blau@nps.edu

ISBN 978-3-95450-126-7

RESULTS AND PERSPECTIVES ON THE FEL SEEDING ACTIVITIES AT FLASH*

Jörn Bödewadt† and Christoph Lechner, University of Hamburg, Hamburg, Germany
for the FLASH seeding team

ABSTRACT

In recent years, several methods of free-electron laser (FEL) seeding, such as high-gain harmonic generation (HGHG), self-seeding, or direct FEL amplification of external seed pulses, have proved to generate intense, highly coherent radiation pulses in the extreme ultraviolet (XUV), soft- (SXR) and hard (HXR) X-ray spectral range. At DESY in Hamburg, the FEL facility FLASH [1] is currently being upgraded by a second undulator beamline (FLASH2, [2]) which allows for the implementation of various seeding schemes. The development of high repetition-rate, high-power laser systems allows for the production of seed sources which match the bunch-train pattern of FLASH. Furthermore, the FLASH1 beamline arrangement is well suited for testing various seeding schemes including HGHG, EEHG, HHG-seeding, and hybrid schemes. In this contribution, we give an overview of latest results and planned FEL seeding activities at FLASH.

INTRODUCTION

The initiation of the FEL process by means of external laser seeding allows to generate fully coherent FEL radiation that is intrinsically synchronized for pump-probe experiments. In recent years, several methods for external laser seeding have been studied, such as high-gain harmonic generation (HGHG), direct FEL amplification, or echo-enables harmonic generation (EEHG) as well as hybrid or cascaded schemes. Among them, the HGHG FEL seeded at the third harmonic of a Ti:sapphire laser has proved to work reliably down to the extreme ultraviolet (EUV) spectral range as shown by the successful operation of the seeded FEL facility FERMI@Elettra [3]. Direct amplification of higher-harmonics from Ti:sapphire laser pulses up to the 21st harmonic has been demonstrated at FLASH in combination with high peak-current electron bunches [4].

The FEL user facility FLASH at DESY has been upgraded recently by a second undulator beamline [5]. This new beamline is going to be commissioned in 2014 for SASE operation. In addition to that, an injection beamline for seed radiation as well as a modulator and a chicane are planned for installation end of 2014. The seed radiation is generated from a high-repetition rate optical parametric chirped pulse amplifier (OPCPA) system currently under development at DESY [6]. It will allow to seed the FEL in the multi-bunch burst mode. Beside the planned seeded FEL user facility at FLASH2, a program for further R&D of seeded FELs is planned at FLASH1 conducted by a collaboration of DESY, Hamburg University, and TU Dortmund University. These activities will first of all provide operational experience for a UV seeded HGHG setup and its performance under variation of different machine parameters. Furthermore, the experimental layout at the FLASH1 beamline offers promising possilities to study EEHG with harmonics down to the EUV.

EXPERIMENTAL LAYOUT

Figure 1 shows the schematic layout of the FLASH facility. A fast kicker-system after the superconducting linac distributes electron bunches into both undulator beamlines, which are shown in more detail in Fig. 2(a) and Fig.2(b).

FLASH1

The FLASH1 beamline is equipped with four different types of undulator systems. The first section contains two 1-m long electromagnetic undulators (ORS1 and ORS2) with an undulator period of 20 cm originally installed for electron diagnostics purposes [7]. Each of these undulators is followed by a magnetic chicane (C1 and C2). ORS1 has a vertical deflection plane, while ORS2 deflects horizontally. The maximum K-value (peak) is 10.8 for both devices. The second undulator system contains a variable-gap undulator with a period of 31.4 mm, an effective length of 10 m, and a maximum K-value of 2.7. It was installed 2009 for direct seeding experiments and covers a wide wavelength range in the EUV. A subsequent magnetic chicane allows to insert a set of mirrors extracting the FEL radiation to dedicated diagnostics. The electron beam further travels through a 10 m long diagnostic and matching section into the fixed-gap undulator system. This 27 m long undulator has a fixed K-value of 1.23 and a period of 27.3 mm. The last undulator is a 4 m long electromagnetic insertion device to generate radiation in the THz spectral range for pump-probe applications.

FLASH2

The new FLASH2 beamline will be equipped with 2.5 m long insertion devices with a period of 31.4 mm and a maximum K-value of 2.7. Behind the radiation shielding wall, twelve of these undulators modules will be installed as indicated in Fig. 2(b). This total active undulator length of

* Supported by the Federal Ministry of Education and Research of Germany under contract No. 05 K13 GU4 and 05 K13 PE3, and the German Research Foundation programme graduate school 1355

† joern.boedewadt@desy.de

ISBN 978-3-95450-126-7

THE CONCEPTUAL DESIGN OF CLARA, A NOVEL FEL TEST FACILITY FOR ULTRA-SHORT PULSE GENERATION

J. A. Clarke[1], D. Angal-Kalinin[1], N. Bliss, R. Buckley[1], S. Buckley[1], R. Cash, P. Corlett[1], L. Cowie[1], G. Cox, G.P. Diakun[1], D.J. Dunning[1], B.D. Fell, A. Gallagher, P. Goudket[1], A.R. Goulden[1], D.M.P. Holland[1], S.P. Jamison[1], J.K. Jones[1], A.S. Kalinin[1], B.P.M. Liggins[1], L. Ma[1], K.B. Marinov[1], B. Martlew, P.A. McIntosh[1], J.W. McKenzie[1], K.J. Middleman[1], B.L. Militsyn[1], A.J. Moss[1], B.D. Muratori[1], M.D. Roper[1], R. Santer[1], Y. Saveliev[1], E. Snedden[1], R.J. Smith[1], S.L. Smith[1], M. Surman[1], T. Thakker[1], N.R. Thompson[1], R. Valizadeh[1], A.E. Wheelhouse[1], P.H. Williams[1], STFC Daresbury Laboratory, Sci-Tech Daresbury, Warrington, UK
R. Bartolini[2], I. Martin, Diamond Light Source, Oxfordshire, UK
R. Barlow, A. Kolano, University of Huddersfield, UK
G. Burt[1], University of Lancaster, UK
S. Chattopadhyay[1], D. Newton, A. Wolski, University of Liverpool, UK
R.B. Appleby[1], H.L. Owen[1], M. Serluca[1], G. Xia[1], University of Manchester, UK
S. Boogert, A. Lyapin, John Adams Institute at Royal Holloway, University of London, UK
L. Campbell, B.W.J. McNeil, University of Strathclyde, UK
V.V. Paramonov, Institute for Nuclear Research of the RAS, 117312 Moscow, Russian Federation
[1] and Cockcroft Institute, Sci-Tech Daresbury, Warrington, UK
[2] and John Adams Institute, University of Oxford, UK.

Abstract

CLARA will be a novel FEL test facility focussed on the generation of ultra-short photon pulses with extreme levels of stability and synchronisation. The principal aim is to experimentally demonstrate that sub-cooperation length pulse generation with FELs is viable, and to compare the various schemes being championed. The results will translate directly to existing and future X-ray FELs, enabling them to generate attosecond pulses, thereby extending their science capabilities. This paper gives an overview of the motivation for CLARA, describes the facility design (reported in detail in the recently published Conceptual Design Report [1]) and proposed operating modes and summarises the proposed areas of FEL research.

INTRODUCTION

Free-electron lasers (FELs) have made huge advances in the past few years with the first successful demonstration of an X-ray FEL at LCLS in the USA in 2009 [2], followed by similar success at SACLA in Japan in 2011 [3]. Whilst the new X-ray FELs are remarkable in their performance the potential for improvements is still great. There are many proposals for improving the FEL photon output in terms of temporal coherence, wavelength stability, increased power, intensity stability and ultra-short pulse generation. However given the low number of operating FELs and the need to dedicate the majority of beam-time for user exploitation many of these ideas remain untested experimentally. This paper describes the design of CLARA (Compact Linear Accelerator for Research and Applications), a dedicated flexible FEL Test Facility, which will be able to assess several of the most promising new schemes. The successful proof of principle demonstration with CLARA will be a vital stepping stone to the implementation of any new scheme on an existing or planned FEL facility. CLARA is effectively a major upgrade to the existing VELA RF photoinjector facility at Daresbury Laboratory [4], targeted at industrial applications and technology developments.

Our vision for CLARA is that it should be dedicated to the production of ultra-short photon pulses of coherent light. Existing FELs are already capable of generating pulses of light that are only tens of femtoseconds in duration, but proposals have been made for generating pulses that are two or three orders of magnitude shorter than this (hundreds or tens of attoseconds) and a recent paper has proposed sub-attosecond pulse generation [5]. Many exciting applications of attosecond pulses have already been demonstrated [6, 7, 8], including coherent X-ray imaging, femtosecond holography, real-time observations of molecular motion and capturing the movement of electrons in atoms and molecules. Attosecond X-ray science could revolutionise how we understand and control electron dynamics in matter.

In order to achieve this vision for ultra-short pulse generation, CLARA must be able to implement advanced techniques, such as laser seeding, laser-electron bunch manipulation, and femtosecond synchronisation. These can only be achieved by developing a state-of-the-art accelerator with the capability to drive current FEL designs. CLARA is therefore of direct relevance to the wider international FEL community and will also ensure that the UK has all the skills required should it choose to develop its own future FEL facility.

ISBN 978-3-95450-126-7

PROGRESS OF THE LUNEX5 PROJECT

M.-E. Couprie#, C. Benabderrahmane, L. Cassinari, J. Daillant, C. Herbeaux, N. Hubert, M. Labat, A. Loulergue, P. Marchand, O. Marcouillé, C. Miron, P. Morin, A. Nadji, P. Roy, T. Tanikawa,
Synchrotron SOLEIL, L' Orme des Merisiers, Saint-Aubin, BP 48, 91 192 Gif-sur-Yvette, France
S. Bielawski, E. Roussel, C. Szwaj, C. Evain, M. Le Parquier,
PhLAM/CERCLA, Univ. Lille, Lille, France
N. Delerue, LAL, Orsay, France
G. Le Bec, L. Farvacque, ESR, Grenoble, France
B. Carré, D. Garzella, CEA/DSM/DRECAM/SPAM, Saclay, France
G. Devanz, M. Luong (CEA/IRFUL SACM, Saclay, France
A. Dubois, J. Lüning, LCPMR, Paris, France
G. Lambert, R. Lehe, V.Malka, C. Thaury, A. Rousse,
LOA, Polytechnique, ENSTA, Palaiseau, France

Abstract

LUNEX5 (free electron Laser Using a New accelerator for the Exploitation of X-ray radiation of 5th generation) aims at investigating the production of short, intense, and coherent pulses in the soft X-ray region. A 400 MeV superconducting linear accelerator and a laser wakefield accelerator (LWFA), will feed a single Free Electron Laser line with High order Harmonic in Gas and Echo Enable Harmonic Generation seeding. After the Conceptual Design Report (CDR), R&D has been launched on specific magnetic elements (cryo-ready 3 m long in-vacuum undulator, a variable strong permanent magnet quadrupoles), on diagnostics (Smith-Purcell, electro-optics). In recent transport studies of a LWFA based on more realistic beam parameters (1 % energy spread, 1 μm beam size and 1 mrad divergence) than the ones assumed in the CDR, a longitudinal and transverse manipulation enables to provide theoretical amplification. A test experiment is under preparation. It is noted in this context that among the French scientific community's interest in experiments at operating FELs is increasing.

INTRODUCTION

Fifty years after the laser discovery, the emergence of several mJ femtosecond X-ray lasers for users in the Angström range at LCLS (USA) in 2009 [1] and in SACLA (Japan) [2] and in the VUV/soft X-ray at FLASH(Germany) [3], SCSS Test Accelerator (Japan) [4] and FERMI (Italy) [5] constitutes a major breakthrough and open unexplored multidisciplinary investigations of matter. Because of the small mirror reflectivity at short wavelength limiting FEL oscillators to the VUV [6], short wavelength FELs are usually operated in the so-called SASE scheme. Though efficient in terms of power, emitted radiation is constituted of random spikes, giving a poor temporal coherence. After the first Coherent Harmonic generation experiments in the VUV [7, 8, 9], since more than one decade ago, seeding with conventional laser has demonstrated the suppression of the spikes, the reduction in gain length and an increase in coherence [10]. FERMI@ELETTRA is the first seeded FEL open for users in the soft X-ray region. It also efficiently up-frequency converts the wavelength along different stages. Short wavelength seeding with High order Harmonics generated in Gas (HHG), demonstrated on the Japanese SCSS FEL [11], on SPARC (Italy) [12], and on FLASH (Germany) [13] enables to decrease the FEL wavelength. The recently proposed self-seeding in particular with a crystal monochromator efficiently cleans the SASE spectrum [14, 15, 16]. The Echo-Enabled Harmonic Generation (EEHG) [17] enabling to generate short wavelengths has been experimentally evidenced so far in the UV [18, 19], opening perspectives for very short wavelength (Å) and short duration at moderate cost.

Present FEL user facilities usually provide only a restricted number of beamlines, making the acceptance of user proposals quite difficult. Superconducting technology enables to produce long electron macro-pulses which can be split into different FEL branches, approaching thus a multi-user facility such as synchrotron radiation light sources. In addition, a superconducting linac enables the operation of the FEL at high repetition rate, beneficial for coincidence experiments for example. The European XFEL, when coming to operation, will provide a major step in this direction [20].

In parallel, novel acceleration schemes such as dielectric ones [21], inverse FELs [22] and Laser Wakefield acceleration [23] are actively developed. Laser Wakefield Acceleration (LWFA) by using intense laser beams interacting with cm long plasmas can now provide high quality electron beams of very short bunches (few fs) with high peak currents (few kA) [24]. Indeed, spontaneous emission from LWFA has already been observed [25], but the presently still rather large energy spread (~1 %) and divergence (mrad) prevent from a straightforward FEL amplification.

#marie-emmanuelle.couprie@synchrotron-soleil.fr

ISBN 978-3-95450-126-7

THE TEST-FEL AT MAX-lab: IMPLEMENTATION OF THE HHG SOURCE AND FIRST RESULTS

F. Curbis*, N. Čutić, F. Lindau, E. Mansten, S. Werin, MAX-lab, Lund University, Sweden
F. Brizuela, B. Kim, A. L'Huillier, Division of Atomic Physics, Lund University, Sweden
M. Gisselbrecht, Division of Synchrotron Radiation Research, Lund University, Sweden

Abstract

The test-FEL at MAX-lab is a development set-up for seeding techniques. After the successful demonstration of coherent harmonic generation from a conventional laser, the new layout now presents a gas target for generation of harmonics. The drive laser will be up-converted and the low harmonics (around 100 nm) will seed the electron beam. The energy modulated electrons will then be bunched in the dispersive section and will radiate in the second undulator. We will detect the second harmonic of the HHG radiation around 50 nm. This experiment has several challenges never tried before: co-propagation of the electron beam and the drive laser, interaction of the electron beam with the gas in the target, no-focusing of the harmonics and no drive laser removal. The commissioning will show if this kind of in-line chamber has advantages with respect to more traditional approaches with optical beam transport. The results are relevant for many facilities that are planning to implement HHG seeding in the near future.

MOTIVATIONS

Seeding a Free-Electron Laser (FEL) with a High Harmonics Generation (HHG) source was firstly demonstrated few years ago [1]. Since then, only a few facilities [2, 3] have tried to implement this technique in a rather conventional way. One of the main challenges lies on the transport and focusing of the harmonics from the emission point to the undulator, where the interacting with electrons happens. The geometry of the accelerators and the radiation safety infrastructures often limit the optimization of the path. Ideally one would like to minimize the number of optical components (mirrors and lenses) from the drive laser (usually an infrared Ti:Sa system) to the gas cell and also limit the optics after the gas cell that are needed for the transverse overlap with the electron beam.

Our idea is to place the HHG source directly in front of the first undulator (modulator), in-line with the electron beam. In this way one can eliminate all optics after the emission of harmonics. The idea behind this is that the harmonics inherit their divergence from the drive laser, so if the production point is very close to the beginning of the undulator, they basically don't need refocusing. An extension of this setup would be possible for any wavelength, because the transport is not limited by the bandwidth of the optics. In this way the tunablity of the FEL source will be limited only by the separation between the (high) harmonics.

The last (but not least) motivation for this experiment is the possbility to achieve modulation of the electron beam at a certain wavelength and generation of higher harmonics in the second undulator (radiator). The combination of HHG source with modulator/dispersive section/radiator has never been tested before (although separately they have been already demonstrated). Due to limitations in the diagnostics we will be able to detect only the second harmonic (at about 50 nm) of the selected HHG line, but this will be sufficient to demonstrate the principle.

EXPERIMENTAL SETUP

The HHG Source

The HHG source is based on a Ti:Sapphire laser system able to provide 8 mJ in 45 fs pulse duration. The repetition rate is up to 1 kHz, but for the seeding the electron beam maximum 2 Hz will be used. The drive laser is locked to the 3 GHz accelerator RF. The HHG chamber has been designed as a duplicate of a working device at the Atomic Physics department in Lund. The main feature is that the drive laser and the electron beam are both passing through a small hole (1-2 mm) which is the gas cell. In Fig. 1 the geometry of the gas target is shown. The additional advantage of our setup is the possibility to change the frequency of the drive laser, using either the infrared beam or converting it with a crystal to 400 nm.

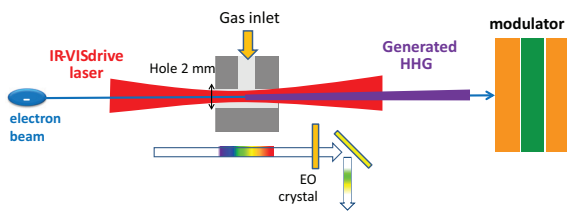

Figure 1: Layout of the HHG source with the path of the electron beam and the drive laser.

Since the testFEL section is connected to the MAX-lab injector, a differential pumping system has been added upstream of the HHG chamber. It consists of a small tube 15 cm long with an inner diameter of 5 mm. Two turbo pumps are equipping the HHG chamber and the nearby

* francesca.curbis@maxlab.lu.se

ISBN 978-3-95450-126-7

SIMULATION STUDIES FOR AN X-RAY FEL BASED ON AN EXTENSION OF THE MAX IV LINAC

F. Curbis*, N. Čutić, O. Karlberg, F. Lindau, A. Mak, E. Mansten, S. Thorin, S. Werin,
MAX-lab, Lund University, Sweden

Abstract

It is well known that the few X-ray FELs around the world are severely overbooked by users. Having a medium energy linac, such as the one now being installed at the MAX IV laboratory, it becomes natural to think about slightly increasing the electron energy to drive an X-ray FEL. This development is now included in the long term strategic plan for the MAX IV laboratory. We will present the current FEL studies based on an extension of the MAX IV linac to 5 GeV to reach the Ångstrom region. The injector for the MAX IV accelerator complex is also equipped with a photocathode gun, capable of producing low emittance electron beam. The bunch compression and linearization of the beam is taken care by two double achromats. The basic FEL layout would consist of short period undulators with tapering for extracting all the power from the electron beam. Self-seeding is considered as an option for increasing the spectral and intensity stability.

BACKGROUND

The MAX IV facility [1], successor of the MAX-lab accelerators at Lund University, Sweden, was already in the initial plans around year 2000 drawn with the idea that the facility could be extended with a FEL in a later stage. Since then the X-ray FELs LCLS [2] and SACLA [3] have been put into operation as well as the UV machines FLASH [4] and Fermi [5]. The European XFEL [6], the SwissFEL [7] and the PAL-XFEL [8] are currently being constructed, indicating the development of the photon science scene worldwide. The MAX IV facility is right now being constructed with the installation of the linac structures (up to 3 GeV), waveguides and magnetic systems almost completed (August 2013) [9]. Swedish users are heavily involved in experiments and the development of experiments in the LCLS and the Euro XFEL projects, as well as the UV FELs FLASH and FERMI [10]. In December 2011 a group of Swedish scientists started the discussions to join forces with the aim of producing a scientific case for X-ray lasers in Sweden [11]. Different concepts have been presented to the MAX IV Laboratory scientific advisory committee which later recommended that an X-ray FEL based on an extended linac (up to 5-6 GeV) should be investigated. The MAX IV laboratory strategy includes a plan for an extension of the facility with an X-ray FEL starting by a conceptual design in near future, followed by a technical design and a tentative operation in 2021. No funding is at the moment available. Figure 1 gives an impression about the different activities connected to the MAX IV FEL.

As a baseline case for the conceptual design a 5 GeV linac and an FEL at 3 Å has been chosen both in Self Amplified Spontaneous Emission (SASE) and seeded mode. Initially the study includes self-seeding by a crystal monochromator and tapering, to increase the extracted power. The goal is a transform limited pulse < 100 fs, > 10 GW peak power, 100 Hz rep rate, 3 Å. The concept will later be complemented by studies including: short pulse operation (< 10 fs), peak power optimization (multi 100 GW), tuning range (1-7 Å), self seeding at > 4 Å, a soft X-ray system based on lower electron energy and beam spreader for several end stations. The MAX IV linac consists of a warm S-band system able to provide > 3 GeV, two bunch compressors [12] able to compress to < 100 fs, two injectors (one thermionic RF gun and one low emittance photo cathode gun). It will provide pulses both for injection into the two storage rings and drive a SPF (Short Pulse Facility) providing spontaneous undulator radiation in 100 fs pulses [13].

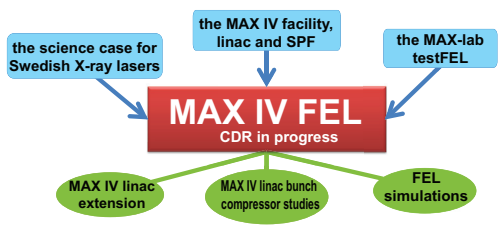

Figure 1: Cartoon showing the current work around the MAX IV FEL.

LAYOUT OF THE X-RAY FEL

The general layout of the MAX IV FEL is shown in Fig. 2. The energy of MAX IV linac will be extended from 3 GeV to about 5 GeV using the same kind of accelerating structures as the main linac [9]. The design of the second bunch compressor allows to use it also as beam spreader. After the accelerating structures, a matching section will allows to prepare the electron beam before entering the undulator chain.

The Injector

The injector consists of an RF gun and an S-band linac structure accelerating up to 100 MeV. The MAX IV FEL will take advantage of the photocathode gun which is foreseen for the SPF. This gun is design to deliver beam with

* francesca.curbis@maxlab.lu.se

ISBN 978-3-95450-126-7

TWO-COLOR SELF-SEEDING AND SCANNING THE ENERGY OF SEEDED BEAMS AT LCLS*

F.-J. Decker, Y. Ding, Y. Feng, M. Gibbs, J. Hastings, Z. Huang, H. Lemke, A. Lutman, A. Marinelli, A. Robert, J.L. Turner, J. Welch, D. Zhang, D. Zhu, SLAC, Menlo Park, CA 94025, USA

Abstract

The Linac Coherent Light Source (LCLS) produces typically SASE FEL pulses with intensities of up to 5 mJ and at high photon energy an FEL bandwidth 0.2% (FWHM) [1]. Self seeding with a diamond crystal reduces the bandwidth by a factor of 10 to 40. The range depends on which Bragg reflection is used, or the special setup of the electron beam like over-compression. The peak intensity level is lower by a factor of only five, giving the seeded beam an advantage of about 2.5 in average intensity over the use of a monochromator with SASE. Some experiments want to scan the photon energy, which requires that the crystal angle be carefully tracked. At certain energies and crystal angles different Bragg lines cross which allows seeding at two or even three different colors inside the bandwidth of the SASE pulse. Out-of plane lines come in pairs, like [1 -1 1] and [-1 1 1], which can be split by adjusting the yaw angle of the crystal, allowing two-color seeding for all energies above 4.83 keV.

INTRODUCTION

Hard x-ray self-seeding with a crystal was introduced just three years ago at the FEL 2010, Malmö, Sweden [2]. A year and a half later the LCLS was upgraded with a chicane to bend the electron beam around a diamond crystal, which provides the necessary seed using Bragg reflections [3]. Understanding the exact setup of the crystal with its many possible Bragg reflections and using them in unforeseen ways will be discussed.

SEEDING CRYSTAL BRAGG LINES

The crystal stage was designed having mainly the Bragg reflection at the [0 0 4] plane in mind, so the main crystal angle (pitch) can be moved from 45° to 90° plus a few degrees on each side which allows for misalignments (Fig. 1).

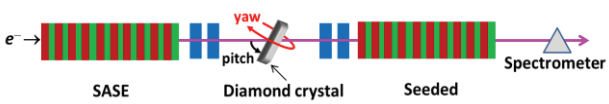

Figure 1: Side view of the HRXSS chicane setup. Undulator 16 (out of 33) was removed to make space for a small chicane (magnets in blue), which bend the electron beam about 2 mm into the paper plane, while the SASE photons go straight through the diamond crystal. The yaw angle axis is vertical when the pitch angle sits at 90° and can move about ± 2.5°.

*Work supported by U.S. Department of Energy, Contract DE-AC02-76SF00515.

Soon it was recognized that there are more lines like the [2 2 0] Laue line [4] where the "reflection" actually goes through the diamond crystal. Figure 2 shows a few more in-plane lines which were used. At the crossing of the two lines at 54.74° and 8.51 keV it is possible to get seeding on two (or more) lines, which was quickly verified (Fig. 3). A long range angle scan from 45° to 75° at 7.2 keV showed that there are more lines to be explained (blue dots in Fig. 2).

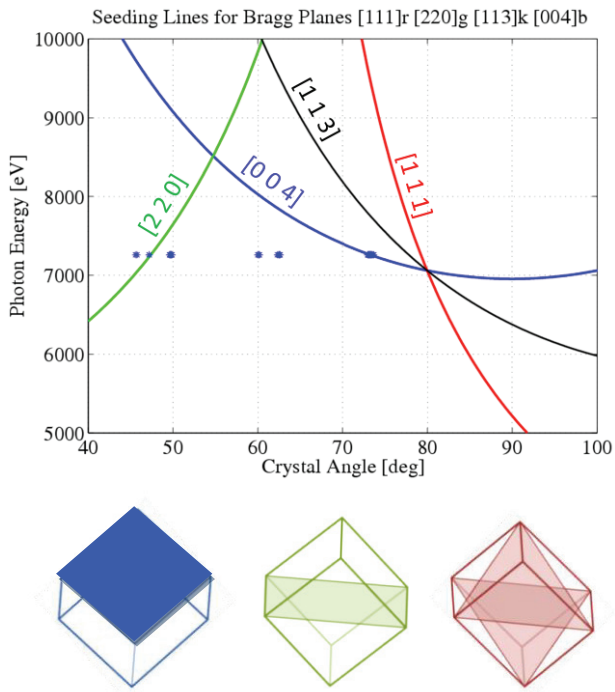

Figure 2: Seeding lines for Bragg reflections with photon energy versus crystal angle for a few basic planes. In blue the [0 0 4] plane corresponds to the surface plane of a cube; its line minimum energy is at 90° (pitch) to the FEL beam. The crystal cube sits then on one of its edges. The [2 2 0] plane cuts diagonally through four corners and its seeding line has a minimum at 0° pitch angle, since its plane would be then 90° to the beam. The [1 1 1] plane cuts through three corners and its perpendicular axis goes through the top, front corner (at 90° pitch). To reach its minimum the pitch angle needs to go further to about 145°. It should be mentioned at this point that with the pitch angle at 90° there are three more corners which have the same angle to the FEL beam and there should be four red lines crossing at the 90° point, the other in-plane line of [-1 -1 1] and the two lines from the out-of-plane planes [-1 1 1] and [1 -1 1]. The perpendicular axes of these out-of-plane planes lie on a cone instead of a plane.

ISBN 978-3-95450-126-7

INCREASED STABILITY REQUIREMENTS FOR SEEDED BEAMS AT LCLS*

F.-J. Decker, W. Colocho, Z. Huang, R. Iverson, A. Krasnykh, A. Lutman, M. Nguyen, T. Raubenheimer, M. Ross, J.L. Turner, L. Wang, SLAC, Menlo Park, CA 94025, USA

Abstract

Running the Linac Coherent Light Source (LCLS) with self-seeded photon beams requires better electron beam stability, especially in energy, to reduce the otherwise huge intensity variations of around 100%. Code was written to identify and quantify the different jitter sources. Some improvements are being addressed, especially the stability of the modulator high voltage of a few critical RF stations. Special setups like running the beam off crest in the last part of the linac can also be used to reduce the energy jitter. Even a slight dependence on the transverse position was observed. The intensity jitter distribution of a seeded beam is still more contained with peaks up too twice the average intensity, compared to the jitter distribution of a SASE beam going through a monochromator, which can have damaging spikes up to 5 times the average intensity.

INTRODUCTION

There have been many efforts over the years from tolerance studies, identifying jitter source to improving stability of LCLS beam [1-7]. The overlap of the SASE photon energy with the narrow crystal line of the seeded beam energy requires that the energy jitter is smaller than the bandwidth of SASE beam or even smaller than some features of its distribution.

INTENSITY VARIATIONS

The main problem of seeded FEL beam stability is its intensity variation dependence on the electron energy. Figure 1 shows the intensity variation of a seeded beam going through a monochromator versus the electron energy measured in DogLeg 2 (DL2). There are two ways to improve the intensity stability, a) by reducing the energy jitter and b) by increasing the acceptance of the undulator or the width of the distribution in Fig. 1.

Effects of Reducing the Energy Jitter

Even without any energy jitter (center part of Fig. 1) there is some intensity fluctuation of about 20 % due to the random FEL process which cannot be much reduced. Ignoring this variation, assuming a perfect Gaussian distribution with a sigma of 0.042%, we can estimate the effect of the jitter on the average intensity and its RMS (Fig. 2). With the jitter equal to the width of the distribution (0.042%) the average intensity is 70% of the maximum and the variation 40%. Reducing the energy jitter to 0.02%, the average intensity would raise by 30% to the 90% of max level, while the intensity variation would be reduced by a factor of four to 10%, which is already smaller than the 20% from the FEL fluctuations, which you would get with not energy jitter. Therefore the goal is to achieve an electron beam energy jitter of 0.02% from the typical 0.04 to 0.06% at high energy. At low energy jitter numbers are typically between 0.1 to 0.15 %.

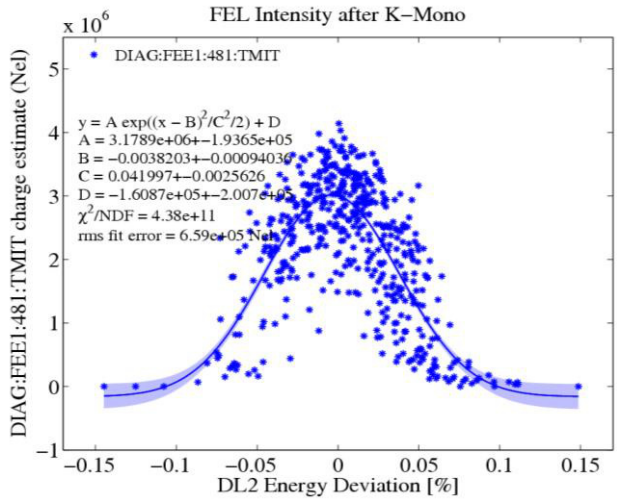

Figure 1: FEL intensity of a seeded beam after the K-monochromator versus DL2 energy. The sigma of the fitted Gaussian is 0.042% and corresponds to the acceptance of the undulator. It is about $\rho/2$ of the undulator and depends also on the beam energy spread.

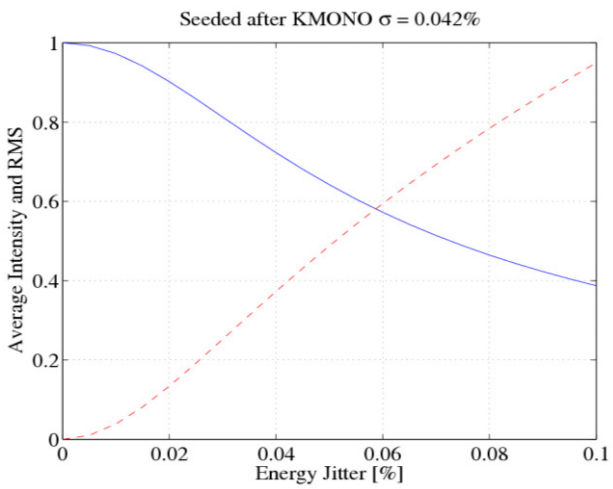

Figure 2: Assuming no SASE FEL fluctuations, the average seeded intensity (solid) is reduced due to jitter and its RMS (dashed) is increased: 0.042% energy jitter gives 70% of the peak and a variation 40%, while 0.020% energy jitter would give 90% of the max intensity with 10% rms variation.

*Work supported by U.S. Department of Energy, Contract DE-AC02-76SF00515.

ISBN 978-3-95450-126-7

COHERENT X-RAY SEEDING SOURCE FOR DRIVING FELS*

A. Novokhatski#, F.-J. Decker, B. Hettel, Z. Huang, H.-D. Nuhn, M. Sullivan
SLAC National Accelerator Laboratory, Menlo Park, CA, USA

Abstract

The success of the hard X-ray self-seeding experiment (HXRSS) at the LCLS is very important in that it provided narrow, nearly transform-limited bandwidth from the FEL, fulfilling a beam quality requirement for experimental applications requiring highly monochromatic X-rays. Yet, because the HXRSS signal is generated from random spikes of noise, it is not a truly continuous monochromatic seed signal and even higher FEL performance would be achieved using a continuous seed source. We propose developing such a source using a low-Q X-ray cavity to achieve a continuous, narrowband X-ray seed signal. The low-Q cavity works like a return path for the fields, produced in the undulator situated within an X-ray cavity. We do not assume that X-ray fields can be coherently stored in the cavity because of the high tolerances on the cavity length. But we assume that the undulator works as a very high gain amplifier, which compensates amplitude loss due to X-ray reflections in the cavity. The cavity may consist of several elements, which can reflect X-rays by several degrees to make a total of 360 degrees. For example, the elements could be four crystals with a corresponding Bragg angle of about 45 degrees each with additional small angle correcting elements. In this case, the amplitude loss is due to the small bandwidth of the reflected fields. The frequency spectrum of the final X-ray signal will be determined by the bandwidth of the reflected elements. This is not a very new idea. A regenerative-amplifier FEL (RAFEL) has been even demonstrated in the infrared wavelength region [1] and discussed in the angstrom wavelength region [2, 3]. In this study we analyze the interaction of X-rays and electron beams with this cavity. The electron beam source in this proposal uses a train of electron bunches initially accelerated in a linear accelerator which then pass through a radiator element situated within an X-ray cavity.

A CONCEPT

The basic schematic is shown in Fig. 1. We suggest using several LCLS undulators [4] as the radiator element inside the X-ray cavity. We may use the same type of crystals that are currently in use in the XCS experiment (The X-ray Split Pulse Experiment) at the LCLS. Two chicanes provide a path for the electron beam around the X-ray cavity crystal mirrors. The electron beam goes through the first chicane avoiding the X-ray cavity mirrors, then passes through the cavity undulator making the X-ray beam for the cavity and then goes through the second chicane again avoiding the X-ray cavity mirrors. Then the beam enters the main part of the LCLS undulators (output undulators). SASE radiation from the leading electron bunch in a bunch train is spectrally filtered by the Bragg reflectors and is brought back to the beginning of the cavity undulator to interact with the second beam bunch. The X-ray pulse that circulates in the cavity repeatedly interacts with consecutive electron bunches in the train, forming a regenerative amplifier FEL. This process yields a growing laser field in the x-ray cavity if the amplification of the field in the cavity undulator is more than the reflection losses. The FEL interaction with these short bunches regeneratively amplifies the radiation intensity because the crystal reflectors filter the radiation, making the frequency bandwidth smaller. The last bunch of a train (or all bunches) after becoming highly monochromatic goes into the main part of the undulators and produces high power monochromatic radiation. Compared to a SASE X-ray FEL, this approach should need a shorter main undulator length. A small number of electron bunches may generate multi-GW x-ray pulses with excellent temporal coherence. The resulting spectral brightness of these x-ray pulses can be another 2 to 3 orders of magnitude higher. It is important to mention that we do use the X-ray cavity in a fundamental way, as a cavity with resonator eigenmodes. We use only the last return X-ray pulse, which modulates the next coming bunch. Due to the large single-pass gain in the X-ray cavity, the output intensity at the cavity exit is orders of magnitude above the input.

As with classical FEL, the beam energy (a few GeV) corresponds to the radiation wavelength. The beam energy spread and beam emittance must not be above the usual FEL requirement. The electron bunch pattern may consist of an initial train of relatively low current bunches followed by a high current bunch. The bunch spacing depends upon the total length of the undulators inside the cavity. However there is no strong requirement on the arrival time because the reflected X-ray pulse length is increased (~ps) due to the frequency filtering (because of the multiple reflections inside the crystal).

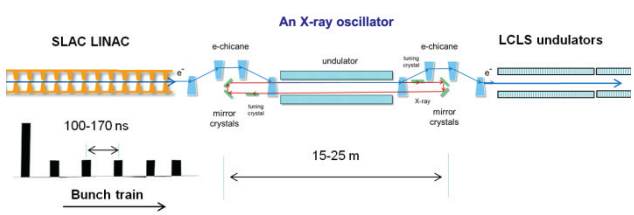

Figure 1: A proposed layout of an X-ray oscillator using high-energy electron beam.

*Work supported by DoE Contract No. DE-AC03-76SF00515
#novo@slac.stanford.edu

ISBN 978-3-95450-126-7

TOWARDS HIGH FREQUENCY OPERATION WITH A MULTI-GRATING SMITH-PURCELL FEL

J. T. Donohue, CENBG, Gradignan, France
J. Gardelle, CEA, Le Barp, France

Abstract

Three-dimensional simulations and experiments have shown that, for a grating equipped with sidewalls, copious emission of coherent Smith-Purcell (SP) radiation at the fundamental frequency of the evanescent surface wave is possible. Since the underlying theory is scale invariant, the wavelength emitted is reduced in proportion to a uniform rescaling of the grating. In order to increase our 5 GHz to 100 GHz, the grating surface would be reduced by a factor of 400, which would lead to greatly reduced power. In addition, the required beam might be hard to generate. To avoid this, we propose to use several gratings in parallel with no overall reduction in the total width and the same beam as in our microwave experiment. For this scheme to succeed, it is essential that the bunching in the different gratings be coherent. . Simulations suggest that this occurs for as much as a ten-fold scale reduction. To test this idea, an experiment is using several gratings is being performed.

INCREASE FREQUENCY BY DOWNSIZING

A demonstration experiment in the microwave domain showed that a Smith-Purcell (SP) free electron laser (FEL), with conducting sidewalls placed at the ends of the grating's grooves, emitted intense radiation at the frequency of the surface wave on the grating [1]. In single shot operation, the ratio of emitted power to beam power exceeded 10 %, and was in reasonable agreement with simulations performed previously [2]. An earlier experiment, on a grating without sidewalls [3], had demonstrated emission of coherent SP radiation at the second harmonic of the surface wave, thereby confirming the scenario proposed in the two-dimensional (2-D) model of Andrews and Brau [4]. But the efficiency was only of order 0.1 %. The sidewalls cause a modification of the dispersion relation for the surface wave [5]. The intersection of the beam line with the new dispersion relation may occur at an allowed SP frequency, which can't happen in the 2-D theory of Reference [3]. Thus the use of sidewalls produces much greater power, albeit at half the frequency. It must be emphasized that the sidewalls protrude only a small distance above the top of the grating, so that the radiation may be emitted in any direction above the grating.

The expressed aim of Andrews, Brau and their collaborators [6] was to develop an intense, compact, and tunable source of THz SP radiation. Theory indicates that a uniform reduction in size of all grating parameters, at constant beam energy, leads to an equal reduction in the wavelength of the SP radiation. This is emitted at the same angle, according to the usual SP formula [7],

$$\lambda = L(1/\beta - \cos\theta_{SP})/|n|.$$

Here λ denotes the wavelength, L the grating period, n the order of diffraction, θ_{SP} the angle with respect to the beam, and β the relative velocity of the electron. Obviously, if all parameters of the grating were reduced by a scaling factor, the wavelength would be reduced by the same factor, at constant beam energy. Such a reduction in size might be expected to greatly reduce the output power. In addition, the beam would have to propagate in a very narrow channel.

MULTI-GRATING ARRAYS

We propose to partially compensate this power loss by superposing in parallel several such gratings with sidewalls, while keeping our flat beam of width a few cm. We have performed 3-D particle-in-cell (PIC) simulations using the code "MAGIC" [8] to study the effect of diminishing the size of the grating, but making a planar array of them so as to maintain a quasi-constant beam width. In order to avoid the problem of beam height above the grating, we simulated a 1 mm-thick beam whose lower edge is flush with the top of the grating, regardless of the individual grating width. Our previous experience with the set-up convinces us that this is feasible. A magnetic field is used to impose approximately linear trajectories on the electrons. The essential question is whether the radiation from the individual channels remains coherent, so that the peak power emitted will scale as the square of the number of channels. For this to happen, the spatial and temporal beam bunching in each channel must be nearly identical. We can use the tools furnished by MAGIC to verify that fields and bunching in the different channels do indeed display the necessary coherence. In these simulations, the number of periods remains fixed (25), so that the reduction in scale leads to successively shorter gratings. In the simulations we have studied reductions of 2, 4, 6, 8 and 10 in size, each compensated by increasing the number of gratings by the same factor. The same beam of 40 A, 80 keV (beam power 3.2 MW) and 1 mm thickness is used in all simulations. The height of the sidewalls above the grating top and their thickness are also scaled down by the same factor. The sidewalls intercept some fraction of the beam, which will make CW operation impossible. The separation of the inner faces of the outermost sidewalls is thus 44-4/N mm, where N denotes the number of channels, and the beam width is equal to this.

ISBN 978-3-95450-126-7

HIGH-RESOLUTION SEEDING MONOCHROMATOR DESIGN FOR NGLS*

Yiping Feng, Juhao Wu, Jerome Hastings, SLAC, Menlo Park, CA94025, USA
Paul Emma, Tony Warwick, Robert Schoenlein, LBL, Berkeley, CA 94720, USA

Abstract

A high-resolution soft X-ray monochromator system is designed for self-seeding the next generation FEL sources. It consists of a single variable-line-spacing (VLS) grating, an exit slit, and pre- and collimating mirrors, and operates in the fixed-focus mode to achieve complete tuning of the seeding energy from 200 to 2000 eV with a nearly constant resolving power of greater than 50000, producing transform-limited seed ranging from 1 ps at 200 eV to 100 fs at 2000 eV. The optical delay is of order 1 ps, matching well with that of an electron chicane of moderate magnetic field strength. The design is based on a coherent Gaussian beam treatment of the FEL beam propagating from the upstream SASE undulator through the entire seeding monochromator system, preserving the transverse beam profile entering the downstream seeding undulator to ensure maximum coupling efficiency with the reentrant electron beam.

INTRODUCTION

SASE FEL starts from the shot noise in the electron bunch and is considered to be chaotic, especially in the temporal or spectral domain [1]. This poses limitations for certain user experiments. Schemes such as self-seeding [2] can effectively improve the temporal coherence of the FEL and provide better correlation between the FEL pulse intensity and the peak electric field, which is critically important for X-ray nonlinear physics. If the seeded FEL pulses approach transform-limited, more precise measurement of the pulse duration can be made using spectral methods. Furthermore, the FEL spectral brightness can be greatly enhanced and thus beneficial to experiments where a monochromator is required as in most spectroscopic/resonant excitation measurements. If brought into saturation, a self-seeded FEL pulse will exhibit far more stable intensity, allowing better control of FEL fluence on samples for measurements. Finally a stable self-seeded pulse will enable FEL high-power (at terawatts level) performance with strong tapering, producing even greater X-ray production and higher spectral brightness.

LCLS has commissioned hard X-rays self-seeding (HXRSS) [3] and has been planning for demonstrating soft X-ray self-seeding (SXRSS) with a moderate resolving power of 5000 [4], limiting the transform-limited pulses to 20 fs at 1 keV. Here in this paper, we present the optical design for a high-resolution soft X-ray monochromator system with a resolving power approaching 50000 and complete tunable from 200 to 2000 eV.

* Work supported by US DOE Office of Basic Energy Sciences under Contract DE-AC02-76SF00515 and US DOE Office of Science Early Career Research Program Award FWP-2013-SLAC-100164.

X-RAY OPTICAL DESIGN

The schematic layout of the seeding grating monochromator system is shown in Fig. 1. M_1 is a cylindrical mirror that deflects the beam vertically, but focuses beam horizontally onto the re-entrance point in the seeding undulator. The planar pre-mirror M_2 also deflects the beam vertically. G is a planar variable-line-spacing type [4], which disperses vertically and tunes the seeding energy by varying both the incident and exit angles in conjunction with the rotation of M_2, and focuses the dispersed beam vertically at the exit slit S, whose width is used for selecting the bandwidth. The mirror M_3 re-collimates the monochromatic but divergent beam from the slit S onto the re-entrant point in the seeding undulator to be re-merged with the electron bunch. The specifications of the grating and mirrors are given in Tables 1 and 2, and the system performance is discussed below.

Table 1: Optics Specifications for the Grating

Parameter	Symbol	Value
Line spacing (μm)	σ	0.393
Linear coefficient ()	$\Delta\sigma/\Delta x$	-2.9091 $\times 10^{-7}$
Groove height (nm)	h	5.21
Grating profile		Blazed
Incident angle (mrad)	θ	3.31 - 10.43
Exit angle (mrad)	θ'	56.3 - 178.2
Included angle (degree)	2θ	176.59 - 169.19
Object distance (m)	$L_{\rm obj}$	~ 8.0
Image distance (m)	$L_{\rm img}$	~ 2.7
Exit slit (μm)	s	0.557 - 1.763

Resolving Power

In the current design, the resolving power of a grating is mainly limited by the number of coherently illuminated grating grooves, which is mainly determined by the beam footprint onto the grating at a given incident angle. Since the FEL is nearly fully coherent, and the exit slit width is adjusted to match the size of the image (at the desired resolving power), the source and image size do not contribute to the resolution function. As such, the resolving power is shown in Fig. 2, approaching 50,000 in the entire energy range from 200 to 2,000 eV. In comparison, the LCLS SXRSS system has a resolving power of only 5,000.

ISBN 978-3-95450-126-7

A FULL BEAM 1D SIMULATION CODE FOR MODELING HYBRID HGHG/EEHG SEEDING SCHEMES FOR EVALUATING THE DEPENDENCE OF BUNCHING FACTOR BANDWIDTH ON MULTIPLE PARAMETERS*

C. Fortgang#, B. Carlsten, Q. Marksteiner, N. Yampolsky, LANL, Los Alamos, NM USA

Abstract

Multiple seeding schemes are available for design of narrow-band, short-wavelength FELS. Analysis of such schemes often focus on the amplitude of the final bunching factor, b, and how far it is above shot noise. Only under ideal conditions is the bandwidth of b Fourier transform limited. We have developed a 1D simulation tool that models complex hybrid seeding schemes using macro properties of the entire beam bunch to assess effects on both the amplitude and bandwidth of b. In particular the effects on bunching factor from using non-ideal beam driven radiators for downstream modulators, energy slew and curvature, and energy spread are investigated with the 1D tool.

INTRODUCTION

High gain harmonic-generation (HGHG) and echo-enabled harmonic generation (EEHG) as seeding schemes for narrowband short-wavelength FELs is an area of active interest. Much of the published analytical work addresses calculating and maximizing the bunching factor considering a single slice of the beam. However, a single slice calculation of b is not sufficient to estimate the bunching factor bandwidth. Producing a nearly Fourier transformed (FT) limited bunched beam is the primary purpose of seeding so having a prediction of b(k) with realistic beam-bunch macro properties is important. In the case of Ref [1] the spectral width of b(k) is estimated analytically and with simulations but only for the case where the laser pulse is short compared to the electron beam bunch. The work presented here uses the entire beam bunch so the results can be directly compared to an ideal FT limited bunching factor.

1D MODEL BENCHMARKING

The 1D equations for modelling HGHG/EEHG schemes has been discussed in numerous publications [2-4]. Our 1D model includes the FEL physics of modulators and radiators as well as the effects of macro beam properties such as; energy chirp or curvature across the entire beam pulse and a Gaussian current profile J(z) which directly impacts the power profile of a radiator. The effects of phase jitter or chirp across the bunch from a non-ideal external laser are also included.

*Work supported by Laboratory Directed Research and Development at LANL (20110067).
#cfortgang@lanl.gov

The following equations are derived from 1D FEL theory [5]. A modulator has to satisfy the condition that $4\pi N_{mod} \eta << 1$ where N_{mod} is the number of modulator periods and $\eta=\Delta\gamma/\gamma$ is the amplitude of the energy modulation. Under this condition electrons are modulated in energy but not in phase.

The amount of laser power required for a desired energy modulation is given by,

$$P_{mod} = \eta^2 \gamma^4 \sigma_L^2 \, Po / (K_{mod}^2 [JJ]^2 L_{mod}^2) \quad \text{where,}$$

σ_L is the laser rms radius and $Po=I_{Alfven}\, mc^2/e = 8.7$ GW.

Some schemes may use a pre-bunched beam to drive a radiator as a source of laser seed power for a subsequent modulator. The power generated by a radiator is given by,

$$P_{rad}(z) = Zo\, K_{rad}^2 [JJ]^2 I_{beam}^2(z) |b(z)|^2 L_{rad}^2/(32\pi \sigma_b^2 \gamma^2)$$

where, Zo=377 ohms, I_{beam} is the beam current along the bunch, b(z) is the bunching factor along the bunch, and σ_b is the rms electron beam radius. In our 1D model where a radiator is used to drive a modulator the relationship between the electron beam size and the laser transverse power profile is given by $\sigma_L^2=\sigma_b^2/2$.

The peak amplitudes of the bunching factor harmonics from a HGHG stage is given by [4],

$$b_h = J_h(-h\, k_{seed}\, R_{56}\, \eta) \exp(-(h\, k_{seed}\, R_{56}\, \sigma_E)^2/2)$$

where h is the harmonic number, R_{56} is the HGHG chicane strength, and σ_E is the intrinsic rms energy spread. None of the above equations are used explicitly in the 1D code but rather are used to verify the code results where applicable.

An EEHG stage uses the analytic analysis as outlined in [6]. Using the notation of [6] the important EEHG parameters are $A_1=\Delta W_1/\sigma_E$, $A_2=\Delta W_2/\sigma_E$, and $B1=R1_{56}\, k_{seed}\, \sigma_E/W_0$ and $B2= R2_{56}\, k_{seed}\, \sigma_E/W_0$ where A1 and A2 are the normalized energy modulations for the 1st and 2nd energy modulators and B1 and B2 are the normalized strengths for the strong (1st) and weak (2nd) EEHG chicanes. In the case of a scheme where an EEHG section follows a HGHG section then $B1=B1^*-B0$ where $B1^*$ would be the strong chicane strength if the HGHG section were absent and B0 is the strength of the HGHG chicane.

ISBN 978-3-95450-126-7

WAKE MONOCHROMATOR IN ASYMMETRIC AND SYMMETRIC BRAGG AND LAUE GEOMETRY FOR SELF-SEEDING THE EUROPEAN X-RAY FEL

G. Geloni, European XFEL GmbH, Hamburg, Germany
V. Kocharyan, E. Saldin, Svitozar Serkez and Martin Tolkiehn, DESY, Hamburg, Germany

Abstract

We discuss the use of self-seeding schemes with wake monochromators to produce TW power, fully coherent pulses for applications at the dedicated bio-imaging beamline at the European X-ray FEL, a concept for an upgrade of the facility beyond the baseline previously proposed by the authors. We exploit the asymmetric and symmetric Bragg and Laue reflections (sigma polarization) in diamond crystal. Optimization of the bio-imaging beamline is performed with extensive start-to-end simulations, which also take into account effects such as the spatio-temporal coupling caused by the wake monochromator. The spatial shift is maximal in the range for small Bragg angles. A geometry with Bragg angles close to $\pi/2$ would be a more advantageous option from this viewpoint, albeit with decrease of the spectral tunability. We show that it will be possible to cover the photon energy range from 3 keV to 13 keV by using four different planes of the same crystal with one rotational degree of freedom. More information and details can be found in [1].

INTRODUCTION

One of the highest priority for experiments at any advanced XFEL facility is to establish a beamline for studying biological objects at the mesoscale, including large macromolecules, macromolecular complexes, and cell organelles. This requires 2-6 keV photon energy range and TW peak-power pulses [2] - [6]. However, higher photon energies (up to 13 keV) are needed to reach the K-edges of commonly used elements, such as Se, for anomalous experimental phasing. Studies at intermediate resolutions need access to the water window at 0.5 keV. The pulse duration should be adjustable from 2 fs to 10 fs.

A basic concept and design of an undulator system for a dedicated bio-imaging beamline at the European XFEL was proposed in [7], and optimized in [8]. All the requirements in terms of photon beam characteristics can be satisfied by the use of a very efficient combination of self-seeding, fresh bunch and undulator tapering techniques [9] - [20]. In particular, a combination of self-seeding and undulator tapering techniques would allow to meet the design TW output power. The bio-imaging beamline would be equipped with two different self-seeding setups. For soft X-ray self-seeding, the monochromator consists of a grating [9]. Starting around the energy of 3 keV it is possible to use a single crystal (wake) monochromator instead of a grating [8].

In [8] we demonstrated that it will be possible to cover the photon energy range between 3 keV and 13 keV using the C(111), C(220) and C(004) symmetric Bragg reflections. In this scenario, three different crystals would enable self-seeding for the different spectral range. In particular, we proposed to exploit the C(111) symmetric Bragg reflection in the photon energy range between 3 keV and 5 keV.

While developing a design for the bio-imaging beamline, the authors first priority was to have it satisfying all requirements. Having achieved that goal, the next step is to optimize the design, making it as simple as possible. The design presented here aims for experimental simplification and cost reduction of the self-seeding setups. In order to improve the original design, here we propose to exploit asymmetric Bragg and Laue C(111), C(113) and C(333) reflections together with the symmetric Bragg reflection C(004). The novel design of the self-seeding setup combines a wide photon energy range with a much needed experimental simplicity. Only one diamond crystal is needed, and only one rotational degree of freedom is required.

While, in this article, we consider applications for the bio-imaging beamline in particular, the present study can also be applied to other beamlines, for example the SASE1-SASE2 lines at the European XFEL as well.

DYNAMICAL DIFFRACTION THEORY AND ASYMMETRIC-CUT CRYSTALS

We begin our analysis of asymmetric-cut crystals by specifying the scattering geometry under study. With reference to Fig. 1, and following the notation in [21] we identify the crystal surface with the unit vector normal to the crystal surface $\vec{n}$, directed inside the crystal. The unit vector $\vec{s}$ indicates the trace of the Bragg planes. The direction of the incident beam is specified by the unit vector $\vec{s}_0$, while that of the diffracted beam is given by $\vec{s}_h$. Always following [21], we call ψ_n the angle between $\vec{n}$ and $\vec{s}$, ψ_0 the angle between $\vec{n}$ and $\vec{s}_0$, and ψ_h the angle between $\vec{n}$ and $\vec{s}_h$. The signs of these angles are univocally fixed by requiring that the angle between $\vec{s}$ and $\vec{s}_0$ is positive (and equal to the Bragg angle θ_B), while the angle between $\vec{s}$ and $\vec{s}_h$ is negative (and equal to -θ_B). Figure 1 shows two generic examples for both Bragg and Laue geometries.

Let us consider an electromagnetic plane wave in the X-ray frequency range incident on an infinite, perfect crystal. Within the kinematical approximation, according to the Bragg law, constructive interference of waves scattered

ISBN 978-3-95450-126-7

FERMI@ELETTRA STATUS REPORT

Enrico Allaria[1], Filippo Bencivenga[1], Carlo Callegari[1], Flavio Capotondi[1], Davide Castronovo[1], Paolo Cinquegrana[1], Ivan Cudin[1], Massimo Dal Forno[1], Miltcho B. Danailov[1], Gerardo D'Auria[1], Raffaele De Monte[1], Giovanni De Ninno[1], Alexander Demidovich[1], Simone Di Mitri[1], Bruno Diviacco[1], Alessandro Fabris[1], Riccardo Fabris[1], William M. Fawley[1], Mario Ferianis[1], Eugenio Ferrari[1], Lars Froehlich[1], Paolo Furlan Radivo[1], Giulio Gaio[1], Luca Giannessi[1,2*], Maya Kiskinova[1], Marco Lonza[1], Benoît Mahieu[1,4], Nicola Mahne[1], Claudio Masciovecchio[1], Fulvio Parmigiani[1], Giuseppe Penco[1], Mauro Predonzani[1], Emiliano Principi[1], Lorenzo Raimondi[1], Fabio Rossi[1], Luca Rumiz[1], Claudio Scafuri[1], Claudio Serpico[1], Paolo Sigalotti[1], Simone Spampinati[1], Carlo Spezzani[1], Michele Svandrlik[1], Cristian Svetina[1], Mauro Trovo[1], Alessandro Vascotto[1], Marco Veronese[1], Roberto Visintini[1], Dino Zangrando[1], Marco Zangrando[1], Paolo Craievich[1,5]

[1]Elettra – Sincrotrone Trieste, 34149 Basovizza, Trieste, ITALY
[2]ENEA C.R. Frascati, Frascati (Roma), ITALY
[3]University of Nova Gorica, Nova Gorica, SLOVENIA
[4]CEA/DSM/DRECAM/SPAM, Gif-sur-Yvette, FRANCE
[5]PSI, Villigen, SWITZERLAND

Abstract

The FERMI@Elettra seeded Free Electron Laser (FEL) is based on two separate FEL lines, FEL-1 and FEL-2. FEL-1 is a single stage cascaded FEL delivering light in the 65-20nm wavelength range, while FEL-2 is a double stage cascaded FEL where the additional stage extends the frequency up-conversion process to the spectral range of 20-4nm.

The FEL-1 beam line has been in operation since the end of 2010, with user experiments carried on in 2011-2013 and user beam time allocated until the first half of 2014. Fermi FEL-2 is the a seeded FEL operating with a double stage cascade in the "fresh bunch injection" mode [1]. The two stages are two high gain harmonic generation FELs where the first stage is seeded by the 3rd harmonic of a Ti:Sa laser system, which is up converted to the 4th-12th harmonic. The output of the first stage is then used to seed the second stage. A final wavelength of 10.8 nm was obtained (the 24th harmonic of the seed wavelength) during the first commissioning in October 2012. The experiment demonstrated that the FEL is capable of producing single mode narrow bandwidth pulses with energy of several tens of microjoules. The commissioning of FEL-2 continued in March and June 2013, where the wavelength of operation was extended down to 4nm and below, demonstrating that an externally seeded FEL is capable of reaching the soft X-ray range of the spectrum.

*Corresponding author: luca.giannessi@elettra.eu. This work has been supported in part by the Italian Ministry of University and Research under grants FIRB-RBAP045JF2 and FIRB-RBAP06AWK3

INTRODUCTION

FERMI@Elettra free electron laser (FEL) is a fourth generation light source at the research centre Elettra – Sincrotrone Trieste, Italy that functions as a user facility producing photons in the ultraviolet and soft X-ray wavelength regions. The scientific case, based on three experimental programs, namely *Diffraction and Projection Imaging* (DiProI), *Elastic and Inelastic Scattering* (EIS), *Low Density Matter* (LDM), calls for stable, high peak brightness, nearly fully coherent (both transversely and longitudinally), narrow bandwidth photon pulses, together with wavelength tunability and variable polarization [2-4].

FERMI is driven by a single-bunch, S-band high brightness electron linac. The linac is presently capable of reaching a final energy up to 1.4 GeV, in conditions of FEL operation (*i.e.*, including energy losses due to the required off crest operation of two linac sections for compression and the X-band cavity for phase space linearization). The linac energy was increased from the previously available 1.2 GeV by an extensive RF conditioning plan program during May 2013. At the same time the machine repetition rate was increased to 50 Hz, with the linac has operating at this rate during all the conditioning of the RF plants. However, the rep rate was reduced back to 10 Hz for the FEL commissioning shifts, in order both to increase the linac reliability for the FEL operation at the higher energy, and to reduce the (expected) cathode aging that was observed on the new 50 Hz gun, delivered by Radia Beam and installed during the winter 2013. In the future the linac energy will be extended further to 1.5 GeV in order to increase the FEL gain in the shortest wavelenght range (at and below 5 nm).

ISBN 978-3-95450-126-7

COMPACT XFEL LIGHT SOURCE*

W.S. Graves#, K.K. Berggren, S. Carbajo, R. Hobbs, K.-H. Hong, W.R. Huang, F.X. Kärtner, P.D. Keathley, D.E. Moncton, E. Nanni, K. Ravi, M. Swanwick, L.F. Velásquez-García, L.J. Wong, Y. Yang, L. Zapata, Y. Zhou, MIT, Cambridge, MA, USA
J. Bessuille, P. Brown, E. Ihloff, MIT-Bates Laboratory, Middleton, MA, USA
S. Carbajo, J. Derksen, A. Fallahi, F.X. Kärtner, F.Scheiba, X.Wu, CFEL-DESY, Hamburg, Germany
D. Mihalcea, Ph. Piot, I. Viti, N. Illinois University, Dekalb, IL, USA

Abstract

X-ray free electron laser studies are presented that rely on a nanostructured electron beam interacting with a "laser undulator" configured in the head-on inverse Compton scattering geometry. The structure in the electron beam is created by a nanoengineered cathode that produces a transversely modulated electron beam. Electron optics demagnify the modulation period and then an emittance exchange line translates the modulation to the longitudinal direction resulting in coherent bunching at x-ray wavelength.

The predicted output radiation at 1 keV from a 7 MeV electron beam reaches 10 nJ or $6X10^8$ photons per shot and is fully coherent in all dimensions, a result of the dominant mode growth transversely and the longitudinal coherence imposed by the electron beam nanostructure. This output is several orders of magnitude higher than incoherent inverse Compton scattering and occupies a much smaller phase space volume, reaching peak brilliance of 10^{27} and average brilliance of 10^{17} photons/(mm^2 mrad^2 0.1% sec). The device is much smaller and less expensive than traditional XFELs, requiring electron beam energy ranging from 2 MeV to a few hundred MeV for output wavelengths from the EUV to hard x-rays. Both laser and THz radiation may provide the undulator fields.

INTRODUCTION

In the course of investigating coherent inverse Compton scattering (ICS) from a nanostructured electron beam [1] it has been found that under certain conditions FEL gain occurs, and that this interaction has significant positive effects on the properties of the radiation emitted. FEL gain for a laser undulator has been previously predicted and studied [2,3] but for very different sets of electron beam and laser parameters than are presented here. In this case the bunch charge and peak current are much lower than earlier studies, as is the electron beam emittance. Furthermore by creating a pre-bunched electron beam via a structured cathode and emittance exchange, the number of gain lengths required to saturate is much reduced, which in turn eases the power, focusing and pulse length requirements on the laser.

*Supported by DARPA N66001-11-1-4192, CFEL DESY, DOE DE-FG02-10ER46745, DOE DE-FG02-08ER41532, and NSF DMR-1042342.
#wsgraves@mit.edu

The net effect of these changes is to allow an XFEL based on collision of a low energy electron beam with a laser that is within present state-of-the-art technologies and results in a very compact and inexpensive x-ray laser. A facility to test these ideas is currently under construction within the DARPA Axis program and is described below. First though the conditions for FEL gain are reviewed as is the method of producing the nanostructured electron beam.

FEL GAIN

For head-on ICS the resonance condition is given by

$$\lambda_x = \frac{\lambda_L}{4\gamma^2}\left(1+\frac{a_0^2}{2}\right) \quad (1)$$

where λ_x is the x-ray wavelength, λ_L is the laser wavelength, γ is the relativistic factor, and a_0 $\frac{eE_L\lambda_L}{2\pi mc^2}$ where E_L is the laser electric field. The Pierce parameter that determines many of the FEL properties is given by

$$\rho_{fel} \quad \frac{1}{2\gamma}\left(\frac{I}{I_A}\frac{\lambda_L^2 a_0^2}{8\pi^2\sigma_x^2}\right)^{1/3} \quad (2)$$

where σ_x is the electron beam size, I is the peak current, and I_A = 17,045 A is the Alfen current. A Bessel function factor in Eq. 2 has been dropped because its value is very close to unity for $a_0^2 \ll 1$ which is true for the present case. The 1D e-folding length for FEL gain is

$$L_G \quad \frac{\lambda_L}{8\pi\sqrt{3}\rho_{fel}} \quad (3)$$

The design goal for the FEL is to have ρ_{fel} large and L_G small. One of the advantages of using a laser undulator is seen in the very short gain lengths possible due to the short period relative to a static undulator.

It is useful to solve Eq. 1 for λ_L with the assumption $a_0^2 \ll 1$ and substitute into Eq. 2 to find how the Pierce parameter scales with electron energy γ, peak current I, and x-ray wavelength λ_x. The beam size is also replaced with σ_x^2 $\frac{\varepsilon_{xN}\beta_x}{\gamma}$, yielding

$$\rho_{fel} \quad \left(\frac{I}{I_A}\frac{\gamma^2\lambda_x^2 a_0^2}{4\pi^2\varepsilon_{xN}\beta_x}\right)^{1/3} \quad (4)$$

ISBN 978-3-95450-126-7

STATUS OF THE FLASH FACILITY

K. Honkavaara*, B. Faatz, J. Feldhaus, S. Schreiber, R. Treusch, M. Vogt,
DESY, Hamburg, Germany †

Abstract

The free-electron laser user facility FLASH at DESY (Hamburg, Germany) finished its 4$^{\text{th}}$ user period in February 2013. In total 2715 hours of SASE radiation have been delivered to user experiments with photon wavelengths between 4.2 nm and 44 nm and up to 5000 photon pulses per second. After a shutdown to connect the second undulator line - FLASH2 - to the FLASH linac, and a following commissioning period, FLASH is scheduled to continue user operation late 2013. The year 2014 will be dedicated to the 5$^{\text{th}}$ period of user experiments. The commissioning of FLASH2 will take place in 2014 in parallel to the FLASH1 operation.

INTRODUCTION

FLASH [1–4], the free-electron laser (FEL) user facility at DESY (Hamburg), delivers high brilliance XUV and soft X-ray FEL radiation for photon experiments. This paper summarizes the performance during the 4$^{\text{th}}$ user period, reports the status of the FLASH II project, and outlines the midterm plans of the FLASH facility. Part of the material discussed here has already been presented in previous conferences [3–6].

FLASH FACILITY

The layout of the FLASH facility, including the second undulator line under construction, is shown in Fig. 1. Typical FLASH operating parameters can be found, for example, in [3].

A laser driven RF-gun produces trains with up to 800 high brightness electron bunches. The bunch train repetition rate is 10 Hz, and the typical bunch charge ranges from 80 pC to 1 nC. The photocathode laser system is based on an actively mode-locked pulse train oscillator with a linear chain of fully diode pumped Nd:YLF amplifiers [7, 8]. The cathode is exchangeable and consists of a thin film of Cs_2Te on a molybdenum plug [9].

During the last three years, severe problems have occurred related to the RF-gun and its RF-window [3] forcing us to exchange the window (autumn 2011) and the RF-gun (June 2012). During the 2013 shutdown a new RF-gun has been installed. In addition, new RF-gun design options and new RF window types are being tested.

The electron beam is accelerated up to 1.25 GeV by seven superconducting TESLA type accelerating modules. Each module has eight 9-cell niobium cavities operated at 1.3 GHz. In order to linearize the longitudinal phase space, four 3.9 GHz (third harmonics of 1.3 GHz) superconducting cavities are installed downstream the first module. Electron bunches are compressed by two magnetic chicane bunch compressors at beam energies of 150 MeV and 450 MeV to achieve the peak current required for the lasing process.

The RF-gun and the accelerating modules are regulated using a sophisticated FPGA based low level RF (LLRF) system [10, 11]. An upgrade to a μTCA based system is under way [12]. Other important developments are improvements on the synchronization and beam arrival time stabilization system including also beam based longitudinal RF-feedbacks [13–15]. A recent novelty is the possibility of on-line monitoring of the electron bunch length and shape using both a transverse deflecting cavity equipped with an off-axis screen and an in-vacuum polychromator measuring coherent radiation in THz and infrared range [16].

The electron beam passes through six 4.5 m long fixed gap (12 mm) undulator modules producing FEL radiation based on the SASE (Self Amplified Spontaneous Emission) process. Undulators consist of permanent NdFeB magnets, the undulator period is 27.3 mm, and the peak K-value 1.23. A planar electromagnetic undulator is installed downstream of the SASE undulators to produce - on request - THz radiation. The produced THz pulses are naturally synchronized with the SASE pulses. A seeding experiment sFLASH [17, 18] with four variable gap undulators is installed between the collimation section and the SASE undulators.

A sophisticated photon diagnostics section provides a possibility to measure and characterize the photon beam parameters. In the experimental hall, five photon beam lines are available for user experiments. Since FLASH has not yet permanent end-stations, each experiment has to provide and install its own measurement hardware. Photon diagnostics and photon beamlines are described in [2].

4$^{\text{TH}}$ USER PERIOD

The 4$^{\text{th}}$ FEL user period started end of March 2012. Unfortunately, after the two first user blocks, the break-down of the RF-gun forced us to stop the operation on June-7, 2012. As a consequence, one four-week user block was postponed from summer 2012 to early 2013. The RF-gun was successfully exchanged and the beam operation quickly re-established such that the next user block in Au-

* katja.honkavaara@desy.de
† for the FLASH team

ISBN 978-3-95450-126-7

RECENT LCLS PERFORMANCE FROM 250 TO 500 eV*

Richard Iverson, John Arthur, Uwe Bergmann, Christoph Bostedt, John Bozek, Axel Brachmann, William Colocho, Franz-Josef Decker, Yuantao Ding, Yiping Feng, Josef Frisch, John N. Galayda, Tom Galetto, Zhirong Huang, Eugene Michael Kraft, Jacek Krzywinski, James Liu, Henrik Loos, Stan Mao, Stefan Moeller, Heinz-Dieter Nuhn, Alyssa Prinz, Daniel Ratner, Tor Raubenheimer, Sayed Rokni, William F. Schlotter, Peter Schuh, Tonee Smith, Michael Stanek, Peter Stefan, Michael Sullivan, James L. Turner, Joshua Turner, James Welch, Juhao Wu, Feng Zhou, SLAC, Menlo Park, California, USA
Paul J. Emma, LBNL, Berkeley, California, USA
Regina Soufli, LLNL, Livermore, California, USA

Abstract

The Linac Coherent Light Source is an x-ray free-electron laser at the SLAC National Accelerator Laboratory. It produces coherent soft and hard x-rays with peak brightness nearly ten orders of magnitude beyond conventional synchrotron sources and a range of pulse durations from 500 to <10 fs. The facility has been operating at x-ray energy from 500 to 10,000 eV. Users have expressed great interest in doing experiments with x-rays near the carbon absorption edge at 284 eV. We describe the operation and performance of the LCLS in the newly established regime between 250 and 500 eV.

INTRODUCTION

In previous work [1] we have described the first lasing of the LCLS x-ray FEL. Recent improvements include femtosecond electron and x-ray beams [2], harmonic lasing [3] and two color lasing [4]. Soft x-ray Self Seeding is scheduled to be commissioned in the fall of 2013 [5]. The layout of LCLS is shown in Fig. 1. This paper reports on initial LCLS FEL performance between 250 and 500eV. For the initial setup, we established 2mJ FEL energy at 500eV. The machine was then ramped down to 300eV and optimized at this energy. In addition to the beam diagnostics in the Front End Enclosure, the x-ray diagnostic chamber (see Fig. 2) located down beam from the undulator was used to measure the x-ray beam profile and to test the survivability of bulk boron carbide (B4C) material used in x-ray stoppers.

FIRST RESULTS

FEL optimization starts with establishing electron beam projected emittance at the injector less than 0.4um in x and y at 150pC bunch charge as shown in Figure 3. This is accomplished by steering the injector laser on the iris before the gun cathode to achieve a nearly Gaussian laser profile then optimizing the gun solenoid. After loading the design optics, dispersion is corrected after each bunch compressor and dogleg 2. Next the emittance is measured and beta functions are matched after each bunch compressor and dogleg 2

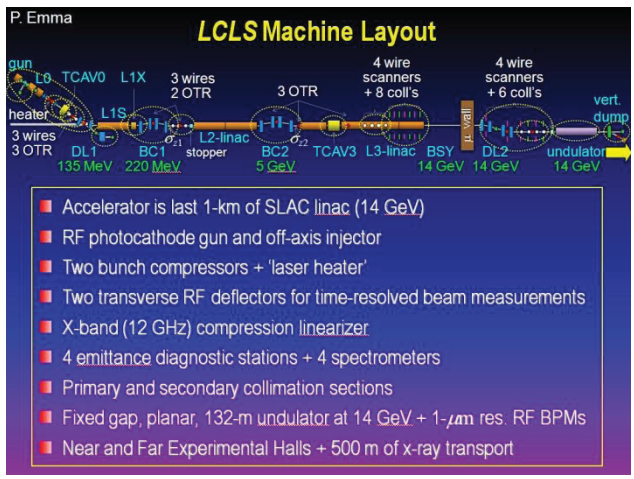

Figure 1: The LCLS machine layout.

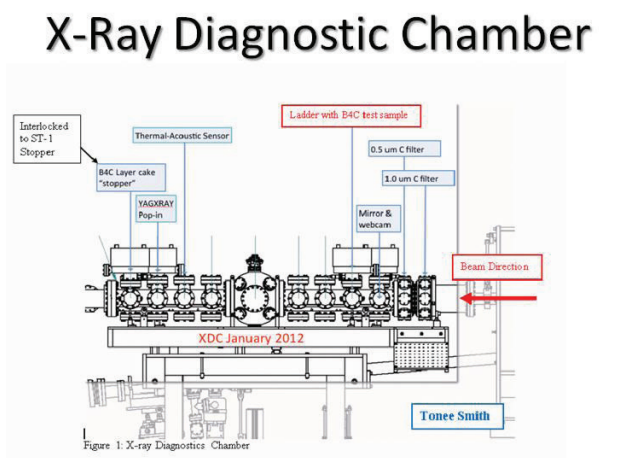

Figure 2: The x-ray Diagnostic Chamber located just down beam of the undulator.

Then the electron beam bunch length, current, beta matching quadrupoles, hard x-ray self seeding chicane delay, laser heater power and undulator taper are optimized to maximize FEL intensity. Figure 4 shows a measurement of the FEL energy after tuning produced 1.3 mJ at 300 eV.

*Work supported by the Department of Energy under Contract Number: DE-AC02-76SF00515

ISBN 978-3-95450-126-7

FAST ELECTRON BEAM AND FEL DIAGNOSTICS AT THE ALICE IR-FEL AT DARESBURY LABORATORY

F. Jackson, D. Angal-Kalinin, D. Dunning, J. Jones, A. Kalinin, T. T. Thakker, N. Thompson,
STFC/DL/ASTeC & Cockcroft Institute, Daresbury Laboratory, Warrington, U.K.

Abstract

The ALICE facility at Daresbury Laboratory is an energy recovery based infra-red free electron laser of the oscillator type that has been operational since 2010. Recently fast diagnostics have been installed to perform combined measurements on pulse-by-pulse FEL energy and bunch-by-bunch electron bunch position and arrival time. These measurements have highlighted and quantified fast instabilities in the electron beam and consequently the FEL output, and are presented and discussed here.

INTRODUCTION

ALICE (Accelerators and Lasers In Combined Experiments) at Daresbury Laboratory is a multifunctional accelerator test facility based on an energy recovery linac and includes an infra-red free electron laser (IR-FEL). The IR-FEL achieved first lasing in 2010 [1, 2] and has been studied and used in scientific applications since then.

The ALICE machine includes a DC electron gun photo-injector (producing electrons at 325 keV), a superconducting booster (accelerating electrons to around 6-7 MeV), and an energy recovery loop including a superconducting linac (accelerating the electrons to around 26 MeV), a four-dipole bunch compressor, and arcs composed of triple-bend achromats. The beam is composed of bunch trains 100 μs long, generated at up to 10 Hz repetition rate. The bunch repetition rate within a train is 16.25 MHz (62 ns bunch spacing) and the bunch charge is nominally 60 pC.

The IR-FEL is of the oscillator type and consists of a 40 period undulator around a metre long. The typical FEL wavelength range is 5.5 - 9.0 μm (via adjustable undulator gap), and the FEL delivers an average saturated radiation power of ~ 10 mW, ~4 mJ per macro-pulse, ~3 μJ energy per micro-pulse [2, 3].

Recently the IR-FEL has been utilised for scanning near field optical microscopy [4]. For this application the long term stability (on the ≳1 sec timescale) of the FEL is important. The stability of FEL radiation power variations is measured to be 3%, while the wavelength fluctuation is < 20 % of the bandwidth [3].

More recently, new diagnostics have been commissioned at ALICE to measure fast instabilities in FEL and accelerator performance. Fast beam position monitor (BPM) electronics and time of arrival (TOA) monitors have been installed to allow measurement of the positions and TOA of individual bunches within the train. In addition, a photoelectromagnetic (PEM) detector was used to simultaneously record the energy of individual FEL pulses (in this paper the term pulse will be used exclusively to refer to an individual FEL radiation pulse; the term macropulse refers to a ~100 μs train of FEL pulses).

DIAGNOSTIC TECHNIQUES

Several different diagnostics at different locations in the lattice were used simultaneously, as illustrated in Fig. 1. These are described in detail in a previous paper [5] and will be summarised briefly here.

A BPM with bunch-by-bunch capability was located after the first dipole in the return arc (location 'C' in Fig. 1). Bunch positions are computed using standard sum/difference formulae of the processed pickup signals, and the calibration relies on simulations performed previously for the EMMA project [6, 7]. The position resolution is estimated to be 30 μm.

TOA monitors were positioned at locations 'A' (just upstream of the FEL) and 'D' (at re-entry to the linac). These use an optical clock system which has been developed at Daresbury [8] to enable high precision beam TOA monitoring utilising existing BPMs. Timing information of the bunches is converted into amplitude modulation which can be accurately measured on a fast oscilloscope (down to 25 ps resolution, or 40 G samples/sec). Using stripline BPMs the electron bunch arrival times were measured with a single-shot resolution of ~280 fs at location A and ~600 fs at location D.

The energy of individual FEL pulses were measured with a photoelectromagnetic detector (PEM-10.6-1x1 from VIGO Systems S. A.) which has a time constant of < 1 ns. The PEM signal was relayed to another fast oscilloscope and the data post-processed to obtain the integrated signal for each pulse as a measure of the FEL pulse energy.

Synchronisation of the diagnostics was achieved through a combination of analogue triggers and time stamping in EPICS. The measurement is initiated with a beam signal from a pickup before the FEL, which triggers the acquisition of the TOA oscilloscope data at locations A and D (the actual arrival times are obtained with post-processing). This TOA oscilloscope then triggers another fast oscilloscope to acquire the data from the FEL pulse energy monitor. The measurements from both oscilloscopes are time-stamped to the local oscilloscope clock which is synchronised to the main EPICS clock of the accelerator control system. For these measurements the ALICE train repetition rate was set to 1 Hz, which enabled the bunch TOA and FEL pulse energy measurements to be matched to the bunch BPM data which is directly time stamped into EPICS.

ISBN 978-3-95450-126-7

INTEGRATING THE FHI-FEL INTO THE FHI RESEARCH ENVIRONMENT – DESIGN AND IMPLEMENTATION ASPECTS

H. Junkes, W. Erlebach, S. Gewinner, U. Hoppe, A. Liedke, G. Meijer [on leave], W. Schöllkopf, G. von Helden, M. Wesemann, FHI, Berlin, Germany
Alan Murray Melville Todd, Lloyd Martin Young, AES, Medford, NY, USA
Hans Bluem, David Dowell, Ralph Lange, AES, Princeton, New Jersey, USA
S.B. Webb, ORNL, Oak Ridge, Tennessee, USA

Abstract

The new mid-infrared FEL at the Fritz-Haber-Institut (FHI) was presented at the FEL12 conference. [1] It will be used for spectroscopic investigations of molecules, clusters, nanoparticles and surfaces. This facility must be easy to use by the scientists at FHI, and should be seamlessly integrated into the existing research environment. The Experimental Physics and Industrial Control System (EPICS) software framework was chosen to build the FHI-FEL control system, and will also be used to interface the user systems. The graphical operator interface is based on the Control System Studio (CSS) package. It covers radiation safety monitoring as well as controlling the complete set of building automation and utility devices, regardless of their particular function. A user interface (subset of the operator interface) allows user-provided experiment-control software (KouDA, LabVIEW, Matlab) to connect with an EPICS Gateway providing secured access. The EPICS Channel Archiver continuously records selected process variable data and provides a web server offering archive and near real-time data. A sample experiment installation demonstrates how this user interface can be used efficiently.

User Experiment: Confirmed Resolved IR-Spectroscopy on Biomolecules

- The function on protein depends on its 3-dimensional structure and shape.
- The study of proteins in the gas phase yields information about isolated molecules and gives insight into intramolecular interactions that govern the protein's structure.
- The gas-phase techniques mass spectrometry (MS), ion mobility spectrometry (IMS), and IR-spectroscopy yield complementary information about the molecule.

The principle of Ion Mobility Spectrometry

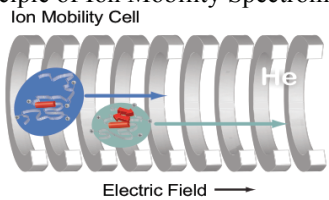

Figure 1: Ion mobility cell.

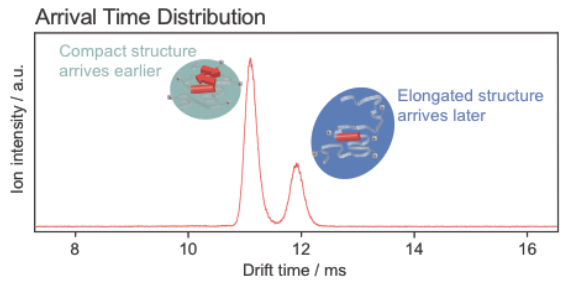

Figure 2: Arrival time distribution.

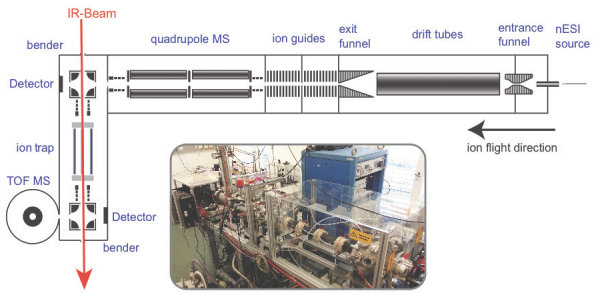

Figure 3: Experimental setup IMS.

- Combination of IMS, MS, and IR-Spectroscopy allows for spectroscopy on m/z- and shape-selected biomolecules.
- Shape- and m/z-selected ions will be stored in a cooled ion trap and irradiated with IR-light.
- The wavelength dependency of the ion-fragmentation will be monitored using LabVIEW programs and NI data acquisition cards. [2]

Operator Console

The operator interface is based on Control System Studio (CSS). This is an Eclipse RCP based development platform and the fundament for many applications like EPICS, TANGO, etc.. As most of these applications deal with process variables and connections to control systems, the CSS Core provides the necessary APIs for dealing with them. Taking advantage of modern graphical editor software technology, Operator Interface (OPI) editor and runtime - Best OPI, Yet (BOY) - has been developed by the CSS collaboration. [3] The Operator Interface is one of the basic components of the standard control system model. It provides not only operators but also scientists and engineers with rich graphical interfaces to view or operate the FEL locally or remotely [Fig. 4].

ISBN 978-3-95450-126-7

THz RADIATION SOURCE POTENTIAL OF THE R&D ERL AT BNL *

Dmitry Kayran[#,1], Ilan Ben-Zvi[1,2], Yichao Jing[1], Brian Sheehy[1]
[1]Collider-Accelerator Department, Brookhaven National Laboratory, Upton, NY 11973, USA
[2]Physics&Astronomy Department, Stony Brook University, Stony Brook, NY 11794, USA

Abstract

An ampere class 20 MeV superconducting Energy Recovery Linac (ERL) is under commissioning at Brookhaven National Laboratory (BNL) for testing concepts for high-energy electron cooling and electron-ion colliders [1-3]. This ERL will be used as a test bed to study issues relevant for very high current ERLs. High repetition rate (9.5 MHz), CW operation and high performance of electron beam with some additional components make this ERL an excellent driver for high power coherent THz radiation source. We present the status and commissioning progress of the ERL. We discuss potential use of BNL ERL as a source of THz radiation and results of the beam dynamics simulation.

INTRODUCTION

The R&D ERL facility at BNL aims to demonstrate CW operation of ERL with average beam current upto 0.3 ampere, combined with very high efficiency of energy recovery. The ERL is being installed in one of the spacious bays in Bldg. 912 of the RHIC/AGS complex (Fig. 1). The bay is equipped with an overhead crane. The facility has two service rooms and a shielded ERL cave. Its control room is located outside of the bay in a separate building. The single story house is used for a high voltage power supply for 1 MW klystron. The two-story unit houses a laser room, the CW 1 MW klystron with its accessories, most of the power supplies and electronics. The intensive R&D program geared towards the construction of the prototype ERL is under way [2]: from development of high efficiency photo-cathodes [4], design, construction and commissioning SRF gun [5], to the development of new merging system compatible with emittance compensation technic [6]. The R&D ERL will test many generic issues relevant with ultra high current continuously operation ERLs: 1) SRF photo-injector (704 MHz SRF Gun, photocathode, laser) capable of 500 mA. 2) Preservation of low emittance for high-charge, bunches in ERL merger; 3) High current 5-cell SRF linac with efficient HOM absorbers; 4) BBU studies using flexible optics; 5) Stability criteria of amp class CW beams.

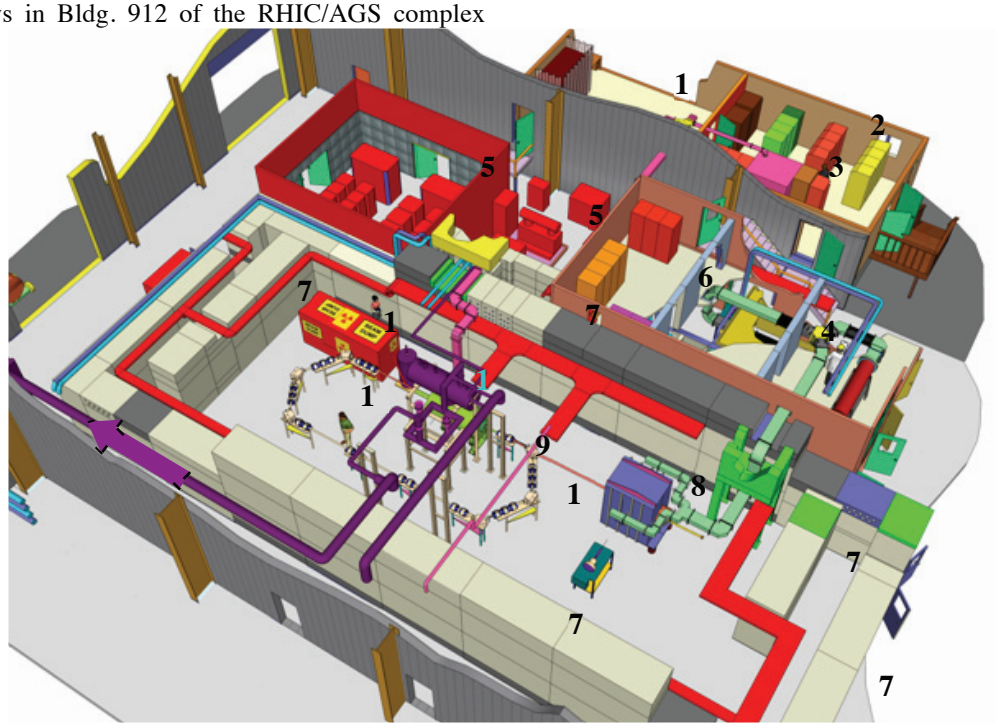

Figure 1: Layout of the R&D energy recovery linac in the shielded vault in bldg 912:1-Control Room; 2-diagnostic and control racks; 3-704 MHz 50 kW CW RF transmitter; 4- 704 MHz 1MW CW klystron; 5- 2MW CW HV power supply for the klystron; 6- magnets power supplies and other controls; 7-shielded ERL vault with removable beams; 8- 2 MeV 704 MHz SRF photo-injector; 9- 15-20 MeV 704MHz 5–cell SRF linac; 10 –return loop; 11- beam dump.

* This work is supported by Brookhaven Science Associates, LLC under Contract No. DE-AC02-98CH10886 with the U.S. DOE.
#dkayran@bnl.gov

ISBN 978-3-95450-126-7

REMOTE RF-SYNCHRONIZATION WITH FEMTOSECOND DRIFT AT PAL

Jungwon Kim, Kwangyun Jung, Jiseok Lim, KAIST, Daejeon, South Korea
Li-Jin Chen, Idesta Quantum Electronics, Newton, NJ, USA
Stephan Hunziker, PSI, Villigen, Switzerland
Franz Kaertner, CFEL, Hamburg, Germany
Heung-Sik Kang and Chang-Ki Min, PAL, Pohang, South Korea

Abstract

We present our recent progress in remote RF synchronization using an optical way at PAL. A 79.33-MHz, low-jitter fiber laser is used as an optical master oscillator (OMO), which is locked to the 2.856-GHz RF master oscillator (RMO) using a balanced optical-microwave phase detector (BOM-PD). The locked optical pulse train is then transferred via a timing-stabilized 610-m long optical fiber link. The output is locked to the 2.856 GHz voltage controlled oscillator (VCO) using the second BOM-PD, which results in remote synchronization between the RMO and the VCO. We measured the long-term phase drift between the input optical pulse train and the remote RF signals using an out-of-loop BOM-PD, which results in 2.7 fs (rms) drift maintained over 7 hours.

INTRODUCTION

In the last decade, optical timing and synchronization techniques, based on CW lasers or pulsed mode-locked lasers, have been intensively investigated for next generation light sources such as X-ray free-electron lasers (XFELs) [1-3]. One of the most important requirements for such femtosecond synchronization systems is precise (e.g., <10 fs rms phase drift) synchronization between multiple, remotely located accelerator-driving RF sources, which may enable lower jitter electron beam generation. For PAL-XFEL facility, we currently investigate the RF synchronization techniques based on an ultralow-jitter femtosecond mode-locked fiber laser as an optical master oscillator (OMO). In this paper, we present our recent progress toward the sub-10-fs drift remote RF synchronization. We used a balanced optical cross-correlator (BOC) [4] for the fiber link stabilization and a balanced optical-microwave phase detector (BOM-PD) [5] for the optical-RF synchronization. We also propose a new remote RF link stabilization scheme based on a fiber loop optical-microwave phase detector (FLOM-PD) [6,7], instead of BOC, to distribute RF through standard single-mode fiber links (such as SMF-28) without dispersion compensating fiber (DCF).

*Work supported by the PAL-XFEL Project, South Korea.
#jungwon.kim@kaist.ac.kr

REMOTE RF SYNCHRONIZATION USING A BOC-STABILIZED FIBER LINK AND BOM-PDS

The first type of a pulsed mode-locked fiber laser-based remote RF synchronization technique uses a BOC-based, timing stabilized fiber link and two BOM-PD-based local optical-RF synchronization units, as shown in Fig. 1. A 79.33-MHz repetition rate Er-fiber laser (manufactured by Toptica Photonics AG) is used as an OMO in this work. The OMO is locked to a 2.856-GHz RF master oscillator (RMO, Agilent E4438C vector signal generator in this work) by using a BOM-PD, which is based on a synchronous detection between the optical pulse train and the RF signal (more detailed information on the BOM-PD can be found in previous publications, such as refs. [1] and [5]). The use of a BOM-PD for optical-RF synchronization enables long-term stable, sub-10-fs precision synchronization between the mode-locked laser and the RF source. To lock the OMO to the RMO, an internal PZT in the OMO is used. The fiber link is a PPKTP-BOC stabilized, dispersion compensated (by connecting 160-m DCF with 450-m SMF-28), 610-m long fiber link, similar to the design shown in [1] and [4]. A PZT stretcher and a fiber coupled motor stage are used to compensate for the length fluctuations in the fiber link.

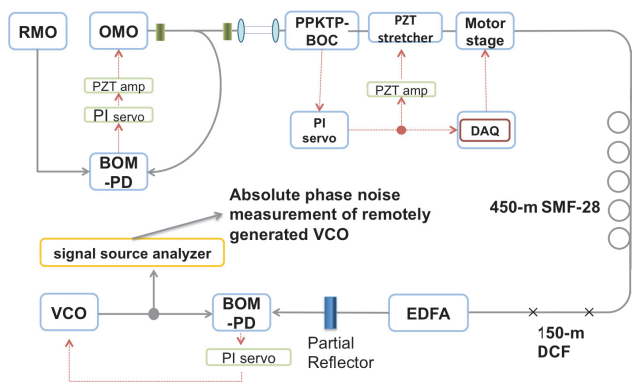

Figure 1: Schematic of remote RF synchronization. PI, proportional-integral; PZT, piezoelectric transducer; DAQ, data acquisition board; DCF, dispersion compensating fiber; EDFA, Er-doped fiber amplifier; VCO, voltage-controlled oscillator.

ISBN 978-3-95450-126-7

PROPOSAL FOR A SCHEME TO GENERATE A 10 TW POWER LEVEL, FEMTOSECOND X-RAY PULSES FOR BIO-IMAGING OF SINGLE PROTEIN MOLECULES AT THE EUROPEAN XFEL

S. Serkez, V. Kocharyan, E. Saldin, I. Zagorodnov, DESY, Hamburg, Germany
G. Geloni, European XFEL GmbH, Hamburg, Germany
O. Yefanov, Center for Free-Electron Laser Science, Hamburg, Germany

Abstract

Crucial parameters for bio-imaging experiments are photon energy range, peak power and pulse duration. For a fixed resolution, the largest diffraction signals are achieved at the longest wavelength supporting that resolution. In order to perform these experiments at the European XFEL, we propose to use a novel configuration combining self-seeding and undulator tapering techniques with the emittance-spoiler method. Experiments at the LCLS confirmed the feasibility of these three techniques. Their combination allows obtaining a dramatic increase the XFEL output peak power and a shortening of the photon pulse duration to levels sufficient for performing bio-imaging of single protein molecules at the optimal photon-energy range between 3 keV and 5 keV. We show here that it is possible to achieve up to a 100-fold increase in peak-power of the X-ray pulses at the European XFEL: the X-ray beam would be delivered in 10 fs-long pulses with 50 mJ energy each at a photon energy around 4 keV. We confirm by simulations that one can achieve diffraction before destruction with a resolution approaching the atomic scale.

INTRODUCTION

Infrastructure of the European XFEL facility offer a unique opportunity to build, potentially, a 10 TW-level x-ray source optimized for single biomolecule imaging. Crucial parameters for this application are photon energy range, peak power, pulse duration, and transverse coherence [1]-[5]. In fact, experimental requirements imply very demanding characteristics for the radiation pulse. In particular, the x-ray beam should be delivered in 10 fs-long pulses in the 10 TW-level, and within a photon energy range between 3 keV and 5 keV.

The baseline SASE undulator sources at the European XFEL will saturate at about 50 GW [6]. While this limit is very far from the 10 TW-level required for imaging of single biomolecules, there is a cost-effective way to improve the output power, when the FEL undulators are longer than the saturation length. All the requirements for single molecular imaging in terms of photon beam characteristics can be satisfied by a simple combination of self-seeding [7]-[26], emittance spoiler foil [27]-[29], and undulator tapering techniques [30]-[39]. Relying on these techniques we discuss a scheme of operation for a bio-imaging undulator source, which could be built at the European XFEL based on start-to-end-simulations for an electron beam with 1 nC charge [40]. We demonstrate that it is possible to achieve up to a 100-fold increase in peak power of the x-ray pulses: the x-ray beam would be delivered in about 10 fs-long pulses with 50 mJ energy each at photon energies around 4 keV.

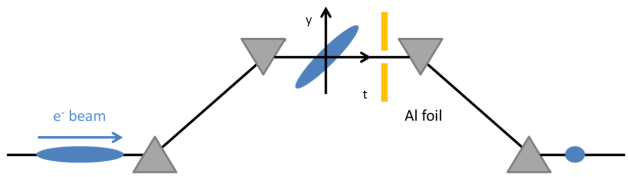

Figure 1: Sketch of an electron bunch at the center of the magnetic bunch compressor chicane (adapted from [28]).

SETUP DESCRIPTION

In order to provide bio-imaging capabilities, x-ray pulses should be provided with a tunable duration between 3 fs and 30 fs. While proposals exist to tune photon pulses at the European XFEL in this range, they require installation of additional hardware in the undulator system [41, 42]. Here we exploit a simpler method to reach the same results still assuming that the undulator system is long enough[1], but making only minimal changes in the undulator system[2]. A proposal [27, 28] and an experimental verification [29] have been made in order to generate femtosecond x-ray pulses at the LCLS by using a slotted spoiler foil located in the center of the last bunch compressor. The method takes advantages of the high sensitivity of the FEL gain process to the transverse emittance of the electron bunch. By spoiling the emittance of most of the beam while leaving a short unspoiled temporal slice, one can produce an x-ray FEL pulse much shorter than in the case when the original electron bunch is sent through the undulator.

Figure 1 shows a sketch of the slotted foil at the center of the third and last bunch compressor BC3 at the European XFEL. The last linac section before the third bunch compressor BC3 is set at an off-crest accelerating rf phase, so that the beam energy at the entrance of BC3 is correlated with time. Due to chromatic dispersion, this chirp transforms into in a $y - t$ bunch tilt in the chicane. At the center of BC3, i.e. at the point of maximum tilt, a thin foil is

[1] 40 undulator cells
[2] Only a single-chicane self-seeding setup with crystal monochromator is needed

ISBN 978-3-95450-126-7

FEMTOSECOND FIBER TIMING DISTRIBUTION SYSTEM FOR THE LINAC COHERENT LIGHT SOURCE*

Heng Li[1,3,4], Li-Jin Chen[5], Haynes Pak Hay Cheng[5], Justin E. May[4],Steve Smith[4], Kerstin Muehlig[4], Akshaya Uttamadoss[4,6], Josef C. Frisch[4], Alan R. Fry[4], Franz X. Kärtner[7,8], Philip H. Bucksbaum[1,2,3,4]

[1] Stanford PULSE Institute, [2] Department of Physics, and [3] Department of Applied Physics, Stanford University, Stanford, CA, USA
[4] SLAC National Accelerator Laboratory, Menlo Park, CA, USA
[5] Idesta Quantum Electronics, LLC, Newton, NJ, USA
[6] Department of Electrical Engineering, Princeton University, Princeton, NJ, USA
[7] Department of Electrical Engineering and Computer Science, and Research Laboratory of Electronics, Massachusetts Institute of Technology, Cambridge, MA, USA
[8] Center for Free-Electron Laser Science, DESY, and Physics Department, University of Hamburg, Hamburg, Germany

Abstract

We present the design and progress of a femtosecond fiber timing distribution system for the Linac Coherent Light Source (LCLS) [1-3] at SLAC to enable the machine diagnostic at the 10 fs level. The LCLS at the SLAC is the world's first hard x-ray free-electron laser (XFEL) with unprecedented peak brightness and pulse duration [1-3]. The time-resolved optical/x-ray pump-probe experiments at this facility open the era of exploring the ultrafast dynamics of atoms, molecules, proteins, and condensed matter [4-6]. However, the temporal resolution of current experiments is limited by the timing jitter between the optical and x-ray pulses [7, 8]. Recently, sub-25 fs root mean squared (rms) jitter is achieved from an x-ray/optical cross-correlator at the LCLS [9], and external seeding is expected to reduce the intrinsic timing jitter [10, 11], which would enable full synchronization of the optical and x-ray pulses with sub-10 fs precision. For such a technique, tight synchronization between seed and pump lasers needs to be implemented [12-16]. Preliminary test results of the major components for a 4 link system will be presented. Currently, the system is geared towards diagnostics to study the various sources of jitter at the LCLS.

INTRODUCTION

The emergence of few fs x-ray pulses generated from state-of-the-art XFELs [2, 3] has enabled the study of ultrafast phenomenon using optical/x-ray pump-probe techniques. In these time-resolved experiments, timing synchronization of x-ray and optical pulses at the precision of or below 10 fs is required, which is beyond the performance of traditional rf-based synchronization systems on the order of 100 fs rms [7]. Although it has been demonstrated recently that sub-10 fs precision can be reached by the x-ray optical cross-correlator and post-analysis [17], such characterization technique requires substantial x-ray pulse energy and it is not practical to install such device at every time-resolved experiment at the LCLS. In order to provide sub-10 fs precision, a pulsed laser timing synchronization and distribution system is adopted. The optical pulse train fulfils two tasks: first, it serves as the means for stabilizing the group delay of the pulses in the fiber link to a multiple of the repetition time of the pulses with femtosecond precision. Secondly, a fraction of the pulse train is coupled out from each end of the fiber link and is used to synchronize microwave or optical sub-systems to the reference rf. The optical-optical and optical-microwave synchronization modules used in the system are all based on balanced detection techniques which are with high dynamic range free of AM-to-PM noise conversion [12-16]. As a result, such systems allow for more accurate timing control in time-resolved experiments at the LCLS. On the other hand, it could serve as an alternative timing diagnostic tool when neither x-ray pulse nor x-ray/optical cross-correlator is available. In this paper, progress towards implementation of the pulsed laser timing system and preliminary experimental results are presented.

* This work is partially supported by the DOE STTR Award DE-SC0004702.

SYSTEM DESIGN AND EXPERIMENT

There are two major challenges in synchronizing the x-ray and optical pulses to the 10-fs level: one is to preserve the timing signal at the experimental hutches hundreds of meters downstream the accelerator RF pickup location [1]; the other is to precisely synchronize the Ti:sapphire lasers and transport the beam to the interaction point of the experiment. The proposed system layout for LCLS is shown in Fig. 1. We use a low-noise Er-doped fiber laser as the optical master clock (OMO). Since the undulator tunnel is usually inaccessible during beam time, the OMO is placed in the laser hall and its pulse train is sent to the end of the undulator tunnel through hundreds meters of timing-stabilized fiber-link (FLS) [12]. The timing signal encoded on the laser pulse train is compared against the accelerator RF picked up by the phase cavity using a balanced-optical microwave phase detector (BOM-PD) [13]. The baseband error signal is fed back to the OMO

ISBN 978-3-95450-126-7

FEASIBILITY STUDIES FOR ECHO-ENABLED HARMONIC GENERATION ON CLARA

I.P.S. Martin[1], R. Bartolini[1,2], N. Thompson[3,4]
[1]Diamond Light Source, Oxfordshire, U.K.
[2]John Adams Institute, University of Oxford, U.K.
[3]STFC Daresbury Laboratory, Sci-Tech Daresbury, Warrington, U.K.
[4]Cockroft Institute, Sci-Tech Daresbury, Warrington, U.K.

Abstract

The Compact Linear Accelerator for Research and Applications (CLARA) is a proposed single-pass FEL test facility, designed to facilitate experimental studies of advanced FEL techniques applicable to the next generation of light source facilities. One such scheme under consideration is Echo-Enabled Harmonic Generation (EEHG). In this paper we explore the suitability of CLARA for carrying out studies of this scheme, combining analytical and numerical calculations to determine likely hardware operating ranges, parameters tolerances and estimated FEL performance. A possible adaptation to convert EEHG into a short-pulse scheme is also considered.

INTRODUCTION

The Compact Linear Accelerator for Research and Applications (CLARA) is a proposed single-pass FEL test facility, the primary purpose of which is to provide a location where advanced FEL techniques can be studied experimentally [1]. The layout for CLARA has been designed to be flexible, with a range of possible experiments considered from an early stage.

The main focus of CLARA is the production of ultrashort pulses of coherent light. Alongside this, there are a large number of other topics of interest, such as novel schemes to improve the FEL intensity and wavelength stability, methods to improve the longitudinal coherence, and demonstrating higher harmonic radiation from bunches conditioned by an external laser seed source.

Echo-Enabled Harmonic Generation (EEHG) [2, 3] is one of the techniques that has been studied explicitly for CLARA. This scheme requires two energy modulation plus chicane stages to be installed upstream of the main radiator section. These are used to induce a fine-structure density modulation in the electron bunch before it passes through the radiators, and so the specifications for these components must be compatible with the requirements for the EEHG scheme. Similarly, it is important to quantify in advance what the spectral and temporal FEL pulse characteristics are likely to be in order to inform the choice of photon diagnostics to be installed on CLARA. It is also important to establish at an early stage whether there are any limiting effects that may prevent successful demonstration of the scheme on CLARA. For example, incoherent synchrotron radiation (ISR) emission in the first chicane could increase the energy spread and blur out the fine-structure energy bands present in the beam. This may not be an issue for CLARA because of the relatively low beam energy. Alternatively, the EEHG-induced micro-bunching could lead to significant coherent synchrotron radiation (CSR) emission in the second chicane, particularly in the final dipole. The bunching could be degraded by R_{51} leakage from the chicanes, by space-charge (SC) or intra-beam scattering (IBS) effects, or during beam transport to the FEL due to the finite beam emittance and energy spread. All of these issues can be investigated in advance using sophisticated particle tracking and FEL simulation codes.

Table 1: Simulated Electron Bunch Parameters at FEL

Parameter	Value
Charge (pC)	250
Energy (MeV)	228
RMS Pulse length (fs)	250
Peak current (A)	400
Normalized emittance (mm.mrad)	0.6
Energy Spread (keV)	75

In this paper we summarise the studies that have been made for EEHG on CLARA, starting with the analytical calculations used to determine likely hardware operating ranges and parameter tolerances. These are supplemented by in-depth numerical simulations of the standard EEHG configuration, followed by preliminary studies of a possible adaptation of EEHG to a short-pulse generation scheme.

ANALYTICAL STUDIES

CLARA Parameters

The main CLARA linac consists of an S-band, normal conducting linac, combined with an X-band 4th harmonic linearising RF cavity and standard C-type bunch compressor [1]. Depending upon the particular experimental requirements, several different operating modes are foreseen for the main linac, including 'SASE' (short bunch), 'seeded' (long bunch), 'single-spike', 'multi-bunch' and 'industrial applications' modes. For EEHG, it is anticipated the linac will be run in the seeded mode, for which the accelerator working point is optimised to produce a flat-top current profile. This is intended to minimise the sensitiv-

ISBN 978-3-95450-126-7

EEHG AND FEMTOSLICING AT DELTA*

R. Molo†, M. Höner, H. Huck, M. Huck, S. Khan, A. Schick, P. Ungelenk
Center for Synchrotron Radiation (DELTA), TU Dortmund University, Dortmund, Germany

Abstract

The ultrashort-pulse facility at DELTA, a 1.5-GeV synchrotron light source operated by the TU Dortmund University, is currently based on the coherent harmonic generation (CHG) technique and will be upgraded using echo-enabled harmonic generation (EEHG) in order to reach shorter wavelengths. Laser-induced energy modulation is employed in the CHG and EEHG schemes to create a periodic electron density modulation, but can also be used to generate ultrashort pulses of incoherent radiation at arbitrary wavelengths by transversely displacing the off-energy electrons (femtoslicing). A new storage ring lattice for DELTA will be presented that not only offers enough space for an EEHG and femtoslicing setup, but also allows to operate both radiation sources simultaneously.

INTRODUCTION

DELTA is a 1.5-GeV synchrotron light source operated by the TU Dortmund University. A sketch of the facility is shown in Fig. 1. The storage ring has a circumference of 115.2 m and comprises two undulators (U55, U250) and a superconducting asymmetric wiggler (SAW). The bunch length, approximately 100 ps, determines the duration of the synchrotron radiation pulses. In contrast to that, state-of-the-art femtosecond laser systems generate radiation pulses with durations of about 20-40 fs, but with wavelengths in the near-visible regime. The techniques outlined below allow for the generation of ultrashort synchrotron radiation pulses by a combination of insertion devices and a femtosecond laser system.

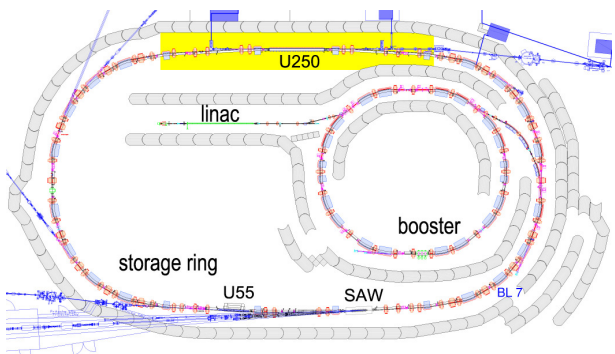

Figure 1: Schematic plan of the DELTA synchrotron radiation facility. The CHG setup is located in the northern part of DELTA denoted by the yellow field.

* Work supported by BMBF, by the DFG, by the Helmholtz ARD Initiative and by the Federal State NRW.
† robert.molo@tu-dortmund.de

Coherent Harmonic Generation (CHG)

The CHG scheme [1–3] is shown schematically in Fig. 2. A short laser pulse co-propagates with a long electron bunch in the first undulator, also referred to as modulator. The laser pulse interacts only with a short slice of the electron bunch, resulting in a sinusoidal modulation of the electron energy with the periodicity of the laser wavelength. A subsequent magnetic chicane converts the energy modulation into a density modulation (microbunching) which gives rise to coherent radiation in the second undulator (also called radiator) that is more intense than the incoherent light generated by the whole bunch.

The radiated power of the nth harmonic of the laser wavelength is given by [4]

$$P_n(\lambda) \sim N^2 b_n^2(\lambda), \tag{1}$$

where N is the number of modulated electrons in the bunch, and $b_n(\lambda)$ is the bunching factor [4]

$$b_n(\lambda) \sim e^{-n^2} \tag{2}$$

that decreases exponentially with the square of the harmonic number for CHG. Due to this intrinsic limitation, the CHG technique is limited to harmonics $n < 10$.

The CHG facility at DELTA is under commissioning [5, 6] and located in the northern part of DELTA (see Fig. 1). Presently, the 5th harmonic of 400 nm from frequency-doubled Ti:sapphire laser pulses can be generated. In future, a seeding wavelength of 266 nm will be used in order to produce shorter wavelengths.

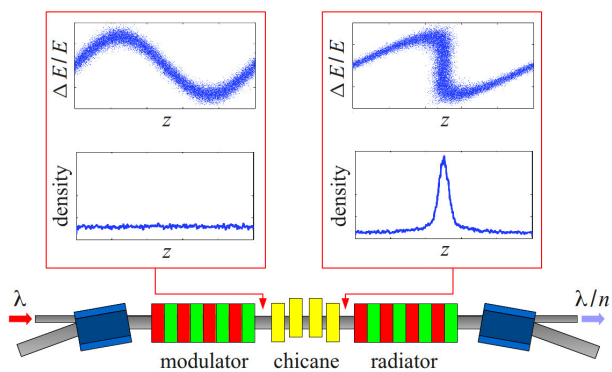

Figure 2: Sketch of the CHG scheme with two undulators and one chicane. The longitudinal phase space plots show the electron distribution before and after the chicane. A peak in the electron density indicates microbunching.

ISBN 978-3-95450-126-7

DESIGN STUDIES FOR FLUTE, A LINAC-BASED SOURCE OF TERAHERTZ RADIATION

S. Naknaimueang, V. Judin, S. Marsching, A-S. Müller, M. J. Nasse, R. Rossmanith, R. Ruprecht, M. Schreck, M. Schuh, M. Schwarz, M. Weber, P. Wesolowski,
KIT, Karlsruhe, Germany
W. Hillert, M. Schedler, University of Bonn, ELSA, Germany

Abstract

FLUTE is a linac-based THz source with a nominal beam energy of 40-50 MeV, which is presently under construction at KIT and in collaboration with PSI and DESY. FLUTE will be operated in a wide bunch charge range of 1 pC-3 nC. The source will allow studies of different mechanisms of THz radiation generation and will serve as a test facility for related accelerator technology. In this paper the basic layout design of FLUTE is discussed.

INTRODUCTION

Terahertz radiation has recently become an important tool in a variety of applications. The production of high-intensity THz radiation with accelerators is based on the compression of electron bunches to lengths of below one picosecond either in storage rings or in linear accelerators. In linear accelerators two compression schemes are known: compression either by velocity bunching (if the energy of the particles is nonrelativistic) or in a chicane (for relativistic particles). In both cases the particle energy must vary as a function of longitudinal position (chirp). In storage rings a so-called low-alpha optics allows the production of short bunches [1]. The reduction of the bunch length is limited by instabilities of the beam [2].

Recently, a new technique to generate coherent THz radiation based on beams produced by laser wake field accelerators was investigated [3]. The advantage of the THz radiation generated by laser wake field accelerators is that the originally produced electron bunch already has a length of only a few femtoseconds. Therefore bunch compression is not necessary. Nevertheless, reproducibility and stability are still a problem with this technique. An overview of laser-based THz sources can be found in [4].

FLUTE will become a linac-based THz source where various techniques of compressing and measuring short bunches can be tested and optimized. With the basic design of FLUTE (final particle energy of 40 to 50 MeV) bunch lengths between 10 fs to 300 fs with a bunch charge ranging from 1 pC to 3 nC can be obtained. After compression, THz radiation can be produced either by coherent synchrotron radiation, - edge radiation or - transition radiation (CSR, CER, CTR).

BASELINE MACHINE DESIGN

The baseline layout of FLUTE [5–7] is shown in Fig. 1. A 3 GHz laser-driven RF gun produces a bunch with a charge from 1 pC to 3 nC and a bunch length of several picoseconds. Such a bunch is then accelerated to 40-50 MeV and compressed subsequently by a magnetic bunch compressor consisting of four dipole magnets (D-shape chicane).

The beam simulation programs ASTRA [8] and CSRtrack [9] are used to minimize the bunch length for the different bunch charges. Since the beam energy of FLUTE is relatively low, CSR effects determine the length of the compressed bunch. In the gun and linac the particle beam is simulated with ASTRA, whereas in the chicane the 1D and 3D routines of CSRtrack are used to simulate the CSR backreaction on the bunch. The 3D option gives a more reliable result for the RMS compressed bunch length (L_{rms}) for our beam energy (≈ 40 MeV).

Table 1: RMS Compressed Bunch Length for Various Bunch Charges

Charge [nC]	Laser pulse length [ps]	Laser spot size [mm]	$-R_{56}$ [mm]	L_{rms} [fs]
3	4	2.25	36.1	270
2	4	1.50	32.5	224
1	3	1.50	34.2	146
0.1	2	0.50	29.5	67
0.001	1	0.50	28.8	13

The simulations showed that the length of the chicane magnets has little influence on the compression factor. From a technical point of view dipole magnets with a length of 20 cm were chosen. The space between the first two and the last two magnets is 30 cm, respectively. The RMS compressed bunch lengths for various bunch charges are shown in Table 1.

The bunch profiles for a 3 nC bunch after the bunch compressor obtained with 1D and 3D simulations are shown in Fig. 2. For a lower bunch charge (1 pC), the differences between 1D and 3D calculations are presented in Fig. 3. For lower bunch charges CSR effects are significantly smaller and results in fewer differences between the 1D and 3D calculations.

On one hand, the longer the compressed bunch length is,

ISBN 978-3-95450-126-7

STUDY ON ELECTRON BEAM STABILIZATION IN KU-FEL

Kensuke Okumura#, Heishun Zen, Motoharu Inukai, Yusuke Tsugamura, Kenta Mishima,
Torgasin Konstantin, Hani Negm, Omer Mohamed, Kyohei Yoshida,, Toshiteru Kii,
Kai Masuda, Hideaki Ohgaki
Institute of Advanced Energy, Kyoto University
Gokasho, Uji, Kyoto, Japan, 611-0011

Abstract

A stable electron beam is essential for a stable FEL operation. In Kyoto University MIR-FEL facility (KU-FEL), a Beam Position Monitor (BPM) system consisting of six 4-button electrode type BPMs and signal processing unit was installed for monitoring of the electron beam position. Fluctuations of the electron beam position have been observed both in horizontal and vertical directions. In horizontal direction, the main fluctuation source could be the energy fluctuation of the electron beam generated by the thermionic RF gun. One of candidate of the energy fluctuation, the cavity temperature of the RF gun has been suspected, because the gun is operated in detuned condition which enhances beam energy dependence on the cavity temperature. Another candidate is the fluctuation of the RF power fed to the RF gun. The both effects were experimentally investigated. We observed a small fluctuation of the beam energy corresponding to the cavity temperature fluctuation. But the large fluctuation of the RF power which was induced by change of temperature of ferrite slabs in the 4-port circulator was clearly observed. A temperature-stabilized water circulation system will be prepared for the ferrite slabs to stabilize the RF power fed to the RF gun.

INTRODUCTION

Stabilization of an electron beam is crucial to stabilize the FEL power fluctuation. We have been working on our resonator type MIR-FEL to supply stable FEL beams to users in Kyoto University FEL facility, KU-FEL. We have introduced 4-button type Beam Position Monitor (BPM) to construct a beam position feedback system. As the result, the beam position displacement in horizontal and in vertical were reduced down to a few tens μm. The FEL power fluctuation was largely reduced from its' original value of 40% to 20% [1]. However, further studies are required to find the source of the fluctuation of electron beam position. In horizontal direction whose position fluctuation is 2-3 times larger than that in the vertical direction, the energy fluctuation of the electron beam should be dominant. Therefore we investigate the energy fluctuation in the electron beam, especially in the RF gun. In this paper we will briefly describe the result of examination, proposed measures, and future plan.

REDUCTION OF FLUCTUATION OF BEAM POSITION BY BPM SYSTEM

The KU-FEL consists of 4.5-cell S-band thermionic RF gun, a 3-m accelerator tube, a 1.8-m Hybrid undulator, and an optical resonator [2]. Figure 1 shows the structure of KU-FEL.

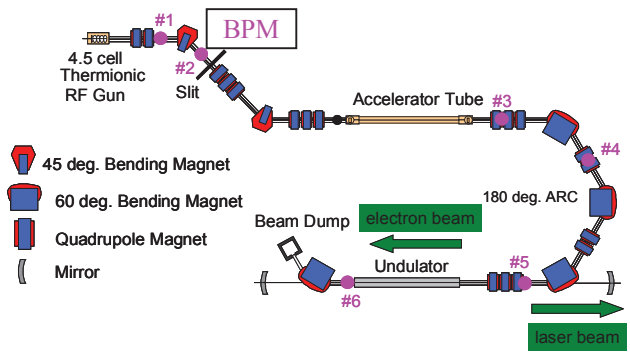

Figure 1: Layout of KU-FEL

In Figure 1, #1-#6 indicate the position of each BPM. We focus on the feedback system in the low-energy part (from RF gun to the entrance of accelerator tube). At first, the set value of Klystron high-voltage power supply (Klystron voltage) was adjusted by using the information of the horizontal movement obtained from BPM #2 to keep the energy of the electron beam constant. The fluctuation of electron beam position was substantially reduced because of this feedback control system. Moreover, the fluctuation of electron beam position which was not able to be compensated by above feedback control system was compensated by the other feedback system which uses the horizontal steering magnet. As the result, it became possible by combining these two feedback systems to reduce the fluctuation of electron beam position in the low energy part. We succeeded to stabilize the FEL power fluctuation [1].

ISBN 978-3-95450-126-7

SIMULATION RESULTS OF SELF SEEDING SCHEME IN PAL-XFEL

Yong Woon Parc#, Heung Sik Kang, Jang Hui Han, Ilmoon Hwang, PAL, Korea
In Soo Ko, Dep. Of Physics, POSTECH, Pohang, Korea
Juhao Wu, SLAC National Accelerator Laboratory, Menlo Park, CA 94025, U.S.A

Abstract

There are two major undulator lines in Pohang Accelerator Laboratory XFEL (PAL XFEL), soft X-ray and hard X-ray. For the hard X-ray undulator line, self-seeding is the most promising approach to supply narrow bandwidth radiation to the users. The electron energy at hard X-ray undulator is 10 GeV and the central wavelength is 0.1 nm. We plan to provide the self-seeding option in the Phase I operation of PAL-XFEL. In this talk, the simulation results for the self-seeding scheme of hard X-ray undulator line in PAL XFEL will be presented.

INTRODUCTION

PAL-XFEL is now under construction in Pohang Accelerator Laboratory (PAL) site [1]. The undulator used in PAL-XFEL hard X-ray undulator hall has 24.4 mm period to make 0.1 nm radiation with 10 GeV electron beam. To supply an X-ray with good longitudinal coherence and high photon flux to users, self-seeding technique will be applied in the hard X-ray undulator line [2]. Using [0 0 4] optical plane of a diamond crystal, we can generate a seed X-ray with 0.15 nm wave length [3]. To meet the resonance condition in the undulator in PAL-XFEL, the electron beam energy will be adjusted as 8.126 GeV in the self-seeding operation. In this study, a preliminary simulation results for the self-seeding scheme for PAL-XFEL are presented with 8.126 GeV electron beam.

BEAM PROPERTIES

Electron beam properties at the entrance of hard X-ray undulator in PAL-XFEL with self-seeding scheme are listed in Table 1.

Table 1: Electron Beam Properties

Beam energy	8.126 GeV
Total charge	100 pC
Peak current	4 kA
Emittance	0.15 mm mrad
Energy spread	0.022 %

In PAL-XFEL, basic target wavelength in hard X-ray beamline is 0.1 nm with 10 GeV energy electron beam. However, for the self-seeding operation in Phase I, the wave length 0.15 nm is chosen [3], beam energy must be adjusted to 8.126 GeV to meet the resonance condition in the undulator.

The detail slice parameters used in this simulation are presented in Fig. 1. The beam current shown in Fig. 1 (a) has no horns and looks like almost a Gaussian profile with 3 um standard deviation. The horizontal direction (x) emittance values keep almost 0.15 mm mrad level. The vertical direction (y) emittance shows a little higher value than x-emittance, however almost values are lower than 0.25 mm mrad. Beam energy in Fig. 1(c) shows an energy chirp which is not a final optimized result for PAL-XFEL operation. γ_0 in Fig. 3 is 15902 which is the relative factor of 8.126 GeV. Energy spread is lower than 0.022 % in all slices as shown in Fig. 1(d).

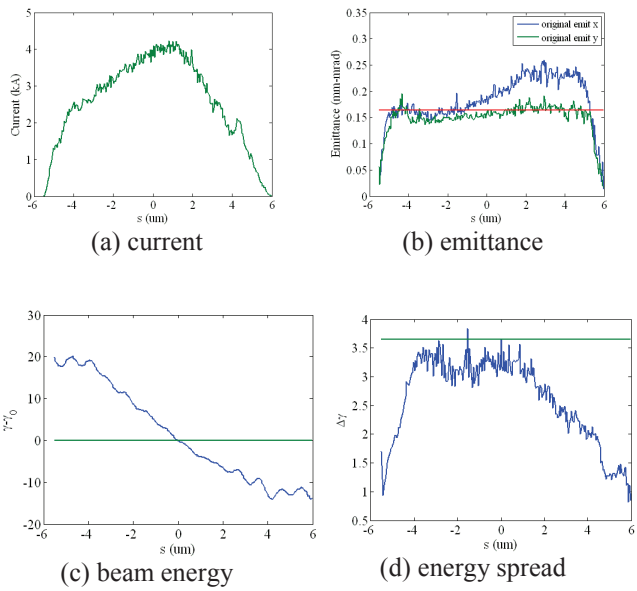

Figure 1: Slice properties of electron beam used in the simulation.

In the first 30 m of undulator line at hard X-ray undulator hall, the electron beam is sent through the undulator to generate 1 GW level radiation as shown in Fig. 2, to make seed radiation using diamond crystal with optical plane [0 0 4] which thickness will be 100 μm. In Fig. 2(a), the steady state simulation result is shown by black line. It reaches 13 GW level at the saturation position. Time dependent simulation result is shown by green line and the current profile is shown by same color line also in Fig. 2(b). Time dependent simulation shows 1 GW radiation power around 30 m position which

#young1@postech.ac.kr

ISBN 978-3-95450-126-7

SIMULATION STUDIES OF FELS FOR A NEXT GENERATION LIGHT SOURCE

G. Penn*, P.J. Emma, G. Marcus, J. Qiang, M. Reinsch, LBNL, Berkeley, CA 94720, USA

Abstract

Several possible FEL beamlines for a Next Generation Light Source are studied. These beamlines collectively cover a wide range of photon energies and pulse lengths. Microbunching and transverse offsets within the electron beam, generated through the linac, have the potential to significantly impact the longitudinal and transverse coherence of the x-ray pulses. We evaluate these effects and set tolerances on beam properties required to obtain the desired properties of the x-ray pulses.

INTRODUCTION

The Next Generation Light Source (NGLS) is envisioned to serve as a powerful soft x-ray FEL user facility with multiple beamlines driven by a CW superconducting linear accelerator. The bunch repetition rate could be up to 1 MHz. Here, we study a self-seeded beamline and a two-stage HGHG beamline driven by a UV laser seed. Both beamlines are capable of yielding up to 10^{12} photons/pulse. We study the performance of these beamlines at different photon energies and using different models for the electron bunches. The focus is on start-to-end (S2E) simulations. We shall see that the performance of the FEL beamline is strongly dependent on the quality and especially uniformity of the electron bunch.

BEAMLINE PARAMETERS

The electron bunch charge is taken to be 300 pC, and it is accelerated to 2.4 GeV. The nominal slice parameters are 500 A current, 150 keV rms energy spread, and 0.6 micron emittance. Various full start-to-end simulations starting from the injector [1] and passing through a SC linac [2] are broadly consistent with those values. The peak current is typically not flat but varies from 450 A to 600 A. The energy spread is controlled by the use of a laser heater [3] in order to damp out microbunching instabilities, but can still varies with position within the bunch, typically in the range 150 keV to 200 keV. The slice emittance ranges between 0.5 micron and 0.7 micron. However, the beamlines are designed to be able to handle a worse beam emittance of up to 0.9 μm, as well as an energy spread of 200 keV.

We focus on undulators using superconducting (SC) technology with relatively short undulator period, to provide the full tuning range with reasonably large (not much smaller than unity) dimensionless undulator parameter at the highest photon energy. SC undulators have the advantage of being able to produce higher magnetic fields for a larger gap, especially for undulator periods shorter than 30 mm. This allows for more compact beamlines, lower energy beams, and larger undulator parameters. There is also the possibility that SC undulators will be more robust to the environment resulting from a high average beam power that could approach 1 MW. The magnetic gap is 6 mm, to allow clearance for an inner diameter beampipe of 4 mm. Superconducting technology is especially critical for the x-ray producing undulators. The undulator sections have a length of 3.3 m, typically with breaks of 1.1 m containing a quadrupole, phase shifter, orbit correctors, and several diagnostics. Both beamlines have a final cross-planar undulator [4] for polarization control.

The self-seeding scheme [5, 6], shown in Fig. 1, uses undulators with a 20 mm period. Using Nb_3Sn technology can yield a peak undulator parameter of $K = 5$ [7], and a tuning range of 0.2 – 1.5 keV. The beamline consists of two stages separated by a chicane. Within the chicane, the electron bunch is displaced from the radiation field, and the radiation is passed through a monochromator with resolution $R = 20,000$ (relative FWHM bandwidth of 5×10^{-5}), and 2% efficiency within that bandwidth. The chicane also serves to debunch the beam, allowing the filtered radiation pulse to act as a low-bandwidth seed in the second stage. Because a significant amount of undulator length is required in addition to what is needed to reach saturation using SASE, the practical tuning range for the self-seeding is 0.2 – 1.2 keV. However, the monochromator can be removed to extend the tuning range up to 1.5 keV under SASE operation.

At a resonant photon energy of 1.2 keV, the gain length is 2.0 m, and the effective FEL parameter is 4×10^{-4}. The effective shot noise power is 35 W. To ensure that shot noise is strongly suppressed in the second stage, we intend to keep the seeding power delivered by the monochromator above 100 times this value, or 3.5 kW.

The HGHG beamline, shown in Fig. 2, uses undulators with a 23 mm period, for a peak undulator parameter of $K = 6.8$ and a tuning range of 0.1 – 1 keV. Because the output x-ray pulse must be generated from a UV laser seed through harmonic upshifting, a reasonable practical limit for the highest output photon energy is 0.72 keV, just above the Fe L-edges. This design closely follows that of the FEL-2 beamline of FERMI@Elettra [8], except that the parameters are pushed for a higher overall harmonic jump and longitudinal coherence.

The laser seed is taken to be tunable over the range 215 – 260 nm. The duration of the pulse can range from 100 fs down to below 20 fs. The nominal peak power is 200 MW, but for the shortest pulse the peak power will have to

* gepenn@lbl.gov

ISBN 978-3-95450-126-7

FLASH2 BEAMLINE AND PHOTON DIAGNOSTICS CONCEPTS

Elke Plönjes#, Bart Faatz, Josef Feldhaus, Marion Kuhlmann, Kai I. Tiedtke, Rolf Treusch
Deutsches Elektronen-Synchrotron, Hamburg, Germany

Abstract

The FLASH II project will upgrade the soft X-ray free electron laser FLASH at DESY into a multi-beamline FEL user facility with the addition of a second undulator line FLASH2 in an additional tunnel. The FLASH linear accelerator will drive both undulator lines and FLASH2 will be equipped with variable-gap undulators to be able to deliver two largely independent wavelengths to user endstations at FLASH1 and FLASH2 simultaneously. A new experimental hall will offer space for up to seven user endstations, some of which will be installed permanently. The beamline system will be set up to cover a wide wavelength range and it will include online photon diagnostics for machine operators and users. Up to three beamlines will be capable of transporting the 5th harmonic at 0.8 nm and a fundamental in the water window while others will cover the longer wavelengths of 6 - 40 nm and beyond. Civil construction and installations of FLASH2 are on-going and first beam is expected for early 2014.

INTRODUCTION

FLASH, the free electron laser user facility for the XUV and soft X-ray range at DESY, has delivered high brilliance radiation for photon experiments since 2005 [1-3]. The FLASH II project will upgrade FLASH into a multi-user facility. The new tunnel and experimental hall have space for two new undulator lines, FLASH2 and FLASH3, with respective beamlines. Within the FLASH II project the first new undulator line FLASH2 is realized with initially one photon beamline.

The FLASH linac drives both the FLASH1 fixed gap undulator line and the new FLASH2 variable gap undulator line as shown in Figure 1. Only moderate modifications in the linear accelerator section are needed, such as a second injector laser, and the addition of an electron kicker to kick the electron bunches into FLASH2. Due to the simultaneous use of one accelerator the electron beam energy is the same for both beamlines. The FLASH2 undulators have gaps variable from 9 to 20 mm to allow for a significant tuning range for FLASH2 at the various wavelength of FLASH1 [4,7]. Thus, FLASH will operate two FEL beams in parallel and double the user beamtime, which is presently overbooked by about a factor of four. Details of FLASH, its parameters, and the necessary modifications of the machine for the FLASH II project are found in [5-8]. Table 1 lists the electron- and photon-beam parameters of FLASH2, including possible upgrades.

The experimental Hall of FLASH2 (and FLASH3) is a civil construction of 60.5 by 33 meters. It will house a 14 m long main photon diagnostics section for users, up to seven FLASH2 and in the future also several FLASH3 beamlines [4]. Similar to FLASH1, a THz beamline [9] and an optical laser system [10] for pump-and-probe experiments complete the user facility. The wide wavelength range, which is covered by FLASH2, poses significant challenges for the optics layout.

PHOTON DIAGNOSTICS

Tunnel

In the new FLASH II tunnel, a set of photon diagnostics serves mainly the machine for optimization of the photon beam. It is positioned directly behind the electron beam dump bending magnet.

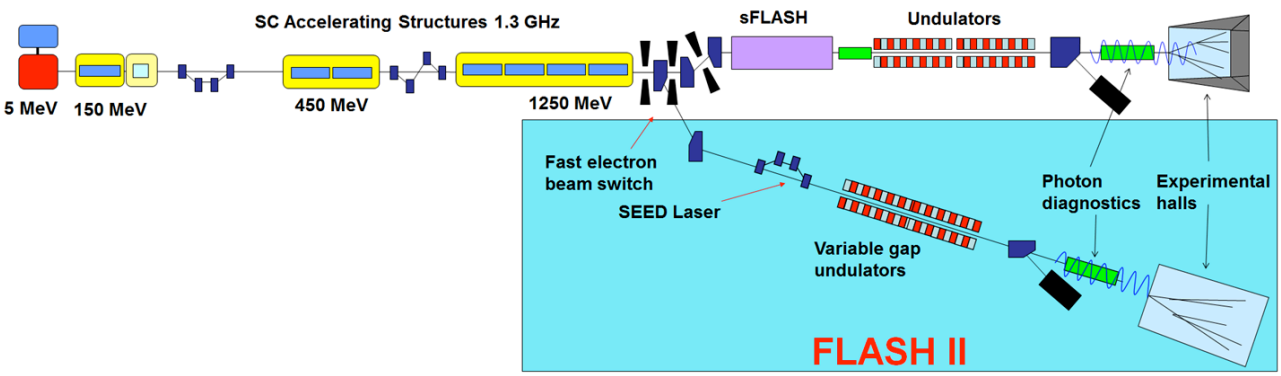

Figure 1: Layout of the FLASH facility with two undulator lines FLASH1 and FLASH2 (not to scale).

#elke.ploenjes@desy.de

ISBN 978-3-95450-126-7

SELF-SEEDING DESIGN FOR SwissFEL

E. Prat and S. Reiche, PSI, Villigen, Switzerland

Abstract

The SwissFEL facility, presently under construction at the Paul Scherrer Institute, will provide SASE and self-seeded FEL radiation at a hard (1-7 Å) and soft (7-70 Å) X-ray FEL beamlines. This paper presents the current status of the self-seeding design for SwissFEL. The layout and full 6D start-to-end simulation results are presented for the hard X-ray beamline. Studies for different charges and optimization of the first and second undulator stages are shown.

INTRODUCTION

Seeding for FELs has several advantages in comparison to SASE radiation: the longitudinal coherence is increased and therefore the FEL brilliance is improved, the pulse to pulse central wavelength is stabilized, the temporal pulse shape is smoothened, the gain length is reduced, etc.

Up to now self-seeding is the only seeding strategy that has been demonstrated with a hard X-ray FEL [1, 2]. A proof-of-principle experiment of the self-seeding scheme based on the proposal of Geloni et al [2] was successfully carried out at LCLS for hard X-rays at the beginning of 2012 [3]. For soft X-rays, self-seeding [4] is presently the only seeding scheme that does not exhibit stringent short wavelength limitations, like all laser-based approaches do, therefore being the most robust and lowest risk strategy to seed a soft X-ray [5]. Self-seeding operation is planned at SwissFEL at 2017 for the hard X-ray beamline for a wavelength down to 1 Å, and at a later phase for the soft X-ray beamline down to a wavelength of 1 nm [6].

Figure 1 shows a generic layout of the self-seeding scheme for soft and hard X-rays. The first undulator stage produces standard SASE-FEL radiation. After that the FEL radiation goes through a monochromator, while the electron beam travels through a magnetic chicane. In the second undulator stage the transmitted radiation overlaps with the electron beam to produce seeded-FEL radiation. The magnetic chicane has three functions: it delays the electron to allow the longitudinal overlap between the electron and photon beams, it smears out the electron bunching created at the first undulator section, and it separates the electrons from the radiation so that intercepting optical elements for the filtering of the X-rays can be placed. The first undulator stage works in the exponential regime before saturation to avoid a blow-up of the energy spread of the electron beam that would prevent the beam to amplify the FEL signal in the second stage. At the same time it has to provide sufficient FEL radiation so that the seed power is well above the shot-noise level at the second undulator stage. The difference between the hard and the soft X-ray is the method to produce a monochromatized signal: for soft X-rays a grating monochromator can be used, while for hard X-rays a Bragg-crystal (e.g. diamond) is employed. For both cases the intersection with the monochromator and the chicane can be presently placed in a space of about 4 m length, i.e. the space occupied by a SwissFEL undulator module.

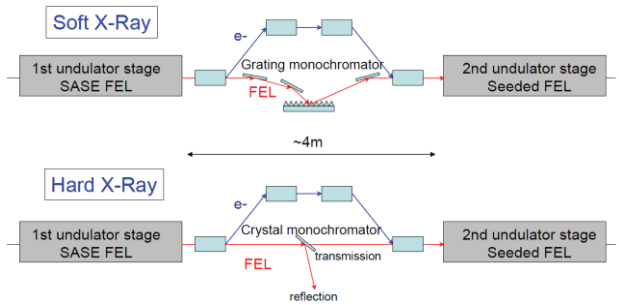

Figure 1: Generic layout of the self-seeding scheme.

SwissFEL will operate with electron beam charges varying between 10 and 200 pC. A study for the hard X-ray beamline for 10 pC using design parameters was shown one year ago at this conference [7]. The main goal of the present work is to analyze if it is possible to produce saturated self-seeded FEL at 200 pC within the available space and equipment (12 undulator modules and the chicane). This time we have used electron distributions obtained from start-to-end calculations as an input for the FEL simulations. We have also redone the simulations for 10 pC with the start-to-end simulation distribution of the electron beam. For both charges we have optimized the number of modules to be used at the first stage (thus the location of the monochromator chicane) and we have applied detuning and tapering to maximize the FEL performance at the second stage. Concerning the soft X-ray beamline, a design based on nominal beam parameters for 200 pC was already done [7]. However, it is still pending to confirm this design with parameters obtained from start-to-end calculations.

LAYOUT AND SIMULATIONS SETUP

The present design lattice for the hard X-ray beamline consists of 12 undulator modules. Each of them is 4 m long, has a period length of 15 mm and a variable gap. The distance between modules is 0.75 m. In addition we have reserved the same space for the crystal monochromator and the chicane. The facility is able to accommodate up to seven more modules for potential future upgrades such as tapering. The beam energy is between 2.1 GeV and 5.8 GeV, corresponding to a radiation wavelength range between 1 Å and 7 Å. The present study is done for a wavelength of 1 Å.

The four dipoles of the magnetic chicane are 0.4 m long each and can deflect the electron beam up to an angle of half a degree at 6 GeV. The drifts between the first and second dipole and between the third and fourth magnet are about 0.35 m long, and the distance between the

ISBN 978-3-95450-126-7

HARMONIC LASING AT THE LCLS

D. Ratner*, Z. Huang, P. Montanez, SLAC, Menlo Park, California, USA
W. Fawley, N. Rodes, LBNL, Berkeley, California, USA
E. Schneidmiller, M. Yurkov, DESY, Hamburg, Germany
E. Allaria, Elettra-Sincrotrone Trieste S.C.p.A., Basovizza, Italy

INTRODUCTION

The fundamental of the Linac Coherent Light Source (LCLS) produces X-FEL radiation to above 10 keV photon energy. Users that require even harder X-rays can make use of the third harmonic, which typically represents 0.5-2% of the total lasing power. This non-linear harmonic radiation is driven by lasing at the fundamental; the resulting microbunching includes sharp density modulations that include high harmonic components. It has been pointed out [1, 2] that linear harmonic production, in which the FEL lases independently at the third harmonic, can produce even higher power radiation.

This paper describes plans to test harmonic lasing using the methods of Ref. [2]. The first half of the FEL produces radiation at both the fundamental and the third harmonic. Inserting an attenuator into the path of the X-ray beam removes the SASE power at the fundamental. A chicane bends the electrons around the attenuator and also resets the microbunching to shot noise. The remaining third harmonic then dominates the startup process in the second half of the FEL. Harmonic lasing will be tested during commissioning of the soft x-ray self seeding system. If tests are successful, it is possible to add additional attenuators or phase shifters to further increase power and create a new LCLS user mode.

LINEAR VS. NON-LINEAR LASING

The normal FEL process produces sharp microbunching of electrons, with each microbunch separated by the resonant wavelength of the undulator. If the microbunching is sufficiently sharp, the Fourier transform of the current density will include strong harmonic components. As a result, we expect exponential growth of coherent emission at the harmonics of the resonant wavelength. This process is known as non-linear harmonic generation. While harmonic bunching is strongest at the second harmonic, the symmetry of a planar undulator suppresses on-axis radiation at even harmonics, so the strongest harmonic radiation is expected at the third harmonic. At LCLS, the third harmonic can typically produce on the order of 1% the power of the fundamental [3].

An alternative approach is to drive the FEL process itself at a harmonic of the undulator's resonant wavelength. At LCLS, the undulators have a K value of 3.5, produces strong coupling at the third harmonic. Typically harmonic lasing would not be observable, because the gain length is shortest at the fundamental; the fundamental saturates and stops the FEL process before the harmonics can grow to a useful level. However, in principle it is possible to suppress the fundamental so that the harmonics are free to saturate. Ref. [1] proposed inserting periodic $2\pi/3$ or $4\pi/3$ phase shifts into the undulator line. The phase shifts suppress the fundamental radiation by forcing the electrons into an inverse-FEL phase, but they have no effect on the third harmonic. As a result, the third harmonic is able to saturate before the fundamental.

The periodic phase shifts are largely ineffective for SASE FELs, where the offset in phase merely shifts the resonant wavelength [2]. However, Ref. [2] shows that it is possible to suppress the SASE fundamental by varying the phase shift between $0, 2\pi/3$ and $4\pi/3$. Inserting an attenuator that preferentially blocks the fundamental further enhances the relative level of the harmonics.

At LCLS, FEL photon energy changes are made through the electron energy, so there are no phase shifters between the undulators and the harmonic phase shift option is not available at this time. However, a chicane is currently under development for the soft X-ray self seeding (SXRSS) project, and it is possible to fit an attenuator into the SASE path where the electrons have been displaced to one side. In addition, the hard X-ray self-seeding chicane [4] can be used as a phase shifter. We propose to use both an attenuator and phase shift to preferentially select lasing at the third harmonic (Fig. 1). We aim to demonstrate and study the principle of harmonic lasing, and if successful motivate development of a new harmonic operation mode at LCLS.

HARDWARE

The attenuator consists of a 450 μm thick piece of sapphire, which can be inserted into the SASE line to establish harmonic operation mode (Fig. 2). The sapphire absorbs all but 10^{-5} of the radiation at 6 keV, but lets through 60% of the 18 keV photons (Fig. 3). The 6 keV fundamental photon energy was chosen as the lowest energy at which the sapphire can be inserted without danger of damaging the crystal. Switching to a diamond attenuator would extend operation to lower photon energies. The upper end is limited by the beam line mirrors, which stop transmitting radiation around 24 keV [3].

The R_{56} of the chicane scrambles the electron phase space, removing any bunching from the upstream undulators, so following the chicane the FEL process restarts from the strong SASE harmonic radiation that remains. The chicane delay must be more than 10 fs to avoid hitting the sap-

* dratner@slac.stanford.edu

ISBN 978-3-95450-126-7

OPTICAL DESIGN AND TIME-DEPENDENT WAVEFRONT PROPAGATION SIMULATION FOR A HARD X-RAY SPLIT-AND-DELAY UNIT FOR THE EUROPEAN XFEL

S. Roling, B. Siemer, F. Wahlert, M. Wöstmann, H. Zacharias, WWU Münster, Germany
L. Samoylova, H. Sinn, European XFEL GmbH, Hamburg, Germany
S. Braun, P. Gawlitza, Fraunhofer IWS, Dresden, Germany
E. Schneidmiller, M. Yurkov, DESY, Hamburg, Germany
F. Siewert, Helmholtz-Zentrum Berlin, Berlin, Germany
E. Ziegler, ESRF, Grenoble, France
O. Chubar, BNL, Upton, NY, USA

Abstract

For the European XFEL [1] an x-ray split-and-delay unit (SDU) is built covering photon energies from 5 keV up to 20 keV [2]. This SDU will enable time-resolved x-ray pump / x-ray probe experiments as well as sequential diffractive imaging [3] on a femtosecond to picosecond time scale. The set-up is based on wavefront splitting, which has successfully been implemented at an autocorrelator at FLASH [4]. The x-ray FEL pulses will be split by a sharp edge of a silicon mirror coated with Mo/B4C and W/B_4C multilayers. Both partial beams will then pass variable delay lines. For different wavelengths the angle of incidence onto the multilayer mirrors will be adjusted in order to match the Bragg condition. Hence, maximum delays between +/- 2.5 ps at hν = 20 keV and up to +/- 23 ps at hν = 5 keV will be possible. The time-dependent wave-optics simulations have been done with SRW software, for the fundamental at hν = 5 keV. The XFEL radiation was simulated using an output of time-dependent SASE code FAST. Main features of the optical layout, including diffraction on the splitter edge, and optics imperfections were taken into account. Impact of these effects on the possibility to characterize spatial-temporal properties of FEL pulses are analyzed.

INTRODUCTION

The advent of new hard x-ray sources providing ultrashort and ultrabright light pulses allows for new classes of x-ray experiments. This is a great challenge for optical instrumentation. In addition to the already operating LCLS at the Stanford Linear Accelerator Center (USA) [5] and SACLA in Japan [6] the European XFEL is now under construction in Hamburg (Germany). Operating at electron bunch energies of 17.5 GeV the machine will provide photon energies between hν = 3 keV and hν = 24 keV at the undulator sources SASE1 and 2. Pulse energies of up to E_{pulse} = 2 mJ and an ultrashort pulse duration from a few fs up to 100 fs [1] are expected. In the burst mode very high pulse rates of 2700 pulses at 4.5 MHz per burst at a pulse rate of 10 Hz are possible, due to superconducting accelerators. In order to gain information about the temporal properties of the x-ray pulses, like temporal coherence and pulse-duration, two jitter-free pulse replicas are needed. Also for x-ray pump / x-ray probe experiments and for time-resolved diffractive imaging a split- und delay unit is required. In this paper we describe the design of a new x-ray split-and-delay unit based on a multilayer mirror coating, that covers photon energies between hν = 5 keV and hν = 20 keV. With this energy range the SDU can be integrated into the SASE 1 or SASE 2 undulator beamlines. Due to the high absorbance and the small reflectivity at large incident angles a grazing incident geometry is utilized. For the xuv- and soft x-ray spectral regime such a set-up has successfully been integrated into the FLASH SASE FEL. With this device the spatio-temporal coherence properties [4,7] as well as the pulse duration [8] of a soft x-ray FEL have successfully been measured for the first time. Further, ionization dynamics in expanding clusters have been investigated by XUV pump / XUV probe spectroscopy [9] and femtosecond sequential imaging has been realized for the first time [3]. The new SDU at the European XFEL will enable similar experiments in the x-ray spectral regime. While for the energy range of FLASH carbon (DLC) coated silicon mirrors still yield a sufficient reflectivity at photon energies up about to hν = 200 eV, this will not be the case for the hard x-ray pulses of the European XFEL. Therefore, Si-substrates coated with multilayers will be utilized.

OPTICAL CONCEPT

The high absorbance and the small reflectivity at large incident angles are severe limitations for optical instrumentation in the x-ray range and therefore demand for a grazing incident geometry.

ISBN 978-3-95450-126-7

OPTIMIZATION OF A DEDICATED BIO-IMAGING BEAMLINE AT THE EUROPEAN X-RAY FEL

G. Geloni, European XFEL GmbH, Hamburg, Germany
V. Kocharyan, E. Saldin, and Svitozar Serkez, DESY, Hamburg, Germany

Abstract

We recently proposed a basic concept for design and layout of a dedicated undulator source for bio-imaging experiments at the European XFEL. Here we present an optimization of that concept. The core of the scheme is composed by soft and hard X-ray self-seeding setups. Using an improved design for both monochromators it is possible to increase the design electron energy up to 17.5 GeV in photon energy range between 2 keV and 13 keV, which is the most preferable for life science experiments. Operating at such high electron energy one increases the X-ray output peak power. Moreover, 17.5 GeV is the preferred operation energy for SASE1 and SASE2 users. This choice will reduce the interference with other undulator lines. We include a study of the performance of the self-seeding scheme accounting for spatiotemporal coupling caused by the use of a single crystal monochromator. This distortion can be easily suppressed by the right choice of diamond crystal planes. The proposed undulator source yields about the same performance as in the case for a X-ray seed pulse with no coupling. Simulations show that the FEL power reaches 2 TW in the 3 keV - 5 keV photon energy range.

INTRODUCTION

The availability of free undulator tunnels at the European XFEL facility offers a unique opportunity to build a beamline optimized for coherent diffraction imaging of complex molecules, like proteins and other biologically interesting structures. Crucial parameters for such bio-imaging beamline are photon energy range, peak power, and pulse duration [1]-[4].

The highest diffraction signals are achieved at the longest wavelength that supports a given resolution, which should be better 0.3 nm. With photon energy of about 3 keV one can reach a resolution better than 0.3 nm with a detector designed to collect diffracted light in all forward directions, that is at angles $2\theta < \pi/2$. Higher photon energies up to about 13 keV give access to absorption edges of specific elements used for phasing by anomalous diffraction. The most useful edges to access are the K-edge of Fe (7.2 keV) and Se (12.6 keV), [5]. Access to the sulfur K-edge (2.5 keV) is required too. Finally, the users of the bio-imaging beamline also wish to investigate large biological structures in the soft X-ray photon energy range down to the water window (0.3 keV – 0.5 keV), [5].

Overall, one aims at the production of pulses containing enough photons to produce measurable diffraction patterns, and yet short enough to avoid radiation damage in a single pulse. This is, in essence, the principle of imaging by "diffraction before destruction" [2]. These capabilities can be obtained by reducing the pulse duration to 5 fs or less, and simultaneously increasing the peak power to the TW power level or higher, at photon energies between 3 keV and 5 keV, which are optimal for imaging of macromolecular structures [5].

The requirements for a dedicated bio-imaging beamline are the following. The X-ray beam should be delivered in ultrashort pulses with TW peak power and within a very wide photon energy range between 0.3 keV and 13 keV. The pulse duration should be adjustable from 10 fs in hard X-ray regime to 2 fs - 5 fs in photon energy range between 3 keV and 5 keV. At the European XFEL it will be necessary to run all undulator beamlines at the same electron energy and bunch charge. Therefore, bio-imaging experiments should be performed without interference with other main SASE1, SASE2 beamlines. This assumes the use of nominal electron energy and electron beam distribution.

A key component of the bio-imaging beamline is the undulator source. A basic concept for layout and design of the undulator system for a dedicated bio-imaging beamline at the European XFEL was proposed in [6]. All the requirements in terms of photon beam characteristics can be satisfied by the use a very efficient combination of self-seeding, fresh bunch, and undulator tapering techniques [7]-[26], [27]-[30]. A combination of self-seeding and undulator tapering techniques would allow to meet the design TW output power. The bio-imaging beamline would be equipped with two different self-seeding setups, one provide monochromatization in the soft X-ray range, and one to provide monochromatization in the hard X-ray range. The most preferable solution in the photon energy range for single biomolecule imaging consists in using a fresh bunch technique in combination with self-seeding and undulator tapering techniques. In [6] it was shown how the installation of an additional (fresh bunch) magnetic chicane behind the soft X-ray self-seeding setup enables an output power in the TW level for the photon energy range between 3 keV and 5 keV. Additionally, the pulse duration can be tuned between 2 fs and 10 fs with the help of this chicane, still operating with the nominal electron bunch distribution [31].

The overall setup proposed in [6] is composed of four undulators separated by three magnetic chicanes. The undulator parts consist of 4,3,4 and 29 cells. Each magnetic chicane compact enough to fit one 5 m-long undulator segment and the FODO lattice will not be perturbed. The undulator system will be realized in a similar fashion as other

ISBN 978-3-95450-126-7

STATUS REPORT OF THE SHORT-PULSE FACILITY AT THE DELTA STORAGE RING*

A. Schick#, M. Höner, H. Huck, M. Huck, S. Khan, R. Molo, P. Ungelenk
Center for Synchrotron Radiation (DELTA), TU Dortmund University, 44221 Dortmund, Germany

Abstract

At DELTA, a 1.5-GeV synchrotron light source operated by the TU Dortmund University, a short-pulse facility employing the CHG (Coherent Harmonic Generation) principle is in operation. Here, the interaction of an intense, ultrashort laser pulse and electrons in an undulator leads to microbunching of a small fraction of the electrons in the bunch. As a consequence, ultrashort, coherent synchrotron radiation pulses in the VUV regime are emitted at harmonics of the incident laser wavelength. In addition, coherent THz pulses on the sub-ps timescale are generated. In this paper, the latest improvements of the facility and recent measurements are presented, including investigation of the transverse coherence and detection of the CHG radiation using photoemission spectroscopy in a VUV beamline.

INTRODUCTION

Pump-probe experiments allow to study phenomena on the timescale of the duration of the pulses used to excite ("pump") a sample and to analyze ("probe") it. Ultrashort (< 100 fs) laser pulses with a wavelength in the near-infrared regime are readily available from Titanium:sapphire laser systems. However, reducing the wavelength of the probe pulse is desirable for many applications.

Synchrotron light sources cover a large part of the electromagnetic spectrum, from the THz to the hard x-ray regime, but the pulse duration is of the order of 30 - 100 ps [1]. Lowering the momentum-compaction factor allows to decrease the pulse length to a few picoseconds, but at a reduced beam current [2].

Accessing the sub-ps regime with conventional synchrotron light sources is possible by using the interaction of ultrashort near-infrared laser pulses with electrons in the storage ring. The femtoslicing method is already in routine operation for several years [3-5], making use of a laser-induced energy modulation of the electrons in an undulator and a consecutive transverse displacement of the modulated electrons due to the dispersion in the following dipole magnet. Using an aperture, ultrashort pulses emitted by a subsequent undulator are extracted at variable photon energies up to the x-ray regime. The drawback of this method is a very low photon rate, because only a very small part of the electron bunch contributes.

* Work supported by DFG INST 212/236-1 FUGG, BMBF and by the Federal State NRW.
# andreas.schick@tu-dortmund.de

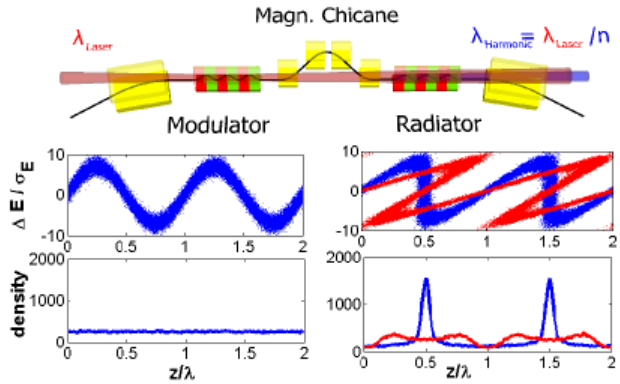

Figure 1: Sketch of an optical klystron (top). The electron energy is modulated sinusoidally (left) by a co-propagating laser pulse in the modulator. The microbunching caused by the magnetic chicane (right) leads to coherent emission of ultrashort synchrotron radiation pulses at harmonics of the laser wavelength in the radiator.

The Coherent Harmonic Generation (CHG) method also uses a laser-induced modulation of the electron energy, here imprinted in the first undulator ("modulator") of an optical klystron, a configuration of two undulators, separated by a magnetic chicane, see Fig. 1. Due to energy-dependent path-length differences in the magnetic chicane, the sinusoidally modulated electron distribution is tilted, forming peaks in the electron density ("microbunching"). The degree of microbunching is described by the bunching factor b_n, which is given by [6]

$$|b_n| = e^{-\frac{1}{2}n^2B^2} J_n(nAB) \qquad (1)$$

where n is the harmonic order, J_n is the Bessel function of the order n, $A = \Delta E/\sigma_E$ is the amplitude of the sinusoidal energy modulation in units of the natural energy spread σ_E and $B = R_{56}\cdot(2\pi/\lambda_{Laser})\cdot(\sigma_E/E)$ is proportional to the transfer matrix element R_{56} of the chicane. The power of the CHG radiation emitted coherently at harmonics of the incident laser wavelength in the radiator scales with the bunching factor squared, which decreases exponentially with harmonic order [6]

$$P_{coherent}(\omega) \propto N_e^2 b_n^2 \propto e^{-n^2} \qquad (2)$$

where N_e is the number of energy modulated electrons. Although only about 0.1 % of the whole electron bunch is modulated, the CHG radiation is 1-2 orders of magnitude more intense than the conventional synchrotron radiation emitted by the rest of the bunch, which only scales

ISBN 978-3-95450-126-7

A POSSIBLE UPGRADE OF FLASH FOR HARMONIC LASING DOWN TO 1.3 nm

E.A. Schneidmiller, M.V. Yurkov, DESY, Hamburg, Germany

Abstract

We propose the 3rd harmonic lasing in a new FLASH undulator as a way to produce intense, narrow-band, and stable SASE radiation down to 1.3 nm with the present accelerator energy of 1.25 GeV. To provide optimal conditions for harmonic lasing, we suggest to suppress the fundamental with the help of a special set of phase shifters. We rely on the standard technology of gap-tunable planar hybrid undulators; total length of the undulator system is 34.5 m. With the help of numerical simulations we demonstrate that the 3rd harmonic lasing at 1.3 nm provides peak power at a gigawatt level and the narrow intrinsic bandwidth, 0.1% (FWHM). Pulse duration can be controlled in the range of a few tens of femtoseconds, and the peak brilliance reaches the value of 10^{31} photons/(s mrad^2 mm^2 0.1% BW). With the given undulator design, a standard option of lasing at the fundamental wavelength to saturation is possible through the entire water window and at longer wavelengths.

INTRODUCTION

FLASH (Free electron LASer in Hamburg) is the first VUV and soft X-ray FEL user facility [1]. Presently, the facility is operated for users with the accelerator energy up to 1.25 GeV and the shortest wavelength of 4.1 nm, i.e. the photon energy is slightly above Carbon K-edge. This makes it possible to perform first experiments in the so-called water window. However, even shorter wavelengths are requested by the FLASH user community. In particular, lasing through the entire water window (i.e. down to 2.34 nm) would be interesting for some experiments. Moreover, resonant magnetic scattering studies would strongly profit from lasing down to 1.3 nm. In this case the L-edges of the most interesting materials would be covered. One of the possible ways to extend wavelength range would be an upgrade of FLASH beyond 2 GeV. However, such an extensive energy upgrade is not possible in the next few years. In this paper we propose an alternative way, namely using the present accelerator energy of 1.25 GeV and the 3rd harmonic lasing in a new undulator.

Harmonic lasing in single-pass high-gain FELs [2–7] is the radiative instability at an odd harmonic of the planar undulator developing independently from lasing at the fundamental wavelength. Contrary to nonlinear harmonic generation (which is driven by the fundamental in the vicinity of saturation), harmonic lasing can provide much more intense, stable, and narrow-band FEL beam which is easier to handle due to the suppressed fundamental. The most attractive feature of saturated harmonic lasing is that the brilliance of a harmonic is comparable to (or even larger than) that of the fundamental. In our recent study [7] we came to the conclusion that the 3rd harmonic lasing in X-ray FELs is much more robust than usually thought, and can be widely used at the present level of accelerator and FEL technology.

In this paper we show that the saturation of 3rd harmonic lasing at 1.3 nm can be achieved within 25 m (net magnetic length) of the optimized undulator at FLASH if we assume that slice parameters of the electron beam are close to those taken from start-to-end simulations [9]. In the same undulator one can lase to saturation at the fundamental wavelength through the entire water window. More details can be found in [8] where we have also considered such additional options as polarization control, bandwidth reduction, self-seeding, X-ray pulse compression, and two-color operation.

MAIN PARAMETERS

A possibility of FLASH operation in the considered wavelength range (down to 1.3 nm) is supported by recent achievements in production of low-emittance electron beams. Start-to-end simulations [9] for FLASH and the European XFEL have shown that low emittances can be preserved during bunch compression and transport of electron beams to the undulator. In Table 1 we present parameters of the electron beam that were used in our FEL simula-

Table 1: Electron Beam and Undulator Parameters

Electron beam	**Value**
Energy	1.25 GeV
Charge	150 pC
Peak current	2.5 kA
Rms normalized slice emittance	0.5 μm
Rms slice energy spread	250 keV
Rms pulse duration	24 fs

Undulator	**Value**
Period	2.3 cm
Minimum gap	9 mm
$K_{\rm rms}$ (at minimum gap)	1
Beta-function	7 m
Net magnetic length	25 m
Total length	34.5 m

ISBN 978-3-95450-126-7

AN OPTION FOR OBTAINING HIGH DEGREE OF CIRCULAR POLARIZATION AT X-RAY FELS

E.A. Schneidmiller, M.V. Yurkov, DESY, Hamburg, Germany

Abstract

Baseline design of a typical X-ray FEL undulator assumes a planar configuration which results in a linear polarization of the FEL radiation. However, many experiments at X-ray FEL user facilities would profit from using a circularly polarized radiation. As a cheap upgrade one can consider an installation of a short helical (or cross-planar) afterburner, but then one should have an efficient method to suppress powerful linearly polarized background from the main undulator. In this paper we propose a new method for such a suppression: an application of the reverse taper in the main undulator. We discover that in a certain range of the taper strength, the density modulation (bunching) at saturation is practically the same as in the case of non-tapered undulator while the power of linearly polarized radiation is suppressed by orders of magnitude. Then strongly modulated electron beam radiates at full power in the afterburner. Considering SASE3 undulator of the European XFEL as a practical example, we demonstrate that soft X-ray radiation pulses with peak power in excess of 100 GW and an ultimately high degree of circular polarization can be produced. The proposed method is rather universal, i.e. it can be used at SASE FELs and seeded (self-seeded) FELs, with any wavelength of interest, in a wide range of electron beam parameters, and with any repetition rate. It can be used at different X-ray FEL facilities, in particular at LCLS after installation of the helical afterburner in the near future.

INTRODUCTION

Successful operation of X-ray free electron lasers (FELs) [1–3], based on self-amplified spontaneous emission (SASE) principle [4], opens up new horizons for photon science. One of the important requirements of FEL users in the near future will be polarization control of X-ray radiation. Baseline design of a typical X-ray FEL undulator assumes a planar configuration which results in a linear polarization of the FEL radiation. However, many experiments at X-ray FEL user facilities would profit from using a circularly polarized radiation. There are different ideas [5–12] for possible upgrades of the existing (or planned) planar undulator beamlines.

As a cheap upgrade one can consider an installation of a short helical afterburner. In particular, an electromagnetic helical afterburner will be installed behind the soft X-ray planar undulator SASE3 of the European XFEL. However, to obtain high degree of circular polarization one needs to suppress (or separate) powerful linearly polarized radiation from the main undulator. Different options for such a suppression (separation) are considered: using achromatic bend between planar undulator and helical afterburner [7]; tuning resonance frequency of the afterburner to the second harmonic of the planar undulator [8]; separating source positions and using slits for spatial filtering [12].

In this paper we propose a new method for suppression of the linearly polarized background from the main undulator: application of the reverse undulator taper. In particular, in the case of SASE3 undulator of the European XFEL, we demonstrate that soft X-ray radiation pulses with peak power in excess of 100 GW and an ultimately high degree of circular polarization can be produced. As for a comparison with the other methods, our suppression method is free, easy to implement, and the most universal: it can be used at SASE FELs and seeded (self-seeded) FELs, with any wavelength of interest, in a wide range of electron beam parameters, and with any repetition rate. It can be applied at different X-ray FEL facilities, in particular at LCLS after installation of the helical afterburner in the near future.

METHOD DESCRIPTION

In a short-wavelength SASE FEL the undulator tapering is used for two purposes: to compensate an electron beam energy loss in the undulator due to the wakefields and spontaneous undulator radiation; and to increase FEL power (post-saturation taper). In both cases the undulator parameter K decreases along the undulator length. The essence of our method is that we use the opposite way of tapering: parameter K increases what is usually called reverse (or negative) taper. We discover that in some range of the taper strength the bunching factor at saturation is practically the same as in the reference case of the non-tapered undulator, the saturation length increases slightly while the saturation power is suppressed by orders of magnitude. Therefore, our scheme is conceptually very simple (see Fig. 1): in a tapered main (planar) undulator the saturation is achieved with a strong microbunching and a suppressed radiation power, then the modulated beam radiates at full power in a helical afterburner, tuned to the resonance.

Note that reverse undulator taper was considered in the

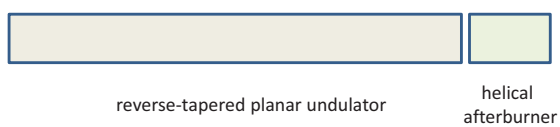

Figure 1: Conceptual scheme for obtaining circular polarization at X-ray FELs.

ISBN 978-3-95450-126-7

THE IR AND THz FREE-ELECTRON LASER AT THE FRITZ-HABER-INSTITUT

W. Schöllkopf, S. Gewinner, W. Erlebach, G. Heyne, H. Junkes, A. Liedke, G. Meijer,
V. Platschkowski, G. von Helden, Fritz-Haber-Institut der Max-Planck-Gesellschaft, Berlin, Germany
H. Bluem, M. Davidsaver*, D. Dowell*, K. Jordan*, R. Lange*, H. Loos*, J. Rathke,
A.M.M. Todd, L.M. Young*, Advanced Energy Systems, Medford, NY, USA
U. Lehnert, P. Michel, W. Seidel, R. Wünsch, HZDR, Rossendorf, Germany
S.C. Gottschalk, STI Optronics, Bellevue, WA, USA

Abstract

A mid-infrared oscillator FEL with a design wavelength range from 4 to 50 μm has been commissioned at the Fritz-Haber-Institut in Berlin, Germany, for applications in molecular and cluster spectroscopy as well as surface science. A second FEL covering the FIR and THz from 40 to 500 μm is planned. The accelerator consists of a thermionic gridded electron gun, a subharmonic buncher and two S-band standing-wave copper structures. The device was designed to meet challenging specifications, including a final energy adjustable in the range of 15 to 50 MeV, low longitudinal emittance (< 50 keV-psec) and transverse emittance (< 20 π mm-mrad), at more than 200 pC bunch charge with a pulse repetition rate of 1 GHz and a macro pulse length of up to 15 μs. In this paper, we present measurements of the electron beam and results from lasing in the wavelength range from 8 to 24 μm.

INTRODUCTION

At the Fritz-Haber-Institut in Berlin, Germany, a new IR and THz FEL has been commissioned for applications in gas-phase spectroscopy of (bio-)molecules, clusters, and nano-particles, as well as in surface science [1-4]. To cover the wavelength range of interest from about 4 to 500 μm, the system design, shown in Fig. 1, includes two FELs; a mid-infrared (MIR) FEL for wavelengths up to about 50 μm and a far-infrared (FIR) FEL for wavelengths larger than about 40 μm. A normal conducting S-band linac provides electrons of up to 50 MeV energy to either FEL.

As of August 2013, commissioning of the accelerator and electron-beam transport system (designed and installed by Advanced Energy Systems, Inc.) is nearing completion [5,6]. Commissioning of the MIR undulator (STI Optronics) [7] and oscillator cavity (Bestec GmbH), as well as of the first five IR user beam lines has been completed. First lasing of the MIR FEL was achieved at a wavelength of 16 μm in 2012 [2]. The FIR FEL has not yet been installed. In this paper, after a brief summary of the electron accelerator, we report on lasing of the MIR FEL in the range from 8 to 24 micron and describe measurements of the electron beam passing through the FEL.

* Consultants to Advanced Energy Systems, Inc.

ELECTRON ACCELERATOR

In Table 1 we summarize the projected top-level electron beam performance. The design of the accelerator and beam transport system has been described elsewhere [2-6]. In brief, it consists of a 50 MeV accelerator driven by a gridded thermionic gun with a beam transport system that feeds two undulators and a diagnostic beamline. The first of two 3 GHz S-band, normal-conducting electron linacs accelerates the electron bunches to a nominal energy of 20 MeV, while the second one accelerates or decelerates the electrons to deliver any final energy between 15 and 50 MeV. A chicane between the structures allows for adjustment of the bunch length as required.

Table 1: Summary of Electron Beam Parameters

Parameter	Unit	Specification	Target
Electron energy	MeV	20 - 50	15 - 50
Energy spread	keV	50	< 50
Energy drift per hour	%	0.1	< 0.1
Bunch charge	pC	200	> 200
Micro-bunch length	ps	1 - 5	1 - 10
Micro-bunch rep. rate	GHz	1	1
Micro-bunch jitter	ps	0.5	0.1
Macro-bunch length	μs	1 - 8	1 - 15
Macro-bunch rep. rate	Hz	10	20
Normalized rms transverse emittance	π mm mrad	20	20

The final design has optimized the specifications of the linac that are most relevant for the IR and THz FEL performance. For instance, the target bunch charge of the micro-pulses, which are repeated at rate of up to 1 GHz, has been increased to 300 pC. In addition, the target length of the macro-bunches has been increased to 15 μs.

MID-INFRARED OSCILLATOR FEL

Both, the MIR FEL and the FIR/THz FEL, consist of an undulator placed within an IR cavity as summarized in Table 2. The MIR FEL includes a 2-m-long planar wedged-pole hybrid undulator manufactured by STI Optronics with a period length of 40 mm. A detailed description of the MIR undulator is provided in Ref. [7]. At a minimum gap of nominally 16.5 mm, a maximum root-mean-square undulator parameter K_{rms} of more than 1.6 is reached. This, in combination with the minimum electron energy of 15 MeV corresponds to a theoretical maximum wavelength of more than 60 μm [2-4].

ISBN 978-3-95450-126-7

EXTENSION OF SASE BANDWIDTH UP TO 2% AS A WAY TO INCREASE NUMBER OF INDEXED IMAGES FOR PROTEIN STRUCTURE DETERMINATION BY FEMTOSECOND X-RAY NANOCRYSTALLOGRAPHY AT THE EUROPEAN XFEL

Svitozar Serkez, Vitali Kocharyan, Evgeni Saldin, Igor Zagorodnov, DESY, Hamburg, Germany
Gianluca Geloni, European XFEL GmbH, Hamburg, Germany
Oleksander Yefanov, CFEL, Hamburg, Germany

Abstract

Experiments at the LCLS confirmed the feasibility of femtosecond nanocrystallography for protein structure determination at near-atomic resolution. These experiments rely on X-ray SASE pulses with a few microradians angular spread, and about 0.2% bandwidth. By indexing individual patterns and then summing all counts in all partial reflections for each index it is possible to extract the square modulus of the structure factor. The number of indexed images and the SASE bandwidth are linked, as an increasing number of Bragg spots per individual image requires an increasing spectral bandwidth. This calls for a few percent SASE bandwidth. Based on start-to-end simulations of the European XFEL baseline, we demonstrate that it is possible to achieve up to a 10-fold increase of the electron energy chirp by strongly compressing a 0.25 nC electron bunch. This allows for data collection with a 2% SASE bandwidth, a few mJ radiation pulse energy and a few fs-pulse duration, which would increase the efficiency of protein determination at the European XFEL. We prove this concept with simulations of lysozyme nanocrystals, with a size of about 300 nm.

INTRODUCTION

X-ray crystallography is currently the leading method for imaging macromolecules with atomic resolution. Third generation synchrotron sources allow for successful structure determination of proteins. The size of a typical single crystal used for conventional protein crystallography is in the order of 50μm -500μm [1]. Obtaining sufficiently large crystals is currently a serious stumbling block as regards structure determination. The new technique of femtosecond nanocrystallography is based on data collection from a stream of nanocrystals, and ideally fills the gap between conventional crystallography, which relies on the use of large, single crystals, and single-molecular x-ray diffraction.

The availability of XFELs allows for a new "diffraction before destruction" approach to overcome radiation damage due to the ultrafast and ultrabright nature of the x-ray pulses, compared to the time scale of the damage process [2]-[6]. In fact, if such time-scale is longer than the pulse duration, the diffraction pattern yields information about the undamaged material. Femtosecond nanocrystallography involves sequential illumination of many small crystals of proteins by use of an XFEL source [7]. The high number of photons incident on a specimen are expected to produce measurable diffraction patterns from nanocrystals, enabling structure determination with high resolution also for systems that can only be crystallized into very small crystals and are not suitable, therefore, for conventional crystallography. Each crystal is used for one exposure only, and the final integrated Bragg intensities must be constructed from "snapshot" diffraction patterns containing partially recorded intensities. Each pattern corresponds to a different crystal at random orientation. Experiments at the LCLS [8] confirmed the feasibility of the "diffraction before destruction" method at near atomic resolution using crystals ranging from 0.2 μm to 3 μm [7]. This method relies on x-ray SASE pulses with a few mJ energy, a few microradians angular spread, and about 0.2% bandwidth with a photon energy range between 2 keV and 9 keV.

The success of nanocrystallography depends on the robustness of the procedure for pattern determination. After acquisition, diffraction patterns are analyzed to assign indexes to Bragg peaks (indexing procedure). Each of the indexed peaks is integrated in order to obtain an intensity. Intensities of corresponding peaks are averaged within the dataset. The table of peak indexes and intensities obtained in this way is used for protein structure determination. Indexing algorithms used in crystallography enable to determine the orientation of the diffraction data from a single crystal when a relatively large number of reflections are recorded. Femtosecond nanocrystallography brings new challenges to data processing [9]. The problem is that single snapshots of crystal diffraction patterns may contain very few reflections, which are not enough for indexing. In this paper we will show how to overcome this obstacle.

The number of Bragg peaks is proportional to the bandwidth of the incident radiation pulse. Considering the baseline configuration of the European XFEL [10], and based on start-to-end simulations, we demonstrate here that it is possible to achieve a tenfold increase in bandwidth by strongly compressing electron bunches with a charge of 0.25 nC up to 45 kA. This allows data collection with a 2% bandwidth, a few mJ radiation pulse energy, a few fs pulse duration, and a photon energy range between 2 keV and 6 keV, which is the most preferable range for nanocrystallography [11].

ISBN 978-3-95450-126-7

GRATING MONOCHROMATOR FOR SOFT X-RAY SELF-SEEDING THE EUROPEAN XFEL

S. Serkez, V. Kocharyan and E. Saldin, DESY, Hamburg, Germany
G. Geloni, European XFEL GmbH, Hamburg, Germany

Abstract

Self-seeding implementation in the soft X-ray wavelength range involves gratings as dispersive elements. We study a very compact self-seeding scheme with a grating monochromator originally designed at SLAC, which can be straightforwardly installed in the SASE3 undulator beamline at the European XFEL. The design is based on a toroidal VLS grating at a fixed incidence angle, and without entrance slit. It covers the spectral range from 300 eV to 1000 eV. The performance was evaluated using wave optics method vs ray tracing methods. Wave optics analysis takes into account the actual beam wavefront of the radiation from the FEL source, third order aberrations, and errors from optical elements. We show that, without exit slit, the self-seeding scheme gives the same resolving power (about 7000) as with an exit slit. Wave optics is also naturally applicable to calculations of the scheme efficiency, which include the monochromator transmittance and the effect of the mismatching between seed beam and electron beam. Simulations show that the FEL power reaches 1 TW, with a spectral density about two orders of magnitude higher than that for the SASE pulse at saturation. A more detailed study and further references can be found in [1].

INTRODUCTION

Self-seeding is a promising approach to significantly narrow the SASE bandwidth and to produce nearly transform-limited pulses [2]-[11]. Considerable effort has been invested in theoretical investigation and $R\&D$ at the LCLS leading to the implementation of a hard X-ray self-seeding (HXRSS) setup that relies on a diamond monochromator in transmission geometry. Following the successful demonstration of the HXRSS setup at the LCLS [12], there is a need for an extension of the method in the soft X-ray range.

In general, a self-seeding setup consists of two undulators separated by a photon monochromator and an electron bypass, normally a four-dipole chicane. The two undulators are resonant at the same radiation wavelength. The SASE radiation generated by the first undulator passes through the narrow-band monochromator. A transform-limited pulse is created, which is used as a coherent seed in the second undulator. Chromatic dispersion effect in the bypass chicane smears out the microbunching in the electron bunch produced by the SASE lasing in the first undulator. The electrons and the monochromatized photon beam are recombined at the entrance of the second undulator, and radiation is amplified by the electron bunch until saturation is reached. The required seed power at the beginning of the second undulator must dominate over the shot noise power within the gain bandpass, which is order of a kW in the soft X-ray range.

For self-seeding in the soft x-ray range, proposed monochromators usually consists of a grating [2], [5]. Recently, a very compact soft x-ray self-seeding (SXRSS) scheme has appeared, based on grating monochromator [13]-[15]. The delay of the photons in the last SXRSS version [15] is about 0.7 ps only. The proposed monochromator is composed of only three mirrors and a toroidal VLS grating. The design adopts a constant, 1 degree incidence-angle mode of operation, in order to suppress the influence of movement of the source point in the first SASE undulator on the monochromator performance.

In this article we study the performance of the soft X-ray self-seeding scheme for the European XFEL upgrade. In order to preserve the performance of the baseline undulator, we fit the magnetic chicane within the space of a single 5 m undulator segment space at SASE3. In this way, the setup does not perturb the undulator focusing system. The magnetic chicane accomplishes three tasks by itself. It creates an offset for monochromator installation, it removes the electron microbunching produced in the upstream seed undulator, and it acts as an electron beam delay line for compensating the optical delay introduced by the monochromator. The monochromator design is compact enough to fit with this magnetic chicane design. The monochromator design adopted in this paper is an adaptation of the novel one by Y. Feng et al. [15], is based on toroidal VLS grating, and has many advantages. It consists of a few elements. In particular, it operates without entrance slit, and is, therefore, very compact. Moreover, it can be simplified further. Quite surprisingly, a monochromatic seed can be directly selected by the electron beam at the entrance of the second undulator. In other words, the electron beam plays, in this case, the role of an exit slit. By using a wave optics approach and FEL simulations we show that the monochromator design without exit slits works in a satisfactory way.

With the radiation beam monochromatized down to the Fourier transform limit, a variety of very different techniques leading to further improvement of the X-ray FEL performance become feasible. In particular, the most promising way to extract more FEL power than that at saturation is by tapering the magnetic field of the undulator [16]-[22]. A significant increase in power is achievable by starting the FEL process from a monochromatic seed rather than from shot noise [20]-[27]. In this paper we propose a study of the soft X-ray self-seeding scheme for the European XFEL, based on start-to-end simulations for an elec-

ISBN 978-3-95450-126-7

LEBRA FREE ELECTRON LASER AS A RADIATION SOURCE FOR PHOTOCHEMICAL REACTIONS IN LIVING ORGANISMS

F. Shishikura#, K. Hayawaka, Y. Hayakawa, M. Inagaki, K. Nakao, K. Nogami, T. Sakai, T. Tanaka,
Laboratory for Electron Beam Research and Application, Nihon University, Chiba, Japan

Abstract

The Laboratory for Electron Beam Research and Application (LEBRA) free-electron laser (FEL) irradiation system has been developed and improved to irradiate single cells at tunable wavelengths ranging from 350 to 6500 nm. The objectives of this research are to determine the unique characteristics of LEBRA-FELs in order to evaluate their ability to control photoreactions in living organisms. The authors examined a well-known photoreaction in lettuce seed germination, which is promoted by red light and inhibited by far-red light. The LEBRA-FELs, centered at 660 nm (average irradiation energy: 20 μJ/pulse) with a half-bandwidth of 8 nm, and at 740 nm (average irradiation energy: 40 μJ/pulse) with a half-bandwidth of 16 nm, could promote and inhibit lettuce seed germination, respectively. This treatment was effective when using natural density filters to reduce radiation energy of the 660 and 740 nm FELs to as low as about 0.05 μJ/pulse (10 min irradiation) and about 0.63 μJ/pulse (10 min irradiation), respectively. The LEBRA-FEL, therefore, promises to be an attractive tool for the non-invasive analysis of photochemical reactions in living organisms.

INTRODUCTION

The radiation sources commonly applied to plants are commercially available lamps developed for human lighting applications (e.g., fluorescent, metal halide, high-pressure sodium, incandescent, light-emitting diode, and laser diode lights). In contrast, free-electron lasers (FELs) such as the one developed by the Laboratory for Electron Beam Research and Application (LEBRA) produce high-energy, tunable pulsed radiation [1, 2]. The advantages of the LEBRA-FEL compared with other lasers [3] are that its peak intensity ranges from 0.9 to 6.5 μm [4] through the use of silver-coated copper mirrors in the FEL resonator [2], that it can generate higher harmonics by means of non-linear optical crystals, and that it can emit wavelengths from 0.35 to 6.5 μm encompassing both the visible (VIS) and infrared (IR) regions. Previously, we established a microscopic irradiation technique for delivering VIS-FEL light to single cells through a tapered glass rod (<10 μm diameter) [5]. However, it is still unclear whether LEBRA-FELs can produce sufficient radiant energy at wavelengths effective for triggering photochemical reactions in living organisms. The aim of this study was to evaluate the effectiveness of LEBRA-FELs through lettuce seed germination tests [6-11]. Results showed promotion by red light (660 nm) and inhibition by far-red light (740 nm), indicating that LEBRA-FELs can be used to control lettuce seed germination and are thus promising as a potent radiation source for photochemical investigations in living organisms.

#shishikura@lebra.nihon-u.ac.jp

MATERIALS AND METHODS

Lettuce Seeds

Lettuce seeds (*Lactuca sativa* L.) from the Red Wave cultivar (a leaf lettuce) were obtained from a commercial supplier (Sakata Seed Co., Yokohama, Japan) and used within the recommended periods. In preliminary germination experiments, the seeds used here exhibited several advantageous characteristics for the evaluation of the LEBRA-FEL as a radiation source for investigating photoreactions in living organisms. Almost no seeds germinate when kept in darkness at 26.5 °C for at least 20-24 h, and average values for induction and inhibition of germination are both over 95±2% upon irradiation with red light and far-red light, respectively. These characteristics were re-examined simply by a 10 min exposure to 660 nm LED light and 735 nm LED light at 26.5 °C in darkness. Both the LEDs were installed in a Photo Germinating Seeds Apparatus (GR-8; Shimadzu Rika Co., Tokyo, Japan).

Setup of FEL Irradiation System

A FEL microscopic irradiation system was set up on an optical bench at the user's laboratory of LEBRA (Figure 1A) as previously published [5]; briefly, an irradiation section of quartz fiber (0.6 mm diameter: Figure 1B) was installed on a fiber holder (H-7; Narishige Group, Tokyo, Japan), which could be readily manipulated by two micromanipulators (MN-153 and MMO-220A; Narishige Group).

Light Sources

According to previous research [6-11], red light promotes germination of lettuce seeds whereas far-red light inhibits it. Therefore, we chose 660 nm red light as a candidate wavelength for the LEBRA-FEL promotion light source, and 740 nm far-red light for the inhibition light source. The tip of the quartz fiber could focus radiation on the surface of the sample seed, which had been inserted into a capillary (Figure 1B), and allowed for accurate direction of the radiation to the targeted sample. The FEL radiation energy could be reduced by means of combined neutral density (ND) glass filters (Kenko Tokina Co. Ltd., Tokyo, Japan), by which the FEL

ISBN 978-3-95450-126-7

PROGRESS WITH THE FERMI LASER HEATER COMMISSIONING*

Simone Spampanati#, Giovanni DeNinno, Sincrotrone Trieste, Italy &
University of Nova Gorica, Nova Gorica, Slovenia
Enrico Allaria, Davide Castronovo, Miltcho B. Danailov,
Alexander Demidovich, Simone Di Mitri, Bruno Diviacco, William M. Fawley, Lars Froelich,
Giuseppe Penco, Carlo Spezzani, Mauro Trovò, Sincrotrone Trieste, Italy
Massimo Dal Forno, Eugenio Ferrari,Sincrotrone Trieste, Italy, University of Trieste, Trieste, Italy
Luca Giannessi, ENEA C.R. Frascati, Frascati (Roma) Italy, Sincrotrone Trieste, Italy

Abstract

FERMI@ELETTRA is a seeded free electron laser facility composed by one linac and two FEL lines named FEL-1 and FEL-2. FEL-1 works in HGHG configuration, while FEL-2 is a HGHG cascade implementing "fresh bunch" injection into the second stage. Performance of FEL-1 and FEL-2 lines have benefited from the use of the laser heater system, which is located right after the injector, at 100 MeV beam energy. Proper tuning of the laser heater parameters has allowed control of the microbunching instability, which is otherwise expected to degrade the high brightness electron beam quality sufficiently to reduce the FEL power. The laser heater was commissioned one year ago and positive effects upon microbunching. In this work we presents further measurements of microbunching suppression in two compressors scheme showing directly the reduction of the beam slice energy spread due to laser heater action. We present measurements showing the impact of the laser heater on FEL2.

INTRODUCTION

FERMI@ELETTRA [1] is a user facility based on two seeded FELs in the VUV (FEL-1 [2]) and soft x-ray (FEL-2 [3]) wavelength regimes. Both FEL lines are driven by a high brightness electron beam produced by the same linac [4]. The very bright electron beam required to drive VUV and X-ray FELs is susceptible to a microbunching instability [5] that produces short wavelength (~1-5μm) energy and current modulations [6]. These can both degrade the FEL spectrum and reduce the power by increasing the slice energy spread. This collective instability takes place as linacs for FEL light sources are equipped with bunch compressors designed to increase the peak current to the level required for photon production. Microbunching instability is presumed to start at the photoinjector exit growing from a pure density and/or energy modulation caused by shot noise and/or unwanted modulations in the photoinjector laser temporal profile. As the electron beam travels along the linac to reach the first bunch compressor (BC1), the density modulation leads to an energy modulation via longitudinal space charge. The resultant energy modulations are then transformed into higher density modulations by the bunch compressor. The increased current non-uniformity leads to further energy modulations along the rest of the linac. Coherent synchrotron radiation in the bunch compressor can further enhance these energy and density modulations [7,8]. The density modulation produced in the first bunch compressor is the source of further energy modulation along the linac and can eventually be amplified by the presence of other compressors. The final slice energy spread is increased and can reduce the FEL performance. A laser heater has been proposed to control these degradations [9,10]. This device can add a small controlled amount of incoherent energy spread to the beam and reduce microbunching instability growth via Landau damping in the bunch compressors. The capability of a laser heater to increase beam brightness has been demonstrated at LCLS where a reduction of the FEL gain length and an increase of the photon flux were observed [11]. The reduction of the final slice energy spread has however not been observed directly. To control microbunching instability in FERMI we have installed a laser heater between the photoinjector and the linac [4]. The FERMI laser heater was commissioned one year ago and positive effects upon microbunching instabilities, reduction of density and energy modulation, and FEL-1 performance was soon observed and reported in [12]. In this work we report further measurements demonstrating the reduction of the beam energy spread resulting to the action of the laser heater and his positive impact on FEL-2.

LINAC LAYOUT

Figure 1 shows the layout of the accelerator that produce the electron beam for FERMI [4].

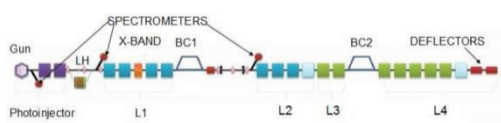

Figure 1: Layout of the electron beam accelerator of FERMI@ELETTRA.

Electrons are generated in the Gun and then pre-accelerated in the photo injector that includes two booster cavities. The first linac section (L1) accelerates the beam and produce the chirp needed for bunch compression in BC1. L1 includes a higher harmonic RF cavity used to

*Work supported in part by the Italian Ministry of University and Research under grants FIRB-RBAP045JF2 and FIRB-RBAP06AWK3
#simone.spampinati@cockcroft.au.uk actually at Liverpool University, Liverpool, Uk and Cockcroft Institute Daresbury, Warrington, Uk

ISBN 978-3-95450-126-7

EFFECT OF COULOMB COLLISIONS ON ECHO-ENABLED HARMONIC GENERATION*

G. Stupakov
SLAC National Accelerator Laboratory, Menlo Park, CA 94025, USA

Abstract

We develop a practical computational technique for evaluation of the effect of intra-beam scattering on Echo-Enabled Harmonic Generation (EEHG). The techniques is applied for calculation of the EEHG seeding for NGLS soft x-ray FEL project being developed at LBNL.

INTRODUCTION

Echo-Enabled Harmonic Generation [1,2] (EEHG) has a remarkable up-frequency conversion efficiency and allows for generation of high harmonics with a relatively small energy modulation. While increasing harmonic number to $\sim 10^2$ in EEHG sets stringent requirements on the seeding system, they can, in principle, be satisfied with increased tolerances on the magnetic field and the quality of the laser beams used for modulation of the beam energy. It was recently realized [3] however that the ultimate limit on harmonic number in EEHG is likely imposed by Coulomb collisions between the particles of the beam (aka intra-beam scattering). This is due to the fact that in the process of EEHG the phase space of the beam is split into stripes that have effective energy spread of the order of the energy spread of the beam divided by the harmonic number, that is much smaller than the beam energy spread. As is well known, the dominant process in Coulomb collisions is a small-angle scattering, which predominantly leads to diffusion in the momentum space. This diffusion smears out the stripes and eventually lead to decreasing of the final bunching factor at the desired harmonic.

The analysis in [3] was limited by an unrealistic assumption that collisions occur in a beam with a constant transverse size and angular spread. In this paper we will get rid of this constraint and consider intra-beam scattering in a lattice where the transverse size of the beam and its angular spread vary along the beam path. Account of these effects leads to the energy diffusion in the beam varying with distance. A convenient technique for treating such a diffusion was developed in recent papers by Yampolsky and Carlsten [4, 5] and is based on Fourier transformation of the beam distribution function in six dimensional phase space and a subsequent solution of the Fourier transformed Vlasov equation. In this paper we briefly outline their technique before applying it to the particular example of EEHG. The technique is applicable for linear beam dynamics when collective effects (wakefields) are neglected.

* Work supported by the U.S. Department of Energy under contract No. DE-AC02-76SF00515.

In a recent report [6] G. Penn developed an alternative approach to the IBS in EEHG and carried out computer simulations for several layouts of EEHG seeding for the NGLS soft x-ray FEL project at LBNL [7].

COULOMB COLLISIONS IN EEHG

A simplified collision term which can be used in EEHG was derived in [3]. It appears on the right-hand side of the Vlasov equation for the distribution function f, and can be written in the following form

$$\frac{df}{ds} = \frac{1}{2} D(s) \frac{\partial^2 f}{\partial \Delta E^2}, \qquad (1)$$

where the full derivative df/ds in (1) is taken along particles' trajectories, s is the path length and ΔE is the energy measured from the nominal energy of the beam. The diffusion coefficient D is

$$D(s) = \frac{\pi^{1/2}\Lambda}{2\gamma\sqrt{\sigma_{\theta x}(s)\sigma_{\theta y}(s)}} \frac{(m_e c^2)^2 r_e}{\sigma_x(s)\sigma_y(s)} \frac{I}{I_A}, \qquad (2)$$

with I the beam current, $I_A = mc^3/e \approx 17$ kA the Alfven current and r_e the classical electron radius. The diffusion coefficient is averaged over the transverse distribution of the beam, which is assumed to be a round Gaussian with the rms transverse sizes σ_x and σ_y and the rms angular spreads $\sigma_{\theta x}$ and $\sigma_{\theta y}$ in x and y directions, respectively.

In Eq. (2) we specifically indicate that the beam dimensions and divergences vary with s due to the variation of the lattice functions. Analysis of Ref. [3] neglected this variation and assumed D constant.

EVOLUTION OF THE DISTRIBUTION FUNCTION IN FOURIER SPACE

The distribution function of the beam f in the six-dimensional phase space, $f(x, \theta_x, y, \theta_y, z, \Delta E, s)$, satisfies the Vlasov equation (we define f as a probability in the phase space, so that its integration over the first 6 variables gives unity). The arguments of f are the transverse coordinates x and y, the transverse angles θ_x and θ_y, the longitudinal coordinate inside the beam z, and the energy deviation from the nominal energy ΔE. If there is no interaction between the particles, so that one actually deals with one-particle dynamics, a solution of the Vlasov equation can be obtained with the help of an R-matrix.

Let $\boldsymbol{X} = (x, \theta_x, y, \theta_y, z, \Delta E)^T$ be a column vector; if the 6×6 matrix $R(s)$ that transforms this vector from $s = 0$ to s is known, then $\boldsymbol{X}(s) = R(s)\boldsymbol{X}(0)$. With the

ISBN 978-3-95450-126-7

OPTICAL CAVITY LOSSES CALCULATION AND OPTIMIZATION OF THz FEL WITH A WAVEGUIDE*

P. Tan#, K. Xiong, Q. Fu, Y. Li, B. Qin, Y. Xiong, Huazhong University of Sci. & Tech., CHINA

Abstract

The optical cavity with waveguide is used in most long wavelength free electron lasers. In this paper, the losses, gains and modes of a terahertz FEL sources in Huazhong University of Science and Technology (HUST) are analysis. Then the radii of curvature of the optical mirrors and shapes of the waveguide are optimized.

INTRODUCATION

Considering wide applications of high power coherent THz radiation sources on biology, imaging and material science etc., a prototype compact terahertz FEL oscillator is proposed at Huazhong University of Science and Technology (HUST), which is considered to generate 50-100μm terahertz radiation. The concept design of the compact THz FEL oscillator is composed of an independently tunable cell (ITC) thermionic RF gun, a linac booster, a planar undulator and a near concentric waveguide optical cavity[1].

The main design parameters of this FEL oscillator are listed in Table 1.

Table 1: Parameters of the THz FEL Oscillator

Parameter	Value
Radiation wavelength λs	50 - 100μm
Beam energy	8.1-11.7 MeV
Energy spread	0.3%
Normalized Emmittance	15πmm·mrad
Charge per pulse	≥200pC
Bunch length	5ps (5-10ps)
Macro pulse length	4-6μs
Undulator parameter K	1.25 (1.0-1.25)
Undulator Period Number	30
Undulator wavelength λu	32 mm
Optical cavity length Lcav	2.940m
Waveguide width	2a=40mm
Waveguide height	2b=10mm
Waveguide length	Lwg=1130mm

In this paper the losses, gains and modes of the THz FEL source with waveguide in HUST are analysis. Then the radii of curvature of the optical mirrors and shapes of the waveguide are optimized.

*Work supported by the Fundamental Research Funds for the Central Universities，HUST：2012QN080

tanping@mail.hust.edu.cn

MODES IN WAVEGUIDE

Compared to the conversional FEL, new issues arise in a long wavelength THz FEL due to the short electron pulse and the radiation diffraction loss. The vacuum duct of undulator is used as the waveguide, which offers the advantage of small wiggler gaps and small mode area is helpful to improve gains and decrease losses in FEL cavity.

In conventional lasers, the oscillating modes are determined by both the radii of curvature of the two mirrors and their separation.

While in a waveguide FEL, the modes of propagation in the waveguide are different from the Gaussian beam. Each end of the waveguide may be considered as a radiating source, each mirror acting as a feedback element coupling the radiation back into the allowed waveguide mode. A part of the radiation is being scattered out of the guide aperture [2].

Consider the simplified waveguide resonator structure shown in Fig.1, in which toroidal mirrors of curvature radius Rx and Ry are positioned at a distance d from the waveguide end, which coincides with the plane z =0. The vacuum duct in the undulator is acted as a rectangular waveguide, and its cross-section is 2a*2b.

Fig.2 gives the coordinate system used in loss calculation.

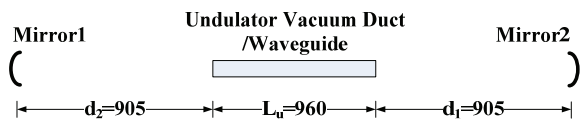

Figure 1: Structure of the waveguide resonator.

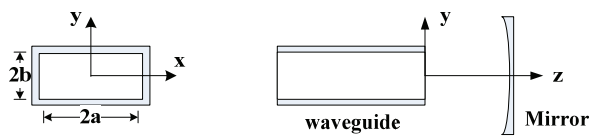

Figure 2: Coordinate system used in calculations.

The transverse dimensions of waveguide in a practical FEL waveguide are usually much larger than the guide wavelength; therefore we are only interested in the overmode, low-mode and low-loss solution.

For convenience, two sets of linearly independent solutions are identified.

The magnetic field of the first class modes is almost completely polarized in the x direction, denoted as: $E^{\sigma}_{pq}\left(H^{\sigma}_{x} \geq H^{\sigma}_{y}, H^{\sigma}_{z}\right)$; that of the second class is polarized in the y direction , denoted as: $E^{\pi}_{pq}\left(E^{\pi}_{x} \geq E^{\pi}_{y}, E^{\pi}_{z}\right)$.With

ISBN 978-3-95450-126-7

FULLY PHASE MATCHED HIGH HARMONIC GENERATION IN A HOLLOW WAVEGUIDE FOR FREE ELECTRON LASER SEEDING

F. Ardana-Lamas[1,3], C. Vicario[1], G. Lambert[2], A. Trisorio[1], V. Malka[2], B. Vodungbo[2], P. Zeitoun[2] and C. P. Hauri[1,3],
[1]SwissFEL, Paul Scherrer Institut, 5232 Villigen-PSI, Switzerland
[2]LOA, ENSTA-CNRS-EP, Palaiseau, France
[3]Ecole Polytechnique Federale de Lausanne, 1015 Lausanne, Switzerland

Abstract

A bright high harmonic source is presented delivering up to 10^{10} photons per second around a central photon energy of 120 eV. Fully phase matched harmonics are generated in an elongated capillary reaching a cut-off energy of 160 eV. The high HHG photon fluence opens new perspectives towards seeding free electron lasers at shorter wavelengths than the state of the art. Characterization of the phase matching conditions in the capillary is presented.

INTRODUCTION

Bright table-top VUV and soft x-ray sources based on laser-field induced ionization in a rare gas found a prominent application in free electron laser facilities, which is seeding. Overlapping a fully coherent seed pulse generated by high-order harmonic generation (HHG) with the electron bunch in the undulator results in locking the FEL longitudinal modes and consequently in an improved longitudinal coherence of the FEL pulse. Proof of principle experiments have been performed at ≈160 nm [1] and at wavelengths around 50 nm [2,3].

Seeding an FEL with a HHG source is one of the most straightforward ways to transfer the coherence properties of an external source to the FEL radiation. In addition to an enhanced longitudinal coherence of the FEL pulse, seeding with an external laser offers a laser pulse, which is inherently synchronized to the FEL x-ray emission. This is most favorable for x-ray/nIR pump-probe investigations in the femtosecond range since the typical arrival time jitter associated to SASE FELs is significantly reduced. At modern SASE FELs, a typical timing jitter of about hundred femtoseconds or more is typically present at the experimental stations.

While seeding at VUV wavelength was successful, injection at wavelengths shorter than 50 nm has remained a challenge using state of the art HHG sources. At shorter wavelengths significantly higher HHG peak power is required since the FEL SASE shot noise scales with λ^{-1}. This requirement is in conflict with the HHG conversion efficiency since the latter decreases for higher photon energy.

In this paper we present recent results on enhanced HHG in an elongated capillary waveguide. One of the limitations to upscale HHG to higher photon fluence and peak power at shorter wavelengths is given by the phase mismatch between the fundamental driving laser wavelength and the harmonics. In the past, different schemes have been studied to overcome this detrimental velocity mismatch in order to enhance the conversion efficiency, such as quasi phase matching, counter propagating beams, modulated waveguides and HHG by a two-color driving laser [4-7]. Since these enhancing techniques complicate the generation process and does not allow phase matching across a large spectral bandwidth we investigated a more simple approach based on an unmodulated, elongated waveguide. We consider direct phase matching by compensating the different HHG dispersion contributions (plasma, neutral gas, waveguide etc.) to be the most efficient and most robust approach for broadband harmonic generation.

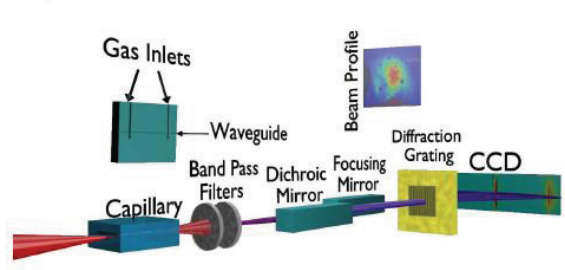

Figure 1: Experimental setup for HHG.. (From ref [8])

EXPERIMENTAL SETUP

For the presented investigations recently published in [8] a 40 fs, 6 mJ Ti:sapphire laser system is used at 1 kHz repetition rate and at a central wavelength of 805 nm. HHG is launched by focusing the laser beam loosely (f=1.5m) into a capillary which is continuously flooded with a rare gas (Fig. 1). The waveguide is made of sapphire glass and carries a 33 mm long laser-drilled channel with an inner diameter of 200 µm. Two gas inlets are arranged orthogonally to the laser waveguide, which is flooded with helium. After the capillary a set of thin metal filters and a pair of dichroic mirrors are used to separate the soft x-ray

ISBN 978-3-95450-126-7

HIGH AVERAGE POWER SEED LASER DESIGN FOR HIGH REPRATE FELs*

R. Wilcox, G. Marcus, G. Penn, LBNL, Berkeley, CA 94720 USA
T. Metzger, M. Schultze, Trump Scientific Lasers, Unterfohring 85774, Germany

Abstract

For two ultrashort pulse X-ray FEL designs, we show that seed or modulating lasers can be built using existing laser technology. An HGHG cascade FEL is seeded with UV from a high average power, frequency quadrupled OPCPA pumped by thin disk regenerative amplifiers. An E-SASE FEL has the electron bunch modulated by a single optical cycle at 2μm, generated by coherently added OPA signal and idler at 1.5 and 3μm.

INTRODUCTION

To be maximally useful as experimental sources X-ray FELs need to control the time-varying parameters of the pulse, that is, instantaneous amplitude and phase. This can be achieved by seeding the FEL with a light pulse generated by a laser or a combination of laser and optical harmonic generation systems. High gain harmonic generation (HGHG) can be used to extend the photon energy range of the FEL beyond that of the seed laser. It is also possible to make a temporally uniform pulse by using a laser to modulate the electron density, generating a current spike with a bandwidth equal to the FEL gain bandwidth, and allowing spontaneous emission during this shortened bunch to seed the FEL process. We have designed FELs using both these schemes [1, 2] and designed seed laser systems which can produce the needed optical pulses. This paper describes the laser designs.

HGHG SEED LASER

For the cascaded HGHG scheme, we seed with a UV pulse in the 220nm range, and multiply frequency in the FEL up to 600eV. Various multiplication factors can be chosen, but since they are integers, the seed laser must be tunable to cover gaps and allow quasi-continuous wavelength tuning. Thus a range of 217 to 261nm is needed. The pulse width range covers 100fs to 10fs, but with peak optical power of ~250MW at 100fs, up to 700MW at 10fs. At 100fs, the pulse energy is 25µJ, and at a repetition rate of 100kHz requires 2.5W at the FEL modulator. At 10fs, the pulse energy at the modulator is 7µJ, with 700mW.

We have initially designed two optical parametric chirped pulse amplifier (OPCPA) laser systems to address the short and long pulse requirements, as it may be difficult to cover the pulse width range with one amplifier setup. While it may be possible to hybridize the design, and at least use the same pumps for two systems, we can at least show that the extremes of the range can be generated. A diagram of the overall seed laser is shown in figure 1, with detail of the OPA amplifier for 100fs (power and energy worst case) shown in figure 2. Also shown in figure 2 are the spectral widths for the two designs).

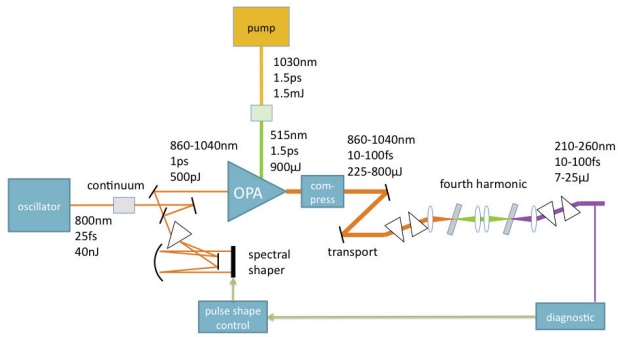

Figure 1: HGHG seed laser design. The diagram shows one of five pump lasers for the OPA.

OVERALL LASER DESIGN

In the seed laser, a titanium sapphire laser emits short (~20fs) pulses which are amplified and then broadened in a nonlinear element to produce a continuum in the 820-1100nm range. A broadband pulse shaper filters the continuum (according to which UV wavelength and pulse width is desired) and controls the spectral phase and amplitude of the resulting pulses, which are subsequently stretched to around 1ps. A five-stage OPA amplifies the stretched pulses to 790µJ (in the 100fs case), after which they are compressed by chirped mirrors [3] and frequency quadrupled to the ultraviolet (238nm in this calculation). Assuming 10% efficiency for fourth harmonic generation, and 30% transmission loss, there will be 24µJ at the FEL. For the 10fs case, 233µJ are needed from the amplifier, assuming the same FHG efficiency and loss).

PUMP LASER

To produce 800uJ at the OPA output, with 100kHz repetition rate, and nominal 20% OPA efficiency, a frequency doubled IR pump with about 400W is needed. With 60% efficient SHG, the IR power is 670W. There currently exist Yb:YAG thin disk regenerative amplifiers

*This work was supported by the U.S. Department of Energy under contract numbers DE-AC02-0SCH11231.

ISBN 978-3-95450-126-7

HARMONIC LASING SELF-SEEDED FEL

E.A. Schneidmiller, M.V. Yurkov, DESY, Hamburg, Germany

Abstract

Numerical studies of the recently proposed concept of a harmonic lasing self-seeded FEL are presented. A gap-tunable undulator is divided into two parts by setting two different undulator parameters such that the first part is tuned to a sub-harmonic of the second part. Harmonic lasing occurs in the exponential gain regime in the first part of the undulator, also the fundamental stays well below saturation. In the second part of the undulator the fundamental mode is resonant to the wavelength, previously amplified as the harmonic. The amplification process proceeds in the fundamental mode up to saturation. In this case the bandwidth is defined by the harmonic lasing (i.e. it is reduced by a significant factor depending on harmonic number) but the saturation power is still as high as in the reference case of lasing at the fundamental in the whole undulator, i.e. the spectral brightness increases. Application of the undulator tapering in the deep nonlinear regime would allow to generate higher peak powers approaching TW level. The scheme is illustrated with the parameters of the European XFEL.

INTRODUCTION

Successful operation of X-ray free electron lasers (FELs) [1–3], based on self-amplified spontaneous emission (SASE) principle [4], opens up new horizons for photon science. However, a poor longitudinal coherence of SASE FELs stimulated efforts for its improvement. Since an external seeding seems to be difficult in X-ray regime, a so called self-seeding has been proposed [5–7]. A particularly simple in technical realization self-seeding scheme [7] is now in operation at the Linac Coherent Light Source (LCLS) [8].

There are alternative approaches to reducing bandwidth and increasing spectral brightness of X-ray FELs without using optical elements. One of them (called iSASE [9]) uses chicanes within an undulator system to increase slippage of the radiation and thus a coherence time. Another approach was proposed by us [10] and is based on combined lasing on a harmonic in the first part of the undulator (with increased undulator parameter K) and on the fundamental in the second part. In this way the second part of the undulator is seeded by a narrow-band signal generated via a harmonic lasing in the first part. Therefore, we suggest here to call this concept HLSS FEL (Harmonic Lasing Self-Seeded FEL). Recently, a very similar concept was proposed in [11]: a purified SASE FEL, or pSASE. The authors of [11] performed numerical simulations of this scheme[1] to confirm the validity of the concept. It was proposed in [11] to have three sections of the undulator: the harmonic lasing section (with increased K-value) is placed in between of the two sections with lower K. We notice here that simply by exchange of the first two sections (smaller K and larger K), both operating as linear amplifiers, the pSASE concept is reduced to our original concept [10]. In other words, pSASE FEL is a more complicated version of the HLSS FEL.

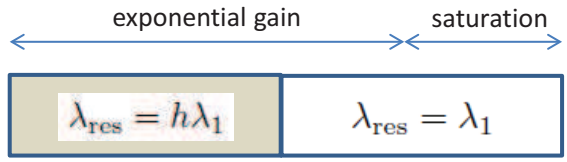

Figure 1: Conceptual scheme of a harmonic lasing self-seeded FEL.

In this paper we present the results of numerical simulations of the HLSS FEL scheme with the parameters of the European XFEL.

SCHEME DESCRIPTION

Typically, gap-tunable undulators are planned to be used in X-ray FEL facilities. If maximal undulator parameter K is sufficiently large, the concept of harmonic lasing self-seeded FEL can be applied in such undulators (see Fig. 1). An undulator is divided into two parts by setting two different undulator parameters such that the first part is tuned to a sub-harmonic of the second part (and the second part is tuned to a wavelength of interest). Harmonic lasing occurs in the exponential gain regime in the first part of the undulator, also the fundamental in the first part stays well below saturation. In the second part of the undulator the fundamental mode is resonant to the wavelength, previously amplified as the harmonic. The amplification process proceeds in the fundamental mode up to saturation. In this case the bandwidth is defined by the harmonic lasing (i.e. it is reduced by a significant factor depending on harmonic number) but the saturation power is still as high as in the reference case of lasing at the fundamental in the whole undulator, i.e. the spectral brightness increases.

Harmonic lasing in single-pass high-gain FELs [10, 13–15] is the radiative instability at an odd harmonic of the planar undulator developing independently from lasing at the fundamental wavelength. Contrary to nonlinear harmonic

[1] Very recently the pSASE scheme was also simulated in [12].

ISBN 978-3-95450-126-7

COHERENCE PROPERTIES OF THE RADIATION FROM FLASH

E.A. Schneidmiller, M.V. Yurkov, DESY, Hamburg, Germany

Abstract

Several user groups at FLASH use higher odd harmonics (3rd and 5th) of the radiation in experiments. Some applications require knowledge of coherence properties of the radiation at he fundamental and higher harmonics. In this paper we present the results of the studies of coherence properties of the radiation from FLASH operating at radiation wavelength of 8.x nm at the fundamental harmonic, and higher odd harmonics (2.x nm and 1.x nm). We found that present configuration of FLASH free electron laser is not optimal for providing ultimate quality of the output radiation. Our analysis shows that the physical origin of the problem is mode degeneration. The way for improving quality of the radiation is proposed.

INTRODUCTION

After an energy upgrade the soft X-ray FEL FLASH at DESY covers a spectral range between approximately 45 nm and 4.2 nm wavelength [1, 2]. With the present undulator (period 2.73 cm, peak field 0.486 T) the minimum wavelength of 4.2 nm is determined by the maximum electron beam energy of approximately 1.25 GeV. There exists clear tendency for users at FLASH to extend available wavelength range to shorter wavelengths. Here we first remember about the so-called water window, i.e. the range between the K-Absorption edges of carbon and oxygen at 4.38nm and 2.34 nm, respectively. Currently minimum wavelength of FLASH is just below the carbon edge. Other range of interest refers to the edges of magnetic elements which spans below water window. In principle, higher odd harmonics of SASE radiation can be used to get radiation. Pioneer experiment for studying magnetic materials using FEL radiation has been performed at FLASH at 1.6 nm wavelength, the 5th harmonic of the fundamental at 8 nm [3]. Many user's experiments rely on coherent properties of the radiation, both temporal and spatial. This concern relates not only to the fundamental harmonic, but to the higher odd harmonics as well.

Previous studies have shown that with given parameters of the electron beam, coherence properties of the radiation strongly evolve during amplification process. At the initial stage of amplification coherence properties are poor, and radiation consists of large number of transverse and longitudinal [4]:

$$\tilde{E} = \int \mathrm{d}\omega \exp[i\omega(z/c-t)] \times \sum_{n,k} A_{nk}(\omega,z)\Phi_{nk}(r,\omega)\exp[\Lambda_{nk}(\omega)z + in\phi] \quad (1)$$

described by the eigenvalue $\Lambda_{nk}(\omega)$ and the field distribution eigenfunction $\Phi_{nk}(r,\omega)$. Here $\omega = 2\pi c/\lambda$ is the frequency of the electromagnetic wave. The fundamental mode (having maximum real part of the eigenvalue) dominates more and more over higher modes when undulator length progresses. Total undulator length to saturation is in the range from about nine (hard x-ray SASE FELs) to eleven (visible range SASE FELs) field gain lengths [5, 6, 9]. Situation with transverse coherence is favorable when relative separation of increments between fundamental and higher modes is more than 20%. In this case degree of transverse coherence asymptotically approaches to unity in the amplification process, and can reach values above 90% in the end of the high gain linear regime [7, 8]. Further development of amplification process in the nonlinear stage leads to visible degradation of the spatial and temporal coherence [5, 6, 9]. Separation of the increments of the beam radiation modes strongly depends on the value of diffraction parameter, and is more pronouncing for stronger focused electron beams [10]. Increase of the energy spread and emittance also leads to better separation of the increments of the beam radiation modes.

In the present experimental situation many parameters of the electron beam at FLASH depend on practical tuning of the machine. Analysis of measurements and numerical simulations shows that depending on tuning of the machine emittance may change from about 1 to about 1.5 mm-mrad. Tuning at small charges may allow to reach smaller values of the emittance down to 0.5 mm-mrad. Peak current may change in the range from 1 kA to 2 kA depending on the tuning of the beam formation system. One (more or less) fixed parameter is average focusing beta function in the undulator which has average value about 10 meters. In this paper we perform thorough analysis of described parameter space with special attention to the coherence properties of the radiation not only for the fundamental frequency, but also for the 3rd and the 5th harmonic. Our conclusion is that spatial coherence of the radiation at FLASH suffers significantly from not sufficient suppression of the higher radiation modes. This happens due to the large value of the diffraction parameter. Our analysis shows that operation with stronger beam focusing, lower emittances and lower peak current will allow to operate FLASH with ultimate quality of the radiation in terms of the degree of transverse coherence exceeding 90%.

For illustration we have chosen specific wavelength of 8 nm. The main reason for this is that this wavelength has been used by several user groups (see, e.g. [3, 12, 13]). Thus, results, presented here, can be used directly for analysis of obtained results and planning future measurements.

ISBN 978-3-95450-126-7

PRESENT STATUS OF KYOTO UNIVERSITY FREE ELECTRON LASER

H. Zen#, M. Inukai, K. Okumura, K. Mishima, K. Torgasin, H. Negm, M. Omer,
K. Yoshida, R. Kinjo, T. Kii, K. Masuda, H. Ohgaki
Institute of Advanced Energy, Kyoto University, Gokasho, Uji, Kyoto, Japan

Abstract

A vacuum duct was newly designed and manufactured to make the undulator gap narrower in order to increase the KU-FEL performance. The width of the undulator duct is 15 mm, but the minimum undulator gap is limited to 16.5 mm due to the small flexure of the duct. After replacing the old undulator duct whose minimum width was around 19.5 mm with new one, the tunable range of KU-FEL has been extended from 5-14.5 μm to 5-21.5 μm. The FEL gain higher than 60% has been observed at largely detuned optical cavity.

INTRODUCTION

An oscillator type Mid-Infrared Free Electron Laser (MIR-FEL) named as KU-FEL has been developed in Institute of Advanced Energy, Kyoto University, for aiding energy related sciences [1]. A 4.5-cell thermionic RF gun is employed as the electron source. After introduction of some cures of back-bombardment effect in the gun [2, 3, 4, 5], we have achieved the first lasing [6], and power saturation in 2008 [7]. However, with trade off relationship between the bunch charge and macro-pulse duration limits the tunable range of the FEL (only 10 to 14 μm). In order to extend the tunable range, the optical cavity mirrors and the undulator have been replaced in January 2012. After those replacements, the tunable range of the FEL has been extended to 5 – 15 μm [8]. We have been still making efforts to increase the FEL gain and to extend the tunable range. For that purpose, we fabricated a new vacuum duct for our undulator, which has the horizontal width of 15 mm. At 15-mm gap, twice FEL gain than 19.5-mm gap (the minimum gap with the old undulator duct) is expected. Commissioning experiments with the new duct have been done in April 2013. The result of the experiment and upgraded performance of KU-FEL are reported in this paper.

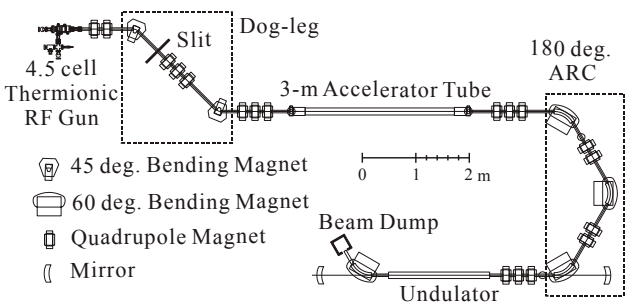

Figure 1: Schematic diagram of KU-FEL accelerator.

#zen@iae.kyoto-u.ac.jp

KU-FEL DEVICE

Figure 1 shows the schematic diagram of KU-FEL device, which consists of a 4.5-cell thermionic RF gun, dog-leg section for an energy filtering, a 3-m accelerator tube, a 180-degree arc section for a bunch compression, an undulator and an optical cavity. Parameters of the undulator and the optical cavity are shown in Table 1.

Table 1: Parameters of Undulator and Optical Cavity

Undulator		
Structure		Hybrid
Period length		33 mm
Number of periods		52
Maximum K-value		1.00 @ 19.5-mm gap* 1.56 @ 15-mm gap**
Minimum Gap		15 mm**
Optical cavity (upstream mirror has out-coupling hole)		
Mirror curvature	Upstream	2.984 m
	Downstream	2.503 m
Diameter of out-coupling hole		1 mm
Cavity length		5.0385 m
Reflectivity of one mirror		99.04%

* Minimum gap limited by old vacuum chamber
** Minimum gap limited by undulator mechanics

DESIGNING AND MANUFACTURING OF NEW UNDULATOR DUCT

As listed in Table 1, the minimum gap given by the undulator itself is 15 mm. Therefore, we decided to design a new undulator duct whose width is 15 mm. In order to give sufficiently high mechanical strength against air pressure, the thickness of undulator duct was selected as 2 mm. Then the clear aperture size in horizontal (gap side) direction was fixed as 11 mm. The vertical aperture was designed to have same size with old one, 56 mm. The comparison between the horizontal aperture size and 6σ–beam size of FEL beam are shown in Fig. 2. The 6σ–beam size in the optical cavity at the wavelength of 20 μm is comparative with the horizontal aperture of the vacuum duct at both ends of the undulator duct. Therefore, optical loss caused by diffraction at the vacuum chamber must be smaller than 1% even at the longest wavelength of our target, 20 μm.

ISBN 978-3-95450-126-7

HIGH-PRECISION ELECTRONICS FOR SINGLE PASS APPLICATIONS

M. Znidarcic, R. Hrovatin, Instrumentation Technologies, Solkan, Slovenia
M. Satoh, High Energy Accelerator Research Organization (KEK), Tsukuba, Japan

Abstract

Monitoring and subsequent optimization of electron Linacs and transfer lines requires specific instrumentation for beam position data acquisition and processing. Libera Single Pass E is the newly developed instrument intended for position and charge monitoring in classical and multi-mode operation Linacs. Development, initial measurements and verification of the instrument performance were conducted in the Instrumentation Technologies laboratories, followed by characterization measurements of the unit carried out at the KEK Linac facility.

INTRODUCTION

Libera Single Pass E is a result of successful collaboration between KEK Linac and Instrumentation Technologies. The KEK 8-GeV Linac injects electron and positron beams with different characteristics into four storage rings: KEKB high-energy ring (HER), KEKB low-energy ring (LER), Photon Factory (PF) and PF-AR. The performance of these machines depends on the injection quality [1]. The BPM system therefore has to provide continuous high-precision monitoring of position for various beam species. It needs to support a wide dynamic range of charge, i.e. charges vary from 0.1 nC to 10 nC. Furthermore, the BPM must auto-detect and further conduct either single-bunch processing or individual processing of two consecutive bunches which are 96.2885 ns apart.

Based on external event announcing, Libera Single Pass E (see Fig. 1), adapts to the beam charge and pattern. It can process various beam structures (single bunch, narrow dual bunch, trains, continuous wave) with large dynamics (over 40 dB). Libera Single Pass E system is based on uTCA modular technologies with IPMI platform management. The system is therefore developed on multiple AMC modules, with each module covering different functionalities.

Figure 1: Libera Single Pass E front panel.

The user can access the functions implemented in the Libera Single Pass E unit through a control system interface, called the Measurement and Control Interface (MCI). This interface was developed to facilitate the integration of Libera Single Pass E into the accelerator's control system software.

CONTROL SYSTEM INTEGRATION

On the top layer, Libera Single Pass E provides the MCI with a development package and Command Line utilities for open interaction in different control systems. On top of the MCI, various adaptors to different control systems can be implemented (EPICS, Tango, etc.). The EPICS interface is part of the standard software package.

EVENT RECEPTION

Libera Single Pass E [3] detects the events announced by the accelerator timing system in order to set the data processing parameters optimally for the expected bunch structure. It enables event reception via the optics/wire event reception in the event receiver module (EvRx) or alternatively via external interfaces (EPICS protocol event generator) [6].

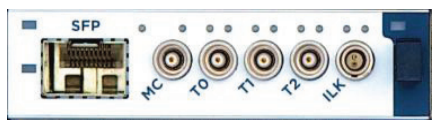

Figure 2: Event receiver module.

The EvRx (see Fig. 2), module receives the optical signal through the SFP transceiver and identifies and extracts the 16-bit event code. Once the code has been extracted, the module decodes the event identification code and triggers specific functions at low latency.

DATA PROCESSING

The data processing is initiated by the external event signal. The short signal from the detector is first shaped by the analog front-end filtering, designed in relation to the accelerator parameters.

Through the configuration of various software parameters, Libera Single Pass E offers processing of various beam types (flavors). After the hardware trigger signal which announces the arrival of the bunch, the search of the bunch signal is started. The bunch signal is detected in comparison with the threshold parameter, then a useful part of the signal is defined with the pre-trigger and post-trigger parameters. The sum of the pre-trigger and post-trigger defines the processing window. The signal energy is calculated from the signal as defined by the processing window. After calculating the four signal amplitudes – Va, Vb, Vc and Vd – the beam position is calculated using formulas for X and Y. Four options can be used for position calculation:

- Diagonal pickup orientation – Linear formula
- Diagonal pickup orientation – Polynomial formula (3rd order)

ISBN 978-3-95450-126-7

DESIGN OF A RESONATOR FOR THE CSU THz FEL

P.J.M. van der Slot,*
University of Twente, Mesa+ Institute for Nanotechnology, Enschede, The Netherlands
Colorado State University, Department of Electrical and Computer Engineering, Fort Collins, USA
S.G. Biedron and S.V Milton,
Colorado State University, Department of Electrical and Computer Engineering, Fort Collins, USA

Abstract

A typical confocal resonator for THz radiation produced by an FEL will have a waist that is larger than the gap of the undulator. Hence waveguiding is required. Here we consider a resonator consisting of two spherical mirrors and a cylindrical waveguide in between. The radii of curvature for the mirrors are chosen to image the ends of the waveguide onto themselves. We discuss the properties of the cold resonator for a wavelength range from 200 to 600 μm and show that the outer radii of the mirrors can be used to control the mode content inside the cylindrical waveguide.

INTRODUCTION

The field of TeraHertz (THz) radiation, which fills the so-called frequency gap between 0.1 and 10 THz (30 μm to 1 mm), has seen significant progress in recent years [1]. The unique properties of THz radiation, together with source and diagnostic developments have enabled applications in medical sciences, non-destructive evaluation, homeland security, control of food quality and in many other areas. Despite the progress, sources with high peak power of 100 kW or more are still lacking. The Colorado State University Accelerator Facilty [2] aims to study, amongst others, various ways to efficiently generate high peak power THz radiation using a FEL. The THz FEL consists of a 6 MeV, L-band, linear accelerator and a fixed gap, equal focussing, linear undulator with $N_u = 50$ periods of $\lambda_u = 2.5$ cm length. The wavelength of this system varies from approximately 200 to 600 μm.

Operating at THz frequencies requires wave guiding to avoid excessive diffraction losses [3]. Usually, parallel plate waveguiding is used, where guiding is provided in one plane and free-space propagation in the other [3, 4]. The effect of cylindrical waveguides on the optical mode propagation has been considered for far-infrared FELs where the wavelengths are such that optical propagation through the cylindrical beam pipe inside the undulator borders between free-space propagation and guided wave propagation [5]. Ref. [5] shows that for sufficiently small wavelengths, the cylindrical waveguide could be replaced by two apertures at the waveguide ends without modifying the wave propagation. At larger wavelengths, the study shows that for the waveguide the optical mode is modified and the roundtrip loss drops below the loss when the waveguide is replaced by two apertures. In order to model the field inside the waveguide, both TE and TM modes were required.

For the CSU THz FEL, the wavelengths are significantly longer and using a resonator consisting only of spherical mirrors would result in a waist diameter that is larger than the gap of the undulator. We therefore consider a geometry where a cylindrical waveguide is used to "image" the waist from one end of the waveguide to the order end. The minimum length of the waveguide is the physical length L_u of the undulator, $L_u = 1.35$ m (note, this is longer than $N_u\lambda_u$). The resonator is completed by two spherical mirrors positioned at either end of the waveguide. Distance and radius of curvature (focal length) are chosen such that the mirror images the end facet of waveguide on to itself. Since the FEL will produce linearly polarised light, it is sufficient to only include TE modes for describing the field inside the waveguide. The resonator is analysed using the Fox-Li method [6]. In the remainder of this paper we first discuss the coupling of a fundamental Gaussian mode to the waveguide and then discuss the properties of the resonator.

COUPLING OF A GAUSSIAN MODE TO A WAVEGUIDE

The resonator consists of a cylindrical waveguide with two spherical mirrors on either side. Propagation of the optical field inside this resonator consists of guided wave propagation inside the waveguide and free-space propagation in between the waveguide ends and the mirrors. It is therefore of interest to determine the coupling of the free-space optical field to the TE_{nm} waveguide modes, which are the only modes of interest for the chosen geometry. The electric field of a linear polarised optical field inside the waveguide can be written as a superposition of TE_{nm} modes as (cylindrical coordinates r, ϕ, z)

$$\mathbf{E}(r,\phi,z,t) = \sum_{n,m} B_{nm}\mathbf{E}_{nm}(r,\phi)e^{i(\omega t-\beta_{nm}z)} \qquad (1)$$

where

$$\mathbf{E}_{nm}(r,\phi) = i\frac{nk_0Z_0}{r}J_n(\kappa_{nm}r)sin(n\phi)\hat{r} + ik_0Z_0\kappa_{nm}\beta_{nm}J_n^{'}(\kappa_{nm}r)cos(n\phi)\hat{\phi}. \qquad (2)$$

In eqs. 1 and 2, B_{nm} is the mode amplitude, $\omega = ck_0$, c being the speed of light in vacuum, $k_0 = \frac{2\pi}{\lambda}$, λ being the free-space wavelength, Z_0 is the vacuum impedance, $\beta_{nm} = \sqrt{k_0^2 - \kappa_{nm}^2}$ is the propagation constant of the

* p.j.m.vanderslot@utwente.nl

ISBN 978-3-95450-126-7

DOUBLE STAGE SEEDED FEL WITH FRESH BUNCH INJECTION TECHNIQUE AT FERMI*

E. Allaria[1,#], D. Castronovo[1], P. Cinquegrana[1], M.B. Danailov[1], G. D'Auria[1], A. Demidovich[1], S. Di Mitri[1], B. Diviacco[1], W.M. Fawley[1], M. Ferianis[1], L. Froehlich[1], G. Gaio[1], R. Ivanov[1], N. Mahne[1], I. Nikolov[1], G. Penco[1], L. Raimondi[1], C. Serpico[1], P. Sigalotti[1], C. Spezzani[1], M. Svandrlik[1], C. Svetina[1], M. Trovo[1], M. Veronese[1], D. Zangrando[1], Benoît Mahieu[1,2], M. Dal Forno[3,1], L. Giannessi[4,1], M. Zangrando[5,1], G. De Ninno [7,1], E. Ferrari[8,1], F. Parmigiani[8,1], D. Gauthier [7]

[1]Elettra-Sincrotrone Trieste S.C.p.A., Basovizza
[2]CEA/DSM/DRECAM/SPAM, Gif-sur-Yvette
[3]DEEI, Trieste
[4]ENEA C.R. Frascati, Frascati (Roma)
[5]IOM-CNR, Trieste
[6]PSI, Villigen PSI
[7]University of Nova Gorica, Nova Gorica
[8]Università degli Studi di Trieste, Trieste

Abstract

Seeding a FEL with an external coherent source has been extensively studied in the last decades as it can provide a way to enhance the radiation brightness and stability with respect to that available from SASE. An efficient scheme for seeding a VUV-soft x ray FEL uses a powerful, long wavelength external laser to induce on the electron beam coherent bunching at the harmonics of the laser wavelength [1]. When the bunching is further amplified by FEL interaction in the radiator, the scheme is called high gain harmonic generation (HGHG) [2]. The need for high power seed sources and small electron beam energy spread are at the main limits for direct extension of the HGHG scheme to short wavelengths. The fresh bunch scheme was proposed as a way to overcome these limitations [3]; the scheme foresees the FEL radiation produced by one HGHG stage as an external seed for a second HGHG stage. We report the latest results obtained at FERMI that uses the two-stage HGHG scheme for generation of FEL pulses in the soft x-ray regime. A characterization of the FEL performance in terms of power, bandwidth and stability is reported. Starting from the FERMI results we will discuss extension of the scheme toward shorter wavelengths.

TWO STAGE HGHG AT FERMI

Operation of FERMI FEL-1 has recently shown the possibility to produce high quality FEL pulses from a single stage HGHG device down to 20nm [4]. Although some coherent emission can be generated at even shorter wavelength with a single stage cascade [5], the amount of power that can be accessed is limited by the large energy spread that is necessary to get a significant bunching at a very large harmonic of the initial seed laser. In order to efficiently produce coherent emission at wavelengths at 10 nm and shorter, a two stage HGHG scheme [3] has been implemented in FERMI's FEL-2 [6]. The layout of the FEL-2 line is sketched in Figure 1. The linear accelerator is not shown as it is the same as used for FEL-1 (see, *e.g.*, [7,8]).

The FERMI FEL-2 layout has a first undulator (MOD) where the electron beam is in resonance with the external seed laser and becomes energy modulated at the laser wavelength (260 nm). The energy modulation is then converted into spatial modulation (bunching) at the laser wavelength and harmonics when the electron beam passes through the first dispersive section (DS1) with an R56 of few tens of microns. The bunched beam emits coherent emission at the desired harmonic wavelength (*e.g.,* 32.5 nm) that is resonant in the following undulators (RAD1. In the delay line (DL) the electron beam is delayed by few hundreds of fs with respect to the FEL pulse produced. The strong dispersion of the delay line also eliminates nearly all residual bunching in the beam at 32.5 nm and harmonics. An additional undulator (MOD2) is tuned again at 32.5 nm so that the head part of the beam can interact with the FEL pulse produced on the first stage. Here the interaction produces energy modulation at 32.5 nm that is converted to coherent bunching at 32.5 nm and higher harmonics by the second dispersive section (DS2) with an R56 of few microns. The electron beam, now bunched at very short wavelengths, enters the final radiator (RAD2) that is tuned to one of the harmonics of 32.5 nm (*e.g.*, 10.8 nm). Here coherent emission is followed by FEL amplification.

*Work partially supported by the Italian Ministry of University and Research under grants FIRB-RBAP045JF2 and FIRB-RBAP06AWK3
#enrico.allaria@elettra.eu

ISBN 978-3-95450-126-7

STABLE OPERATION OF HHG-SEEDED EUV-FEL AT THE SCSS TEST ACCELERATOR

H. Tomizawa, K. Ogawa, K. Togawa, T. Tanaka, T. Hara, M. Yabashi, H. Tanaka, and T. Ishikawa, RIKEN, SPring-8 Center, Kouto 1-1-1, Sayo, Hyogo 679-5148, Japan
T. Togashi, S. Matsubara, Y. Okayasu, and T. Watanabe, Japan Synchrotron Radiation Research Institute, Kouto 1-1-1, Sayo, Hyogo 679-5198, Japan
E. J. Takahashi and K. Midorikawa, RIKEN Center for Advanced Photonics, Hirosawa 2-1, Wako, Saitama 351-0198, Japan
M. Aoyama and K. Yamakawa, Japan Atomic Energy Agency, Umemidai 8-1-7, Kizugawa, Kyoto 619-0215, Japan
T. Sato, S. Owada, A. Iwasaki, and K. Yamanouchi, The University of Tokyo, Hongo 7-3-1, Bunkyo-ku, Tokyo 113-0033, Japan

Abstract

We completed HHG (Higher-order Harmonic Generation) optical laser-seeded FEL (Free Electron Laser) operation at a 61.2-nm fundamental wavelength with an HHG pulse seeding source from a Ti:sapphire laser at the EUV (Extreme Ultraviolet) -FEL test accelerator. The HHG-seeded FEL scheme must synchronize the seeding laser pulse to the electron bunch. We constructed a relative arrival timing monitor based on EO (Electro-Optic) sampling. Since the EO-probe laser pulse was optically split from the HHG-driving laser pulse, the arrival time difference of the seeding laser pulse, with respect to the electron bunch, was measured in real time. This non-invasive EOS (EO Sampling) monitor made uninterrupted, single shot monitoring possible even during the seeded FEL operation. The EOS system was used for the arrival timing feedback with a hundred-femtosecond adjustability for continual operation of the HHG-seeded FEL. Using the EOS locking system, the HHG-seeded FEL was operated over half a day with a 20 – 30% effective hit rate. The output pulse energy was 20 μJ at the 61.2-nm wavelength. A user experiment was performed using the seeded EUV-FEL at SCSS, and a clear difference was observed between the SASE FEL and the seeded FEL with a high contrast.

INTRODUCTTION

FEL (Free Electron Laser), which was proposed in the early 1970s, is one of the most promising coherent light sources with arbitrary wavelength [1]. Today, using SASE (Self-Amplified Spontaneous Emission) scheme, FEL is available in wide regions up to hard X-rays [2].

SCSS (SPring-8 Compact SASE Source) [3], which is the prototype FEL machine at SPring-8, was constructed for feasibility tests of new components to realize our FEL machine concept. This SASE FEL generated an EUV (Extreme Ultraviolet) pulse at wavelengths from 50 to 60 nm. This EUV-FEL contributed to a variety of user experiments, especially research on the resonance absorption of atomic or molecular lines in AMO (Atomic, Molecular, and Optical physics).

SASE starts from shot noise (spontaneous emission) and is amplified through electromagnetic interaction with a high-brightness electron bunch in a single pass (without an optical cavity). Based on this mechanism, the SASE pulse fluctuates in its spectrum due to the temporal multimode. Its spectrum fluctuates shot-to-shot, because of its shot-noise seeding source. The SASE characteristics are not reliable for AMO experiments that aim at a specific wavelength for resonance absorptions. To provide a spectrum with a targeting single peak on the demand of user experiments, a full-coherent seeding source is required instead of shot noise for FEL machines without an optical cavity in shorter wavelengths below the EUV region.

In the methodology, seeding schemes, which have been intensively developed worldwide, are roughly categorized into two kinds of approaches. One is called self-seeding, which utilizes a SASE pulse monochromized just after the first undulator section as the seeding source for the second undulator section by itself [4]. The self-seeding scheme is reliable for seeding in the hard X-ray region.

In the other scheme, an external laser pulse is prepared and directly used as a full-coherent seeding pulse. Up to now, an optical laser can be generated up to the water window region. However, the pulse energy is limited and insufficient for seeding in a shorter wavelength. To extend FEL seeding in a shorter wavelength, this seeding scheme is often combined with HGHG (High-Gain Harmonic-Generation) [5]. In the user facility at FERMI (Elettra), the 3rd order harmonic pulse of a Ti:Sapphire laser is used as optical seeding and generates FEL seeded at its 13th harmonics with HGHG [6]. For our SCSS, we directly developed external seeding with HHG pulses at the SASE's wavelength. These corresponding HHG's orders of a Ti:Sapphire laser (800 nm) were prepared as follows: 13th (61.7 nm), 15th (53.3 nm), and 17th (47.1 nm).

ISBN 978-3-95450-126-7

THREE UNIQUE FEL DESIGNS FOR THE NEXT GENERATION LIGHT SOURCE

G. Penn*, D. Arbelaez, J. Corlett, P.J. Emma, G. Marcus, S. Prestemon, M. Reinsch, R. Wilcox,
LBNL, Berkeley, CA 94720, USA
A. Zholents, ANL, Argonne, IL 60439, USA

Abstract

The NGLS is a next generation light source initiative spearheaded by the Lawrence Berkeley National Laboratory and based on an array of free-electron lasers (FEL) driven by a CW, 1-MHz bunch rate, superconducting linear accelerator. The facility is being designed to produce high peak and high average brightness coherent soft x-rays in the wavelength range of 1 nm – 12 nm, with shorter wavelengths accessible in harmonics or in expansion FELs. The facility performance requirements are based on a wide spectrum of scientific research objectives, requiring high flux, narrow-to-wide bandwidth, broad wavelength tunability, femtosecond pulse durations, and two-color pulses with variable relative timing and polarization, all of which cannot be encompassed in one FEL design. In addition, the cost of the facility requires building in a phased approach with perhaps three initial FELs and up to 9-10 FELs in the long term. We describe three very unique and complementary FEL designs here as candidates for the first NGLS configuration.

INTRODUCTION

The NGLS is conceived as a soft x-ray free-electron laser (FEL) user facility with high repetition rate and multiple beam lines. It will be based on a CW superconducting (SC) linac accelerating bunches with a 1-MHz bunch rate. These bunches will be distributed through an array of FEL beamlines. We present three distinct beamlines which each address different experimental needs.

The first beamline is self-seeded [1, 2]: it starts from noise like a SASE FEL, then has the radiation pass through a monochromator to seed a second stage. This scheme produces a large number of photons in a narrow bandwidth close to that specified by the monochromator. Not needing an external laser seed, this beamline is consistent with a high repetition rate, although heating of the monochromator optics may become an issue. The output pulse will have a duration roughly equivalent to the region of the beam where the electron energy is close to the nominal value and the peak current is high. This portion of the beam is referred to throughout this paper as the "usable" portion of the beam.

The second beamline uses a conventional external laser as a seed, which determines the output pulse timing and duration. The repetition rate is then limited to that of the external laser. X-rays are produced through two stages of high-gain harmonic generation (HGHG), with a "fresh-bunch" delay in between stages [3]. Due to the fresh bunch scheme, the output pulse duration cannot be more than about 1/3 of the usable portion of the beam. The duration can be as short as 5 fs. This provides control of both the pulse duration and bandwidth, which together remain close to the transform limit.

The third beamline also uses an external laser but in an unconventional manner, to generate energy and/or current modulations which then shape the output pulse during SASE [4]. The combination of the chirped electron beam and undulator tapering produces very narrow pulses, of a few femtoseconds, with a high bandwidth mostly due to a roughly linear frequency chirp. Because radiation tends to be suppressed outside of a small region of the beam, two independent pulses can be generated with independent control over their wavelengths and relative timing. The repetition rate is again limited by that of the external laser. This beamline can provide both pulses of a pump-probe measurement.

BEAMLINE PARAMETERS

The nominal parameters, which are broadly consistent with simulation studies, are shown in Table 1. However, the beamlines are designed to be able to handle a worse beam emittance, of up to 0.9 μm, or a lower peak current of 400 A. The energy spread is adjustable by the use of a laser heater [5] to damp out microbunching instabilities.

Table 1: Electron beam parameters, both slice and projected where relevant. The usable bunch duration is defined as the portion of the beam with relatively flat beam energy and high peak current.

	Whole Bunch	Slice
Bunch charge	300 pC	-
Electron energy	2.4 GeV	-
Energy spread	1.1 MeV	0.15 MeV
Transverse emittance	1.0 μm	0.6 μm
Peak current	-	500 A
Rms bunch length	50 μm	-
Usable bunch duration	300 fs	-

We focus on undulators using superconducting (SC) technology with relatively short undulator period, to provide a large tuning range with reasonably large dimensionless undulator parameter. Photon energy tuning will

* gepenn@lbl.gov

ISBN 978-3-95450-126-7

TRANSVERSE GRADIENT UNDULATORS FOR A STORAGE RING X-RAY FEL OSCILLATOR*

R.R. Lindberg† and K.-J. Kim, ANL Advanced Photon Source, Argonne, IL 60439, USA,
Y. Cai, Y. Ding, and Z. Huang, SLAC National Accelerator Laboratory, Menlo Park, CA 94025, USA

Abstract

An x-ray FEL oscillator (XFELO) is a fully coherent 4th generation source with complementary scientific applications to those based on self-amplified spontaneous emission. While the naturally high repetition rate, intrinsic stability, and very small emittance produced by an ultimate storage ring (USR) makes it a potential candidate to drive an XFELO, the energy spread is typically an order of magnitude too large for sufficient gain. On the other hand, Smith and coworkers showed how the energy spread requirement can be effectively mitigated with a transverse gradient undulator (TGU): since the TGU has a field strength that varies with transverse position, by properly correlating the electron energy with transverse position one can approximately satisfy the FEL resonance condition for all electrons. Motivated by the recent work in the high-gain regime we investigate the utility of a TGU for low gain FELs at x-ray wavelengths. We find that a TGU may make an XFELO realizable in the largest ultimate storage rings now under consideration (e.g., in either the old Tevatron or PEP-II tunnel).

INTRODUCTION

Storage rings have served the synchrotron radiation community with bright x-rays from spontaneous emission for over fifty years. Additionally, some have produced coherent, intense radiation in the infrared to ultraviolet spectral range using free-electron laser (FEL) oscillators. Hence, it is natural to consider whether the storage rings of today might also drive an FEL oscillator operating at x-ray wavelengths. As shown in Ref. [1], such an x-ray FEL oscillator (XFELO) is feasible with current linac-based e-beams using a stabilized Bragg crystal-based x-ray optical cavity. Unfortunately, the equilibrium electron beam brightness of modern third generation storage rings is not sufficient for the XFELO: both the transverse emittance and the energy spread is too large to provide sufficient FEL gain. With the recent advances in minimum emittance lattices, however, so-called "ultimate storage rings" are being designed that can satisfy the transverse emittance condition $\varepsilon_x \sim \varepsilon_y \lesssim \lambda/4\pi$ at hard x-ray wavelengths. On the other hand, the longitudinal brightness in a storage ring is still too poor: the equilibrium energy spread is more than an order of magnitude too large, with a typical value $\sigma_\gamma/\gamma \equiv \sigma_\eta \sim 0.1\%$.

To make the large energy spread of a storage ring beam compatible with FEL operation, Smith and collaborators [2] proposed designing the undulator field such that the dimensionless deflection parameter $K \equiv eB_0/mck_u$ varies transversely as shown in Fig. 1 (here B_0 is the peak magnetic field, $k_u \equiv 2\pi/\lambda_u$ is the undulator wave-vector, and e, m, c are the electron charge magnitude, mass, and speed of light). Then, by combining this transverse gradient undulator (TGU) field with an electron beam whose energy is also correlated with transverse position, one can imagine preserving FEL gain even in the presence of large energy spreads. The TGU concept was recently revisited for high-gain FELs driven by large energy spread beams produced by laser-plasma accelerators in Ref. [3], and for high-gain FELs in a USR by Ref. [4].

In this paper we investigate to what extent one might leverage the advances in ultimate storage ring design with a TGU to drive an x-ray free-electron laser oscillator (XFELO). First, we begin by reviewing some basic low-gain TGU physics, and show that the parameter regime for XFELOs is somewhat different than that used in Refs. [5, 6]. Hence, we reinterpret some of their results, and then use some relatively simple analytic expressions to describe the TGU effect as it pertains to x-ray parameters. These expressions can be derived from the more complete 3D gain analysis that we sketch in the Appendix. Next, we discuss how the ideas developed for the TGU-FEL can be applied at x-ray wavelengths, and show how XFELO operation may become viable in a TGU with an electron beam whose energy spread is of order 0.1%, provided the emittance is $\lesssim \lambda/4\pi$. Finally, we begin to explore what additional constraints are imposed if this e-beam is derived from a stable, high brightness, ultimate storage ring (USR). It appears to be quite difficult to operate the XFELO in a USR without some sort of bypass line, and we further find that maintaining sufficient peak current and realistic kicker times are quite challenging. Nevertheless, we show that there are a set of parameters for which a storage ring TGU-XFELO is compatible with the PEP-X ring design [7].

FEL PHYSICS WITH A TGU

FEL gain requires a resonant interaction between the electrons and the radiation field. Writing the fundamental radiation wavelength as $\lambda_1 \equiv 2\pi/k_1$, the FEL interaction requires that

$$\lambda_1 = \lambda_u \frac{1 + K^2/2}{2\gamma^2} \quad (1)$$

* Work supported by U.S. Dept. of Energy, Office of Science, Office of Basic Energy Sciences, under Contract No. DE-AC02-06CH11357
† lindberg@aps.anl.gov

ISBN 978-3-95450-126-7

THE POTENTIAL USES OF X-RAY FELS IN NUCLEAR STUDIES

Wen-Te Liao*, Christoph H. Keitel and Adriana Pálffy,
Max-Planck-Institut für Kernphysik, Saupfercheckweg 1, D-69117 Heidelberg, Germany

INTRODUCTION

The intent of this study is to theoretically extend the territory of quantum optics to the fields of nuclear physics [1–3] and x-ray optics [4]. Typically, nuclear transition have energies above 10 keV and a very narrow linewidth, rendering optical lasers unsuitable to control nuclei. However, the novel X-ray Free Electron Laser (XFEL) [5, 6] delivers very bright hard x-rays providing completely new opportunities to study the light-nucleus interaction. Encouraged by this coming revolution, in the first part of this work the technique of stimulated Raman adiabatic passage and the two π-pulse method are investigated in the context of controlling the nuclear population with two Lorentz boosted XFEL pulses. In the second part of this work we consider another promising aspect of novel coherent x-ray sources, namely that the spot size of a tightly focused hard x-ray beam can be essentially smaller than a single atom. Thus, using hard x-ray photons as the information carriers for the future photonic circuits may lead to sub-nm architectures. As the first step, the coherent control of single hard x-ray photons with the help of the 14.4 keV transition of the ^{57}Fe Mössbauer nucleus is addressed in what follows.

NUCLEAR COHERENT POPULATION TRANSFER

Coherent control of nuclear states remains so far challenging [7–9]. Typically, the traditional way of shifting nuclei from one internal quantum state to another is by incoherent photon absorption, i.e., incoherent γ-rays (usually bremsstrahlung) illuminate the nuclear sample and excite the nuclei to some high-energy states. Subsequently, some of the excited nuclei may decay to the target state by chance, according to the corresponding branching ratio. This kind of method is rather passive, and its efficiency is low. Encouraged by the development of the XFEL, a promising setup for nuclear coherent population transfer in a three-level system using the quantum optics technique of stimulated Raman adiabatic passage (STIRAP) [10] has been proposed [11, 12]. Two overlapping x-ray laser pulses drive two nuclear transitions and allow for coherent population transfer directly between the nuclear states of interest without loss via incoherent processes. This would enable actively manipulating the nuclear state by using coherent hard x-ray photons and lay an important milestone in the new developing field of nuclear quantum optics [13].

* wen-te.liao@mpi-hd.mpg.de

Efficient control of the nuclear population dynamics in a three-level system as the one shown in Fig. 1 (also referred to as Λ-type system) is in particular interesting due to its association to level schemes necessary for isomer depletion. Nuclear metastable states, also known as isomers, can store large amounts of energy over longer periods of time. Isomer depletion, i.e., release on demand of the energy stored in isomers, has received a lot of attention in the last one and a half decades, especially related to the fascinating prospects of nuclear batteries [14]. As shown in Fig. 1, by shining only the pump radiation pulse, depletion occurs when the nuclear population in isomer state $|1\rangle$ is excited to a higher triggering level $|3\rangle$ whose spontaneous decay to other lower levels, e.g., state $|2\rangle$ is no longer hindered by the long-lived isomer. However, such nuclear state control is achieved by incoherent processes (spontaneous decay) and its efficiency is therefore low. In this summary we consider the efficient coherent nuclear population transfer setup proposed in Ref. [11, 12]. Two x-ray laser pulses, the pump and the Stokes pulse, drive the two nuclear transitions $|1\rangle \rightarrow |3\rangle$ and $|2\rangle \rightarrow |3\rangle$, respectively. Since most of the nuclear transition energies are higher than the energies of the currently available coherent x-ray photons, an accelerated nuclear target is envisaged, i.e., a nuclear beam produced by particle accelerators [13]. This allows for a match of the x-ray photon and nuclear transition frequency in the nuclear rest frame.

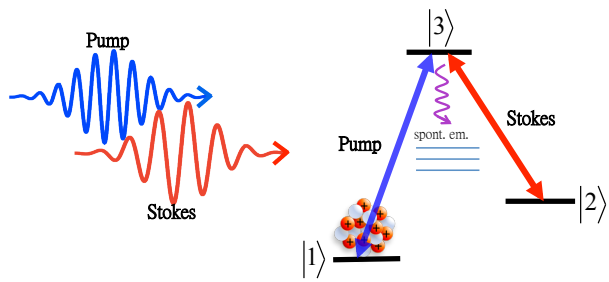

Figure 1: The Λ-level scheme. The blue arrow illustrates the pump pulse, and the red arrow depicts the Stokes pulse. All initial population is in state $|1\rangle$.

STIRAP versus π Pulses

The interaction of a Λ-level scheme with the pump laser P driving the $|1\rangle \rightarrow |3\rangle$ transition and the Stokes laser S driving the $|2\rangle \rightarrow |3\rangle$ transition is depicted in Fig. 1. In STIRAP, at first the Stokes laser creates a superposition

ISBN 978-3-95450-126-7

JITTER-FREE TIME RESOLVED RESONANT CDI EXPERIMENTS USING TWO-COLOR FEL PULSES GENERATED BY THE SAME ELECTRON BUNCH

M. Zangrando, Elettra-Sincrotrone Trieste and IOM-CNR, Trieste, Italy
L. Giannessi, ENEA, Frascati, Italy; Elettra-Sincrotrone Trieste, Trieste, Italy
E. Allaria, F. Bencivenga, F. Capotondi#, D. Castronovo, P. Cinquegrana, M.B. Danailov, A. Demidovich, S. Di Mitri, B. Diviacco, W.M. Fawley, E. Ferrari, L. Froehlich, R. Ivanov, M. Kiskinova, B. Mahieu, N. Mahne, C. Masciovecchio, I. Nikolov, E. Pedersoli, G. Penco, L. Raimondi, C. Serpico, P. Sigalotti, S. Spampinati, C. Spezzani, C. Svetina, M. Trovo, Elettra-Sincrotrone Trieste, Trieste, Italy
D. Gauthier, University of Nova Gorica, Nova Gorica, Slovenia
G. De Ninno, University of Nova Gorica, Nova Gorica, Slovenia and Elettra-Sincrotrone Trieste, Trieste, Italy
D. Fausti, Università degli Studi di Trieste, Trieste, Italy

Abstract

The generation of two-color FEL pulses by the same electron bunch at FERMI-FEL has opened unprecedented opportunity for jitter-free FEL pump-FEL probe time resolved coherent diffraction imaging (CDI) experiments in order to access spatial aspects in dynamic processes. This possibility was first explored in proof-of-principle resonant CDI experiments using specially designed sample consisting of Ti grating. The measurements performed tuning the energies of the FEL pulses to the Ti M-absorption edge clearly demonstrated the time dependence of Ti optical constants while varying the FEL-pump intensity and probe time delay. The next planned CDI experiments in 2013 will explore transient states in multicomponent nanostructures and magnetic systems, using the controlled linear or circular polarization of the two-color FEL pulses with temporal resolution in the fs to ps range.

INTRODUCTION

In the last years the FEL pump-FEL probe experiments have been based either on time-delayed holography [1], or autocorrelator devices [2,3]. These approaches give access only to single color experiments. In 2013, at LCLS [4] it has been generated a pair of temporally and spectrally separate soft X-ray FEL pulses via a double undulator scheme. However, due to the underlying self-amplified spontaneous emission configuration, these pulses have partial longitudinal coherence and limited shot-to-shot repeatability in both energy and central wavelength. In the present paper we report the successful generation of two FEL pulses with precisely controlled time delay, wavelength and intensity ratio, using two-color, two-pulse external laser seeding of the High Gain Harmonic Generation (HGHG)-based FERMI@Elettra FEL. These highly coherent FEL pulse pairs are used in a proof-of-principle XUV pump - XUV probe experiment examining the dynamics of a thin-metal layer structure exposed to high intensity XUV excitation.

flavio.capotondi@elettra.eu

GENERATION OF TWIN FEL PULSES

In a HGHG FEL [5,6] like FERMI@Elettra the output radiation properties (spectrum, duration, arrival time) are very tightly correlated with those of the input seed laser pulse. This scheme has demonstrated outstanding performances in terms of stability10, wavelength and polarisation tenability [7]. As proposed by Freund *et. al.* [8], a straightforward method for the generation of multiple X-ray pulses from an HGHG FEL consists of seeding the electron bunch with multiple laser pulses. In the specific configuration demonstrated here, we use two ultraviolet (UV), 180 fs-long (FWHM) seed pulses at slightly different central wavelengths (independently tunable in the 260-262 nm range) with variable time separation and intensity ratio. As schematically shown in Fig. 1a these pulses are focused in the modulator stage of the HGHG FEL and interact with a 750 fs-long electron bunch, for which attention was devoted in preserving the temporal uniformity of the beam parameters (mainly current and energy) using also the X-band RF cavity to linearize the longitudinal phase space of the electron beam to obtain a nominally flat current. After acceleration to 1.2 GeV, the electron beam is first energy-modulated by the seed pulses (in the modulator) and then density-modulated into two regions in which the phase/amplitude properties of the two seed pulses are encoded into the electrons. In the radiator undulator sections, having the magnetic strengths (K) tuned for fundamental FEL resonance with the N^{th} harmonic ($N = 7$ in this case) of the average seed wavelength, the two regions emit two temporally and spectrally independent XUV pulses having wavelengths scaled by a factor of 7 with respect to the seeding pulses. Tuning the delay between the input

ISBN 978-3-95450-126-7